Sources of non-methane volatile organic compounds in Delhi, India

Gareth James Stewart

Doctor of Philosophy

University of York

Chemistry

March 2021

Abstract

Cities in India consistently feature amongst the most polluted in the world, with air quality problems driven by rapid and poorly regulated economic growth and development. Many sources emit non-methane volatile organic compounds (NMVOCs), which degrade local and regional air quality through the photochemical formation of tropospheric ozone and secondary organic aerosol (SOA). Large uncertainties in the understanding of NMVOC sources specific to India result in poorly constrained regional policy and global chemical transport models. Consequently, the drivers of the consistently observed poor air quality remain poorly understood.

This thesis presents measurements of NMVOCs made in Delhi during pre- and post-monsoon seasons in 2018. The sources of NMVOCs were examined, which showed that NMVOC emissions were principally from petrol and diesel related sources. Very high NMVOC concentrations were measured at night during the post-monsoon campaign. These were shown to be emissions from the local area and were enhanced due to stagnant conditions caused by very low planetary boundary layer heights and windspeeds.

Solid fuels represent a large energy source to India, with potentially significant impacts to air quality. Consequently, a detailed source study of organic emissions from solid-fuel combustion sources was conducted. Firstly, a new method for collecting intermediate-volatility and semi-volatile organic gases and particles onto solid-phase extraction disks and Teflon filters, followed by solvent extraction with analysis by two-dimensional gas chromatography coupled to time-of-flight mass spectrometry was evaluated. Secondly, an extremely detailed set of emission factors of NMVOCs were measured with a range of online gas-phase techniques. These results were then mapped onto a volatility-basis dataset and the SOA production potential and OH reactivity of different sources compared. Finally, a high-resolution bottom-up emission inventory was developed for India from 1993-2016. This found that burning of cow dung cake had a disproportionately large impact to NMVOCs from residential combustion.

List of contents

List of tables

List of figures

List of accompanying material

The concentration-time series measured in chapter 2 are available at https://catalogue.ceda.ac.uk/uuid/ee3900d930c34730bacc4cf5ada98a7d

The emission factors presented in chapter 3 are available at https://doi.org/10.5194/acp-21-2407-2021

The emission factors presented in chapter 4 are available at https://doi.org/10.5194/acp-21-2383-2021

The emission inventories presented in chapter 6 are available at http://dx.doi.org/10.5285/fdb8960260a64c5faf652f8f47c4df81

Acknowledgements

I would like to thank Prof Jacqueline Hamilton for the continued help, guidance, and support that you have given me during my time at York, particularly your ability to laugh off the logistical disaster that this project turned out to be. Your contagious smile and good humour throughout really helped. I really appreciate that you came to India to help me setup and always gave detailed and timely feedback on my written work. It really helped to develop ideas, explore new areas, and improve the content presented in this thesis. I would also like to thank Prof James Lee for the support you have given me as a second supervisor, particularly during the times we were both in India and ensuring that we made time to see the Taj Mahal!

Dr Jim Hopkins is one of the most good-natured people I have ever encountered and is a real asset to WACL. I really appreciate that you have repeatedly gone out of your way to make time to help me during this project, particularly in fixing the GC×GC-FID during the post-monsoon field campaign, but also all the other times you have helped me with smaller problems and never made me feel like a burden. Likewise, a very big thank you to Prof Ranu Gadi and Shivani for your similarly good nature in making a special effort to facilitate ambient measurements and helping to navigate logistical difficulties faced in Delhi.

Dr Joe Acton, Dr Adam Vaughan, and Beth Nelson were great company and support during all three Delhi field campaigns. You are all very funny people and were fantastic whilst away and really helped take my mind off all the troubles we faced. Thank you for being there during all the good (and bad) times and making this project happen, particularly during the burning studies. Beth also deserves a special thank you for sorting out the gas cylinders, how such an apparently easy job could end up so complicated I will never know! Thank you also to Dr Ernesto Reyes-Villegas for being so amusing whilst away and for later sharing data with me to help with interpretation of our own measurements. I would also like to thank all the other co-authors of the papers presented as part of this thesis, your help during the experimental sections and expert critical evaluation of the data really helped to spot things I may have missed.

Thank you also to my family and Syu for encouraging me to pursue a PhD, as well as your love and support throughout.

Author's declaration

I declare that this thesis is original work, which I undertook at the University of York from 2017-2021. Except where stated, all the work contained within this thesis represents the original contribution of the author. This work has not previously been presented for an award at this, or any other, University. All sources are acknowledged as references. The majority of chapters 2-5 have been published as the following papers.

Gareth J. Stewart, Beth S. Nelson, Will S. Drysdale, W. Joe F. Acton, Adam R. Vaughan, James R. Hopkins, Rachel E. Dunmore, C. Nicholas Hewitt, Eiko Nemitz, Neil Mullinger, Ben Langford, Shivani, Ernesto Reyes-Villegas, Ranu Gadi, Andrew R. Rickard, James D. Lee and Jacqueline F. Hamilton. *Faraday Discuss*., 2021. https://doi.org/10.1039/D0FD00087F

Gareth J. Stewart, Beth S. Nelson, W. Joe F. Acton, Adam R. Vaughan, Naomi J. Farren, James R. Hopkins, Martyn W. Ward, Stefan J. Swift, Rahul Arya, Arnab Mondal, Ritu Jangirh, Sakshi Ahlawat, Lokesh Yadav, Sudhir K. Sharma, Siti S. M. Yunus, C. Nicholas Hewitt, Eiko Nemitz, Neil Mullinger, Ranu Gadi, Lokesh. K. Sahu, Nidhi Tripathi, Andrew R. Rickard, James D Lee, Tuhin K. Mandal and Jacqueline F. Hamilton. *Atmos. Chem. Phys.*, 21, 2407-2426, 2021. https://doi.org/10.5194/acp-21-2407-2021

Gareth J. Stewart, W. Joe F. Acton, Beth S. Nelson, Adam R. Vaughan, James R. Hopkins, Rahul Arya, Arnab Mondal, Ritu Jangirh, Sakshi Ahlawat, Lokesh Yadav, Sudhir K. Sharma, Rachel E. Dunmore, Siti S. M. Yunus, C. Nicholas Hewitt, Eiko Nemitz, Neil Mullinger, Ranu Gadi, Lokesh. K. Sahu, Nidhi Tripathi, Andrew R. Rickard, James D Lee, Tuhin K. Mandal and Jacqueline F. Hamilton. *Atmos. Chem. Phys.,* 21, 2383–2406, 2021. https://doi.org/10.5194/acp-21-2383-2021

Gareth J. Stewart, Beth S. Nelson, W. Joe F. Acton, Adam R. Vaughan, James R. Hopkins, Siti S. M. Yunus, C. Nicholas Hewitt, Eiko Nemitz, Tuhin K. Mandal, Ranu Gadi, Lokesh. K. Sahu, Andrew R. Rickard, James D Lee and Jacqueline F. Hamilton. *Environmental Science*: *Atmospheres*, 1, 104-117, 2021. https://doi.org/10.1039/D0EA00009D

Chapter 1

Introduction

1.1. Introduction to project

The Atmospheric Pollution and Human Health in an Indian Megacity programme (APHH-India) was a research project focused on the sources of air pollution in the Delhi area of India, the atmospheric processing of these emissions and the impacts of air pollution on human health. The project was formed of 5 different research themes.

ASAP-Delhi: A project focussed on the sources, formation processes, burden, and characteristics of particulate matter (PM) in Delhi and the National Capital Region.

DelhiFlux: A project focussed on the sources of pollutants in the Delhi area which intended to measure new emission factors, compile new emission inventories, and compare current and new inventories to *in situ* flux measurements.

Promote: A project to analyse the contribution of primary and secondary aerosols to air pollution in Delhi, examine the impacts of boundary layer meteorology and long-range transport, and to examine which emission control measures would be effective in reducing air pollution in Delhi.

DAPHNE: A project to look at the impact of air pollution on key health metrics such as birth weight and acute respiratory infections in children less than 2 years old and on asthma in adolescents aged between 12-18 years old.

CADTIME: A project to identify the key sources and emission trends of air pollutants and the key legislation determining these. It was also intended to examine the impacts of air pollution mitigation strategies on future air quality in 2030 and 2050 scenarios in Delhi.

This thesis formed part of the DelhiFlux research project focused on understanding the sources of non-methane volatile organic compounds (NMVOCs) in Delhi, measurement of emission factors of NMVOCs from solid fuel combustion sources widely used across Delhi and development of new emission inventories of NMVOCs from solid fuel combustion sources in India. This introductory chapter looks at the chemistry of organic gases in the troposphere, the measurement techniques used to analyse NMVOCs and state-of-the-art studies focussed on NMVOC air pollution in Delhi.

1.2. Non-methane volatile organic compounds

A variety of pollutants are present in the atmosphere from a range of biogenic and anthropogenic sources. Examples of gas-phase pollution include nitrogen monoxide (NO), nitrogen dioxide (NO_2), carbon monoxide (CO), ozone (O_3), sulphur dioxide (SO_2) and NMVOCs. Aerosol phase pollution contains a complex mixture of chemical species including organic aerosol (OA), cations from dust such as Mn^{2+} and $Fe^{2+/3+}$, metals from combustion such as Pb^{-}, Cu^{2+}, K^{+}, NH_4^{+} and Zn^{2+} and anions such as Cl^{-}, NO_3^{-} and SO_4^{2} as well as black carbon and water.

The chemistry of NMVOCs in the atmosphere is complex due to the tens of thousands of species present (Goldstein and Galbally, 2007). Table 1.1 shows some of the different functionalities present. NMVOCs are released into the atmosphere from a variety of biogenic sources such as vegetation and anthropogenic sources like drying paint, petrol vapours and combustion (Went, 1960). Biogenic emissions dominate global NMVOC emissions (see Table 1.2) and are greatest in the tropics. Isoprene is the largest contributor to biogenic NMVOC emissions (Wells et al., 2020), with other NMVOCs such as monoterpenes, sesquiterpenes, methanol, ethene and formaldehyde contributing smaller amounts (Sindelarova et al., 2014).

Table 1.1. NMVOCs present in the atmosphere. Reproduced from: Seinfeld and Pandis, (2012).

Functionality	Formula	Example
Alkane	R-H	CH_3CH_3 (ethane)
Alkene	$R_1{=}CR_2$	$CH_2{=}CH_2$ (ethene)
Alkyne	RC≡CR	HC≡CH (acetylene)
Aromatics	C_6R_6	C_6H_6 (benzene)
Alcohols	R-OH	CH_3OH (methanol)
Aldehydes	RCH(O)	HCH(O) (formaldehyde)
Ketone	RC(O)R	$CH_3C(O)CH_3$ (acetone)
Peroxides	R-OOH	CH_3OOH (methylhydroperoxide)
Phenolics	C_6R_5OH	C_6H_5OH (phenol)
Furans	C_4H_3OCHO	$C_5H_4O_2$ (furfural)
Carboxylic acids	R-COOH	HC(O)OH (methanoic acid)
Organic nitrates	$R\text{-}ONO_2$	CH_3ONO_2 (methyl nitrate)
Alkylperoxy nitrates	RO_2NO_2	$CH_3O_2NO_2$ (methyl peroxynitrate)
Peroxyacyl nitrates	$R\text{-}C(O)OONO_2$	$CH_3C(O)O_2NO_2$ (peroxyacetyl nitrate)
Polycyclic aromatic hydrocarbons	$C_{10}H_8$	$C_{10}H_8$ (naphthalene)
Biogenics	C_5H_8 / $C_{10}H_{16}$	Isoprene, monoterpenes
Multifunctional		Glyoxal

Table 1.2. Global biogenic NMVOC emission estimates where A = anthropogenic and B = biogenic.

Inventory	Annual flux / TgC yr^{-1}	Year	A/B	Type	Ref
MEGAN	760	2010	B	Gridded	(Sindelarova et al., 2014)
Ehhalt (1999)	654.8	1999	B	Total budget	(Ehhalt, 1999)
TAR	377	2001	B	Total budget	(Dentener et al., 2001)
ACCMIP	130	2000	A	Gridded	(Lamarque et al., 2010)
EDGAR	169	2012	A	Gridded	(Huang et al., 2017)
TAR	161	2001	A	Total budget	(Dentener et al., 2001)

The effect of NMVOCs on the atmosphere is 3-fold: they can be directly harmful to human health, lead to O_3 production and their oxidation products can produce secondary organic aerosol (SOA). In urban areas, species such as benzene can cause severe problems as they are carcinogenic and mutagenic (Huff, 2007). Tropospheric O_3 can originate from stratospheric air or as a secondary pollutant produced by the oxidation of reactive NMVOCs in the atmosphere. Ozone leads to respiratory inflammation and can increase the prevalence of asthma in children (Sheffield et al., 2015). SOA is formed of low volatility organic products, often produced by the oxidation of more volatile species.

Understanding of the chemistry of NMVOCs in the atmosphere is complicated by the exponential increase in the number of isomers present with carbon number. 10^4-10^5 NMVOCs have been measured, with this suggested to only represent a fraction of the total amount of NMVOCs present in the troposphere (Goldstein and Galbally, 2007). Different NMVOCs have different influences on the formation of O_3 and SOA.

1.2.1. Formation of secondary pollutants

Gas-phase organic compounds are of interest because they contribute to the formation of secondary pollutants, such as tropospheric O_3 and SOA. Tropospheric O_3 is formed from the oxidation of organic gases in the presence of radical species in the atmosphere. The simplest hydrocarbon in the atmosphere is methane (CH_4), which is present at a concentration of around 1.75 ppmv (Ehhalt, 1999). The oxidation scheme of methane is given through a series of steps, shown in R1.1-R1.14,

$$CH_4 + {}^{\cdot}OH \rightarrow CH_3{}^{\cdot} + H_2O \qquad \text{(R1.1)}$$

where $k_{R1.1}^{o}$ = 6.3 x 10^{-15} molecule^{-1} s^{-1} (Atkinson et al., 1997). CH_4 takes a long time to degrade in the atmosphere (lifetime ~ 12 years) because R1.1 is slow (IPCC, 2007). R1.1 is around 24 times faster in the tropics and accounts for around ~ 80% of the global CH_4 sink (Bloss et al., 2005). R1.2 shows how the methyl peroxy radical ($CH_3O_2^{\cdot}$) is formed, through reaction of $CH_3^{\cdot}$ with oxygen.

$$CH_3^{\cdot} + O_2 + M \rightarrow CH_3O_2^{\cdot} + M \quad \text{(R1.2)}$$

$CH_3O_2^{\cdot}$ then oxidises NO to NO_2 in polluted environments through R1.3.

$$CH_3O_2^{\cdot} + NO \rightarrow CH_3O^{\cdot} + NO_2 \quad \text{(R1.3)}$$

$CH_3O^{\cdot}$ goes onto produce formaldehyde with O_2:

$$CH_3O^{\cdot} + O_2 \rightarrow HCH(O) + HO_2^{\cdot} \quad \text{(R1.4)}$$

and $^{\cdot}OH$ is produced by the oxidation of NO by HO_2 radicals.

$$NO + HO_2^{\cdot} \rightarrow {}^{\cdot}OH + NO_2 \quad \text{(R1.5)}$$

Aldehydes can either be photolyzed or react with OH/NO_3 radicals, however, the reaction with NO_3 is minor (Seinfeld and Spyros, 2006). CO can be generated directly by the photolysis of HCH(O) through R1.6 (Monks, 2005):

$$HCH(O) + h\nu \rightarrow H_2 + CO \ (\lambda \leq 330 \text{ nm}) \quad \text{(R1.6)}$$

or the steps given in R1.7-R1.8 (Sander et al., 2011).

$$HCH(O) + h\nu \rightarrow HC^{\cdot}(O) + H^{\cdot} \ (\lambda \leq 361 \text{ nm}) \quad \text{(R1.7)}$$

$$HC^{\cdot}(O) + O_2 \rightarrow HO_2^{\cdot} + CO \quad \text{(R1.8)}$$

Formaldehyde and $^{\cdot}OH$ also generate HCO which is then oxidised to CO via. R1.9-R1.10:

$$HCH(O) + {}^{\cdot}OH \rightarrow HC^{\cdot}(O) + H_2O \quad \text{(R1.9)}$$

$$HC^{\bullet}(O) + O_2 \rightarrow HO_2^{\bullet} + CO \quad \text{(R1.10)}$$

R1.11 usually initiates the formation of photochemical smog:

$$^{\bullet}OH + CO \rightarrow H^{\bullet} + CO_2 \quad \text{(R1.11)}$$

with HO_2 produced through:

$$H^{\bullet} + O_2 + M \rightarrow HO_2^{\bullet} + M \quad \text{(R1.12)}$$

and OH reformed by R1.5. NO_2 then undergoes photolysis (Holloway and Wayne, 2010):

$$NO_2 + h\nu \rightarrow NO(X^2\pi) + O(^3P) \quad \text{(R1.13)}$$

to produce $O(^3P)$ which leads to the formation of O_3.

$$O(^3P) + O_2 + M \rightarrow O_3 + M \quad \text{(R1.14)}$$

Figure 1.1 shows the overall reaction from R1.11-R1.14, which is given in R1.15.

$$CO + 2O_2 + h\nu \rightarrow CO_2 + O_3 \quad \text{(R1.15)}$$

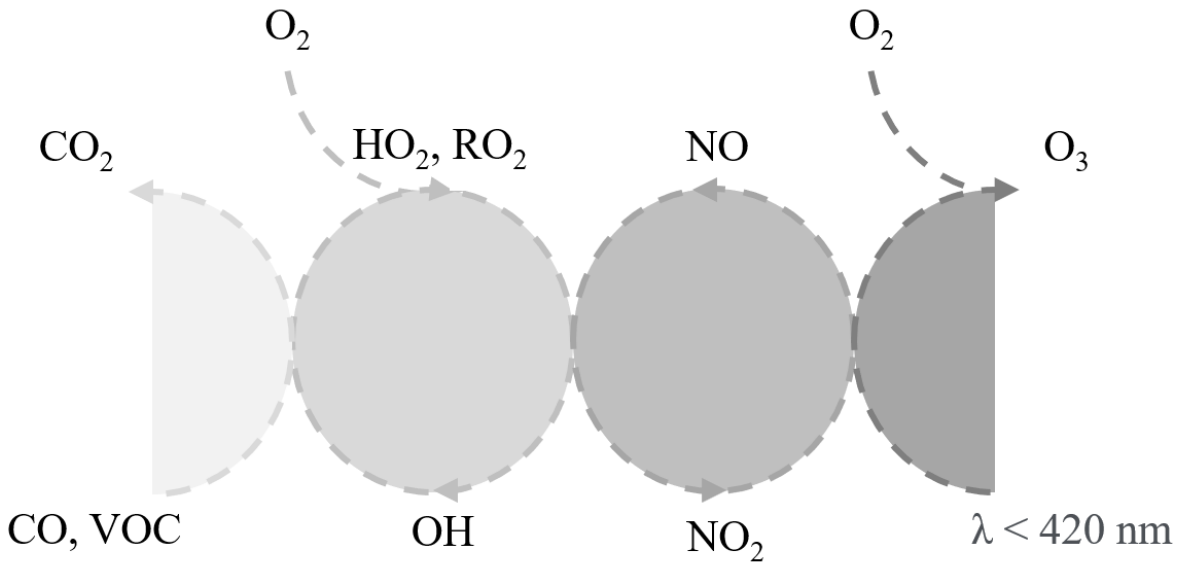

Figure 1.1. O_3 production in the oxidation of CO to CO_2 due to catalytic cycles linked by HO_x and NO_x.

Studies focus on NMVOCs, as despite the chemistry being analogous, the reactions with the OH radical are much faster than for methane (e.g. $k_{CH4,\ 298K}$ = 0.00618 x10^{-12} cm^3 $molecule^{-1}$ s^{-1} whereas $k_{dodecane,\ 298K}$ = 18 x10^{-12} cm^3 $molecule^{-1}$ s^{-1} (Atkinson, 1997)).

The oxidation of larger hydrocarbons is far more complicated, with a multitude of possible reaction products. An example is of aromatic oxidation, which occurs through two main pathways with OH: H abstraction reactions from the aromatic ring and alkyl groups attached to it or OH addition to the aromatic ring.

The vapour pressure of a NMVOC is determined by molecular weight and polarity. Functional groups such as carboxylic acids, which can allow hydrogen bonding, are significantly more polar than those such as ketones and result in NMVOCs with lower vapour pressures. As NMVOCs become increasingly oxidised in the atmosphere, their vapour pressures are reduced and they are more likely to partition to the aerosol phase.

Organic aerosol (OA) is responsible for ~ 50% of sub-micron aerosol mass globally (Putaud et al., 2004; Murphy et al., 2006; Zhang et al., 2007) and the contribution of SOA to organic aerosol is significant and varies from 20 – 80% (Dechapanya et al., 2004; de Gouw et al., 2005; Yu et al., 2007; Lanz et al., 2007; Lanz et al., 2008). Globally the SOA budget is very uncertain, ranging from 12 – 1820 Tg yr^{-1}, with the relative contributions of biogenic, anthropogenic and biomass burning sources still under debate (Spracklen et al., 2011). Intermediate-volatility and semi-volatile organic compounds (I/SVOCs) are an important class of air pollutant due to their contribution to aerosol formation (Bruns et al., 2016; Lu et al., 2018).

The volatility regions organic components are classified by are defined by their effective saturation concentration, C^*. Figure 1.2 shows the two-dimensional volatility basis dataset (VBS) of organic emissions, with volatility indicated along the x axis. Intermediate-volatility organic compounds (IVOCs) have $\log_{10}(C^*)$ = 2.5-6.5 and are predominantly in the vapour phase. Once oxidised, their lower volatility products can partition into the aerosol phase (Donahue et al., 2006). Semi-volatile organic compounds (SVOCs) have $\log_{10}(C^*)$ = -0.5-2.5 (Donahue et al., 2012) and can partition between the gas and particle phases. Low-volatility organic compounds (LVOCs) have $\log_{10}(C^*)$ = -3.5 to -0.5 and extremely low-volatility organic compounds (ELVOCs) have $\log_{10}(C^*)$ < -3.5. Lower volatility, higher molecular

weight, NMVOCs are important to the formation of SOA, due to their ability to partition from the gas to particle phase. Figure 1.2 demonstrates that organic emissions from particular sources, for example biomass burning, are released as both vapours and organic aerosol (BBOA). Figure 1.2 also shows the volatility distribution of anthropogenic and biogenic emissions, with anthropogenic sources releasing a larger mass fraction of I/SVOC species.

The y axis shows the oxidation state ($\overline{OS}C$) or approximate O:C ratios. The $\overline{OS}C$ is defined as the oxidation state of a carbon atom if it were to lose all electrons in more electronegative bonds, but gain those from bonds with less electronegative atoms (Kroll et al., 2011). It can be seen that species with increased oxidation state are generally less volatile (e.g. LV-OOA).

Better measurement techniques are required to understand the range, complexity and impacts of NMVOCs present in the atmosphere. Better characterisation is required of the sources of NMVOCs to understand the key species at emission. This can allow further laboratory studies to understand the chemistry of these key species and evaluate their atmospheric impact. This is required to properly understand the drivers of poor air quality.

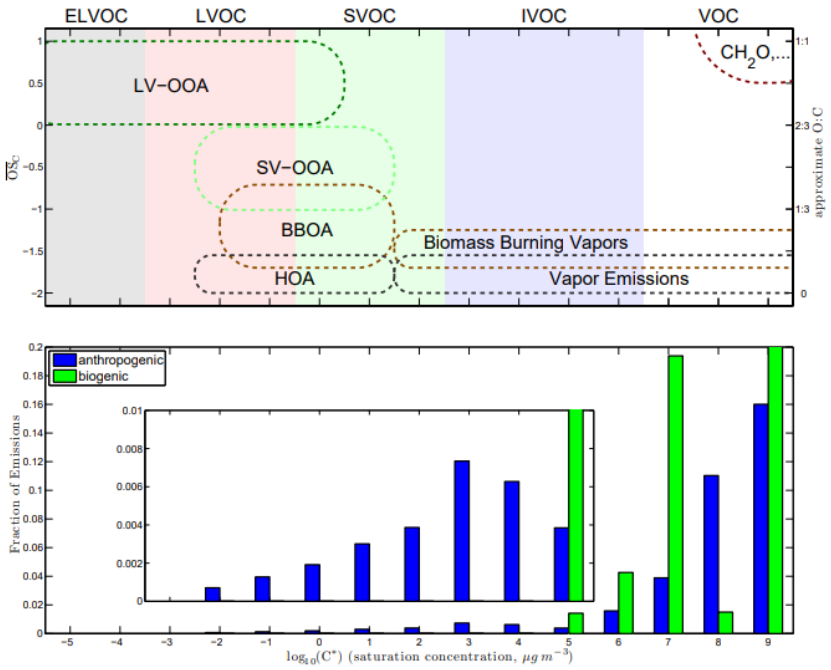

Figure 1.2. Top: Volatility basis dataset of atmospheric organic species with volatility along the x axis and oxidation state ($\overline{OS}C$) and approximate O:C ratios along the y axis. Bottom: Volatility distribution of anthropogenic and biogenic emissions, copied from Donahue et al. (2012).

1.3. Measurement techniques of NMVOCs

Measurement of NMVOCs in the atmosphere presents a difficult analytical challenge as species are present over a wide range of volatilities, functionalities and isomers (Goldstein and Galbally, 2007). A range of techniques have been developed to measure NMVOCs such as gas chromatography (GC), proton transfer reaction-time of flight-mass spectrometry (PTR-ToF-MS) and iodine clustering chemical ionisation mass spectrometry (I^-CIMS).

1.3.1. Gas chromatography

Gas chromatography is a widely used analytical technique for the detection of chemical species at low quantities in a range of applications, such as environmental measurements, petrochemical analysis and pharmaceutical quality control.

The mixture to be analysed needs to contain organic components which can be vaporised without degradation. The mixture is injected into a column through which a mobile phase, usually H_2 or He, is flowing. Separation relies upon the equilibrium of analytes between a stationary and mobile phase, which is influenced by the different chemical and physical properties of analytes (Dettmer-Wilde and Engewald, 2014). The temperature of the oven is slowly ramped in GC to allow the species of interest to be gradually volatilised from the column, pass through, and be separated. The separation can be influenced by the choice and length of column, the mobile phase pressure or flow rates and the oven temperature ramp (Pravallika, 2016). The choice of column is one of the most important considerations as the molecular properties of the stationary phase dictate the level of interaction, and thus retention time, of analyte and column.

The analytes are then measured using a detector. A variety of detectors are used such as the flame ionisation detector (FID), mass spectrometer (MS) and electron capture detector (ECD). FIDs have a wide dynamic range and are excellent for quantifying most organic species, mass spectrometers are useful for providing qualitative information on analytes and ECDs are used for quantifying organic species containing halogens. Species are quantified against the response of a standard, which is of known concentration, injected into the column. Species are qualified using either comparison of retention times of known compounds or through comparison of characteristic fragmentation patterns to databases.

GC is a robust technique which has been widely used for long-term monitoring of ambient air samples. GC can provide information on the isomeric speciation of emissions, with setups designed to allow ambient measurements of a range of alkanes, alkenes and oxygenated volatile organic compounds (OVOCs) (Hopkins et al., 2003). The main drawbacks of GC are that this technique is of limited use in untargeted measurements of complex emissions unless an MS is used, preconcentration of gas samples is usually required and many different column configurations and detectors are required to provide information on different chemical classes to avoid missing important emissions. The nature of a chromatographic separation means that separations usually take minutes to hours. This can be partly alleviated by collecting multiple whole air samples (WAS) at a higher time resolution than the separation and pumping into sample canisters or bags with subsequent analysis (Sirithian et al., 2018; Wang et al., 2014; Barabad et al., 2018), but this can introduce artefacts (Lerner et al., 2017). A pre-treatment water removal stage is also required prior to sample analysis which can cause carryover between samples and limit the volatility range of analysis.

1.3.2. Comprehensive two-dimensional gas chromatography

Liu and Phillips, (1991) developed two-dimensional chromatography (GC×GC) and it has since been used for a vast range of analyses (Liu and Phillips, 1991; Phillips and Xu, 1995). Some of the most exciting have been the revelation of the complexity of organic compounds urban air (Lewis et al., 2000) and the demonstration of over 10,000 organic components in $PM_{2.5}$ (Hamilton et al., 2004). GC×GC has also been used for a wide variety of petrochemical analyses (Adahchour et al., 2006a), fragrance analyses (Adahchour et al., 2006a) and studies of third hand cigarette smoke (Ramírez et al., 2015).

GC×GC couples together two columns with different separation mechanisms via. a modulator (see Figure 1.3) (Liu and Phillips, 1991; Phillips and Xu, 1995). Typically, a nonpolar primary column (B in Figure 1.3) is used for a volatility-based separation and is connected to a short polar secondary column to create a fast polarity-based separation (D in Figure 1.3). The chromatogram is displayed as a 2D contour plot, with families of chemical species sorted into bands based on functionality. This overcomes a major limitation of one-dimensional gas chromatography in that different NMVOCs with similar

vapour pressures, but different polarities, can coelute. Using GC×GC, quantitative analysis of extremely complex mixtures is possible (Vendeuvre et al., 2007). Figure 1.4 shows an example GC×GC chromatogram from measurements made in London in 2012 (Dunmore et al., 2015). The C_3 substituted monoaromatics would coelute in the same region as C_{10}-C_{11} alkanes/alkenes in a conventional one-dimensional boiling point separation. Using GCxGC, these NMVOCs have different polarities and thus are well separated into different bands. This increases the peak capacity of the system (where n_x = peak capacity of column x) from the sum of the two columns for a heart-cut system, to a maximum of the product of the two columns as shown in R1.16 (Hamilton and Lewis, 2007). The higher peak capacity in R1.16 also means that sample preparation is often not required before analysis (Eiserbeck et al., 2014).

$$n_1 \text{x } n_2 \approx n_{\text{total}} \qquad \text{(R1.16)}$$

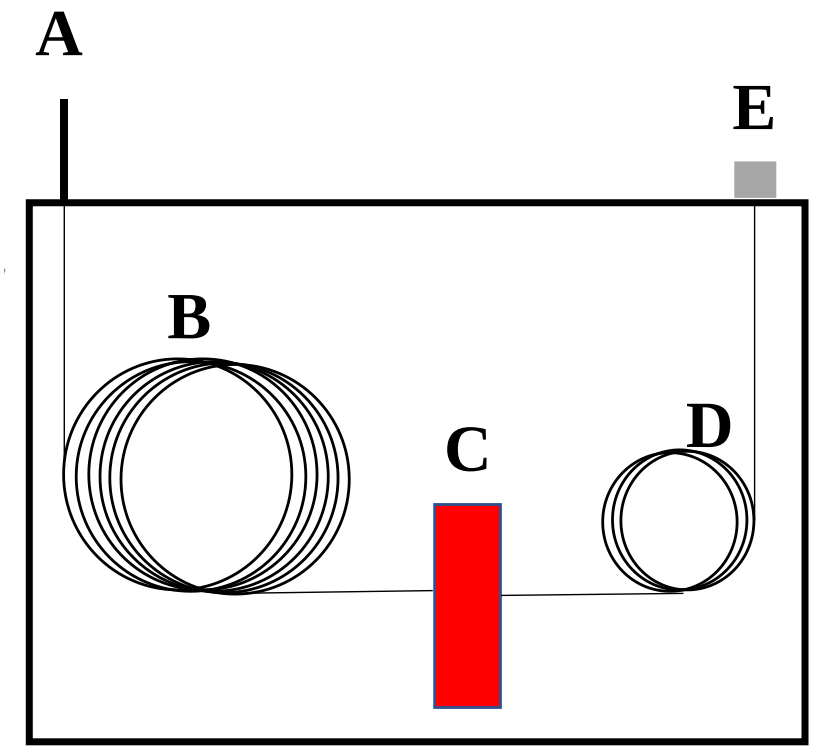

Figure 1.3. GC×GC detection scheme where A = injection to GC×GC, B = primary column, C = modulator, D = secondary column (different separation mechanism to B) and E = detection/data processing.

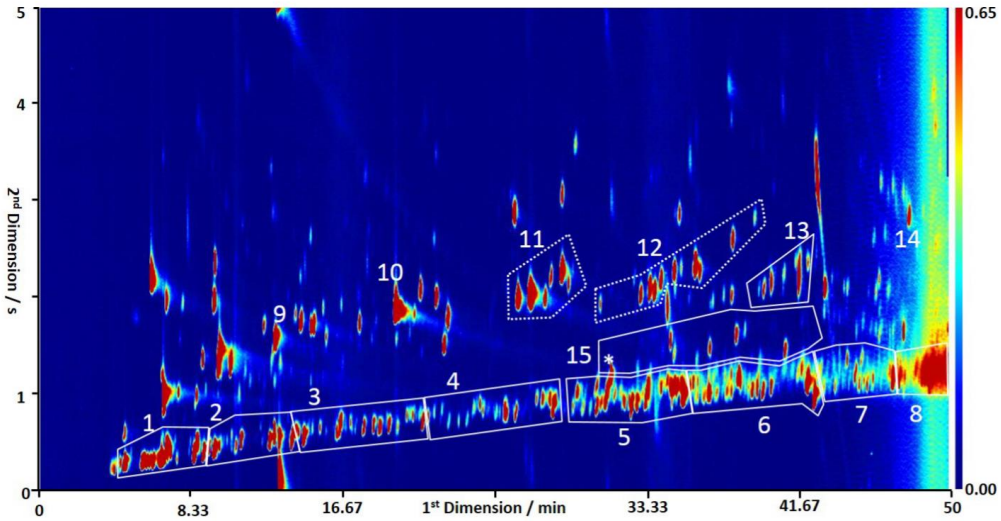

Figure 1.4. Two-dimensional gas chromatogram for C_6-C_{13} where 1 = C_6 alkanes, 2 = C_7 alkanes, 3 = C_8 alkanes, 4 = C_9 alkanes, 5 = C_{10} alkanes, 6 = C_{11} alkanes, 7 = C_{12} alkanes, 8 = C_{13} alkanes, 9 = benzene, 10 = toluene, 11 = C_2 substituted aromatics, 12 = C_3 substituted aromatics, 13 = C_4 substituted monoaromatics, 14 = naphthalene and 15 = C_{10} monoterpenes. Taken from: Dunmore et al. (2015).

The two columns are connected by a modulator (C in Figure 1.3) which captures the eluent from the end of the primary column and transfers it to the secondary column in discrete bands. The peak width of the primary column should be several times the modulation frequency. It is important to ensure that there are enough sub peaks in the second dimension to accurately characterise the peak. If there are only one or two sub peaks from a peak in the second dimension, little extra information is gained from performing the two-dimensional separation. The modulation period is selected as a balance between two competing factors. If a very long modulation period is used, more NMVOCs which have been separated on the primary column will be mixed again before injection into the secondary column and this can result in loss of the initial separation. If the modulation period is too fast, NMVOCs may not be through the secondary column before the next modulation and may wrap around into other bands of NMVOCs on the chromatogram (Eiserbeck et al., 2014).

Numerous modulators have been tested, such as thermal desorption, cryogenic and valves (Cortes et al., 2009). Thermal modulation uses either heating or cryogenic cooling to provide modulation. With heating, a thick film of stationary phase is used between the columns to trap eluent from the primary column and then this is periodically heated to

around 100 ^{o}C more than the oven temperature to allow desorption to occur (Liu and Phillips, 1991; Phillips et al., 1999; Vendeuvre et al., 2007). Thermal desorption was used in many early GC×GC systems; however, electrically heated modulators were unreliable, sweeper motors created a volatility range restriction so could not analyse > C_{25} (Serrano et al., 2012) and other modulators designs have since proven to be more effective (Adahchour et al., 2006b).

Cryogenic modulators use endothermic expansion of cryogenic liquids such as CO_2 or N_2 to create low temperatures to trap eluent after a primary separation. Marriott et al. (1997) pioneered the longitudinally modulated cryogenic system, which used expanding liquid CO_2 to cool the start of the second column to trap small bands of eluent from the primary column (Marriott and Kinghorn, 1997; Kinghorn and Marriott, 1998). Longitudinal movement of this system allowed the release of the eluent for a secondary separation. This method showed poor trapping of highly volatile NMVOCs. This was also developed into a dual-jets CO_2 system (Beens et al., 2001). Jet based systems have been improved with nitrogen gas passed through liquid nitrogen and allowed analysis of C_1-C_{36} (Adahchour et al., 2006b). This technique is best suited to lab studies, due to cryogenic liquids, and samples are routinely collected in the field, transported and then analysed offline in the lab.

Differential flow modulation was introduced by Bueno et al. (2004) and has been used (Bueno and Seeley, 2004; LaClair et al., 2004; Micyus et al., 2005) and developed in subsequent publications (Seeley et al., 2006; Kochman et al., 2006; Seeley et al., 2007a; Seeley et al., 2007b; Seeley et al., 2008b; Seeley et al., 2008a; Poliak et al., 2008; Gu et al., 2010; Manzano et al., 2011). This technique has been demonstrated to offer comparable performance to thermal modulation (Semard et al., 2011) and is able to trap particularly volatile NMVOCs as it does not rely on a temperature differential.

Narrow peak widths are observed from the second column in GC×GC and it is therefore important to have a detector with a high acquisition speed. A range of detectors have been used such as FID, ToF-MS, micro electron capture detectors and element specific detection such as nitrogen or sulphur chemiluminescence. Nitrogen specific detection has been used in studies of nitrosamines (Kocak et al., 2012), nitro compounds (Ramírez et al., 2015) and

nitriles (Özel et al., 2011). Sulphur specific detection has been used to examine mercaptans, sulphides, thiophenes, benzothiophenes, dibenzothiophenes (Wang and Walters, 2007) and sulphur-bound hopanes and steranes (Li et al., 2008). The most powerful detection method for qualification of extremely complex mixtures is high frequency ToF-MS. ToF-MS can be run at 5 kHz which allows a good signal to noise ratio with narrow peak widths from GC×GC of around 50 ms (Eiserbeck et al., 2014). FID does not provide structural information but can also be run at high frequency (~ 200 Hz) and structural elucidation can occur thanks to comparison with retention times of standard molecules. The eluent can also be split between both ToF-MS and FID to provide qualitative and quantitative information.

Valve based modulators have proven to be particularly advantageous because they can trap the most volatile components, there is no need for cryogenics and fast second column separations are possible (Adahchour et al., 2006b). Initial modulators lacked sensitivity because only part of the eluent was transferred from the first to second column (Hamilton and Lewis, 2007). Bruckner et al. (1998) connected the primary and secondary columns using a commercial diaphragm valve (Bruckner et al., 1998). Several improvements have been made, such as Seeley et al. (2000) who used differential flow modulation with a sample loop on a 6-port diaphragm valve to allow 80% of the sample to pass through the secondary column (Seeley et al., 2000). Bueno et al. (2004) refined this by creating a flow switching device which allowed total transfer between the two columns (Bueno and Seeley, 2004). This improved trace gas analysis by transferring all the eluent from the primary to secondary column. This study created a relatively simple setup where eluent from the primary column could be alternately injected into two different sample loops and whilst one loop was filling, the other would be venting to the secondary column (Bueno and Seeley, 2004). Other total transfer devices have been investigated. Lidster et al. (2011) investigated the use of rotary and diaphragm valves (Lidster et al., 2011), with the latter successfully deployed on field campaigns outside of usual laboratory operating conditions (Dunmore et al., 2015). The main limitation of valves previously used is the upper operating temperature of usually around 175 ^{o}C (Adahchour et al., 2006b) which restricted the temperature range of separation.

1.3.3. Chemical ionisation mass spectrometry

The high energy of Electron Ionization (EI) in mass spectrometry can result in complete fragmentation of compounds and means that the parent ion is not measured and therefore important information about the molecular weight of the analyte is lost. Recent developments in mass spectrometry have developed techniques which are ideally suited to online measurements of NMVOCs using softer ionisation techniques.

PTR-ToF-MS uses chemical ionisation with the hydronium ion (H_3O^+) to measure most polar and unsaturated NMVOCs in gas samples. Lower ionisation energies are used, which means that less fragmentation occurs compared to EI. H_3O^+ ions are generated using a hollow-cathode discharge through water vapor (Blake et al., 2009). The H_3O^+ ions produced by this ion source then react with a NMVOC of interest through R1.17.

$$H_3O^+ + M \rightarrow MH^+ + H_2O \qquad \text{(R1.17)}$$

The protonated analyte then passes into a drift tube of around 10 cm long held at a pressure of approximately 2.0-4.0 mbar with a voltage of 600-700 V to create the desired electric field strength. The drift tube temperature is around 40 – 60 ^oC (Yuan et al., 2017). The ions have band broadening reduced using a reflectron and are measured using a microchannel plate detector.

The PTR-ToF-MS is very sensitive with very low detection limits of tens to hundreds of pptv, measurements possible over a wide mass range of 10 – 500 Th and fast acquisition rates of up to 10 Hz (Yuan et al., 2016). Measurements have been made of a wide array of aromatics, oxygenated aromatics, alkenes, furans and nitrogen containing volatile organic compounds (Warneke et al., 2011; Yokelson et al., 2013; Stockwell et al., 2015; Koss et al., 2018). The main limitations of measurements using PTR-ToF-MS are fragmentation of the parent ion leading to uncertainty in quantification, an inability to measure alkanes as it is only possible to detect species with a proton affinity greater than water and the inability to speciate isomers as PTR-ToF-MS can only provide information about a specific mass and not the isomeric contributions to this mass (Stockwell et al., 2015).

The use of reagent ions other than H_3O^+ allows the measurement of species which do not react with water (Yuan et al., 2017). Measurements have been made for example using an

iodide-clustering time-of-flight chemical ionization mass spectrometer (I^--CIMS), which is well suited to measuring acids and multifunctional oxygenates (Lee et al., 2014) as well as isocyanates, amides and nitrates (Priestley et al., 2018).

1.4. Air quality in the developing world

Poor urban air quality is a major global public health concern, particularly in the developing world, as rapid urban growth has increased emissions to harmful levels. This issue remains at the forefront of many governmental policies, as by 2050 approximately 66% of the global population are expected to live in urban environments (United Nations, 2014). Globally, an estimated 4.2 million premature deaths were a result of poor ambient air quality in 2016, mainly caused by exposure to PM and O_3 (World Health Organization, 2018a) with a further 3.8 million estimated premature deaths as a result of household air pollution caused by inefficient solid fuel use for cooking (World Health Organization, 2018b). NMVOCs are key precursors to PM and O_3. Figure 1.5 shows a breakdown of deaths attributable to air pollution by region and the cause of death. The Western Pacific and South East Asian regions have the highest premature death rate per capita attributable to poor ambient air quality. In India, air quality related deaths were estimated to be 1.2 million in 2017 (Health Effects Institute, 2019).

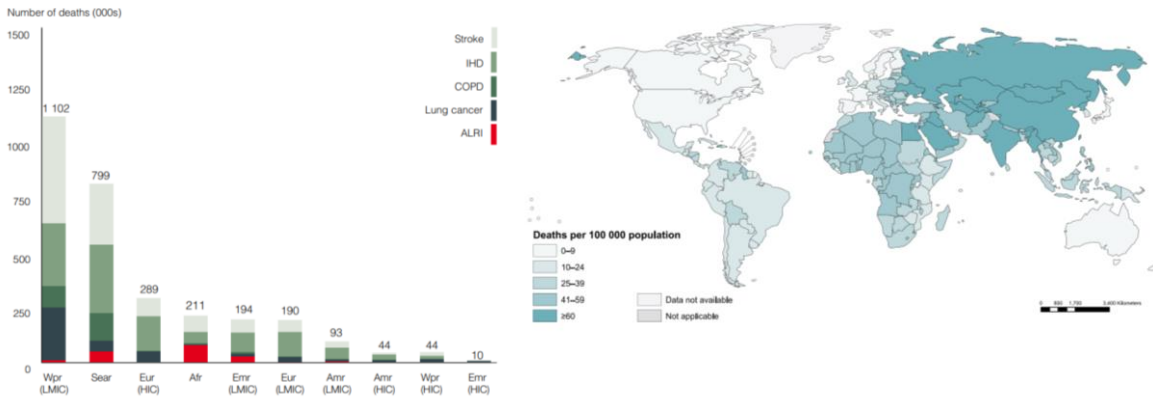

Figure 1.5. Global premature deaths caused by ambient air pollution (left) where Afr: Africa; Amr: Americas; Emr: Eastern Mediterranean; Eur: Europe; Sear; South-East Asian region; Wpr: Western Pacific region; LMIC: Low- and Middle-Income Countries; HIC: High-Income Countries; COPD: Chronic Obstructive Pulmonary Disease; IHD: Ischeaemic Heart Disease. Global deaths per 100,000 population due to poor ambient air quality (right). Copied from: World Health Organisation, (2016).

Air pollution leads to a range of health problems such as chronic bronchitis, chronic obstructive pulmonary disease, lung cancer, childhood pneumonia, acute lower respiratory infections, low birth weight of children, sore eyes and problems with the nervous system (World Health Organisation, 2018a,b). The impact of poor air quality remains significant in the developing world, with high but poorly understood emissions. The sources of NMVOC pollution in the developing world can be different to those measured from developing countries and can include sources which are currently poorly characterised, such as the burning of municipal solid waste in landfill sites, residential burning of waste, solid fuel combustion for heating and cooking, varied and unregulated industrial sources, different vehicle fleets, lower grade fuels and poorly serviced diesel generators (Kumar et al., 2015). Few local source profiles have been developed and used in local spatially disaggregated inventories, which means that the relative importance of key source sectors remains unknown. For successful mitigation to occur, policy must be informed by reasoned and well-evaluated scientific studies. New studies in poorly understood and highly polluted atmospheres are therefore essential in limiting the impact of pollution on human health.

1.4.1. Delhi metrics

Delhi is in the north of India with a latitude 28°40’0”N and longitude 77°10’0”E and had a population of around 17 million in 2011 (Department of Economics and Statistics, 2011) which is forecast to grow to 39 million by 2030 (United Nations, 2019). Figure 1.6 shows the location of Delhi within India and a gives a breakdown of the regions of Delhi state. Delhi is an area of high population density, with population densities of the respective regions in the 2011 census of North West (8254 persons km^{-2}), North (8254 persons km^{-2}), North East (36,155 persons km^{-2}), East (27,132 persons km^{-2}), New Delhi (4057 persons km^{-2}), Central (27,730 persons km^{-2}), West (19,563 persons km^{-2}), South West (5446 persons km^{-2}) and South (11,060 persons km^{-2}) (Directorate of Census Operations, 2011). There are 5 main seasons: winter (December-January), spring (February-March), summer (April-June), monsoon (July-mid-September) and autumn (mid-September-November) (Delhi Tourism, 2016). Figure 1.7 shows mean temperatures and precipitation for Delhi in 2017.

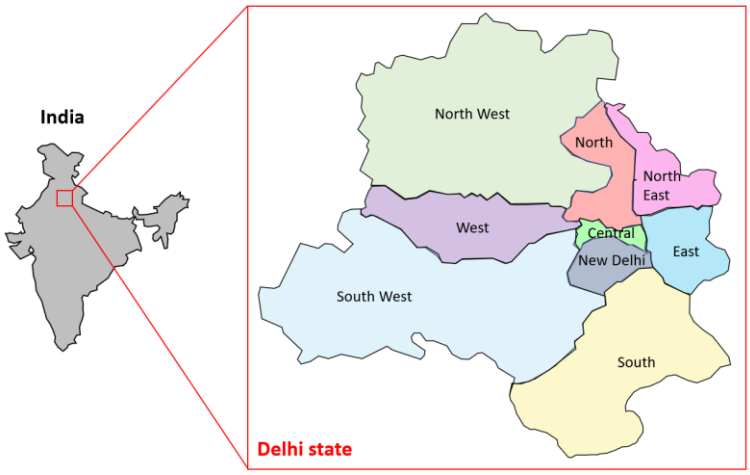

Figure 1.6. Maps showing location of Delhi state within India and regions of the state.

Urban air pollution remains at the forefront of global media and many measures to improve the situation in both Delhi and India have been undertaken. These started with the 1981 Air Act and new measures have been implemented such as using compressed natural gas for light good vehicles, the implementation of vehicle emissions regulations and the construction of a modern metro system (see Figure 1.8). Some mitigation measures to improve air quality in India have been reported to be successful, for example reducing benzene content in fuels from 5% to 3% in Kolkata was reported to reduce roadside benzene levels from 214.8 µg m^{-3} to 30.8 µg m^{-3} (Talapatra and Srivastava, 2011). Monitoring of NMVOCs in Delhi has been conducted through three different approaches: studies reported in published literature, wider government studies and continuous measurement programs.

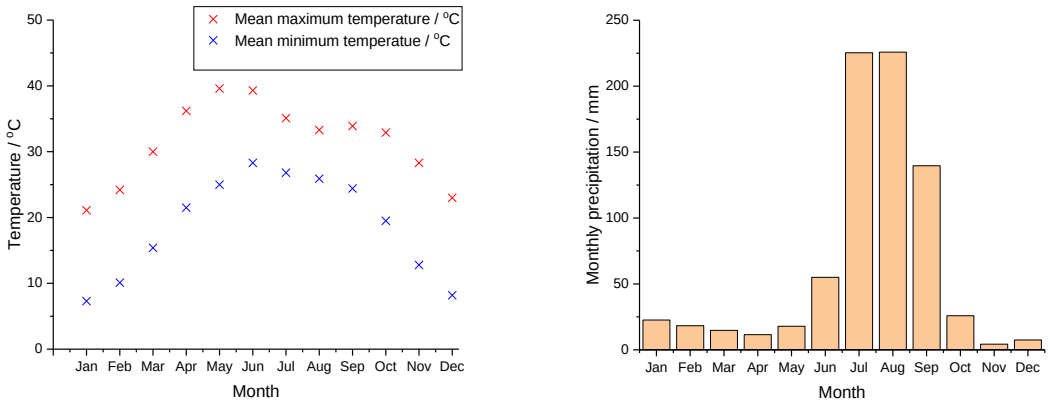

Figure 1.7. Metrological data for Delhi. Mean monthly temperature (left) and mean total monthly precipitation (right). Data taken from: Indian Meteorological Office, (2018).

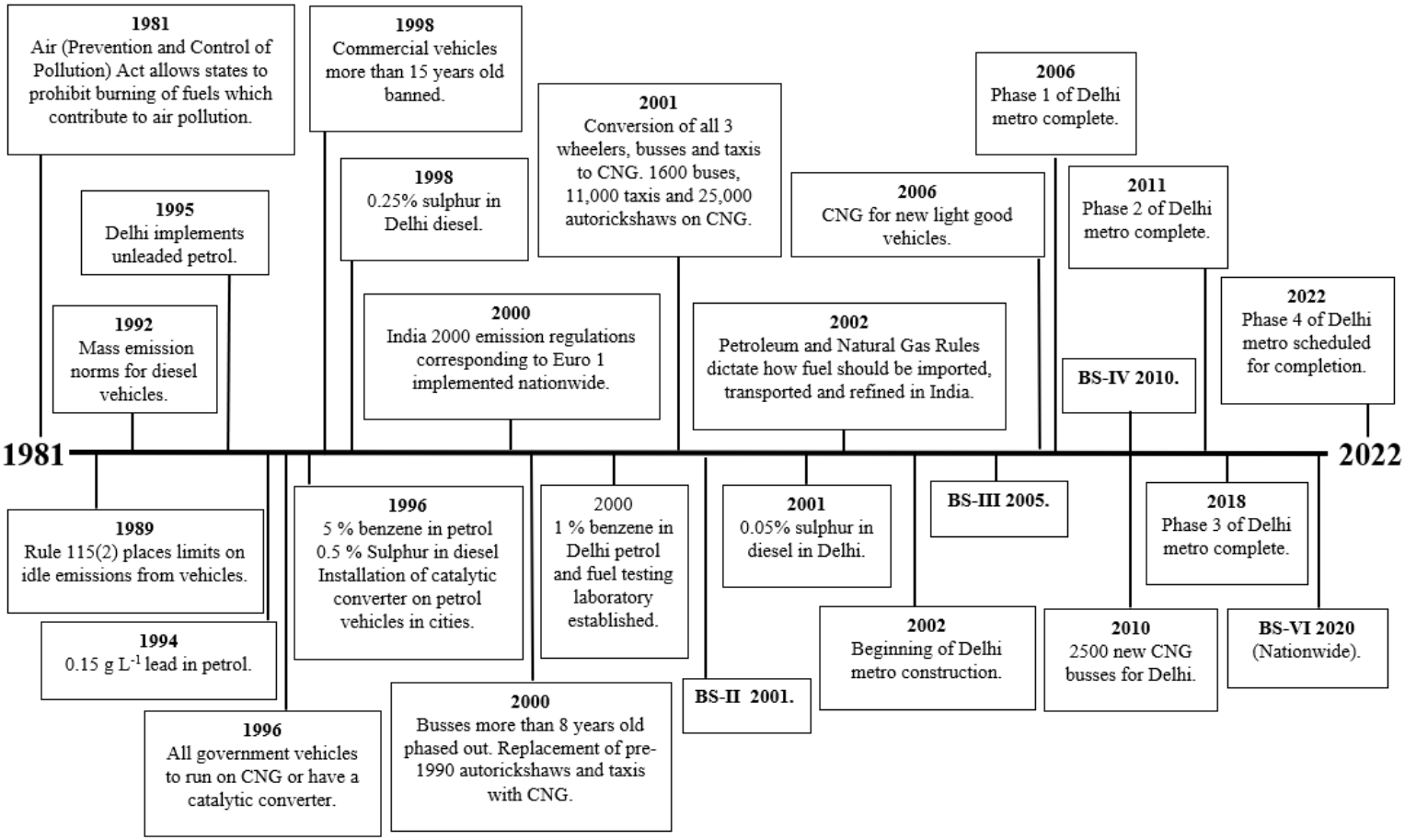

Figure 1.8. Timeline of changes to transport to improve air quality in Delhi from 1981- 2022. BS = Bharat stage, which correspond to equivalent Euro standards and only affects future fleet. BS dates correspond to implementation in Delhi. CNG = compressed natural gas. Constructed using information from: Parliament of India, (1982), Government of NCT Delhi, (1989), Khillare, (2008), NEERI, (2008) and Goel and Guttikunda, (2015).

1.4.2. Delhi specific NMVOC inventories

Since the 1990s, a limited range of inventories and measurements have attempted to estimate NMVOC emissions from Delhi. NMVOC emission estimates have been the subject of several studies and were estimated to be approximately 100 kt y^{-1} in 1990 (Bose and Anandalingam, 1996), 148 kt y^{-1} in 1995 (Gurjar et al., 2004) and ~ 150 kt y^{-1} in 2010 (Sharma et al., 2015), with most NMVOC emissions related to transport and solvent use. Despite this, the investigation of Sharma et al. (2015) was limited as the grids were 36 km x 36 km and thus too large to be truly Delhi specific. Additionally, China specific speciation factors were used, which may not be accurate for India. A different study provided a 1 km × 1 km gridded emission inventory for Delhi covering an 80 km × 80 km area and provided total unspeciated NMVOC emissions by sector (Guttikunda and Calori, 2013). Other studies have focussed on specific sources. Goel and Guttikunda (2015) estimated vehicular NMVOC emissions using fleet average emission factors of 180 kt y^{-1} in mid 1990s to ~ 80 kt y^{-1} in 2014. Srivastava et al. (2009) produced an emission inventory of evaporative emissions in Delhi and reported the evaporative emissions in Delhi to be higher than in Mumbai, Chennai and Kolkata (Srivastava and Majumdar, 2009).

Table 1.3 shows their finding that vehicles dominate NMVOC evaporative emissions. These were from running vehicles and smaller contributions from transit/breathing losses, hot soak emissions after a trip from heated fuel and lines, diurnal heating of the vehicle and resting emissions.

Table 1.3. Contribution to NMVOCs in Delhi from evaporative emissions, according to Srivastava et al. (2009).

NMVOC source	Contribution kg yr^{-1}	NMVOC source	Contribution kg yr^{-1}
Running vehicles	1.71 $x10^9$	Printing	3.06 $x10^5$
Vehicle transit	1.84 $x10^7$	Graphical art applications	3.58 $x10^6$
Vehicle hot soak	6.06 $x10^7$	Consumer products	9.24 $x10^6$
Vehicle diurnal	2.15 $x10^7$	Surface coating	1.84 x 10^6
Vehicle resting	4.87 $x10^6$	Auto refining	6.50 $x10^4$
Petrol loading / unloading	1.31 $x10^6$	Dry cleaning	1.32 $x10^6$
Petrol refiling	4.02 x 10^6		

1.4.3. Previous literature relating to Delhi NMVOCs

Previous studies making measurements of NMVOCs at sites in Delhi have been limited either covering total NMVOCs or benzene, toluene, ethylbenzene and xylenes (BTEX). Very few studies have offered an insight into speciated NMVOC emissions in Delhi (see Table 1.4). A range of sampling techniques have been used for NMVOC analysis such as whole air samples (Padhy and Varshney, 2000), pre-concentration onto TENAX sorbent tubes (Kumar, 2006), activated charcoal diffusion tubes (Hoque et al., 2008) and real-time monitors such as the handheld PGM-7600 which used a photoionization detector to detect NMVOCs (Singh et al., 2010). A recent study by Wang et al. (2020) was the most detailed to date and used PTR-ToF-MS at urban and suburban sites to conduct source apportionment using positive matrix factorisation (PMF). The conclusion of this study was that anthropogenic traffic related emissions were the dominant source of NMVOCs at the urban site representing 56.6% of the total mixing ratio and remained important at the suburban site (36.0% of total mixing ratio). The contribution of solid fuel combustion was of similar importance at urban (33.6%) and suburban (30.4%) sites. Secondary formation was responsible for 15.9% of total mixing ratio at the urban site and 33.6% at the suburban site.

1.4.4. Government studies of NMVOCs

In 2008 a wider programme was undertaken focussed on pollution sources in Delhi, Mumbai, Bangalore, Chennai, Kanpur and Pune (CPCB, 2010). The aim of this study was to undertake pollutant monitoring, produce new emission inventories and carry out receptor and dispersion modelling. The National Environmental Engineering Research Institute (NEERI) created a 2 km x 2 km gridded emission inventory for a 32 km x 30 km area of hydrocarbon emission estimates for area sources, industrial sources and vehicular sources across Delhi (see Figure 1.9). The conclusion of this study was similar to Srivastava et al. (2009), indicating that vehicular sources dominate city-wide NMVOC emissions. Despite this, obvious limitations are apparent, such as only sampling for 1 or 7 days during the experiment.

Table 1.4. Measurements of NMVOCs made in Delhi during field campaigns.

Measurement details	Example mixing ratio/ ppbv	Dates	Reference
Sampling at 13 sites every 15 days by grab sample in syringes and storing the sample in a glass vial before measuring by GC-FID.	Total NMVOCs 1300 – 32500	Nov 1994-Jun 1995	(Padhy and Varshney, 2000)
NMVOC measurements at 10 sites across Delhi using GC-FID for polyaromatic hydrocarbons, *n*-alkanes, hopane, sterane, methyl-alkane, branched alkane, cycloalkane, alkenes and levoglucosan.	-	Summer, monsoon, post monsoon 2008	(NEERI, 2008)
BTEX species were sampled at 3 sites in Delhi using carbon sorbent tubes and subsequently analysed by GC-FID. Results presented as monthly means alongside monthly minimum and maximum values.	Mean values of benzene (18.9), toluene (43.2), ethylbenzene (11.4) and xylene (5.8)	Jan-Jun 2015	(Guar et al., 2016)
Measurements of BTEX at a residential site with vegetation, commercial site, industrial site with high traffic density and near a traffic intersection. NMVOCs adsorbed onto charcoal diffusion tubes with one tube a week and then analysed by GC-FID.	Mean yearly benzene at residential (15.0), commercial with heavy traffic (30.4) and industrial (27.9) sites as well as at a traffic intersection (34.4)	Oct 2001-Sept 2002	(Hoque et al., 2008)
Measurements of benzene and toluene at a petrol pump, roadside and residential area onto TENAX sorbent tubes and then GC-FID.	Benzene (10.5-54.65) and toluene (11.94-60.72)	7 days from Apr – Jun 2002	(Kumar, 2006)
Measurements of benzene at a commercial site, residential site and busy traffic intersection in 2007 and comparison to Hoque et al. (2008). Analysis with diffusion tubes followed by GC-FID to allow comparison pre- and post-compressed natural gas implementation.	Mean benzene concentrations for residential (18.5), commercial with heavy traffic (67.9) and near the traffic intersection (89.8)	Oct 2001-Sept 2002 and Jan – Feb 2007	(Khillare et al., 2008)
Mean values and ranges of 21 species measured at 15 sites for monsoon, winter and summer using sorbent tubes with GC-MS.	-	Aug 2001 – Jul 2002	(Srivastava et al., 2005a)

Table 1.4 continued.

Measurement details	Example mixing ratio/ ppbv	Dates	Ref
Source apportionment using same data set as (Srivastava et al., 2005a) suggesting that diesel combustion emissions dominate in Delhi (26 – 54% total NMVOCs).	-	Aug 2001 – Jul 2002	(Srivastava et al., 2005c)
Measurements once a month of 17 NMVOCs at 3 petrol stations in Delhi using thermal desorption from sorbent tubes with GC-MS.	-	Mar-Feb 2001-2002	(Srivastava et al., 2005b)
Measurement of BTEX at the Sirifort monitoring station published as a mean yearly concentration for each pollutant. Measured online using thermal desorption GC-FID.	Benzene (2.5), toluene (3.9), *o*-xylene (1.1), *m-/p*-xylene (1.6) and ethylbenzene (1.1)	2006	(CPCB, 2006)
Measurements of benzene at a busy roadside, petrol pump and residential area.	Range of benzene near a petrol pump (100-2500)	Oct 2007 - Feb 2008	(Singh et al., 2010)
Measurements of BTX at 6 sites across Delhi by adsorption onto activated carbon sample tubes and then measurement with GC-FID.	Mean benzene (2.7-7.8), toluene (5.8-22.3) and xylenes (2.3-5.1)	May-Apr 2010	(Singh et al., 2012)
Benzene, toluene and xylene measured at 40 petrol stations around Delhi. Measurements carried out by adsorption onto sample tubes and then measurement with GC-FID. Each site measured twice for 8 hours in rainy and dry seasons.	Mean winter benzene (470), toluene (400) and xylenes (580). Mean summer benzene (190), toluene (160) and xylenes (460)	2009-2010	(Sehgal et al., 2011)
Measurements of BTEX at 8 sites in Delhi including intersections, residential areas and at petrol pumps. Measurements carried out by adsorption onto sample tubes and then measurement with GC-FID.	Maximum values of benzene (0.18), toluene (0.12), xylenes (0.47) and ethylbenzene (0.02) 200-300m from intersection	Oct/Nov 2013 and Jan/Feb/Mar/May 2014	(Singh et al., 2016)
PTR-ToF-MS measurements at urban and suburban sites in Delhi.	Total NMVOC mixing ratios from 10-200 ppbv at urban site	Jan-Mar 2018	(Wang et al., 2020)

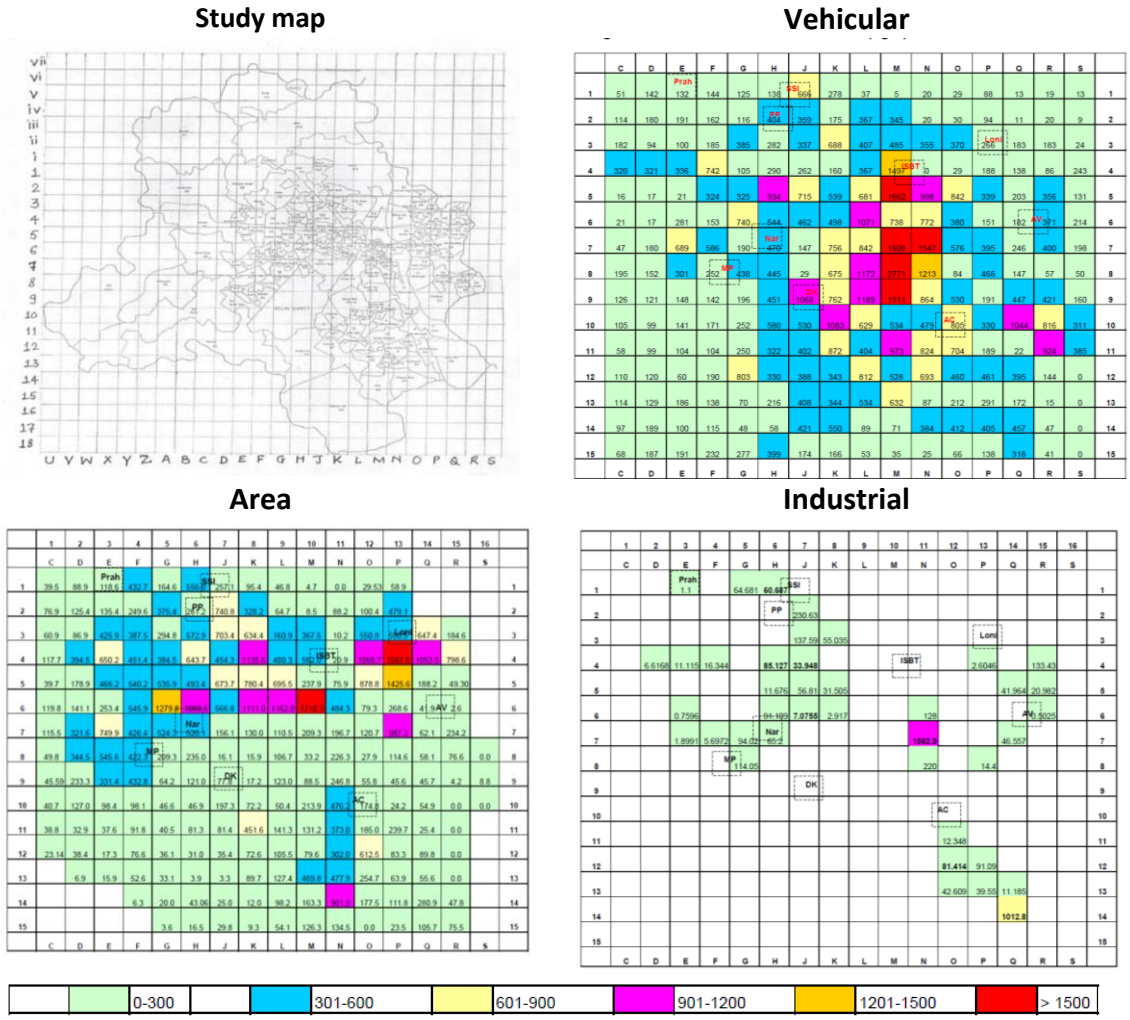

Figure 1.9. Gridded hydrocarbon emission estimate for Delhi (kg day^{-1}) for vehicular, area and industrial sources. Taken from: NEERI, (2008).

1.4.5. Continuous monitoring of NMVOCs in Delhi

The Central Pollution Control Board (CPCB) is a governmental organisation which oversees the National Air Quality Monitoring Program of 683 stations across India. The CPCB regulate air quality, and Table 1.5 shows the regulations for criteria pollutants. For NMVOCs, the annual mean benzene concentration should be < 5µg m^{-3} (Talapatra and Srivastava, 2011).

20 CPCB monitoring stations are across the metropolis of Delhi (see Figure 1.10 for map, see Table 1.6 for species measured) and the values are published online (CPCB, 2018). Despite this, large periods of data are often absent, for example the CPCB claim to have measured BTEX at Lodhi Road from September 2017 – February 2018, but essentially no data is present. The measurement site at Shadipur (yellow circle on Figure 1.10, located at

a metro station in North-West Delhi) has one of the most detailed measurements sets for BTEX (see Table 1.7 for mean annual values).

Table 1.5. Ambient air quality standards in India. Reproduced from: CPCB, (2011).

	Industrial, Residential and rural annual	Industrial, Residential and rural 24 hours	Ecologically sensitive area 24 annual	Ecologically sensitive area 24 hours
SO_2 / µg m^{-3}	50	80	20	80
NO_2 / µg m^{-3}	40	80	30	80
PM_{10} / µg m^{-3}	60	100	60	100
$PM_{2.5}$ / µg m^{-3}	40	60	40	60
O_3 / µg m^{-3}	100	180	100	180
Pb / µg m^{-3}	0.5	1.0	0.5	1.0
CO / mg m^{-3}	2	4	2	4
NH_3 / µg m^{-3}	100	400	100	400
Benzene / µg m^{-3}	5		5	
Benzo(a)Pyrene / ng m^{-3}	1		1	
As / ng m^{-3}	6		60	
Ni / ng m^{-3}	20		20	

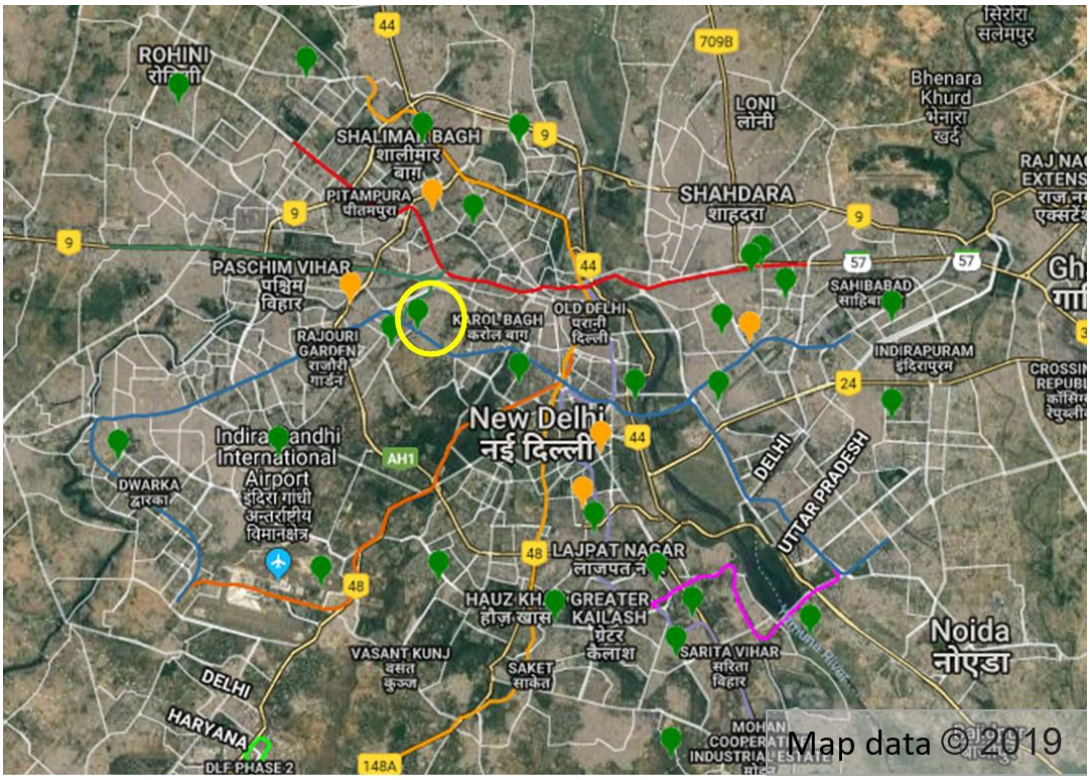

Figure 1.10. Map of CPCB measurement sites in New Delhi with Shadipur measurement site marked by a yellow circle. Sites indicated by green and orange markers, where green represents live data and orange a delay in data at the time the map was copied. Map data © 2019 Google.

Table 1.6. Central Pollution Control Board measurements sites in Delhi and the NMVOCs they monitor. Present is reference to March 2018.

Site	Benzene	Toluene	Ethylbenzene	*o*-Xylene	*m*-+*p*-Xylene	*p*-Xylene	Methane	NMHC	Data availability
CRRI Mathura road	✓	✓	✓						Jan-Apr 2015, Sep 2017-present
Mandir Marg	✓								May-Oct 2011, Jan 2012-Jan 2013, Apr 2015-present
Income Tax Office									
Siri Fort									
Aya Nagar	✓	✓	✓						Sep 2017 – Feb 2018
R. K. Puram	✓	✓				✓			May-Oct 2011, Jan-May + Nov-Dec 2012, Apr 2015-present
IGI Airport Terminal-3									
NSIT Dwarka	✓	✓	✓	✓	✓				Jan 2009-Dec 2012, Jan 2014-May 2015, Oct 2017-present
Pusa	✓		✓						Sept 2017-present
Shadipur	✓	✓	✓	✓	✓				Jan 2009-present
Punjabi Bagh	✓	✓				✓			May-Oct 2011, Jan-Feb + Nov-Dec 2012, Apr 2015-present
Lodhi Road	✓	✓	✓						Jan-Apr 2014, Sept 2017-present
Anand Vihar	✓	✓				✓			Aug 2012-Feb 2013, Apr 2015-present
East Arjun Nagar Delhi-CPCB	✓								Jun 2016-present
IHBAS							✓	✓	Jan 2009-present
Technological University									
Civil lines									
North Campus	✓	✓	✓						September 2017-present
Burari Crossing									

Table 1.7. Mean yearly mixing ratios of BTEX at Shadipur in ppbv from 2010 – 2017.

Year	Ethylbenzene	*m*-, *p*-Xylene	Benzene	Toluene
2010	2.02	2.61	4.58	15.21
2011	3.24	3.81	4.44	17.85
2012	1.25	2.35	2.63	17.21
2013	2.12	3.51	2.88	7.98
2014	0.93	1.34	1.66	3.79
2015	0.55	0.92	1.15	3.39
2016	2.61	1.83	2.20	5.66
2017	1.45	2.25	1.72	5.60

Figure 1.11-Figure 1.12 show the mean weekly diurnal and daily diurnal profiles of mixing ratio for benzene and toluene, as well as monthly and daily mean values at Shadipur, plotted using the Openair R package (Carslaw and Ropkins, 2012). The 95% confidence intervals in mean values are indicated by the shaded areas on the plots. Benzene and toluene reach a maximum at midnight, which may be attributed to a decrease in the height of the boundary layer due to decreased solar irradiation. Throughout the year a small increase is observed around June-August and the largest peak is seen in winter from November-December. The winter peak is potentially because of stagnant conditions and lower boundary layer heights (Gani et al., 2019). During the week values were at a minimum on Sunday, with a maximum around Wednesday-Thursday and reducing towards the weekend. This could be caused by less heavy vehicles being on the road at weekends. Erroneous values appear to be contained within this dataset, for example the reduction in ethylbenzene mixing ratios in 2014/2015 appears inconsistent (see Table 1.7). Equally on the 24 January 2016, values were recorded which were around an order of magnitude larger than other values in 2016 and these points have been removed from Table 1.7 and Figure 1.11-Figure 1.12.

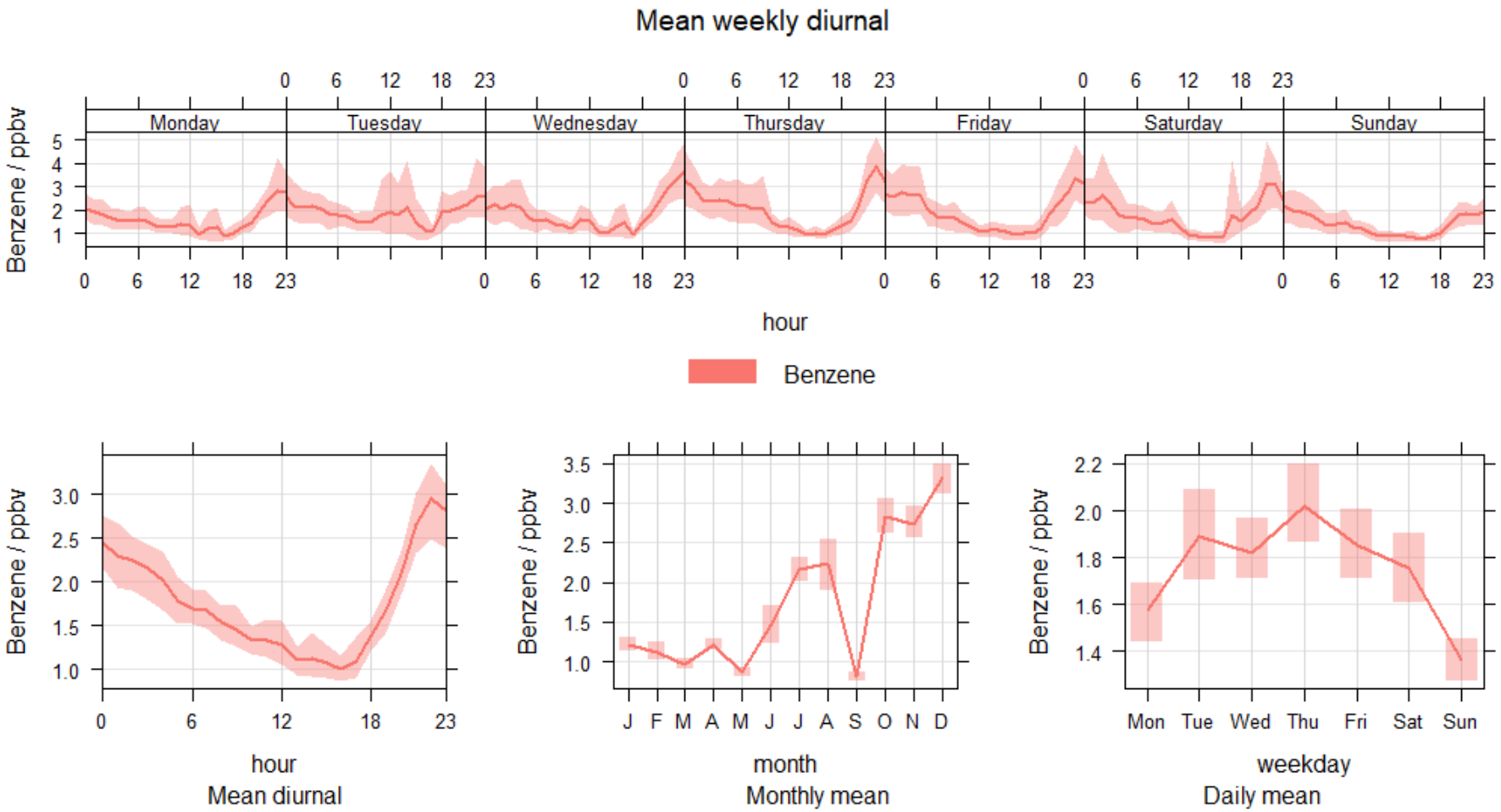

Figure 1.11. Time variation for benzene at Shadipur in 2016 with shaded regions representing 95% confidence interval in mean values. Top: mean benzene diurnal across 2016. Bottom left: mean daily benzene diurnal across 2016. Bottom middle: mean monthly benzene mixing ratio across 2016. Bottom right: mean daily benzene mixing ratio by day across 2016.

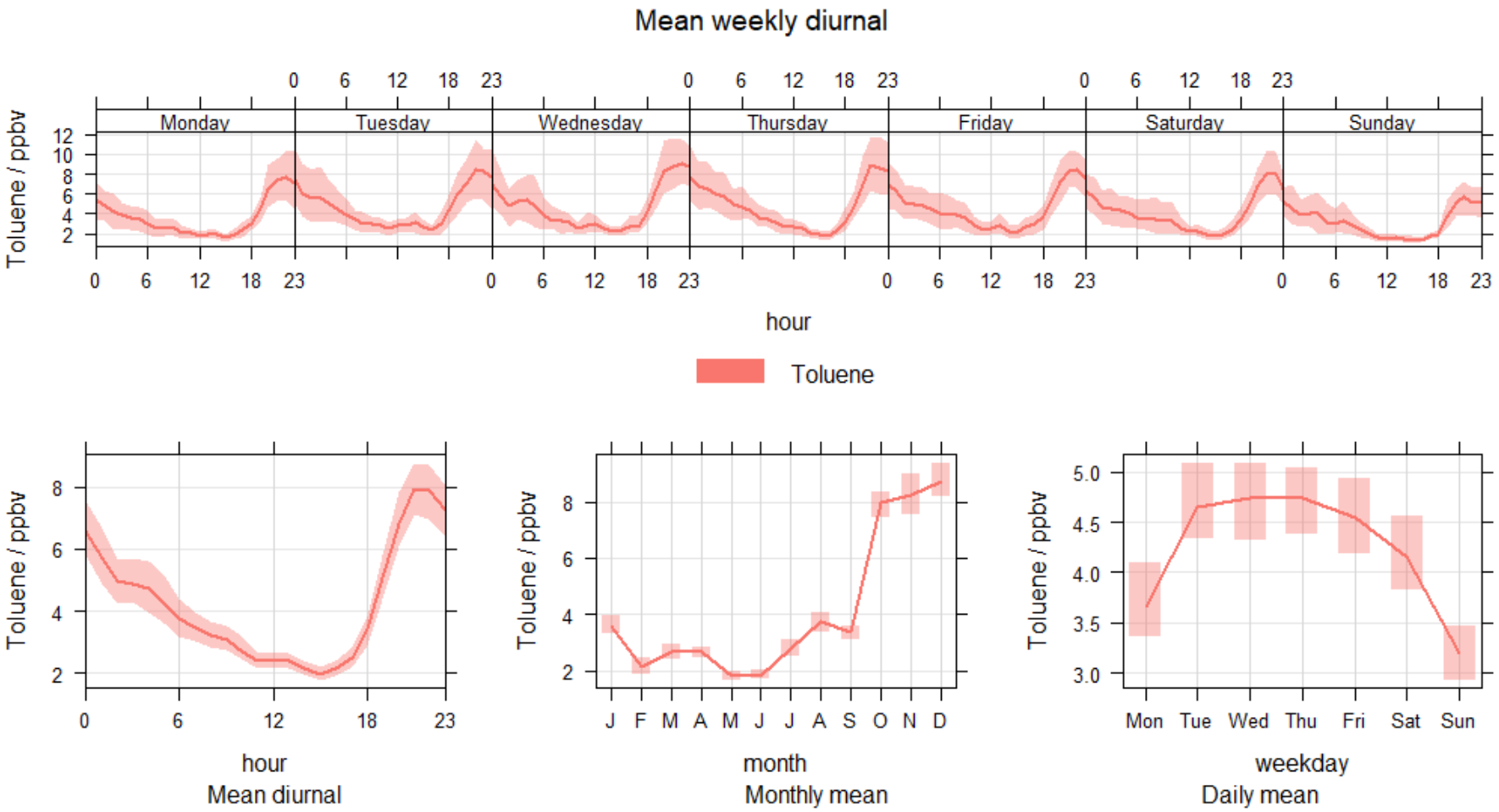

Figure 1.12. Time variation for toluene at Shadipur in 2016 with shaded regions representing 95% confidence interval in mean values. Top: mean toluene diurnal across 2016. Bottom left: mean daily toluene diurnal across 2016. Bottom middle: mean monthly toluene mixing ratio across 2016. Bottom right: mean daily toluene mixing ratio by day across 2016.

A comparison of benzene and toluene at Shadipur during May and September/October 2016 provides context for the pre- and post-monsoon measurement campaigns in Chapter 2. Table 1.8 shows that mean September/October mixing ratios were ~ 2-6 times greater than May values. This was likely caused by colder, stagnant conditions resulting in lower boundary layer heights (Gani et al., 2019) as well as increased generator usage and solid fuel combustion for heating (Nagpure et al., 2015).

Figure 1.13 shows diurnal cycles for benzene and toluene from May (Figure 1.13A-B) and September-October 2016 (Figure 1.13C-D). Benzene and toluene peaked at night which was likely caused by lower boundary layer heights (Gani et al., 2019) and particularly polluting vehicles, such as heavy goods vehicles, only being allowed access to New Delhi at night (Dahiya, 2016). In September/October, night-time emissions may also be driven by the need to heat both affluent and deprived houses (Nagpure et al., 2015), whilst in summer the use of private air conditioning at night by those who can afford it may increase levels of pollution from increased generator usage. The lowest mixing ratios were always present from 12:00-18:00, which was likely caused by heating and expansion of the boundary layer and increased reactive chemistry as the sun is most intense at midday.

Figure 1.13A-B shows peaks from about 06:00 – 10:00 in May which may coincide with a morning rush hour. This trend was not really present in the September data in Figure 1.13C-D. Lower summer mixing ratios in the pre monsoon may make this appear more pronounced, and increased temperatures may increase the influence of evaporative emissions. Pre- and post-monsoon night-time trends were similar, with a clear peak around midnight and a second smaller peak from 02:00-04:00 in the post monsoon.

Whilst some data exists from previous studies of NMVOCs in Delhi, it is of limited use in accurately characterising the sources of NMVOCs. Without a proper understanding of NMVOC sources and their strengths, accurate and meaningful mitigation based on a firm understanding of the key sources controlling poor air quality is not possible.

Table 1.8. Mean mixing ratios of BTEX (ppbv) at Shadipur from 12:00 2nd May 2016 - 23:00 31st May and 00:00 1st September 2016- 23:00 31st October 2016.

	Benzene	**Toluene**	**Ethylbenzene**	***m*-, *p*-Xylene**
May 2016	0.76	1.56	0.25	0.50
Sept-Oct 2016	1.85	5.72	1.29	2.98

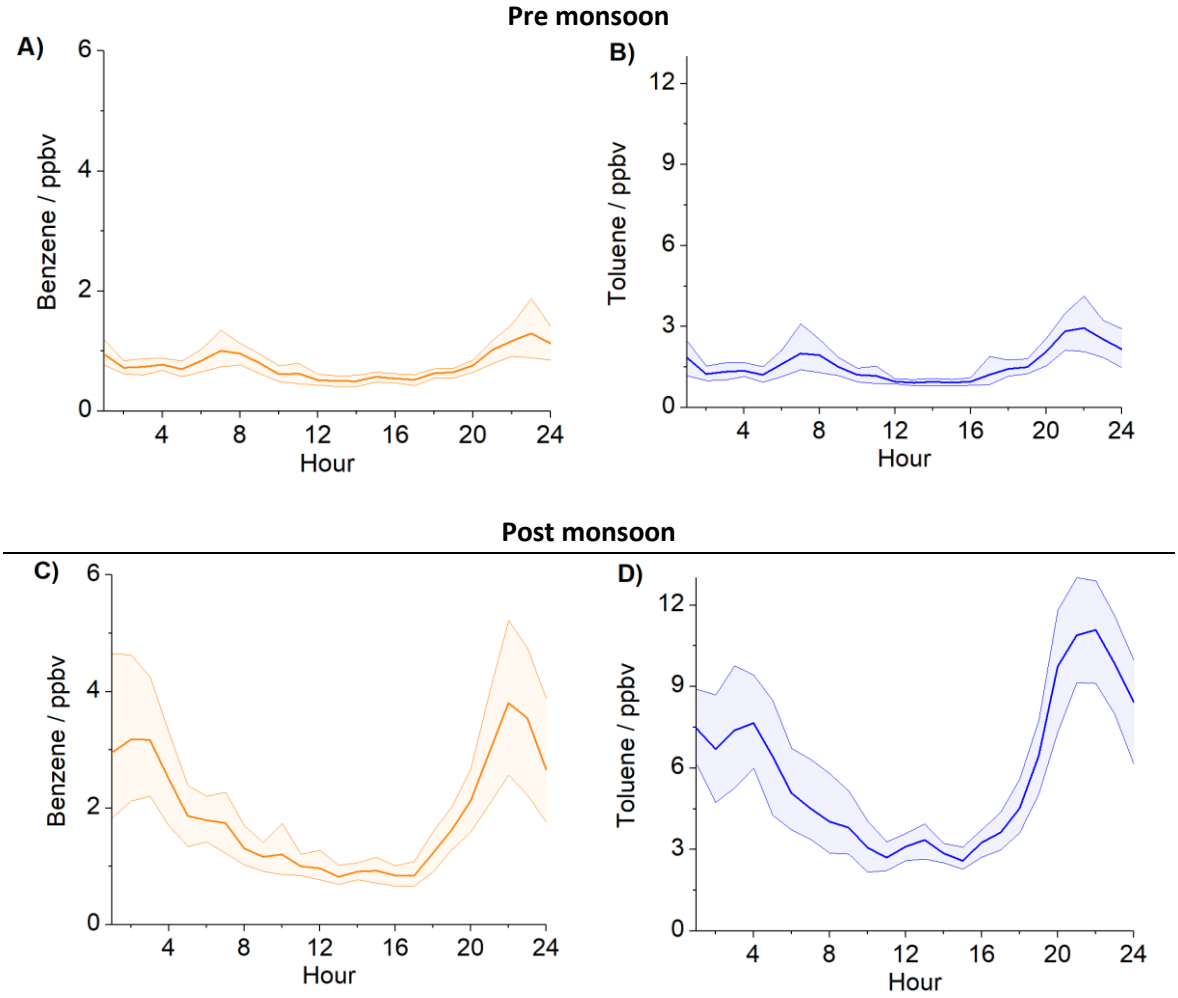

Figure 1.13. Diurnal cycles at Shadipur for A = benzene and B = toluene from 12:00 2nd May 2016 - 23:00 31st May 2016 and C = benzene and D = toluene from 00:00 1st September 2016- 23:00 31st October 2016 with shaded areas representing 95% confidence intervals in the mean.

1.4.6. India specific NMVOC inventories

Emission estimates of NMVOCs from India have been the focus of many studies. Streets et al. (2000), Ohara et al. (2007), Zhang et al. (2009), Li et al. (2014) and Kurokawa et al. (2013) produced Asian specific emission inventories which estimated NMVOC emissions from India to be 8630 kt y^{-1}, 9680 kt y^{-1}, 10,767 kt y^{-1}, 10,800 kt y^{-1} and 15,950 kt y^{-1} for the years 2000, 2003, 2006, 2006 and 2008, respectively. Varshney et al. (1998) estimated NMVOC emissions specifically from India for 1998 at 8100 kt y^{-1}. These studies, except for Varshney et al. (1998), covered other key pollutants, but the production of state, or city, specific estimates of speciated NMVOC emissions were not included. Sharma et al. (2015) produced one of the most insightful India specific inventories using a 36 km × 36 km grid for 2010.

They estimated total NMVOC emissions from India at 9810 kt y^{-1} and included a vast range of speciated sources (Sharma et al., 2015). Major alkane sources were attributed to oil/gas extraction, refining and distribution alongside residential fuel combustion. Alkenes and alkynes were released with residential fuel combustion and aromatics via. solvent use, traffic, and residential fuel combustion. Despite this, large uncertainties still exist over the contributions of unconventional and unmanaged sources to air quality in India and their relative contributions to urban and rural environments (Garaga et al., 2018). This poor understanding of the drivers of poor air quality results in high levels of pollution and significant impacts to human health.

1.5. Thesis outline

This thesis presents work carried out during the DelhiFlux project which intended to provide better characterisation of NMVOC sources in India.

Chapter 2 presents NMVOC measurements using two-dimensional gas chromatography during pre- and post-monsoon seasons in 2018 at an urban site in Delhi. It characterises the sources of NMVOCs from C_2-C_{14} using measurements from two GC instruments, as well as quantifying and qualifying a wide array of monoterpenes present. This study then evaluates the meteorological drivers of high night-time concentrations of NMVOCs in the post monsoon and uses multiple source apportionment techniques to understand different NMVOC emission sources to allow their impact on O_3 production to be assessed in future studies. The results of this study compare well to recent literature and show that traffic related emissions were the largest NMVOC source in urban Delhi. This can provide information to allow policy makers to make informed judgments on the key NMVOC pollution sources to be controlled in the urban environment in Delhi to mitigate air pollution.

Chapter 3 presents a new method developed for collection and extraction of I/SVOCs from residential combustion onto solid-phase extraction disks and PTFE filters. The method resolves many thousands of peaks for complex samples, is evaluated for suitability for quantitative I/SVOC measurements and aerosol-phase molecular markers are evaluated from burning sources in India. I/SVOC emissions are shown in the gas phase to have a large contribution from phenolic and furanic species and levoglucosan is an important

contributor to the aerosol phase. The results of this study are used to produce emission factors of 21 polycyclic aromatic hydrocarbons emitted from the burning of wood, cow dung cakes, municipal solid waste, charcoal and LPG.

Chapter 4 presents results of NMVOC measurements made using two-dimensional gas chromatography of a range of solid fuel combustion experiments from samples collected across Delhi. This chapter compiles measurements made with another GC instrument and a PTR-ToF-MS instrument to produce emissions factors for 192 NMVOCs released from burning, with on average 94% speciation of the total mass of measured NMVOC released. Variability in emission factors by different samples are examined and diagnostic ratios are compared from burning and liquid fuel sources to potentially allow better identification of NMVOC sources in ambient samples.

Chapter 5 combines the results of chapters 3 and 4 and maps emissions onto a volatility basis dataset to better understand SOA formation from biomass burning emissions by providing comprehensive, model-ready profiles for solid fuels collected from India. This shows little semi-volatile organic compound emissions from wood and charcoal samples. This study then shows that emissions from fuel wood, cow dung cakes and municipal solid waste burning contribute significantly more to the SOA production potential and the OH reactivity of emissions than LPG. The chemical drivers are then explored, with phenolic and furanic species shown to be likely important contributors to SOA formation and furanic species to OH reactivity. This is intended to provide guidance to policy makers on the need to mitigate burning sources to limit the impact on human health.

Chapter 6 combines the results of chapters 3 and 4 and is used to produce a 1 km^2 bottom-up emission inventory estimate of NMVOCs released in India from 1993-2016 due to the burning of fuel wood, cow dung cakes, municipal solid waste, charcoal and LPG. Fuel consumption data is collected from a range of different sources to provide a well evaluated estimate of emissions. Emissions from crop residue burning on fields are estimated for 2011, using recently measured emission factors collected from literature to allow evaluation of the relative contributions of different burning sources to emissions. Emissions of 13 (5-38) Mt are estimated for 2011 principally from residential combustion (53%), the open burning of municipal solid waste (23%) and crop residue burning (23%) with a small (< 1%) contribution from LPG.

PAH emissions are estimated for combustion of fuel wood, cow dung cakes, municipal solid waste, charcoal and LPG in 2011 of 121 (52-326) kt with contributions from fuel wood (48%), cow dung cakes (22%) and municipal solid waste (30%). NMVOC emissions from the burning of cow dung cakes are shown to be much higher per user than fuel wood and LPG, representing only 6 – 14% of total users but 27 – 53% of total residential combustion emissions. The effect of 400 million new LPG users from 1993-2016 is evaluated to give a net emissions benefit of 2924 (708-14,688) kt in 2016 but this failed to lead to meaningful emissions reduction as it failed to outpace population growth.

This study evaluates the relative importance of emissions from different burning sources to provide information to policy makers on the quantity of NMVOCs released from the combustion sources studied as part of this project. This can allow well targeted mitigation of specific source sectors to significantly reduce emissions.

Chapter 7 summaries the main findings and limitations of this study and provides discussion of future work.

Chapter 2

Sources of non-methane hydrocarbons in surface air in Delhi

The majority of this chapter has been published as a manuscript under the same name:

Gareth J. Stewart, Beth S. Nelson, Will S. Drysdale, W. Joe F. Acton,' Adam R. Vaughan, James R. Hopkins, Rachel E. Dunmore, C. Nicholas Hewitt, Eiko Nemitz, Neil Mullinger, Ben Langford, Shivani, Ernesto Reyes-Villegas, Ranu Gadi, Andrew R. Rickard, James D. Lee and Jacqueline F. Hamilton. *Faraday Discuss*., 2021. https://doi.org/10.1039/D0FD00087F

The data collected as part of this chapter have also been used as part of a separate study:

Lewis, A., Hopkins, J., Carslaw, D., Hamilton, J., Nelson, B., Stewart, G., Dernie, J., Passant, N., and Murrells, T.: An increasing role for solvent emissions and implications for future measurements of Volatile Organic Compounds, Philosophical Transactions of the Royal Society of London. Series A, Mathematical and Physical Sciences, 378, 2020. https://doi.org/10.1098/rsta.2019.0328

2.1. Introduction

Poor urban air quality is a major global public health concern, particularly in the developing world, as rapid urban growth has increased concentrations to harmful levels. This issue remains at the forefront of many governmental policies, as by 2050 approximately 66% of the global population are expected to live in urban environments (United Nations, 2014). Globally, an estimated 4.2 million premature deaths were a result of poor ambient air quality in 2016 (World Health Organization, 2018a), mainly caused by exposure to particulate matter (PM) and ozone (O_3). Non-methane hydrocarbons (NMHCs) are key precursors to PM and O_3 and some, such as aromatic species, are carcinogenic themselves (Huff, 2007). Globally biogenic volatile organic compound emissions are the dominant source with an estimated flux of 377-760 TgC yr^{-1} (Ehhalt, 1999; Dentener et al., 2001; Sindelarova et al., 2014). However, anthropogenic emissions, which have been estimated to be 130-169 TgC yr^{-1} (Dentener et al., 2001; Lamarque et al., 2010; Huang et al., 2017), can be important drivers of poor air quality in densely populated urban environments.

NMHC emissions from India are high and poorly understood, with emissions estimated to be the second largest in Asia, after China (Kurokawa et al., 2013; Kurokawa and Ohara, 2020). Several emission inventories have been produced for India, which included a range of NMHC sources (Varshney and Padhy, 1998; Streets et al., 2003; Ohara et al., 2007; Zhang et al., 2009; Kurokawa et al., 2013; Sharma et al., 2015). However, inventories remain hard to evaluate without knowledge of unaccounted for and unregulated sources and their strength.

Delhi (28°40’0”N, 77°10’0”E) had a population of around 29 million in 2018 (United Nations, 2019) and has been ranked as the worst of 1600 cities in the world for air pollution, based on available data (WHO, 2014). As a result, 1/3 of adults and 2/3 of children in Delhi have experienced respiratory symptoms owing to poor air quality (Kumar et al., 2013). NMHC pollution has been previously highlighted as coming from uncontrolled and unregulated sources in and surrounding Delhi and amplified by an unfavourable geographic location (Kumar et al., 2015). NMHCs are a key driver of air pollution in Delhi: the composition of fine particulates (PM_1) in Delhi has been found to be dominated by oxygenated organic aerosol which derives from NMHC precursors (Gani et al., 2019; Reyes-Villegas et al., 2020;

Cash et al., 2020), whilst ozone production has been found to be in a regime where NO_x emissions reduction, without simultaneous reduction in NMHCs, would lead to an increase (Chen et al., 2020).

A range of inventories have been produced for NMHC emissions from 1990-2010 in Delhi which have estimated emissions between 100-261 kt yr^{-1} (Bose and Anandalingam, 1996; Gurjar et al., 2004; Guttikunda and Calori, 2013; Sharma et al., 2015). Other inventories have focussed on specific sources, such as traffic emissions and estimated NMHC emissions using fleet average emission factors to be around 180 kt y^{-1} in 1995, to approximately 80 kt y^{-1} in 2014 (Goel and Guttikunda, 2015). Current inventories for Delhi are limited by the lack of activity data and emission factors specific to Indian NMHC sources which include brick kilns, residential solid fuel combustion, agricultural waste burning, poor quality coal, cooking, burning of organic and plastic waste for heating and combustion of municipal solid waste (Kumar et al., 2015). Poorly serviced and regulated diesel generators using inferior quality fuel are also an important pollution source throughout the year in areas with a poor electricity infrastructure (Kumar et al., 2015). The highest resolution inventory (1 km^2) used China specific factors and calculated the importance of different sources to NMHCs as transport (51%), diesel generators (14%), power plants (13%), brick kilns (9%), domestic (7%), industrial (5%) and waste burning (1%) (Guttikunda and Calori, 2013).

Recent studies have focussed on improving understanding of NMHC emissions from Indian sources. These included a detailed study of north-Indian solid fuel sources which showed many hundreds to thousands of organic components can be released into the aerosol phase, measured emissions factors of non-methane volatile organic compounds released from burning, developed comprehensive source profiles of different fuel sources and showed cow dung cakes to be a highly polluting fuel source (see chapters 3-6).

Previous studies focussed on making NMHC measurements in Delhi have limitations, concentrating on total NMHCs (Padhy and Varshney, 2000) or small subsets of NMHCs such as benzene, toluene, ethylbenzene and xylenes (BTEX) (Kumar, 2006; Hoque et al., 2008; Singh et al., 2010; Khillare et al., 2008; Sehgal et al., 2011; Singh et al., 2012). Only a few studies have included a greater variety of NMHCs (Srivastava et al., 2005a; Srivastava et al., 2005c). These have been complimented by a 2008 study with 7 day “snap shot” intensive observations of a range of species of atmospheric interest during the summer, post-

monsoon and winter periods (NEERI, 2008). These measurements were used to create a gridded emission inventory (2 km^2 over an area of 32 km x 30 km) of hydrocarbon emissions for area sources (including emissions from cooking, crematoria, open burning, waste incinerators and diesel generator sets), industrial sources and vehicular sources. This formed part of a source apportionment study focussed on pollutant monitoring, creation of new emission inventories, and receptor and dispersion modelling in Delhi, Mumbai, Bangalore, Chennai, Kanpur and Pune (CPCB, 2010). The Central Pollution Control Board (CPCB) also measure BTEX at 12 of their 20 sites in Delhi, although there is generally very limited-data coverage. A detailed recent study made measurements at an urban and background site in Delhi using proton-transfer-reaction time-of-flight mass spectrometry (PTR-ToF-MS) and determined the relative NMHC contributions at the urban site of traffic (56.6%), solid fuel (27.5%) and secondary formation (15.9%). This result echoed the findings of several studies and available emission inventories which have concluded that transport emissions are the dominant NMHC source in Delhi (NEERI, 2008; Srivastava and Majumdar, 2009; Guttikunda and Calori, 2013; Sharma et al., 2015; Wang et al., 2020).

Attempts to improve air quality in Delhi, which started with the 1981 Air Act (Parliament of India, 1981), have heavily focussed on limiting transport related emissions. Examples include reducing the concentration of benzene in petrol to < 1%, phasing out vehicles > 15 years old, the introduction of improved vehicle regulations, time restrictions placed on when heavy goods vehicles can enter the city, the introduction of compressed natural gas (CNG, mainly methane) for light goods vehicles, mandatory for public transport vehicles, and the construction of a modern metro system (Khillare et al., 2008; Goel and Guttikunda, 2015); however, air pollution has remained stubbornly high. This is because improvements have not taken into account the significant unregulated population growth, which is expected to continue as Delhi is estimated to become the most populous city in the world in 2030 with an estimated population of 39 million (United Nations, 2019). Consequently, the risks due to elevated levels of air pollution remain of great concern. Accurate measurements of a wide range of ambient NMHC species are vital to understand the sources of NMHCs in Delhi, as rapid development and limited measurements have resulted in a lack of reliable data to determine the key drivers of the consistent poor air quality

observed. This is crucial to allow the development of well targeted legislation to improve air quality and limit the impact on human health at a reasonable economic cost.

During this study, measurements of a range of NMHCs were made at an urban site located in old Delhi during the pre- and post-monsoon seasons in 2018. Exceptionally high levels of NMHC pollution were measured at night during the post-monsoon period. The meteorological drivers of this elevated pollution are explored in detail and the contributions from different sources are evaluated using a range of complementary source apportionment techniques. The findings of this study are placed in context using recent receptor model and inventory studies.

2.2. Methods

Delhi has five main seasons: winter (December to January), spring (February to March), pre-monsoon (April to June), monsoon (July to mid-September) and post-monsoon (mid-September to November). Measurements were made during two field campaigns in the pre- and post-monsoon seasons using dual-channel gas chromatography with flame-ionisation detection (DC-GC-FID) and two-dimensional gas chromatography (GC×GC-FID) at the Indira Gandhi Delhi Technical University for Women (IGTDUW), near Kashmiri gate, within the historical area of Old Delhi. The site is located in the central district of Delhi (Figure 2.1A), an area of high population density (27,730 people km^{-2}, as per the 2011 census). Old Delhi railway station is approximately 0.5 km to the southwest (Figure 2.1B), National Highway 44 about 0.3 km to the east (Figure 2.1C) and Chandi Chowk market about 1.5 km south.

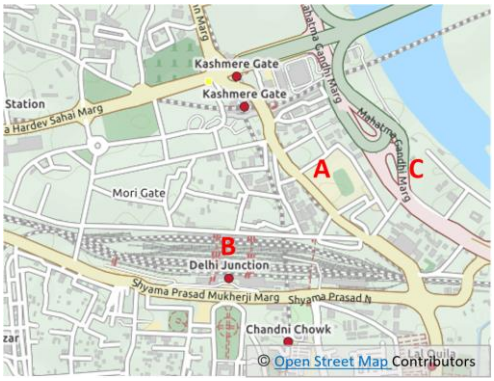

Figure 2.1. Location of field site in Delhi where A = IGTDUW, B = Old Delhi railway junction and C = National Highway 44. © OpenStreetMap contributors.

2.2.1. Gas chromatography

The dual-channel gas chromatography instrument with flame ionisation detection (DC-GC-FID) was operated by Beth Nelson at the University of York from 28-May to 05-Jun 2018 and 5- to 27-Oct 2018, with 31 C_2-C_7 NMHCs and C_2-C_5 oxygenated volatile organic compounds measured (Hopkins et al., 2003). A 500 ml sample (1.5 L pre-purge of 100 ml min^{-1} for 15 mins, sample at 25 ml min^{-1} for 20 mins) was collected (Markes International CIA Advantage), passed through a glass finger at -30 ^oC to remove water and adsorbed onto a dual-bed sorbent trap (Markes International ozone precursors trap) at - 20 ^oC (Markes International Unity 2). The sample was thermally desorbed (250 ^oC for 3 mins) in a flow of helium carrier gas then split 50:50 and injected into two separate columns for analysis of NMHCs (50 m × 0.53 mm Al_2O_3 PLOT) and oxygenated volatile organic compounds (10 m × 0.53 mm LOWOX with 50 µm restrictor to balance flow). The oven was held at 40 ^oC for 3 mins, then heated at 12 ^oC min^{-1} to 110 ^oC and finally heated at 7 ^oC min^{-1} to 200 ^oC with a hold of 20 mins.

The two-dimensional gas chromatography instrument with flame ionisation detection (GC×GC-FID) made measurements from 29-May to 05-Jun 2018 and 11-Oct to 04-Nov 2018. It was used to measure 64 C_7-C_{12} hydrocarbons (alkanes, monoterpenes and monoaromatics). The mean, minimum and maximum mixing ratios measured using both GCs from both campaigns are summarised in the Supplementary Information 8.1. The GC×GC-FID collected 2.1 L samples (70 ml min^{-1} for 30 mins) using an adsorption-thermal desorption system (Markes International Unity 2). NMHCs were trapped onto a sorbent (Markes International U-T15ATA-2S) at - 20 ^oC with water removed in a glass cold finger (-30 ^oC). The sample was thermally desorbed (250 ^oC for 5 mins) and injected splitless down a transfer line. It was refocussed for 60 s using liquid CO_2 at the head of a non-polar BPX5 held at 50 psi (SGE Analytical 15m × 0.15 µm × 0.25 mm) which was connected to a polar BPX50 at 23 psi (SGE Analytical 2 m × 0.25 µm × 0.25 mm) via. a modulator held at 180 ^oC (5 s modulation, Analytical Flow Products MDVG-HT). The oven was held for 2 mins at 35 ^oC, then ramped at 2.5 ^oC min^{-1} to 130 ^oC and held for 1 min with a final ramp of 10 ^oC min^{-1} to 180 ^oC and hold of 8 mins. GC systems were tested for breakthrough to ensure trapping of the most volatile components (see Figure 2.2 for example from GC×GC-FID). Calibration was carried out using a 4 ppbv gas standard containing a range of NMHCs purchased from

the British National Physical Laboratory (NPL, UK). The linearity of the detector response at higher mixing ratios was confirmed post-campaign by carrying out a calibration using multiple injections at a range of mixing ratios of benzene up to 3 times greater than the maximum observed ambient mixing ratio (see Figure 2.3). The inlet used by both instruments was located approximately 5 m above the ground with sample lines run down ½" PFA tubing to the laboratory.

NMHCs not in the gas standard were quantified using the relative response of liquid standard injections to toluene. This included quantification and qualification of a range of monoterpenes (see Figure 2.4 for examples) and quantification of C_{12}-C_{14} alkanes.

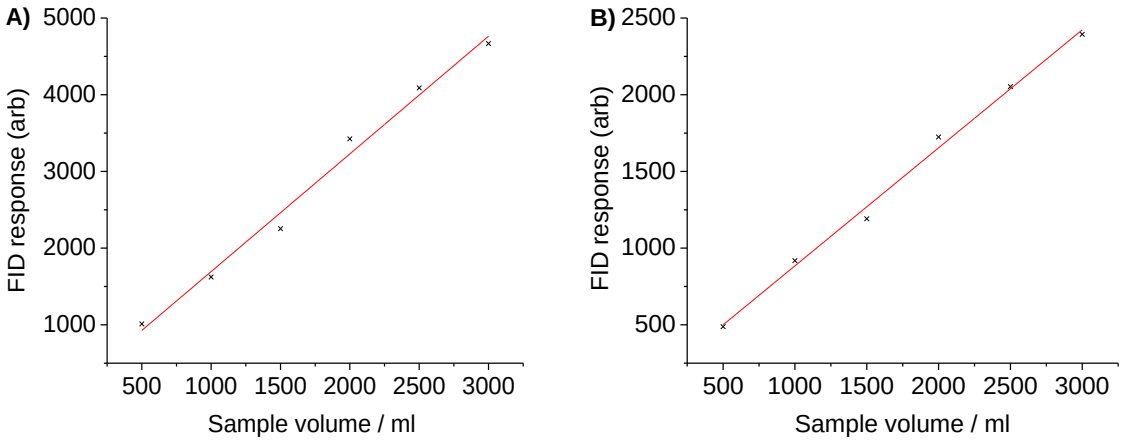

Figure 2.2. Breakthrough testing for GC×GC-FID for A = benzene and B = *n*-octane.

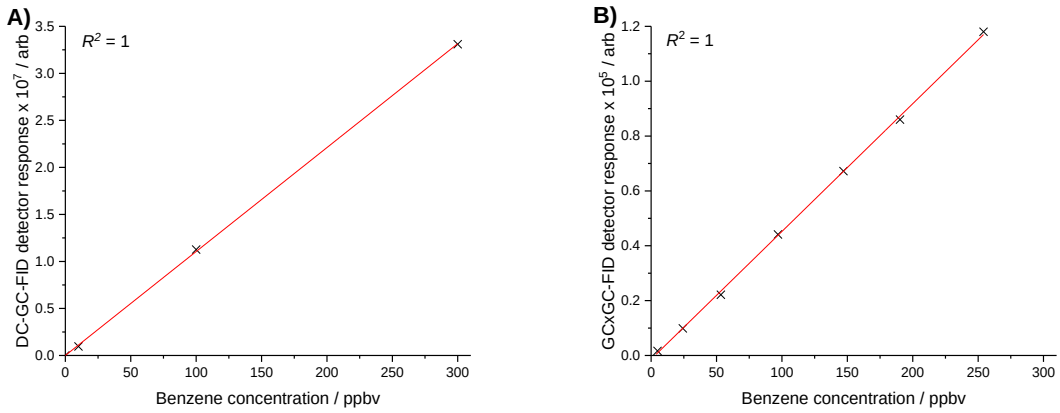

Figure 2.3. High concentration calibrations of DC-GC-FID and GC×GC-FID instruments to benzene.

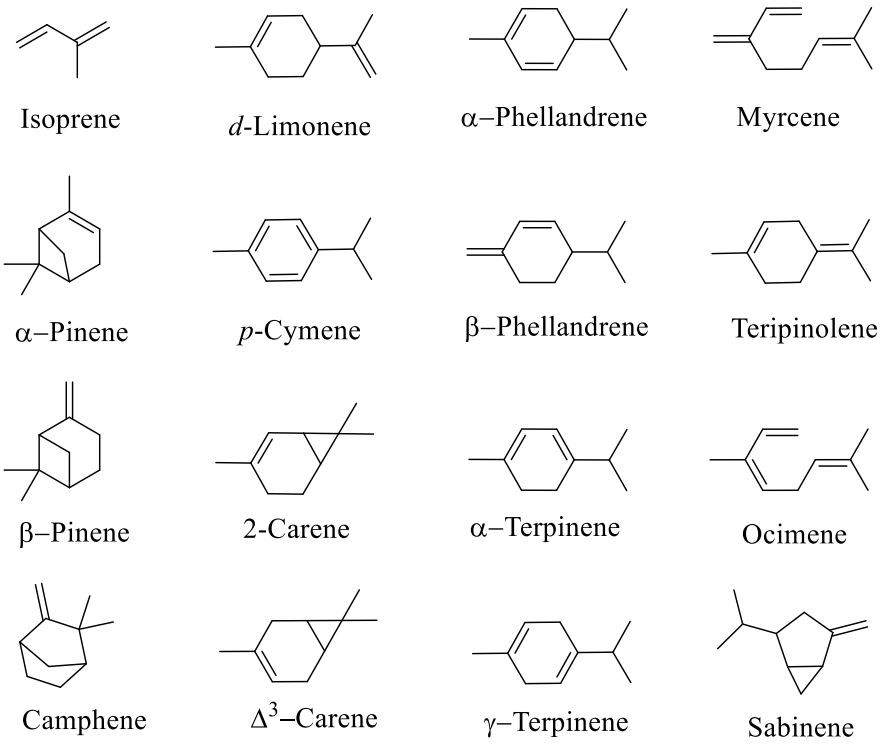

Figure 2.4. Common biogenic NMVOCs (Seinfeld and Pandis, 2012).

Monoterpenes present in the ambient air of Delhi were qualified through stepwise addition (see Figure 2.5). Kováts retention indices (*I*) were calculated for offline liquid injections, an ambient sample from 27/10/2018 at 08:13 and compared to literature to assist with peak qualification (see Table 2.1). The Kováts retention index allows unidentified eluents to be identified by comparing their position in the chromatogram relative to *n*-alkanes,

$$I = 100 \times \left[n_l + (N_h - n_l) \frac{t_{r(\text{unknown})} - t_{r(n_l)}}{t_{r(N_h)} - t_{r(n_l)}} \right] \quad \text{(E2.1)}$$

where I = Kováts retention index, N_h = carbon number of *n*-alkane of higher boiling point than unidentified eluent, n_l = carbon number of *n*-alkane of lower boiling point than unidentified eluent, $t_{r(\text{unknown})}$ = retention time of unidentified eluent, $t_{r(\text{nl})}$ = retention time of *n*-alkane of lower boiling point than unidentified eluent and $t_{r(\text{Nh})}$ = retention time of *n*-alkane of higher boiling point than unidentified eluent.

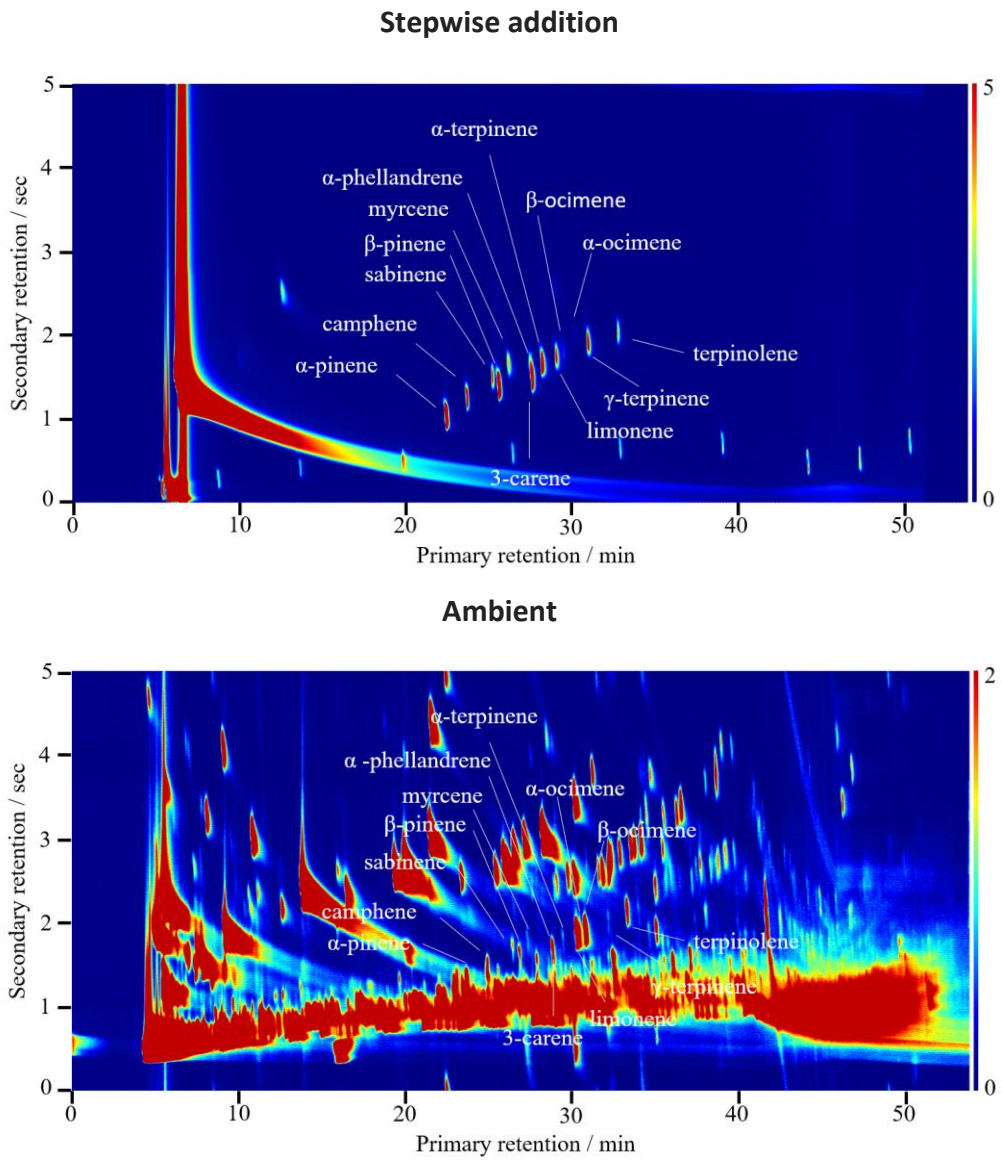

Figure 2.5. Stepwise qualification of monoterpenes.

Table 2.1. Qualification of monoterpenes through Kováts retention indices.

NMVOC	$Kovát_{liquid}$	$Kovát_{ambient}$	$Kovát_{literature}$	Ref
α -Pinene	940.7	940.5	941	(Charles et al., 2001)
Camphene	959.3	959.5	958	(Charles et al., 2001)
Sabinene	981.5	982.3	983	(Charles et al., 2001)
β-Pinene	985.3	988.6	990	(Charles et al., 2001)
Myrcene	996.3	996.2	995	(Charles et al., 2001)
α -Phellandrene	1017.9	1018.0	1017	(Charles et al., 2001)
3-Carene	1017.9	1018.0	1022	(Guy et al., 2004)
α -Terpinene	1027.0	1028.2	-	-
Limonene	1039.8	1041.1	1040	(Charles et al., 2001)
β-Ocimene	1047.5	1048.8	1051	(D. Flatt et al., 2015)
α-Ocimene	1055.2	-	-	-
γ-Terpinene	1069.2	1070.5	1069	(Guy et al., 2004)
Terpinolonene	1097.4	1097.3	1096	(Vilaseca et al., 2004)

Quantification has been carried out by measuring the response of a known quantity of these components to a known quantity of toluene in solution which was then used to develop a detector response factor. Standards were prepared by dissolving 0.1 g into 10 ml of ethyl acetate (EtOAC) to give a stock solution concentration of 10000 µg m^{l-1}. This was diluted to give a concentration of 500 µg ml^{-1} by dissolving 0.5 ml of stock solution into 9.5 ml EtOAc. This solution was diluted to 100 µg ml^{-1} prior to analysis by dissolving 0.2 ml into 0.8 ml of EtOAc.

A 1 µL sample was injected split (100:1) into a liner held a 170 ^{o}C connected to a non-polar BP5 held at 50 psi (15 m x 0.25 µm x 0.25 mm) which was connected to a polar BPX50 (30 psi; 2 m x 0.25 µm x 0.25 mm) via. a modulator held at 180 ^{o}C (5 s modulation, Analytical Flow Products ELDV2-MT). The oven was held at 35 ^{o}C for 2 mins then ramped at 2.5 ^{o}C min^{-1} to 130 ^{o}C and held 1 min then ramped 10 ^{o}C min^{-1} to 180 ^{o}C with a final hold of 8 mins. The syringe was cleaned prior to injection with EtOAC by 3 × pre-/post- injection washes in two different solvent wash bottles.

2.2.2. Supporting measurements

Nitrogen oxides (NO_x = NO + NO_2) were measured using a dual-channel chemiluminescence instrument (Air Quality Designs Inc., Colorado). Carbon monoxide (CO) was measured using a resonance fluorescent instrument (Model AL5002, Aerolaser GmbH, Germany). Ozone measurements were made using a 49i (Thermo Scientific) with a limit of detection of 1 ppbv. The CO and NO_x instruments were calibrated regularly (every 2 – 3 days) throughout both campaigns using standards from the NPL, UK. The setup and calibration procedures were identical to those described by Squires et al. (2020). These measurements were made by Will Drysdale from the University of York.

PTR-QiToF-MS (Ionicon Analytik, Innsbruck) measurements were made by Joe Acton from the University of Lancaster from 26/05/2018 to 09/06/2018 in the pre-monsoon campaign and from 04/10/2018 to 23/11/2018 in the post-monsoon campaign. For the pre-monsoon and post-monsoon campaign up until 05/11/2018, the sample inlet was positioned 5 m above the ground adjacent to the inlet used for GC measurements. The PTR-QiToF-MS subsampled from a ½" PFA common inlet line running from this inlet to an air-conditioned

laboratory where the instrument was installed with a flow of around 20 L min^{-1}. From 05/11/2018 to 23/11/2018, the inlet was moved to a flux tower approximately 30 m above ground level. The PTR-QiToF-MS was operated with a drift pressure of 3.5 mbar and a drift temperature of 60 °C giving an *E*/*N* (the ratio between electric field strength and buffer gas density in the drift tube) of 120 Td.

The PTR-QiToF-MS was calibrated daily using a 19 component 1 ppmv gas standard (Apel Riemer, Miami) dynamically diluted into zero air to provide a 3-point calibration. Volatile organic compounds were then quantified using a transmission curve (Taipale et al., 2008). Mass spectral analysis was performed using PTRwid (Holzinger, 2015).

Windspeed and direction were taken from measurements at Indira Gandhi International Airport in 2018, approximately 16 km southwest of the site. Modelled Planetary Boundary Layer Height (PBLH) data was downloaded (Lat. 28.625, Lon. 77.25) from the fifth-generation reanalysis (ERA5) from the European Centre for Medium-Range Weather Forecasts at 0.25 degree resolution with a 1-hour temporal resolution (European Centre for Medium-Range Weather Forecasts, 2019).

2.2.3. Receptor models

The mixing ratio of NMHC *i* in the k^{th} sample, C_{ik}, can be described by equation (E2.2 (Miller et al., 2002):

$$C_{ik} = \sum_{j=1}^{p} F_{ij} S_{jk} + \varepsilon_{ik} \qquad i = 1, \dots, m, \; k = 1, \dots, n \tag{E2.2}$$

where F_{ij} = chemical composition of source, S_{jk} = source contribution, p = total number of sources, m = total number of NMHCs, n = number of measurements and ε_{ik} = residual error, which is minimised.

Principal component analysis (PCA) is a type of factor analysis which has been used to decompose many different NMHCs measured into a set of factors which are used to represent their sources (Bruno et al., 2001; Miller et al., 2002; Guo et al., 2004; Seinfeld and Spyros, 2006; Wang et al., 2010). It is appropriate to use with datasets with only a few underlying factors. Principal component analysis has been performed in R on the data

collected in this study, retaining the 4 factors with eigen values >1 (Seinfeld and Spyros, 2006). This process is well described elsewhere (Miller et al., 2002).

The contribution of each source was determined by absolute principal component scores (APCS) (Thurston and Spengler, 1985; Guo et al., 2004; Wang et al., 2010). The first step involves normalisation of NMHC, Z_{ik}:

$$Z_{ik} = \frac{(C_{ik} - C_i)}{\sigma_i} \quad \text{(E2.3)}$$

where σ_i = standard deviation of NMHC *i* of all samples included in the analysis and C_i = mean mixing ratio of species *i*. The factor scores from the PCA are normalised with mean = 0 and σ = 1. An artificial value with mixing ratio of species *i* = 0 is created in equation E2.4 to compensate for this.

$$(Z_0)_i = \frac{(0 - C_i)}{\sigma_i} = \frac{- C_0}{\sigma_i} \quad \text{(E2.4)}$$

The source contributions are determined by equation E2.5:

$$C_i = (b_0)_i + \sum_{k=1}^{p} \text{APCS}_k^* b_{ki} \qquad p = 1, 2, \ldots, n \quad \text{(E2.5)}$$

where $(b_0)_i$ = constant for pollutant *i*, APCS_k* is determined by subtracting the factor scores from the true sample in E2.3 from those obtained in E2.4 (Guo et al., 2004), b_{ki} = coefficient of regression for source *k* for NMHC *i* (Bruno et al., 2001) and *p* = number of sources. The product $\text{APCS}_k^* b_{ki}$ shows the contribution to the airborne mixing ratio of NMHC *i* from source *p*. E2.5 is solved through multiple linear regression analysis. Due to the potentially colinear nature of many diurnal profiles in Delhi, factors with small non-meaningful contributions to chemical species (< 20%) have been deemed to be insignificant and filtered out from the analysis. Furfural, measured by PTR-QiToF-MS, has been included as a tracer for burning emissions to help with the identification of factors (Stockwell et al., 2015; Coggon et al., 2016). The result from PCA/APCS has been compared to those calculated using the EPA Unmix 6.0 source apportionment toolkit (Henry, 2007), which has been previously applied to many air quality datasets (Hopke, 2016). The use of multiple source apportionment methods should result in a more robust conclusion.

2.3. Results and discussion

2.3.1. Meteorological overview

Figure 2.6 shows seasonal wind rose plots for windspeed and direction measured at Indira Gandhi International Airport in 2018, downloaded from the Integrated Surface Database provided by the National Oceanic and Atmospheric Administration (NOAA) (Carslaw and Ropkins, 2012; NOAA, 2019). Air masses predominantly approached Delhi from the west/north west in winter and spring. During the pre-/post-monsoon and monsoon seasons, air masses generally approached from either the west/north west or east/south east. Conditions were most stagnant in the winter and post-monsoon seasons with the lowest windspeeds (averages of 1.8 and 1.9 m s^{-1}, respectively) and the largest percent of calm periods, where the wind speed was below < 0.5 m s^{-1} (25.7-28.0%). Windspeeds were higher in spring, pre-monsoon and monsoon seasons (with averages in the range 2.6 to 3.3 m s^{-1}, respectively), with the lowest number of calm periods in the pre-monsoon and monsoon seasons (6.4 and 7.5%, respectively).

Figure 2.7 shows 10 m 96 h NOAA HYSPLIT (Hybrid Single Particle Lagrangian Integrated Trajectory) back trajectories clustered (Angle) from pre- and post-monsoon campaigns with mean toluene mixing ratio coloured by cluster (Carslaw and Ropkins, 2012). Back trajectories in the pre-monsoon campaign were generally long (C2-C4 at around 1000 km over 96 h), suggesting higher windspeeds with monsoon-type wind patterns, and resulted in low toluene mixing ratios. C1 was important from 27-29/05/18 and followed a much shorter trajectory and resulted in higher toluene mixing ratios, highlighting the impact of shorter, slower moving trajectories in allowing the build-up of local pollution. Trajectories in the post-monsoon campaign were generally shorter, and toluene mixing ratios higher.

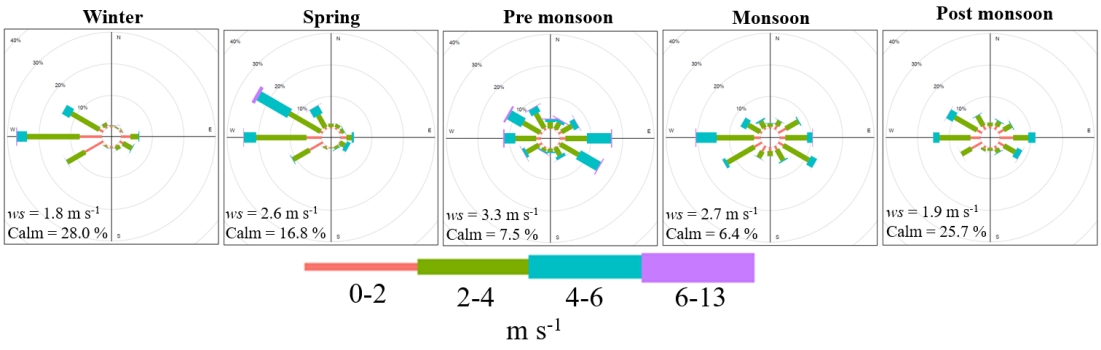

Figure 2.6. Seasonal wind rose plots at Indira Gandhi International Airport in 2018.

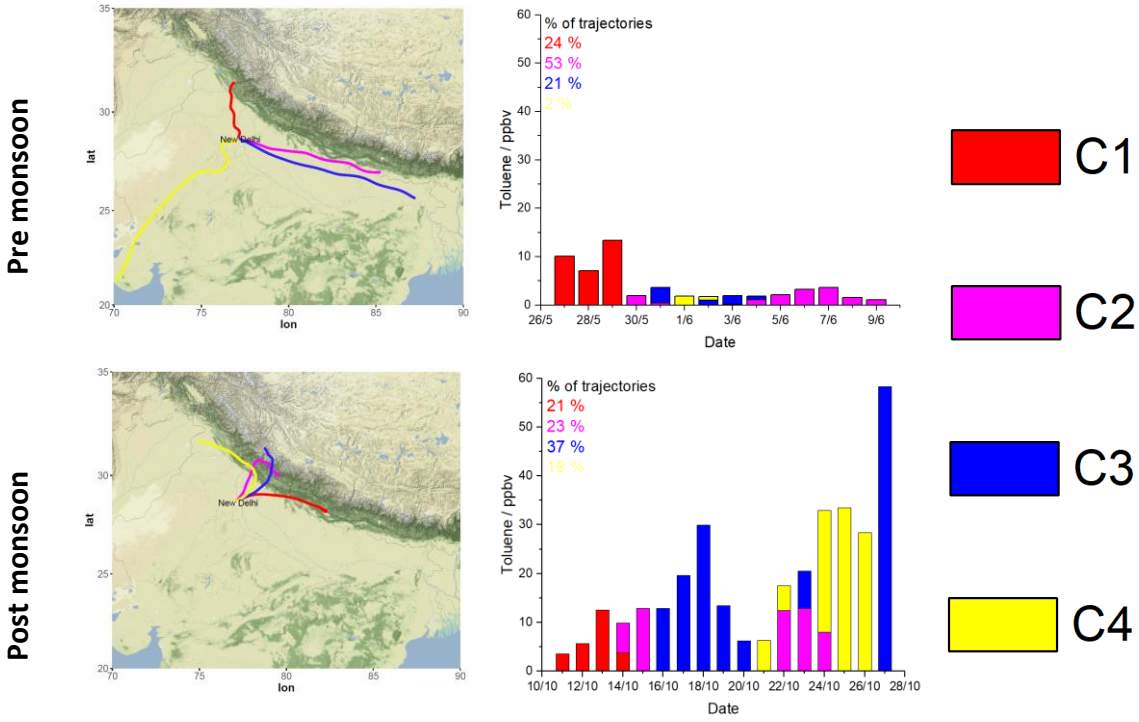

Figure 2.7. Clustered NOAA Hysplit back trajectories from pre- and post-monsoon campaigns (left) and mean toluene mixing ratios by cluster (right).

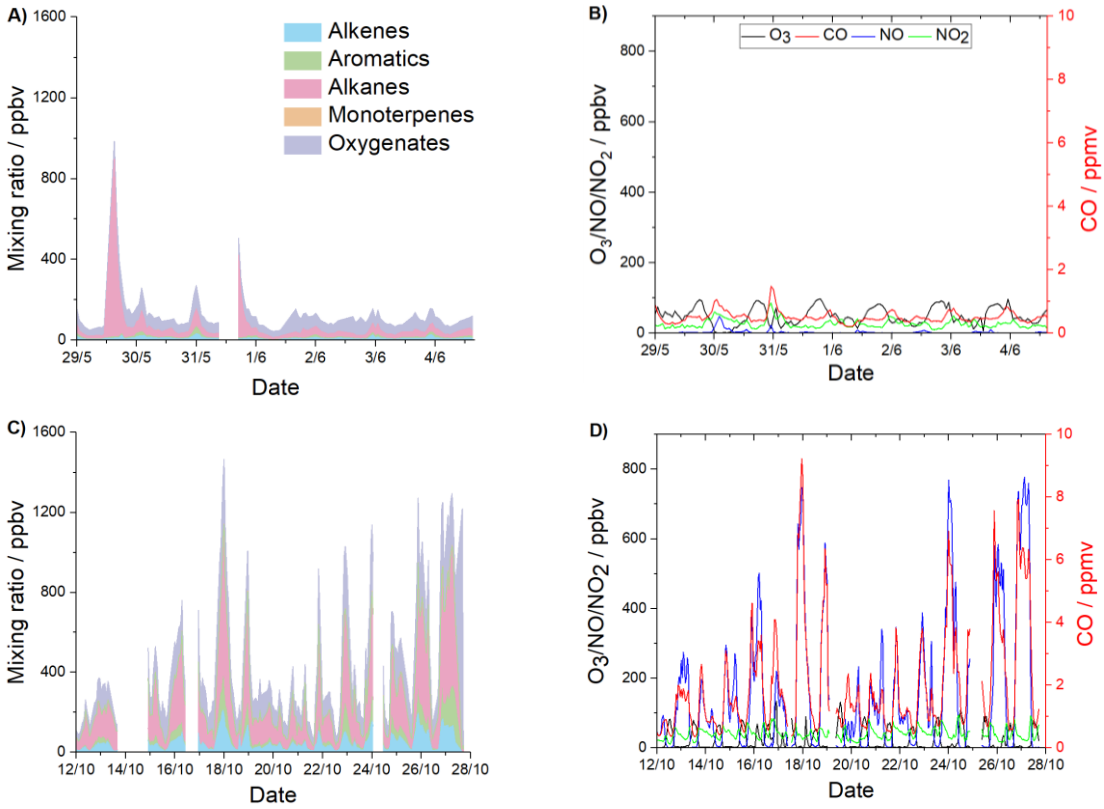

Figure 2.8. Concentration-time series of A = pre-monsoon NMHCs (stacked), B = pre-monsoon O_3, NO, NO_2 and CO, C =post-monsoon NMHCs (stacked) and D = post-monsoon O_3, NO, NO_2 and CO. Zoomed in versions for the pre-monsoon campaign are available in the Supplementary Information 8.2.

2.3.2. NMHC mixing ratios and diurnal cycles

Hourly measurements of 90 individual NMHCs were obtained from both GC instruments over the two campaigns. Relatively high mixing ratios of NHMCs were observed during both campaigns, but with significant enhancements observed from 17/10/2018 until the end of the post-monsoon measurement period on the 27/10/2018. Figure 2.8A and Figure 2.8C show stacked area plots of NMHC mixing ratios during pre- and post-monsoon campaigns. NMHC concentrations in the pre-monsoon were generally much lower, except for two large alkane spikes caused by very large concentrations of propane and butane (Figure 2.8A). In the post-monsoon, NMHC concentrations at night were significantly larger than in the pre-monsoon. Figure 2.8B and Figure 2.8D show concentration-time series of O_3, CO and NO_x from pre- and post-monsoon campaigns. Significant night-time enhancement of CO and NO_x was observed in the post-monsoon. O_3 peaked in the pre-monsoon at around 80-90 ppbv and around 60-90 ppbv in the post-monsoon.

Figure 2.9 shows the mean diurnal profiles using data combined from both campaigns for propane (A), *n*-hexane (B), isoprene (C), toluene (D), *n*-tridecane (E) and ethanol (F). These have been chosen as they are typical NMHC tracers from different sources. Diurnal profiles of individual data from the pre- and post-monsoon campaigns are given in the Supplementary Information 8.3. The diurnal profiles observed for propane, *n*-hexane, toluene and *n*-tridecane were similar, peaking at night between 8 pm and 6 am with a minimum in the afternoon. For propane, large spikes were present around midday, with the spikes present but less pronounced in the post-monsoon campaign. These large increases in mixing ratios have been attributed to emissions from LPG, a mixture of propane and butane, from lunchtime cooking activities. The average diurnal profile for *n*-hexane during the pre-monsoon (see the Supplementary Information 8.3) showed a small peak around lunchtime likely from midday traffic. A small peak was present for toluene from 8-10 am, potentially from the morning rush hour before the boundary layer begins to expand. Isoprene showed a typically distinct biogenic diurnal profile and peaked around midday. However, mixing ratios remained high at night (around 0.5 ppbv), possibly indicating an additional anthropogenic source (Borbon et al., 2001; Wagner and Kuttler, 2014; Sahu and Saxena, 2015; Sahu et al., 2016). A pronounced diurnal profile was present for *n*-tridecane which was highest at night, potentially amplified by night-time residential generator usage

and restrictions which allow the entry of heavy good vehicles to the city only at night. A peak was present for ethanol around midday, which was most pronounced in the pre-monsoon campaign and may be from increased volatilisation due to increased temperature and radiation.

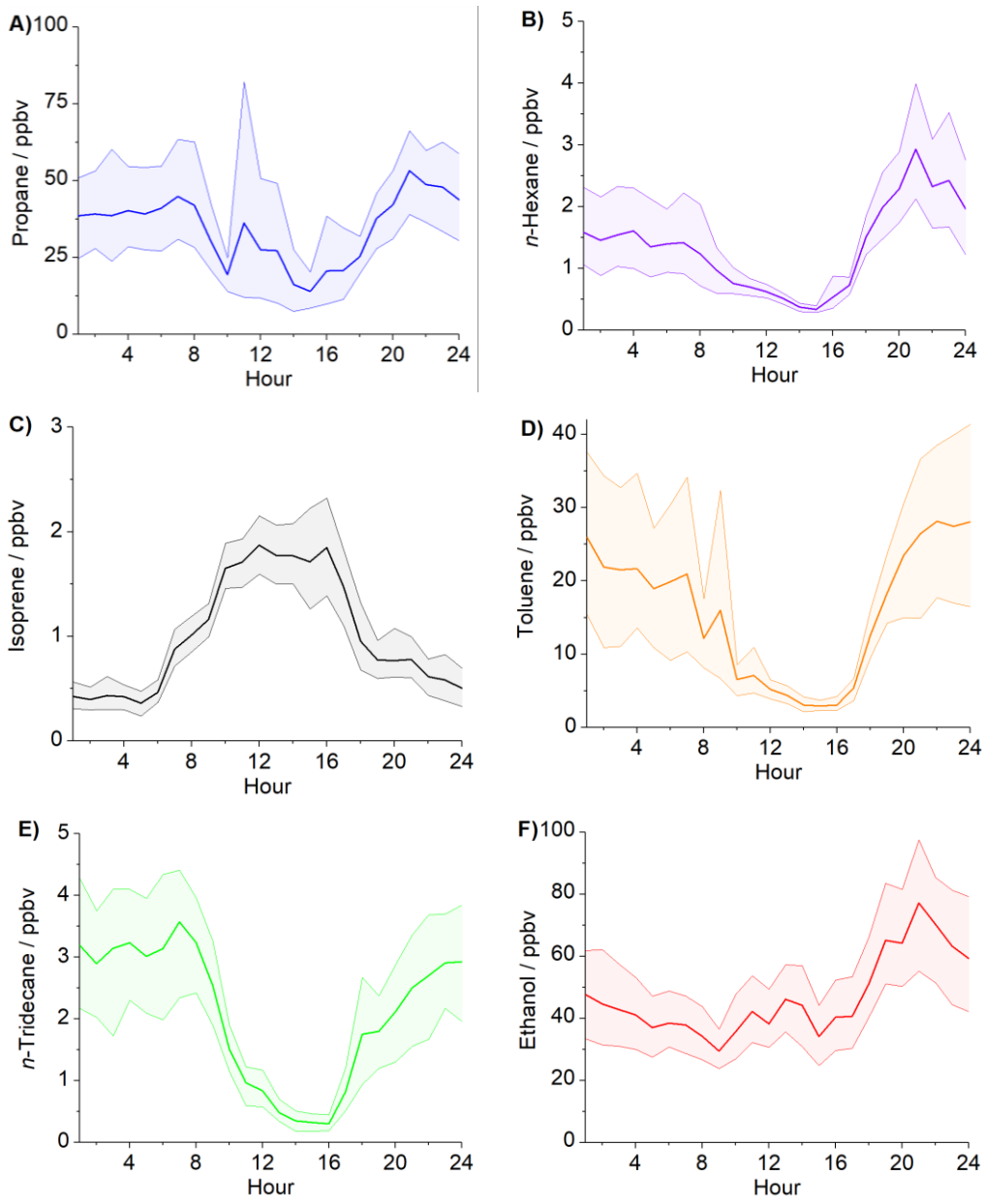

Figure 2.9. Diurnal profiles of selected NMHCs from pre- and post-monsoon campaigns for A = propane, B = *n*-hexane, C = isoprene, D = toluene, E = *n*-tridecane and F = ethanol. The shaded region indicates the 95% confidence interval in the means.

In order to compare the composition of NMHCs during the two campaigns, average diurnal profiles were calculated for all NHMC during the two campaigns and split according to functionality (alkanes, aromatic, monoterpenes). Figure 2.10A-B shows the average diurnal profiles for all alkanes. During the pre-monsoon campaign, the largest alkane mixing ratios were from 10:00-14:00 and caused by very large mixing ratios of propane and butane, with the mean for both campaigns peaking at around 150 ppbv. Outside of these peaks, the highest mixing ratios were observed at 20:00 at approximately 50 ppbv. The lowest mixing ratios of 20 ppbv were observed at 04:00. In the post-monsoon campaign, mixing ratios were high from 20:00-08:00 and peaked at around 360 ppbv at 21:00.

Figure 2.10C-D show the average diurnal profiles for aromatic species from the pre- and post-monsoon campaigns. Both campaigns showed peaks likely from traffic between 08:00-12:00. During the pre-monsoon, mixing ratios peaked at 19 ppbv at 19:00 and reduced to around 5 ppbv at midnight and remained low until the rush hour. In the post-monsoon, the mean diurnal variation of aromatic mixing ratios peaked at 96 ppbv at 21:00. The mixing ratio at 12:00 in the post-monsoon campaign was around 3 times larger (14 ppbv) than at the same time in the pre-monsoon average diurnal profile (5 ppbv). The lowest mixing ratios observed in the pre-monsoon campaign were at 15:00 (4.2 ppbv) and at 14:00 in the post-monsoon campaign (8.8 ppbv).

Figure 2.10E shows that in the average diurnal profile during the pre-monsoon the monoterpenes peaked at 07:00 (0.19 ppbv) and 22:00 (0.18 ppbv), likely due to biogenic emissions before the effect of photochemical degradation was too pronounced. Post-monsoon monoterpenes (Figure 2.10F) peaked from 22:00-07:00. The largest contributors to post-monsoon mixing ratios were limonene (31%) and β-ocimene (25%). The contribution of β-ocimene was similar in the pre-monsoon, with a lower contribution of limonene (8%) and larger contributions of α-pinene (28%), α-phellandrene (14%) and 3-carene (12%). The lowest monoterpene mixing ratios observed were in the afternoon at similar mixing ratios in the pre- (0.07 ppbv) and post-monsoon periods (0.09 ppbv), with a minimum at 15:00. The diurnal profile of the monoterpenes in the post-monsoon period was very similar to the anthropogenic NHMCs, with high concentrations of very reactive monoterpenes observed. In the time series in Figure 2.8C, up to 6 ppbv of monoterpenes were measured.

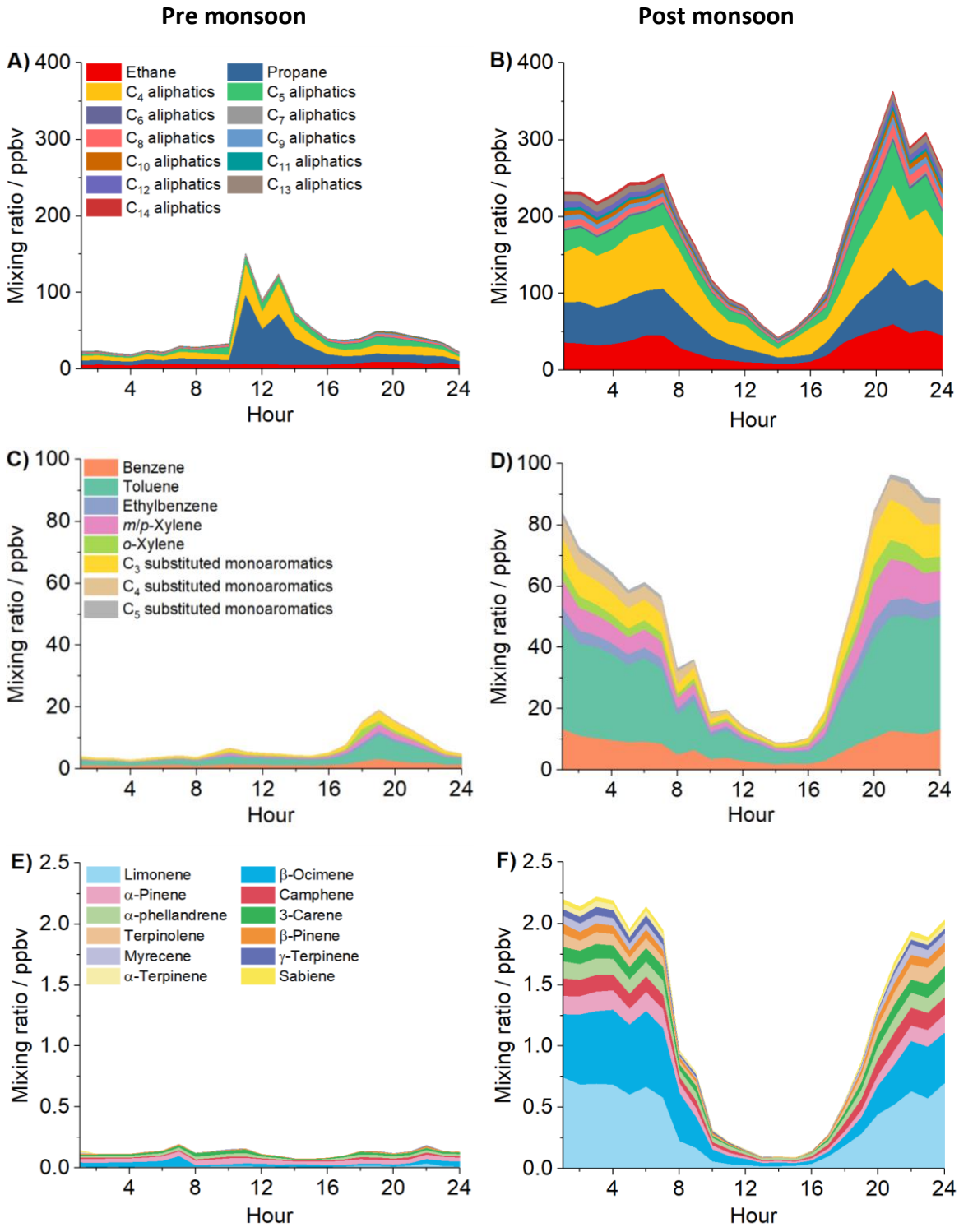

Figure 2.10. Stacked average diurnal profiles of alkanes (A-B), aromatics (C-D) and monoterpenes (E-F) measured during the pre- and post-monsoon campaigns in Delhi in 2018. Zoomed in stacked diurnals from the pre-monsoon campaign are given in the Supplementary Information 8.4.

Figure 2.11A-B show the diurnal variation of the toluene mixing ratio, PBLH and windspeed during the pre- and post-monsoon campaigns. The shape of the toluene diurnal was similar in both campaigns, but the mixing ratio of toluene much larger in the post-monsoon campaign. The windspeed in the pre-monsoon campaign (3-4 m s^{-1}) was consistent throughout the day and the night-time PBLH was around 300 m. In the post monsoon both night-time windspeed (~ 0.9 m s^{-1}) and PBLH (~ 60 m) were lower, resulting in higher toluene mixing ratios.

Figure 2.11C-D show the average diurnal profiles of the O_3, NO, NO_2 and CO measured during the pre- and post-monsoon campaigns. In the pre-monsoon campaign, mean O_3 peaked at 14:00 (90 ppbv) and remained high from 20:00-08:00 at ~ 30 ppbv. Average mixing ratios of NO (24-55 ppbv) and CO (0.67-1.3 ppmv) were elevated at night, with NO reducing to ~ 1.3 ppbv from 14:00-15:00 and CO to 0.4-0.5 ppmv from 12:00-16:00. In the post-monsoon campaign, mean O_3 was low (< 5ppbv) from 18:00-08:00 and peaked at 81 ppbv at 13:00. Night-time mixing ratios of NO (around 200 ppbv) and CO (approximately 2-3 ppmv) remained high from around 20:00-08:00. NO_2 showed less variability, with a mean mixing ratio of around 40 ppbv from 00:00-08:00 with two peaks at 09:00 (55 ppbv) and 17:00 (65 ppbv). There was a clear enhancement of primary pollutants NO, CO and NMHCs in Delhi during the post-monsoon at night, which appears to be driven, at least in part, by a very shallow and stagnant boundary layer.

A bivariate polar plot of the toluene concentration measured using PTR-QiToF-MS during pre- (26/05/18-09/06/18) and post-monsoon (07/10/18-23/11/18) seasons is shown in Figure 2.11E and for CO in pre- (28/05/18-05/06/18) and post-monsoon (07/10/18-23/11/18) campaigns in Figure 2.11F. Most of the NHMCs presented in this paper show a similar trend, with the highest mixing ratios observed under low windspeeds and PBLH indicating they are likely the result of emissions from the local area, perhaps with a larger source directly to the East.

The IGTDUW site was located close (around 0.3 km) to the national highway 44, the longest running north-south highway in India at over 3800 km in length, as well as old Delhi railway station (around 0.5 km). There were also many congested roads close to the site passing by shops selling automotive parts. These were both likely large sources of petrol and diesel

related emissions and likely to have a large impact on the composition of the measurements made at the IGTDUW site.

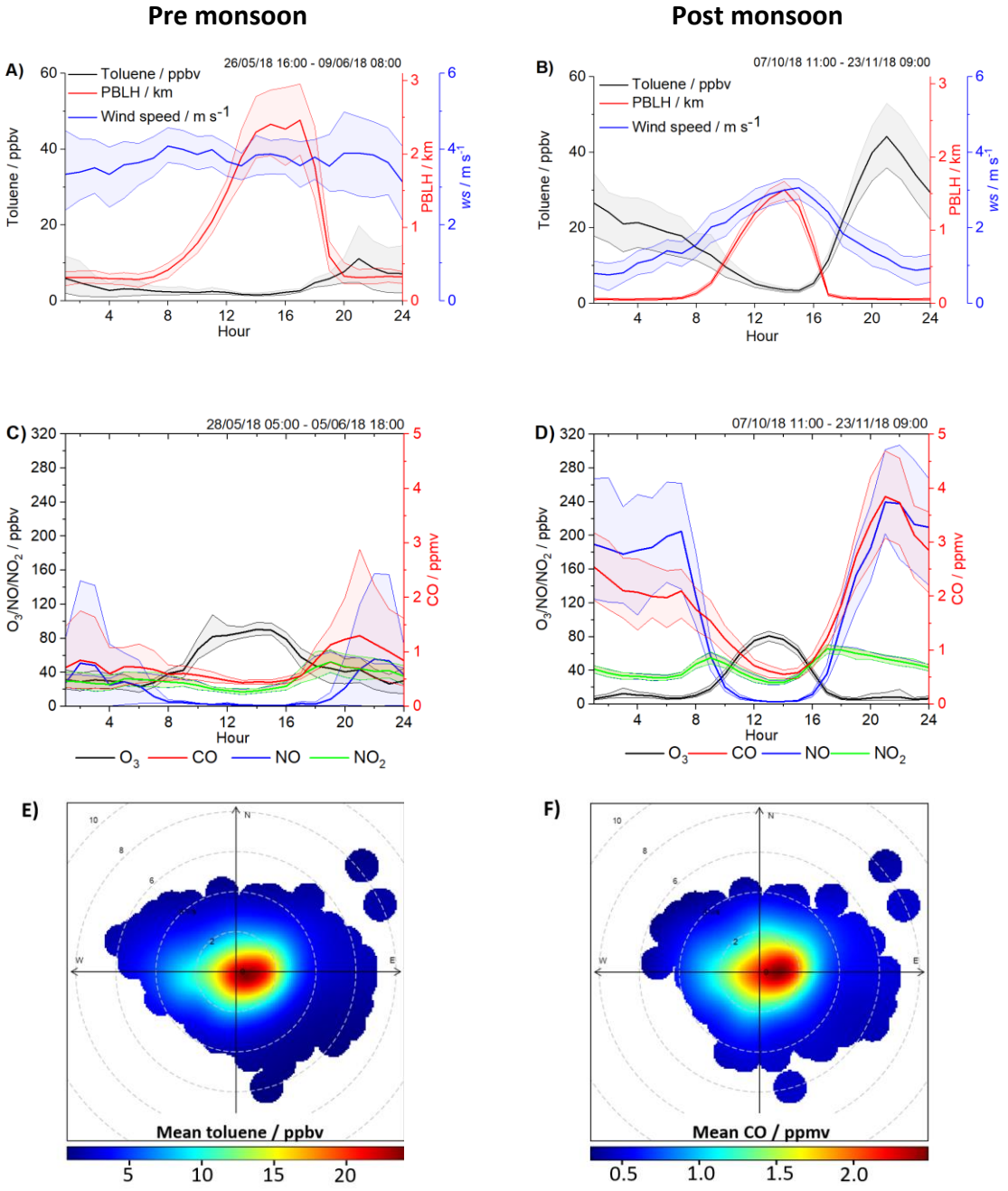

Figure 2.11. Variation of toluene mixing ratio, PBLH and windspeed in A = pre-monsoon campaign from 26/05/18-09/06/18 and B = post-monsoon campaign from 06/10/18-23/11/18. Mean diurnal profiles of O_3, NO, NO_2 and CO in C = pre- and D = post-monsoon campaigns. Shaded areas represent the 95% confidence intervals in the mean. Polar plots of E = toluene from 26/05/18-09/06/18 and 06/10/18-23/11/18 and F = CO from 28/05/18-05/06/18 and 07/10/18-23/11/18, with the radial component reflecting wind speed in m s^{-1} (Carslaw and Ropkins, 2012).

2.3.3. Regression analysis

In order to determine the relative source strength of different NMHCs, a number of different regression techniques were used. The observed mixing ratios of NMHCs were plotted against the mean CO and acetylene (tracers for petrol vehicles) measured during the concurrent GC sample time, with the regression coefficient of determination, R^2, examined. Figure 2.12 shows the observed R^2 values for different carbon numbers with the points coloured by functionality. Shaded regions have been added to group NMHCs that were indicative of major emission sources. C_3-C_4 alkanes, normally attributed to LPG emissions (Gamas et al., 2000; Bon et al., 2011), were grouped together with low R^2 values in the pre-monsoon campaign (< 0.4) and shaded in red. The low R^2 value to CO indicated that these likely were fugitive emissions from LPG rather than combustion. Removal of the few measurement points which caused the large peaks in propane and butane, shown as large spikes in alkanes between 11:00-13:00 in Figure 2.10A, confirmed this and remaining measurements had much higher R^2 to CO and acetylene (shown as red shaded area with red dashed line). C_5-C_{10} alkanes, as well as some C_4 alkenes (green shading), were grouped with R^2 values ~ 0.7-0.9 and may be from a petrol source as CO is a conventional tracer for petrol vehicular exhaust emissions. The R^2 value then decreased for C_{10}-C_{15} alkanes, which could be indicative of a different source (blue shading), with a poorer relationship to CO such as diesel or burning. Aromatic species are located in the regions characteristic of petrol and diesel emissions, and isomers with C_{10} showed the greatest variability spanning a range of R^2 values with CO from 0.1-0.9. Monoterpenes were also placed onto Figure 2.12 and a range of R^2 values were observed, possibly indicating a range of sources for these species. The overall shape between the two campaigns appeared similar, however, the R^2 values for the post-monsoon campaign were greater, and may be driven by strong meteorological influences, higher levels of pollution and reduced photochemistry. The monoterpenes in particular showed a much stronger correlation with CO during the post-monsoon period suggesting an anthropogenic source (Stockwell et al., 2015; Zhang et al., 2020). This conclusion is similar to that reported by Wang et al. (2020), who suggested that biogenic molecules may be explained by vehicular or burning sources in Delhi.

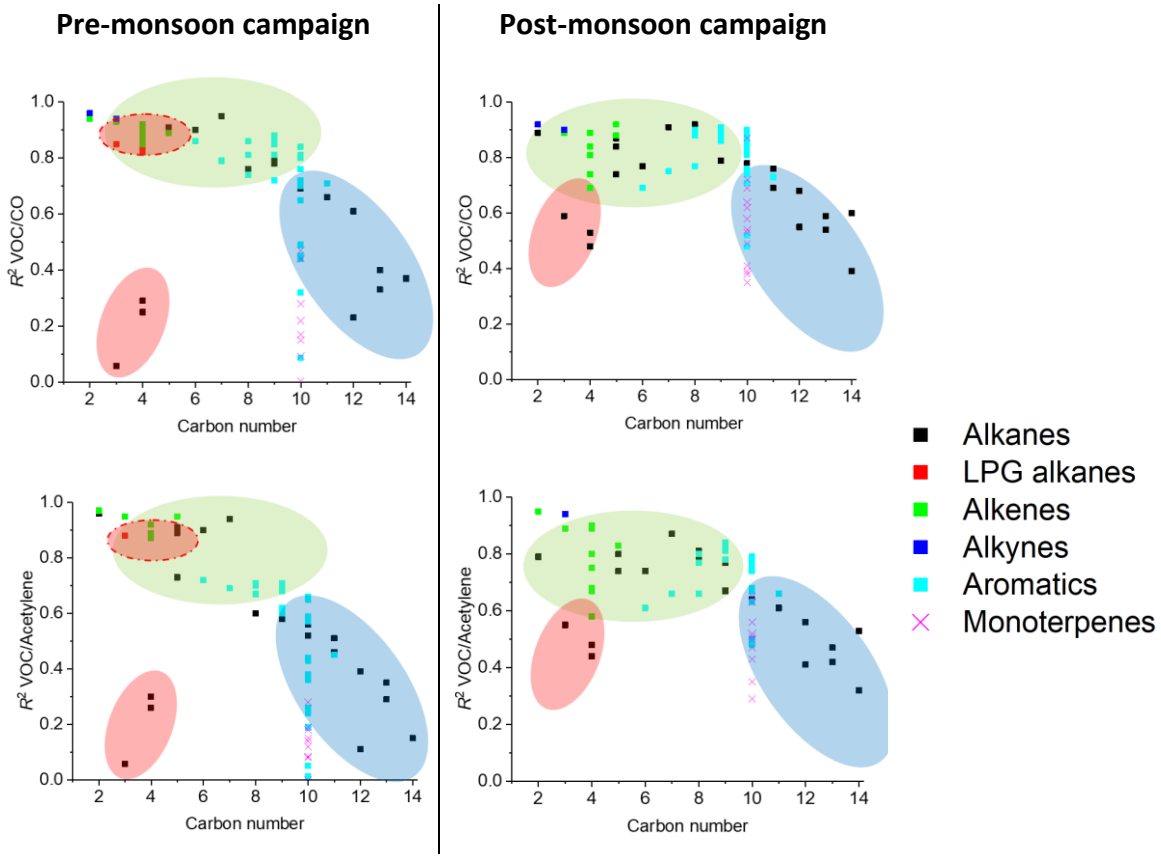

Figure 2.12. R^2 as a function of carbon number from regression analysis of NMHCs against CO and acetylene during pre- and post-monsoon campaigns. See text for discussion of the shaded ellipses.

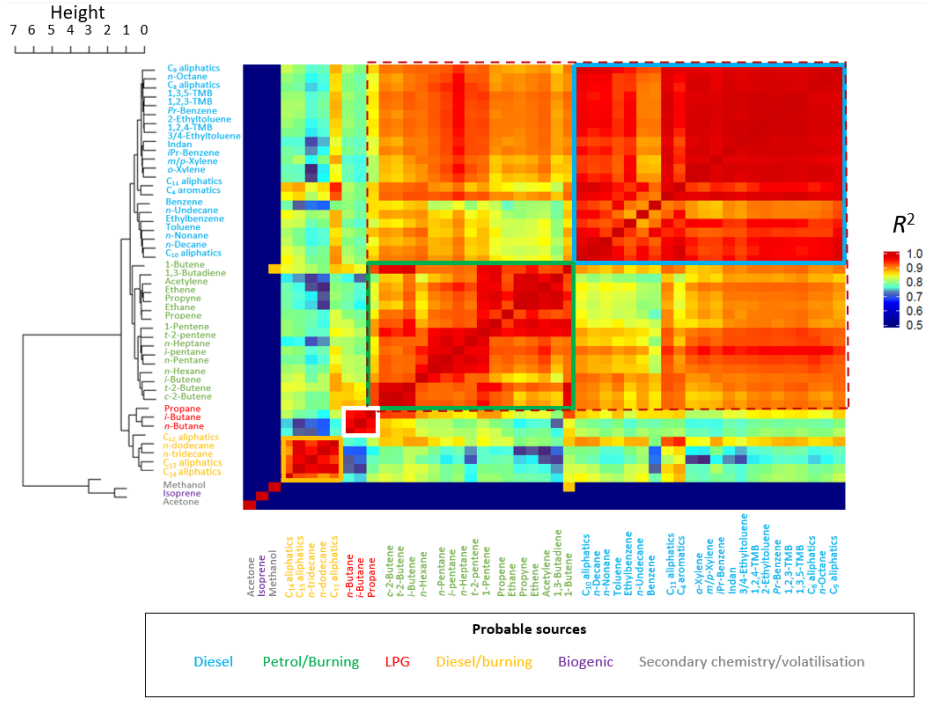

Figure 2.13. Correlation and hierarchical cluster analysis of NMHC mixing ratios using a combined dataset from both pre- and post-monsoon campaigns. Light blue shaded region corresponds to hydrocarbons typically associated with diesel fuel, green region to petrol, white region to LPG and orange region to diesel/burning.

Figure 2.13 shows the R^2 of linear regression plots of different NMHCs measured during pre- and post-monsoon campaigns ordered according to hierarchical cluster analysis, created with data extracted from the corPlot function of openair (Carslaw and Ropkins, 2012). A region is marked with a red dashed line which contained two closely correlated regions with NMHCs characteristic of diesel (blue) and petrol (green) fuels. There was likely some crossover of C_8-C_{10} species in this region, owing to similar diurnal profiles of NMHCs characteristic of petrol/diesel emissions. Benzene and toluene also sat with the diesel region but were likely to come from both vehicular sources, and toluene showed a stronger correlation with C_4-C_6 tracers than benzene. A further region with propane and butane (white square) was identified and characteristic of emissions from LPG fuels. Acetone and methanol were poorly correlated to other NMHCs, indicating a different source, which was assumed to be secondary chemistry or volatilisation for methanol. Isoprene was poorly correlated to other NMHCs, with an assumed daytime biogenic source due to the diurnal profile in Figure 2.9C. A further small region was identified (orange square) containing C_{11}-C_{14} aliphatic species, which were tentatively identified as coming from a mixture of diesel/burning sources. These species showed strong correlations to each other but poorer correlation with other NMHCs.

2.3.4. Emission ratio evaluation

The ratio of specific NMHC tracer pairs in ambient samples can be indicative of their emission source(s). The atmospheric lifetimes of *i*-pentane and *n*-pentane are similar (Jobson et al., 1998); a concentration ratio of 0.8-0.9 is typically observed for natural gas drilling, 2.2-3.8 for vehicular emissions, 1.8-4.6 for evaporative fuel emissions and 0.5-1.5 for biomass burning (Li et al., 2019). Figure 2.14 shows the *i*-/*n*-pentane ratio measured in this study, which was 2.6. This was compared to vehicular exhaust emissions reported from the Pearl River Tunnel in Guangzhou, China, where the ratio was found to be 2.9 (Liu et al., 2008). The ratio in Delhi was similar to another site considered to be highly influenced by traffic emissions (Jingkai community, Zhengzhou, China in 2017) which had a ratio of 2.6 (Li et al., 2019). The high R^2 of 0.98 in the Delhi measurements indicated a constant pollution source (mix), with a ratio close to that characteristic of vehicular emissions.

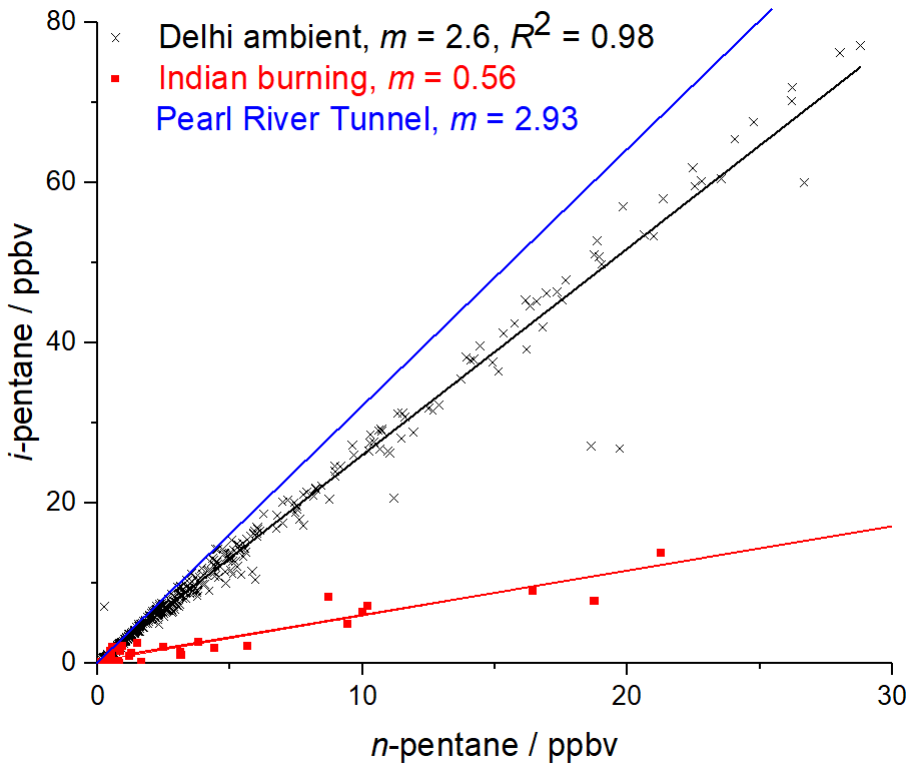

Figure 2.14. Comparison of *i*/*n*-pentane ratios between Delhi (black), Indian solid fuel combustion from data presented in chapter 4 (red) and the Pearl River Tunnel China (blue) (Liu et al., 2008).

The ratio of benzene to toluene in ambient samples has also been compared to those from different sources. During the post-monsoon campaign, the mean benzene/toluene ratio was 0.36. This has been compared to the ratios measured from the headspace of petrol (0.4) and diesel (0.2) liquid fuel samples collected from Delhi and presented in chapter 4 and that of 0.3 reported for traffic exhaust emissions (Hedberg et al., 2002). Whilst there is uncertainty in the exact ratio of benzene/toluene at emission due to the increased reactivity of toluene relative to benzene, the presence of a significantly greater molar ratio of toluene to benzene in ambient samples underlines the importance of petrol and diesel emissions to NMHCs in Delhi, as this could not be explained by the solid fuel combustion sources measured in chapter 4 for which benzene/toluene ratios were 2.3 for wood and 0.9 for cow dung cake.

2.3.5. Source apportionment modelling

Figure 2.15 shows the mean contribution of the 4 factors selected to pollutant mixing ratios from the PCA/APCS model. The PCA/APCS model was initially run with 3-7 factors, however, inclusion of > 4 factors did not lead to a significantly improved output and running EPA Unmix 6.0 with > 4 factors often led to solutions which would not converge. Sources in this study have been attributed to factors according to the species which they predict and those suggested in previous studies which showed emissions of C_2-C_5 for natural gas, C_2-C_{10} for petrol and diesel emissions > C_8 (Passant, 2002). The LPG factor in this study contributed to C_3-C_4 hydrocarbons. The petrol factor contributed to C_2-C_{12} hydrocarbons and contributed significantly to alkanes from C_5-C_9. The petrol factor had a smaller contribution to C_{11}-C_{12} hydrocarbons and was probably due to slight collinearity of petrol and diesel factors due to similar diurnal profiles and strong meteorological influences. The diesel factor increased in importance from C_8-C_{14} NMHCs, as expected of a diesel source. The inclusion of a small number of factors was beneficial to factor identification in this study, as the diurnal profiles of all NMHCs in the post monsoon were very similar. It was not possible to resolve a second diesel factor, which could be explained by diesel emissions from vehicles and generators. The assignment of petrol and diesel factors compared well with previous studies which showed that aromatics and alkanes were the dominant emission from 4-stroke motorcycles, light petrol vehicles and diesel trucks (Yao et al., 2015; Cao et al., 2016; Dhital et al., 2019).

The burning factor was rationalised using furfural as a tracer and contributed to C_2-C_7 hydrocarbons and > C_{12} hydrocarbons. North Indian burning sources are examined in detail in chapters 3-4 and shown to release substantial amounts of furfural and had significant emission factors of smaller alkanes such as ethane. The open burning of municipal solid waste is shown to contribute to emissions of heavier alkanes. Previous studies have also reported emissions of *n*-alkanes from the burning of municipal solid waste (Karasek and Tong, 1985). It is noteworthy that very low mean mixing ratios of furfural (0.8 ppbv) were measured by PTR-QiToF-MS in the post-monsoon campaign compared to other NMHCs such as monoterpenes (1.3 ppbv) and toluene (18 ppbv), which is suggestive of a small burning source.

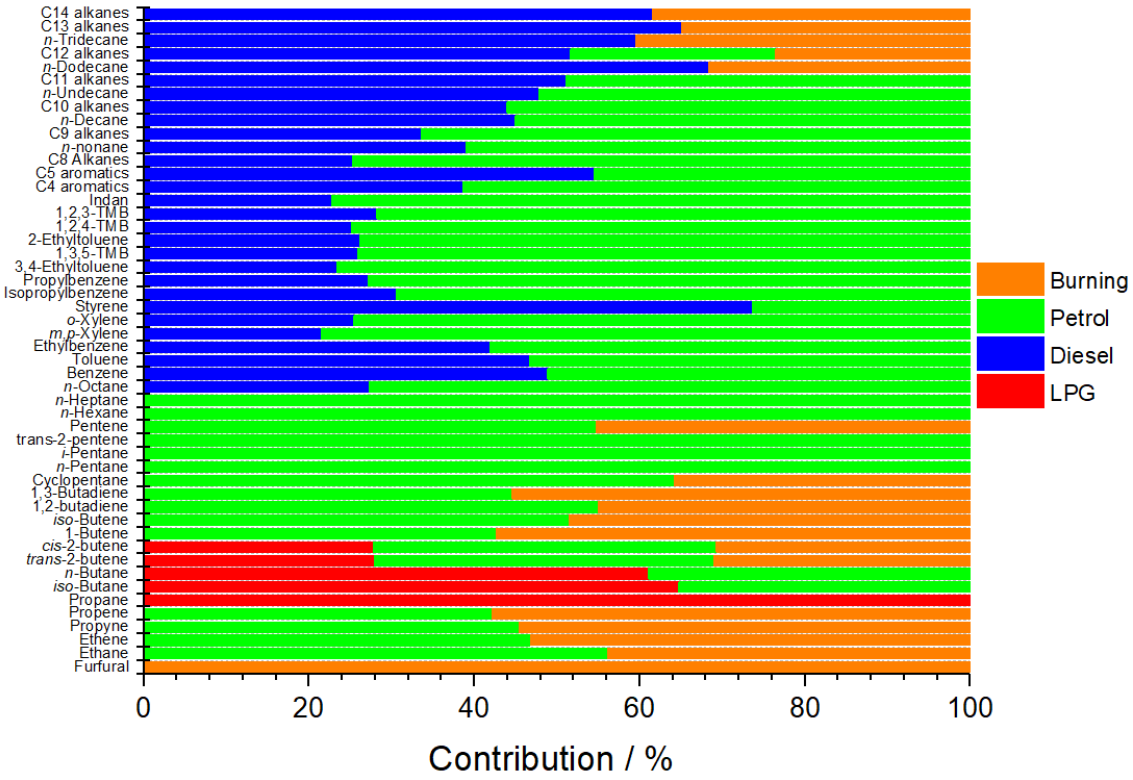

Figure 2.15. Mean contribution of sources to NMHCs measured in Delhi by PCA/APCS. Unmix 6.0 outputs are given in the Supplementary Information 8.5.

Table 2.2. Estimated source contributions to mean total NMHC mass and mixing ratios (M.R) observed in ambient samples.

Method	By	LPG	Burning	Petrol	Diesel
PCA/APCS	M.R	30	15	44	11
EPA Unmix 6.0	M.R	34	18	32	16
PCA/APCS	Mass	23	10	47	20
EPA Unmix 6.0	Mass	25	18	30	27

Table 2.2 shows the estimated source contributions to mean mixing ratio (M.R) and mass observed in ambient samples predicted by PCA/APCS and the EPA Unmix 6.0 toolkit. This study showed that traffic related emissions, which also included some emissions from static diesel generators, were the dominant source of NMHCs at the site, with relative mean mixing ratio contributions predicted by the PCA/APCS and Unmix models from petrol automobiles and motorbikes (38%), diesel trucks, trains and generators (14%), LPG from cooking (32%) and open burning of biomass and municipal solid waste (16%). The mean mass contributions were petrol (39%), diesel (23%), LPG (24%) and burning (14%). High

mixing ratios of aromatics were dominated by traffic related sources and meant that the contribution of biomass burning to these was insignificant.

This study compared well to the limited previous literature focussed on NMHC source apportionment in Delhi from ambient measurements (Wang et al., 2020) and inventories which have shown the importance of vehicular emissions (Gurjar et al., 2004; Guttikunda and Calori, 2013; Sharma et al., 2015). Gujar et al. (2004) showed that from 1990-2000 transport represented > 80% of NMHC emissions with 47% of emissions from motorcycles (Gurjar et al., 2004) and the study led by NEERI in 2008 showed vehicular related emissions to be the largest citywide source. Petrol emissions were the largest source shown by Srivastava et al. (2009) and the inventory for India produced by Sharma et al. (2015) commented that large built-up areas like Delhi were dominated by petrol traffic related emissions. The most recent study led by Wang et al. (2020) determined that traffic was responsible for 57% of the mixing ratio of NMVOCs at an urban site in Delhi, with 16% from secondary sources and 27% from biomass burning (Wang et al., 2020). The larger contribution of traffic related emissions and lower contribution of burning emissions in this present study were explained by the proximity of major roads to the IGTDUW site. It was also explained by the fact that the GC instrumentation used in this study was specifically targeted to NMHCs, in comparison to PTR-ToF-MS which is more suited to measuring oxygenated species commonly from secondary sources and burning. The contribution by mass of petrol and diesel sources in this study (62%) is in good agreement with that suggested by a 1 km^2 gridded inventory of Delhi (65%) (Guttikunda and Calori, 2013).

The results of the PCA/APCS and Unmix 6.0 models were compared to 3-6 factor unconstrained solutions from EPA PMF 5.0 run on individual pre-/post-monsoon datasets as well as the combined dataset. Although PMF is widely accepted as a more powerful receptor model due to being able to find more factors, PMF explored variance within the petrol and diesel factors before finding the factor attributed to LPG (see the Supplementary Information 8.6 for comparison of the 4-factor solution using the combined dataset). The instrumental uncertainty in the large fugitive spikes in propane and butane was not large, and so these points had not been down weighted within the model for this reason. Inclusion of benzene/toluene ratios and propane/butane ratios of factors in the PMF model did not lead to a significantly improved result and PMF was only able to identify the LPG

factor in the 6-factor pre-monsoon dataset. Factor identification for model runs with inclusion of additional factors was increasingly difficult to interpret. This may be partly driven by the limited data collected during the short measurement periods of this study. For these reasons, the results from the PMF model were not included in this study. Whilst studies criticise source apportionment in India using PCA/APCS and Unmix (Pant and Harrison, 2012), the results of the PCA/APCS and Unmix models were considered beneficial to include as they agreed well with other source apportionment analyses in this study and compared well to literature.

This work shows that NMHC emissions near an urban site in Delhi were predominantly the result of traffic related emissions. This study only focussed on the major sources of NMHCs in Delhi. The large contributions of petrol and diesel related emissions likely masked smaller contributions from other sources further from the site to the ratios of benzene/toluene and *i*-/*n*-pentane examined and are therefore not accounted for in the conclusions of this study. It is expected that any CNG transport related emissions which may be > C_1, potentially from poor maintenance and lubricant emissions, are grouped with petrol emissions. The influence of burning closer to slum sites and landfill is likely to be larger, and unaccounted for in the conclusions of this study. The contribution of LPG emissions from cooking and transport was also larger than estimated in current inventories.

It is highly likely that there were more smaller sources contributing to the NMHCs in Delhi than the 4 identified with the PCA/APCS and Unmix models, such as the contributions from industry, powerplants and brick kilns. The source of the 12 highly reactive monoterpenes measured at the IGTDUW site was not clear, and may be related to automotive emissions, cooking, personal care products, biogenic, burning of solid fuels, spices related to cooking or from incense burnt for religion reasons. These species are highly reactive and likely to be contributors to OH reactivity and SOA formation. Future studies should measure direct fluxes of NMHC to remove the strong meteorological influences impacting concentration measurements in Delhi. This could lead to a better understanding of the impact of NMHC sources on daytime NMHC emissions.

2.4. Conclusions

This study presents a comprehensive suite of NMHC measurements performed at an urban site in Delhi during the pre- and post-monsoon seasons in 2018. Extremely high night-time mixing ratios were measured during the post-monsoon campaign, caused by stagnant conditions and a shallow boundary layer. A range of source apportionment techniques have been used, which appear self-consistent and arrive at similar conclusions for correlation analysis to CO, acetylene and other NHHCs as well as hierarchical cluster analysis. The absolute contributions of different sources have been determined through receptor models, with factors rationalised using recent studies focussing on emissions from petrol, diesel and solid fuel combustion sources and confirmed through comparison of characteristic *i*-/*n*-pentane and benzene/toluene ratios which are close to those of liquid automotive fuels. These results are in line with bottom-up emission inventory and top-down receptor modelling approaches from recent literature. Unusually high levels of very reactive monoterpenes were observed at night during the post-monsoon campaign, with similar diurnal profiles to NHMCs typical of petrol and diesel sources. This suggested that these species were emitted from anthropogenic sources in Delhi rather than the conventional biogenic source seen in other locations. The impact of prolonged exposure to elevated NMHC concentrations at night during the post-monsoon campaign is likely to lead to significant health impacts and result in the production of high levels of other harmful secondary pollutants, when photochemical oxidation can occur the following day. In order to reduce the high levels of NMHCs during the post-monsoon period, policies that target vehicle emission reductions are critical.

Chapter 3

Emissions of intermediate-volatility and semi-volatile organic compounds from domestic fuels used in Delhi, India

The majority of this chapter has been published as a manuscript under the same name:

Gareth J. Stewart, Beth S. Nelson, W. Joe F. Acton, Adam R. Vaughan, Naomi J. Farren, James R. Hopkins, Martyn W. Ward, Stefan J. Swift, Rahul Arya, Arnab Mondal, Ritu Jangirh, Sakshi Ahlawat, Lokesh Yadav, Sudhir K. Sharma, Siti S. M. Yunus, C. Nicholas Hewitt, Eiko Nemitz, Neil Mullinger, Ranu Gadi, Lokesh. K. Sahu, Nidhi Tripathi, Andrew R. Rickard, James D Lee, Tuhin K. Mandal and Jacqueline F. Hamilton. *Atmos. Chem. Phys.*, 21, 2407-2426, 2021. https://doi.org/10.5194/acp-21-2407-2021

3.1. Introduction

Biomass burning is one of the most important global sources of trace gases and particles to the atmosphere (Simoneit, 2002; Chen et al., 2017; Andreae, 2019), with residential solid fuel combustion and wildfires emitting significant quantities of organic matter (Streets et al., 2003; Barboni et al., 2010; Chen et al., 2017; Liu et al., 2017; Kiely et al., 2019). Emissions of volatile organic compounds (VOCs) and particulate matter (PM) from biomass burning are of interest due to their detrimental impact on air quality. VOCs react to form ozone and secondary organic aerosol (SOA). Intermediate-volatility and semi-volatile organic compounds (I/SVOCs) are also a significant emission from biomass burning (Stockwell et al., 2015; Koss et al., 2018). I/SVOCs are an important class of air pollutant due to their contribution to aerosol formation (Bruns et al., 2016; Lu et al., 2018). I/SVOC emissions are poorly, if at all, represented in regional inventories and chemical transport models. Consequently, their impacts to air quality in developing regions, where solid fuel combustion is a dominant fuel source, are not well understood. Recent studies have shown that the inclusion of I/SVOCs leads to better agreement between modelled and measured values (Ots et al., 2016; Woody et al., 2016; Murphy et al., 2017; Jathar et al., 2017). Global I/SVOC emissions to the atmosphere from biomass burning were estimated to be ~ 54 Tg yr^{-1} from 2005-2008 (Hodzic et al., 2016), with I/SVOCs contributing in the range 8-15.5 Tg yr^{-1} to SOA (Cubison et al., 2011; Hodzic et al., 2016).

SOA formation from biomass burning emissions is poorly understood globally. Important factors include the formation of less volatile products from the oxidation of NMVOCs which partition into the aerosol phase, heterogeneous oxidation of aerosol phase organics, as well as plume dilution followed by evaporation and further gas-phase oxidation (Lim et al., 2019). Ahern et al. (2019) showed that for burning of biomass needles, biogenic VOCs were the dominant class of SOA precursor. This study also found that for wiregrass, furans were the most important SOA precursor. Bruns et al. (2016) showed that SOA formation from combustion of beech fuel wood was dominated by 22 compounds, with phenol, naphthalene and benzene contributing up to 80 % of the observed SOA. SOA formation from biomass burning has been shown to be significant in laboratory studies, with SOA yields from the burning of western U.S. fuels reported to be 24±4 % after 6 h and 56±9 %

after 4 d (Lim et al., 2019). However, the effect of atmospheric of aging on I/SVOCs still remains poorly understood (Liu et al., 2017; Decker et al., 2019; Sengupta et al., 2020).

Better understanding of the quantity and composition of I/SVOCs from biomass burning is needed to evaluate their impact on the atmosphere. This is a difficult analytical task, not well suited to conventional analysis with gas chromatography coupled to mass spectrometry (GC-MS). The reason for this is because of the exponential growth of potential isomers with carbon number, which results in a large number of coeluting peaks (Goldstein and Galbally, 2007). The high resolution of two-dimensional gas chromatography (GC×GC) has been demonstrated as an ideal technique to overcome this issue when analysing complex organic samples in both gas (Lewis et al., 2000; Stewart et al., 2021) and particle phases (Hamilton et al., 2004; Lyu et al., 2019). The application of GC×GC to biomass burning emissions has shown hundreds of gaseous I/SVOCs using adsorption-thermal desorption cartridges (Hatch et al., 2015) or solid phase extraction (SPE) disks (Hatch et al., 2018). GC×GC has also been used to analyse the particle phase with samples collected onto PTFE or quartz filters (Hatch et al., 2018; Jen et al., 2019), with the latter study quantifying 149 organic compounds which accounted for 4-37 % of the total mass of organic carbon. The process used by Hatch et al. (2018) demonstrated high recoveries of non-polar species from PTFE filters, with lower recoveries from SPE disks. This study highlighted the need for further evaluation of samples collected onto PTFE filters and SPE disks, ideally improving the method to remove undesirable steps such as trimethylsilylation derivatisation, the use of pyridine and centrifuging which led to high evaporative losses. The need to develop improved sampling and measurement techniques for I/SVOCs has also been highlighted. This is because these species often do not transmit quantitatively through the inlet and tubing when measured using online gas-phase techniques (Pagonis et al., 2017).

Residential combustion, agricultural crop residue burning and open municipal solid waste burning in the developing world are large, poorly characterised pollution sources with the potential to have a significant impact on local and regional air quality, impacting human health (Venkataraman et al., 2005; Jain et al., 2014; Wiedinmyer et al., 2014). Hazardous indoor air pollution from combustion of solid fuels has been shown to be the most important factor from a range of 67 environmental and lifestyle risk factors causing disease

in South Asia (Lim et al., 2012). Despite this, nearly 76 % of rural Indian households depend on solid biomass for their cooking needs (Gordon et al., 2018), using biofuels such as fuel wood, cow dung cake and crop residue. Combustion often takes place indoors, without efficient emission controls, which significantly increases the mean household concentration of pollutants, particularly particulate matter with a diameter less than 2.5 µm ($PM_{2.5}$). The health effects from this are significant, with an estimated 3.8 million premature deaths globally due to inefficient indoor combustion from cooking (World Health Organization, 2018b).

Few detailed studies have been conducted examining the composition of I/SVOC emissions from solid-fuel combustion sources from South Asia. Sheesley et al. (2003) used solvent extraction followed by GC-MS to produce emission factors and examine molecular markers from combustion of coconut leaves, rice straw, cow dung cake, biomass briquettes and jackfruit branches collected from Bangladesh. A more recent study extracted $PM_{2.5}$ samples followed by analysis with GC-MS from motorcycles, diesel- and gasoline-generators, agricultural pumps, municipal solid waste burning, cooking fires using fuel wood and cow dung cake, crop residue burning and brick kilns in Nepal (Jayarathne et al., 2018). Lack of knowledge regarding major pollution sources hinders our ability to predict air quality, but also the development of effective mitigation strategies for air pollution which leads to health impacts ranging from respiratory illness to premature death (Brunekreef and Holgate, 2002). This results in many people living with high levels of air pollution (Lelieveld et al., 2015; Cohen et al., 2005) and 13 Indian cities ranking amongst the top 20 cities in the world with the highest levels of ambient $PM_{2.5}$ pollution, based on available data (Gordon et al., 2018).

In this study we develop a more efficient extraction step for the SPE/PTFE technique developed by Hatch et al. (2018), using accelerated solvent extraction into ethyl acetate, which showed high recoveries of non-polar I/SVOCs. Domestic fuels characteristic to Northern India were gathered and organic I/SVOC samples collected onto SPE disks and PTFE filters from controlled laboratory combustion experiments of a variety of fuel woods, cow dung cakes, municipal solid waste samples, crop residues, charcoal and liquefied petroleum gas (LPG). The samples were extracted using this new technique and analysed with GC×GC coupled to time-of-flight mass spectrometry (GC×GC-ToF-MS). Molecular

markers were examined from different fuels and the limitations for quantification of the extremely complex samples using a mass spectrometer were examined.

3.2. Methods

3.2.1. Fuel collection and burning facility

The state of New Delhi was gridded (0.05×0.05) and a diverse range of fuel types collected from across the state (see Figure 3.1). Fuels were stored in a manner akin to local practices prior to combustion, to ensure that the moisture content of fuels were similar to those burnt across the state. A range of solid biomass fuels were collected which included 17 fuel wood species, cow dung cake, charcoal and sawdust (see Table 3.1). Three crop residue fuel types were collected and consisted of dried stems from vegetable plants such as cabbage (*Brassica spp*) and aubergines (*Solanum melongena*) as well as coconut husk (*Cocos nucifera)*. Municipal solid waste was collected from Bhalaswa, Ghazipur and Okhla landfill sites. A low-cost liquefied petroleum gas (LPG) stove was also purchased to allow direct comparison to other combustion sources.

Fuels were burnt at the CSIR-National Physical Laboratory (NPL) New Delhi under controlled conditions using a combustion dilution chamber that has been well described previously (Venkataraman et al., 2002; Saud et al., 2011; Saud et al., 2012; Singh et al., 2013). In summary, 200 g of dry fuel was rapidly heated to spontaneous ignition with emissions driven into a hood and up a flue by convection to allow enough dilution, cooling and residence time to achieve the quenching of typical indoor environments. This process was designed to replicate the immediate condensational processes that occur in smoke particles approximately 5-20 mins after emission, yet prior to photochemistry which may change composition (Akagi et al., 2011). A low volume sampler (Vayubodhan Pvt.Ltd) was used to collect particulates and low volatility gases passing from the top of the flue through a chamber with a flow rate of 46.7 L min^{-1}. As detailed in Table 3.1, samples were collected from 30 fuels alongside 8 blank measurements. Prior to sample collection, SPE disks (Resprep, C_{18}, 47 mm) were prewashed with 2 × 5 mL acetone (Fisher Scientific analytical reagent grade), and 1 × 5 mL methanol (Sigma-Aldrich HPLC grade), then packed in foil and sealed in airtight bags. Samples were collected onto a PTFE filter (Cole-Parmer, 47 mm, 1.2 µm pore size) placed on top of an SPE disk in a filter holder (Cole-Parmer, 47 mm, PFA) for

30 mins at a flow rate of 6 L min^{-1}, maintained by a mass flow controller (Alicat 0-20 SLM) connected to a pump. Samples were removed from the filter holder immediately after the experiment and wrapped in foil, placed inside an airtight bag and stored at – 20 °C. Samples were then transported to the UK for analysis using an insulated container containing dry ice via. air freight and stored at – 20 °C for around 2 months prior to analysis.

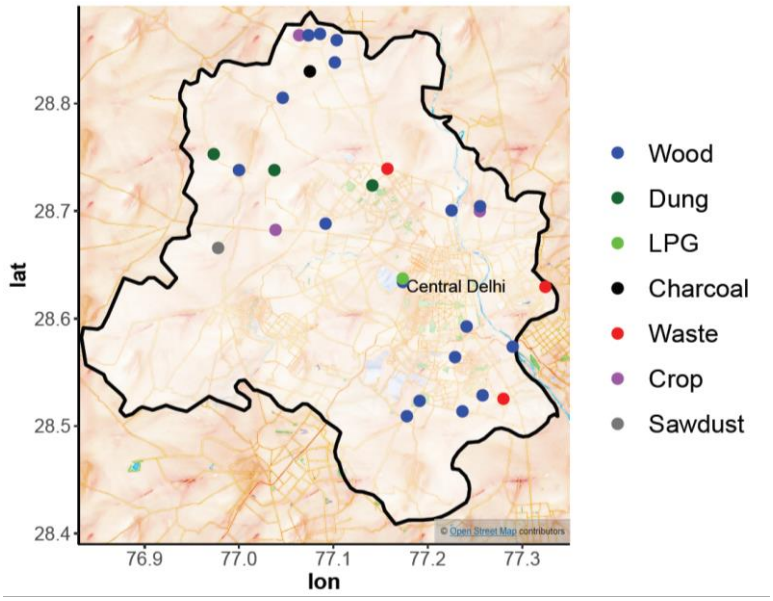

Figure 3.1. Locations across Delhi used for fuel collection. Map tiles by Stamen Design. Data by © OpenStreetMap contributors 2020. Distributed under a Creative Commons BY-SA License.

Table 3.1. Types of fuel sampled where *n* = number of burns of a specific fuel type, SPE and PTFE = number of blank corrected peaks detected on SPE disks and PTFE filters, respectively.

Fuel woods	***n***	**SPE**	**PTFE**	**Other**	***n***	**SPE**	**PTFE**
Plywood	1	201	516	Cow dung cake	3	1235	1562
Azadirachta indica	1	557	862	*Cocos nucifera*	1	620	1197
Morus spp	1	805	1132	Charcoal	1	439	280
Shorea spp	1	296	360	Sawdust	1	1112	1486
Ficus religiosa	1	500	712	Waste	3	948	1182
Syzygium spp	1	661	571	LPG	1	-	-
Ficus spp	1	306	292	Blank	8	-	-
Vachellia spp	1	697	800	Cow dung cake mix	1	931	1241
Dalbergia sissoo	1	501	611	*Brassica spp*	1	652	536
Ricinus spp	1	424	271	*Solanum melongena*	1	314	559
Holoptelea spp	1	274	324				
Saraca indica	1	525	484				
Pithecellobium spp	1	525	235				
Eucalyptus spp	1	238	144				
Melia azedarach	1	444	213				
Prosopis spp	1	248	144				
Mangifera indica	1	387	628				

3.2.2. Extraction

SPE disks and PTFE filters were spiked with an internal standard (50 µL at 20 µg mL^{-1}) containing 6 deuterated PAHs (1,4-Dichlorobenzene-d_4, naphthalene-d_8, acenaphthene-d_{10}, phenanthrene-d_{10}, chrysene-d_{12}, perylene-d_{12}; EPA 8720 Semivolatile Internal Standard Mix, 2000 µg mL^{-1} in DCM) to result in a final internal standard concentration of 1 µg mL^{-1} in solution. The solvent from the internal standard was allowed to evaporate and then SPE disks and PTFE filters were cut and extracted into ethyl acetate (EtOAc) using accelerated solvent extraction (ASE 350, Dionex, ThermoFisher Scientific). Extractions were performed at 80 °C and 1500 psi for three 5 min cycles. After each cycle, the cell was purged for 60 secs into a sample collection vial. Samples were then reduced from 15 mL to 0.90 mL over a low flow of N_2 in an ice bath over a period of 6-8 hours (Farren et al., 2015). Samples were then pipetted (glass Pasteur) to sample vials (Sigma-Aldrich, amber glass, 1.5 mL), with ASE vials rinsed with 2 × 50 µL washes of EtOAC, then added to the sample vial and sealed (Agilent 12 mm cap, PTFE/silicone/PTFE). The mass of the sample vial and cap for each sample was measured before and after to determine the exact volume of solvent in each sample. Extracts were frozen prior to analysis to reduce evaporative losses.

3.2.3. Organic composition analysis

GC×GC-ToF-MS: PTFE samples were analysed using GC×GC-ToF-MS (Leco Pegasus BT 4D) using a splitless injection (1 µL injection, 4mm taper focus liner, SHG 560302). The primary dimension column was a RXI-5SilMS (Restek, 30 m × 0.25 µm × 0.25 mm) connected to a second column of RXI-17SilMS (Restek, 0.25 µm × 0.25 mm, 0.17 m primary GC oven, 0.1 m modulator, 1.42 m secondary oven, 0.31 m transfer line) with a He flow of 1.4 mL min^{-1}. The primary oven was held at 40 °C for 1 min then ramped at 3 °C min^{-1} to 322 °C where it was held for 3 min. The secondary oven was held at 62 °C for 1 min then ramped at 3.2 °C to 190 °C after which it was ramped at 3.6 °C min^{-1} to 325 °C and held for 19.5 mins. The inlet was held at 280 °C and the transfer line at 340 °C. A 5 s cryogenic modulation was used with a 1.5 s hot pulse and 1 s cool time between stages. Using two separate wash vials, the syringe (10 µL Gerstel) was cleaned prior to injection with two cycles of 3 × 5 µL washes in EtOAc and rinsed post injection with two cycles of 2 × 5 µL washes in EtOAc. Samples with high concentrations of levoglucosan were reanalysed using a faster method,

injected split (75:1 and 125:1) with the primary oven held at 40 ^{o}C for 1 min, then ramped at 10 ^{o}C min^{-1} to 220 ^{o}C. The secondary oven was held at 62 ^{o}C for 1 min and then ramped at 10 ^{o}C min^{-1} to 245 ^{o}C.

SPE samples were injected split (10:1) and analysed with a shorter analysis time with the primary oven held at 40 ^{o}C for 1 min then ramped at 3 ^{o}C min^{-1} to 202 ^{o}C where it was held for 4 secs. The secondary oven was held at 62 ^{o}C for 1 min then ramped at 3.2 ^{o}C min^{-1} to 235 ^{o}C. A 75:1 split injection was used for quantitation of concentrations outside of the detector response range for furanics, phenolics, benzaldehydes, naphthalenes and benzonitrile. Peaks were assigned through comparison of retention times with known standards and comparison with the National Institute of Standards and Technology (NIST) mass spectral library. Peaks with no genuine standard available were tentatively identified if the NIST library hit was > 700. Peaks with a hit > 900 reflect an excellent match, 800-900 a good match and 700-800 a fair match (Stein, 2011). The uncertainty in this approach has been shown to be low for peaks with hits > 800, with the probability of incorrect identification being around 30% for hits between 800-900 and 14% for matches above 900 (Worton et al., 2017). Integration was carried out within the ChromaTOF 5.0 software package (Leko, 2019). Calibration was performed using a 6-point calibration using either a linear or second-order polynomial fit covering the ranges 0.1-2.5 μg ml^{-1} (splitless), 0.5-15 μg ml^{-1} (10:1 split), 15-400 μg ml^{-1} (75:1 split) and 400-800 μg ml^{-1} (125:1 split). Eight blank measurements were made at the beginning and end of the day by passing air from the chamber (6 L min^{-1} for 30 mins) through the filter holder containing PTFE filters and SPE disks. Blank corrections were applied by calculating the average blank value for each compound using blank samples collected using the same sample collection parameters as real samples before and after the relevant burning experiments.

PTR-ToF-MS: Online measurements of naphthalene, methylnaphthalenes and dimethylnaphthalenes were made by Joe Acton from the University of Lancaster using a proton transfer reaction-time of flight-mass spectrometer PTR-ToF-MS (PTR 8000; Ionicon Analytik, Innsbruck) and assigned as masses 129.058, 143.08 and 157.097, respectively. Additional details of the PTR-ToF-MS from Physical Research Laboratory (PRL), Ahmedabad used in this study are given in previous papers (Sahu and Saxena, 2015; Sahu et al., 2016). A ¼ inch OD PFA sample line ran from the top of the flue to the instrument which was

housed in an air-conditioned laboratory with a sample flow rate of 4.3 L min^{-1}. The sample air was diluted either 5 or 6.25 times into zero air, generated by passing ambient air (1 L min^{-1}) through a heated platinum filament at 550 ^{o}C, before entering the instrument with an inlet flow of 250 ml min^{-1}. The instrument was operated with a reduced electric field strength (*E*/*N*, where *N* is the buffer gas density and *E* is the electric field strength) of 120 Td. The drift tube temperature was 60 °C with a pressure of 2.3 mbar and 560 V applied across it.

Calibrations of the PTR-ToF-MS were performed twice a week using a gas calibration unit (Ionicon Analytik, Innsbruck). The calibration gas (Apel-Riemer Environmental Inc., Miami) contained 18 compounds: methanol, acetonitrile, acetaldehyde, acetone, dimethyl sulphide, isoprene, methacrolein, methyl vinyl ketone, 2-butanol, benzene, toluene, 2-hexanone, *m*-xylene, heptanal, α-pinene, 3-octanone and 3-octanol at 1000 ppb (±5%) and β-caryophyllene at 500 ppb (±5%). This standard was dynamically diluted into zero air to provide a 6-point calibration. The normalised sensitivity (ncps/ppbv) was then determined for all masses using a transmission curve derived from these standard compounds (Taipale et al., 2008).

Mass calibration and peak fitting of the PTR-ToF-MS data were performed using PTRwid software (Holzinger, 2015). Count rates (cps) of each mass spectral peak were normalised to the primary ion (H_3O^+) and water cluster ($H_3O.H_2O)^+$ peaks and mixing ratios were then determined for each mass using the normalised sensitivity (ncps). Where compounds known to fragment in the PTR-ToF-MS were identified, the mixing ratio of these species was calculated by summing parent ion and fragment ion mixing ratios. Before each burning study, ambient air was sampled to provide a background for the measurement.

3.2.4. Quantification of recovery and breakthrough

Standards were used for 136 species (see Figure 3.2) including two commercially available standard mixes containing 33 alkanes (C_7-C_{40} saturated alkane standard, certified 1000 µg m^{-1} in hexane, Sigma Aldrich 49452-U) and 64 semi volatiles (EPA CLP Semivolatile Calibration Mix, 1000 µg mL^{-1} in DCM:benzene 3:1, Sigma Aldrich 506508). Further standards were produced in-house, by dissolving high quality standards (> 99% purity), for a range of additional species also found in samples including nitrogen containing NMVOCs,

furans, alkyl-substituted monoaromatics, oxygenated aromatics, ketones, aldehydes, methoxy phenols, aromatic acids, PAHs and levoglucosan. Stock solutions of around 1000 µg mL^{-1} were prepared by dissolving 0.01 g into 10 mL EtOAc. Polar components, such as levoglucosan, were dissolved into methanol (MeOH) for stock solutions and those not soluble at room temperature were heated and pipetted using hot pipette tips to make quantitative dilutions.

Six separate PTFE filters and SPE disks were spiked with the standard solution containing 136 compounds (50 µL at 20 µg mL^{-1}), extracted and analysed. Recovery levels were calculated by comparing the signal to direct injection of the diluted standards to the GC×GC-ToF-MS. The recoveries are shown in Table 3.2. SPE disks showed poor recoveries (S_{rec}) of *n*-nonane to *n*-tridecane and C_2 substituted monoaromatics, likely due to volatilisation of these more-volatile components. Poorer recoveries were also observed of nitroanilines and levoglucosan. Non-polar species showed good recoveries, with high recoveries of C_{14}-C_{20} alkanes, furans, phenols, chlorobenzenes and PAHs. PTFE filters demonstrated high recoveries (P_{rec}) of PAHs with more than three rings in their structure (81.6-100%). Recoveries were low, or zero, for volatile components with boiling points < 200 °C, indicating no retention, which is consistent with the method being well-suited to target the aerosol phase. The recoveries of non-polar species into EtOAc from SPE disks were higher than those reported into MeOH (Hatch et al., 2018).

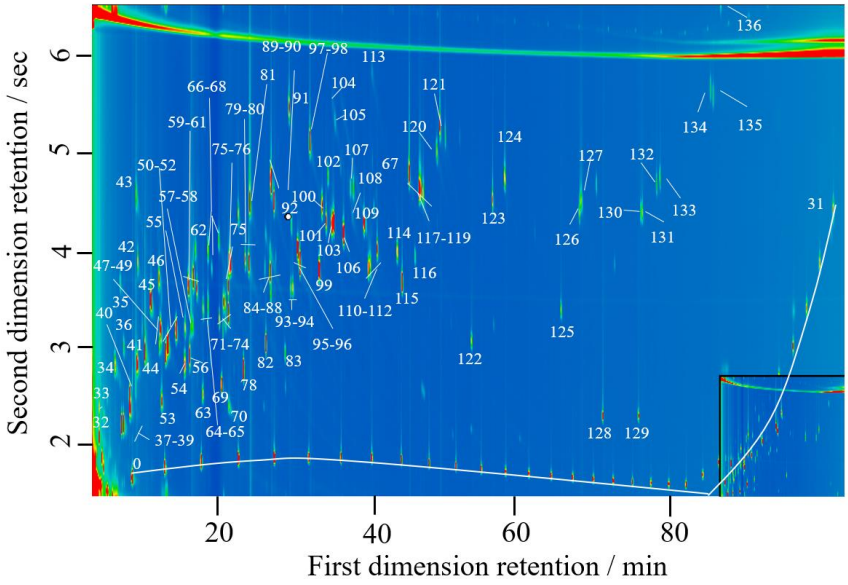

Figure 3.2. GC×GC-ToF-MS chromatogram of a mixed standard, numbered according to species listed in Table 3.2.

Table 3.2. Results of recovery tests where No. refers to the peak number in Figure 3.2, Q_{ms} = split method used for SPE quantitation, Q_{mp} = split method used for PTFE quantitation, S = splitless method, S_{rec} = % recovery SPE, P_{rec} = % recovery PTFE, [a] = Sigma-Aldrich *n*-alkanes standard, [b] = Sigma-Aldrich semivolatiles standard, [c] = Sigma-Aldrich deuterated internal standard, [d] = in-house solution and **-** = not measured either due to being outside of SPE method range or due to volatilisation from PTFE filters. Slight over-recoveries of > 100% are reported as 100% and accounted for in blank subtractions.

No.	Species	Q_{ms}	Q_{mp}	S_{rec}	P_{rec}	No.	Species	Q_{ms}	Q_{mp}	S_{rec}	P_{rec}
Alkane						**Nitrogen containing NMVOC**					
0	*n*-Nonane [a]	10:1	S	60.0	-	32	Pyridine [d]	10:1	S	75.1	-
1	*n*-Decane [a]	10:1	S	77.6	19.5	33	*n*-Nitrosodimethylamine [b]	10:1	S	-	-
2	*n*-Undecane [a]	10:1	S	100	57.2	44	2,3-lutidine [d]	10:1	S	99.4	-
3	*n*-Dodecane [a]	10:1	S	85.7	22.0	46	Benzonitrile [d]	75:1	S	86.9	-
4	*n*-Tridecane [a]	10:1	S	91.4	75.0	57	*n*-Nitrosodipropylamine [b]	10:1	S	100	-
5	*n*-Tetradecane [a]	10:1	S	97.8	97.8	62	Nitrobenzene [b]	10:1	S	88.5	-
6	*n*-Pentadecane [a]	10:1	S	99.7	92.3	67	2-Nitrophenol [b]	10:1	S	100	-
7	*n*-Hexadecane [a]	10:1	S	100	100	68	Pyrrole 2-carbonitrile [d]	10:1	S	-	-
8	*n*-Heptadecane [a]	10:1	S	100	98.0	77	4-chloroanaline [b]	10:1	S	7.78	-
9	*n*-Octadecane [a]	10:1	S	100	99.9	98	2-Nitroanaline [b]	10:1	S	100	-
10	*n*-Nonadecane [a]	10:1	S	100	98.9	102	2,6-dinitrotoluene [b]	10:1	S	99.9	-
11	*n*-Eicosane [a]	10:1	S	100	96.8	105	3-Nitroanaline [b]	10:1	S	34.2	-
12	*n*-Heneicosane [a]	10:1	S	-	100	107	2,4-Dinitrotoluene [b]	10:1	S	100	-
13-23	*n*-Docosane [a] – *n*-Dotriacontane [a]	10:1	S	-	100	108	4-Nitrophenol [b]	10:1	S	-	-
24	*n*-Tritriacontane	-	-	-	96.5	112	Azobenzene [b]	10:1		100	100
25	*n*-Tetratriacontane	-	-	-	78.9	113	*p*- Nitroaniline [b]	10:1	S	64.5	-
26	*n*-Pentatriacontane	-	-	-	58.3	121	Caffeine [d]	10:1	S	-	-
27	*n*-Hexatriacontane	-	-	-	49.9	**Aromatics**					
28	*n*-Heptatriacontane	-	-	-	35.4	37	Ethylbenzene [d]	10:1	S	44.6	-
29	*n*-Octatriacontane	-	-	-	32.1	38	*m*-Xylene [d]	10:1	S	34.5	-
30	*n*-Nonatriacontane	-	-	-	29.1	39	*o*-Xylene [d]	10:1	S	32.4	-
31	*n*-Tetracontane	-	-	-	27.9	40	Styrene [d]	10:1	S	58.4	-
PAH						69	Pentylbenzene [d]	10:1	S	99.0	24.4
76	Naphthalene [b/c]	75:1	S	93.9	37.1	82	Pentamethylbenzene [d]	10:1	S	68.6	39.5
81	Quinoline [d]	10:1	S	28.6	-	**Halogenated**					
87	2-Methylnapthalene [b]	75:1	S	90.8	72.4	48	2-Chlorophenol [b]	10:1	S	100	-
89	Indole [d]	10:1	S	81.6	-	50	1,3-Dichlorobenzene [b]	10:1	S	85.5	-
90	Azulene [d]	10:1	S	38.5	-	51	1,4-Dichlorobenzene [b,c]	10:1	S	87.2	-
91	1(3H)-Isobenzofuranone [d]	10:1	S	100	-	52	1,2-Dichlorobenzene [b]	10:1	S	70.3	-
96	Biphenyl [d]	10:1	S	99.5	75.0	56	Hexachloroethane [b]	10:1	S	83.7	-
97	1,4-Naphthoquinone [d]	10:1	S	100	-	74	2,4-Dichlorophenol [b]	10:1	S	100	83.9
99	2,3-Dimethylnaphthalene [d]	10:1	S	100	-	75	1,2,4-trichlorobenzene [b]	10:1	S	85.6	-
100	Acenaphthylene [b]	10:1	S	98.5	84.1	78	Hexachlorobutadiene [b]	10:1	S	61.6	-
103	Acenapthene [b/c]	10:1	S	100	88.2	83	Hexachlorocyclopentadiene [b]	10:1	S	100	-
106	Dibenzofuran [b]	10:1	S	100	86.4	88	4-Chloro-3-methylphenol [b]		S	90.8	-
109	Fluorene [b]	10:1	S	100	86.0	93	2,4,6-Trichlorophenol [b]	10:1	S	95.8	-
117	9H-Fluoren-9-one [d]	10:1	S	100	100	94	2,4,5-Trichlorophenol [b]	10:1	S	100	-
118	Phenanthrene [b]	10:1	S	100	96.7	95	2-Chloronapthalene [b]	10:1	S	99.6	-
119	Anthracene [b]	10:1	S	98.6	95.9	110	4-Chlorophenylphenylether [b]	10:1	S	100	-
120	Carbazole [b]	10:1	S	100	85.2	114	4-Bromophenylphenylether [b]	10:1	S	100	-
123	Fluoranthene [b]	10:1	S	100	97.2	115	Hexachlorobenzene [b]	10:1	S	100	-
124	Pyrene [b]	10:1	S	-	100	116	Pentachlorophenol [b]	10:1	S	100	-
126	Benzo(a)anthracene [b]	-	S	-	100	**Furans**					
127	Chrysene [b/c]	-	S	-	100	34	Furfural [d]	75:1	S	84.3	-
130	Benzo(b)fluoranthene [b]	-	S	-	100	35	Maleic anhydride [d]	10:1	S	54.9	-
131	Benzo(k)fluoranthene [b]	-	S	-	100	36	α-Angelica lactone [d]	10:1	S	52.1	-
132	Benzo(a)pyrene [b]	-	S	-	89.5	43	2-5(H)-furanone [d]	75:1	S	100	-
133	Perylene-D12 [c]	-	S	-	92.4	**Phthalates**					
134	Indeno(1,2,3-CD)pyrene [b]	-	S	-	94.0	101	Dimethyl phthalate [b]	10:1	S	100	-
135	Dibenz(A,H)anthracene [b]	-	S	-	92.9	111	Diethyl phthalate [b]	10:1	S	100	-
136	Benzo(G,H,I)perylene [b]	-	S	-	96.6	122	Di-*n*-butyl-phthalate [b]	10:1	S	-	-
Oxygenated aromatics						125	Benzyl butyl phthalate [b]	-	S	-	92.0
41	Anisole [d]	10:1	S	20.4	-	128	Bis(2-ethylhexyl)phthalate [b]	-	S	-	97.4
42	*p*-Benzoquinone [d]	10:1	S	94.8	-	129	Di-*n*-octyl phthalate [b]	-	S	-	90.6
45	Benzaldehyde [d]	10:1	S	82.8	-	**Others**					
47	Phenol [b]	75:1	S	100	-	49	Bis(2-chloroethyl)ether [b]	10:1	S	84.5	-

Table 3.2. continued.

No.	Species	Q_{ms}	Q_{mp}	S_{rec}	P_{rec}	No.	Species	Q_{ms}	Q_{mp}	S_{rec}	P_{rec}
55	*o*-Cresol [b]	10:1	S	100	-	53	2-Octanone [d]	10:1	S	97.0	-
58	*p*-Cresol [b]	75:1	S	100	-	54	Bis(2-chloro-1-methylethyl)ether [b]	10:1	S	100	-
59	3-Methylbenzaldehyde [d]	10:1	S	99.9	-	63	Nonanal [d]	10:1	S	100	52.3
60	2-Methylbenzaldehyde [d]	75:1	S	100	-	65	Isophorone [b]	10:1	S	96.4	-
61	2-Methoxyphenol [d]	75:1	S	100	-	70	1-nonanol [d]	10:1	S	98.6	-
64	2,6-Dimethylphenol [d]	75:1	S	100	100	72	Bis(2-chloroethoxy)methane [b]	10:1	S	100	-
66	2,3-dimethyl-2,5-cyclohexadiene-1,4-dione [d]	10:1	S	100	-	84	Pinane diol [d]	10:1	S	-	-
71	2,4-dimethylphenol [b]	10:1	S	89.5	-	104	Levoglucosan [d]	10:1	S	0	70.0
73	Benzoic acid [d]	10:1	S	-	-						
79	Mequinol [d]	10:1	S	60.4	-						
80	*m*-Guaiacol [d]	10:1	S	44.0	-						
85	Hydroquinone [d]	10:1	S	34.8	-						
86	Resorcinol [d]	10:1	S	76.0	-						
92	2,6-Dimethoxyphenol [d]	10:1	S	93.6	-						

To quantify the additional effect of breakthrough during sampling, tests were conducted for SPE disks to examine the retention of components adsorbed to their surface when subject to an air flow equivalent to the sample volume. SPE disks were spiked with the calibration mixture containing 96 compounds of interest (50 µL at 20 µg mL^{-1}, n = 4) and subject to a purified air flow of 6 L min^{-1} for 30 mins. The samples were extracted and analysed, and the signal compared with 4 × 50 µL spikes directly into 0.95 mL EtOAc. Figure 3.3 shows the relative enhancement of unpurged over purged samples. For more volatile components a value greater than zero was observed (Figure 3.3), which indicated breakthrough of the most volatile components and indicated good retention of components with a boiling point of around 225 °C (see the Supplementary Information 8.7 for results of individual species, see the Supplementary Information 8.8 for results of breakthrough testing). Concentrations measured for *n*-alkanes on SPE disks were also compared with concurrent measurements made during burning experiments using online thermal-desorption two-dimensional gas chromatography coupled to a flame ionisation detector. The measured concentrations for *n*-alkanes from *n*-nonane to *n*-dodecane were compared using both techniques, with measured concentrations similar for *n*-undecane/*n*-dodecane (bp = 216 °C, see the Supplementary Information 8.9) but not the smaller alkanes. This was interpreted to indicate little breakthrough for components less volatile than *n*-dodecane. These findings are in line with the US EPA certified methods for Resprep SPE disks (525.1, 506, 550.1, and 549.1), when used to quantitatively analyse drinking water, which show their suitability for quantitative measurement of species with a molecular weight of around naphthalene/acenaphthylene (bp = 218-280 °C). These results

indicate that for more volatile species with boiling points below 250 °C, SPE disks can only be used to make qualitative measurements at these sample times and flow rates.

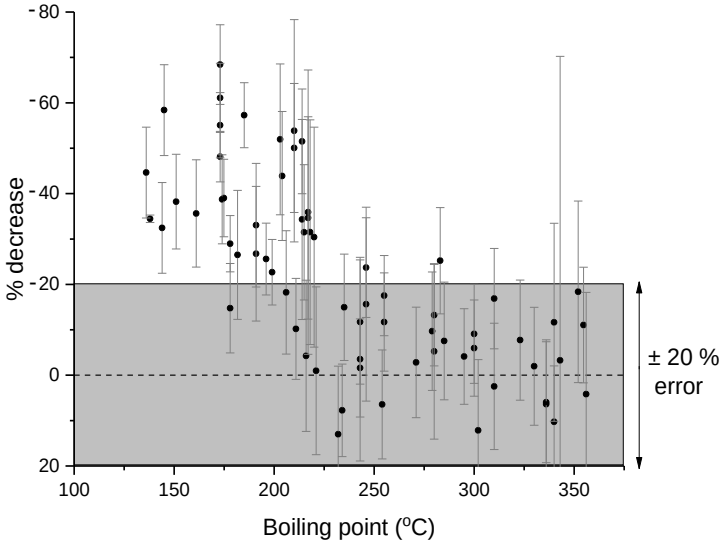

Figure 3.3. Relative reduction of purged over unpurged samples, presented as a percentage decrease of purged to unpurged signal. The standard deviation of replicate measurements is indicated by the error bars.

3.3. Results

3.3.1. Chromatography

Figure 3.4 shows chromatograms from I/SVOCs in the gas and particle phase from burning a cow dung cake sample collected from SPE disks and PTFE filters during a whole 30-minute burn, after passing through a dilution and cooling chamber. The saturation concentration C_i^* at 298 K is provided as an alternative x-axis and was calculated for each *n*-alkane, *i*, using:

$$C_i^* = \frac{M_i 10^6 \zeta_i P^o_{L,i}}{760RT} \qquad \text{E3.1}$$

where M_i = molecular weight of NMVOC *i* (g mol^{-1}), ζ_i = activity coefficient of NMVOC *i* in the condensed phase (assumed to be 1), $P^o_{L,i}$ = liquid vapour pressure of NMVOC *i* in Torr, *R* = gas constant (8.206×10^{-5} m^3 atm mol^{-1} K^{-1}) and *T* = temperature in Kelvin (Lu et al., 2018). The constant 760 Torr has been used to convert between units of atm and Torr where 1 atm = 760 Torr. $P^o_{L,i}$ values have been calculated from EPA Estimation Programme Interface Suite data at 298 K (EPA, 2012).

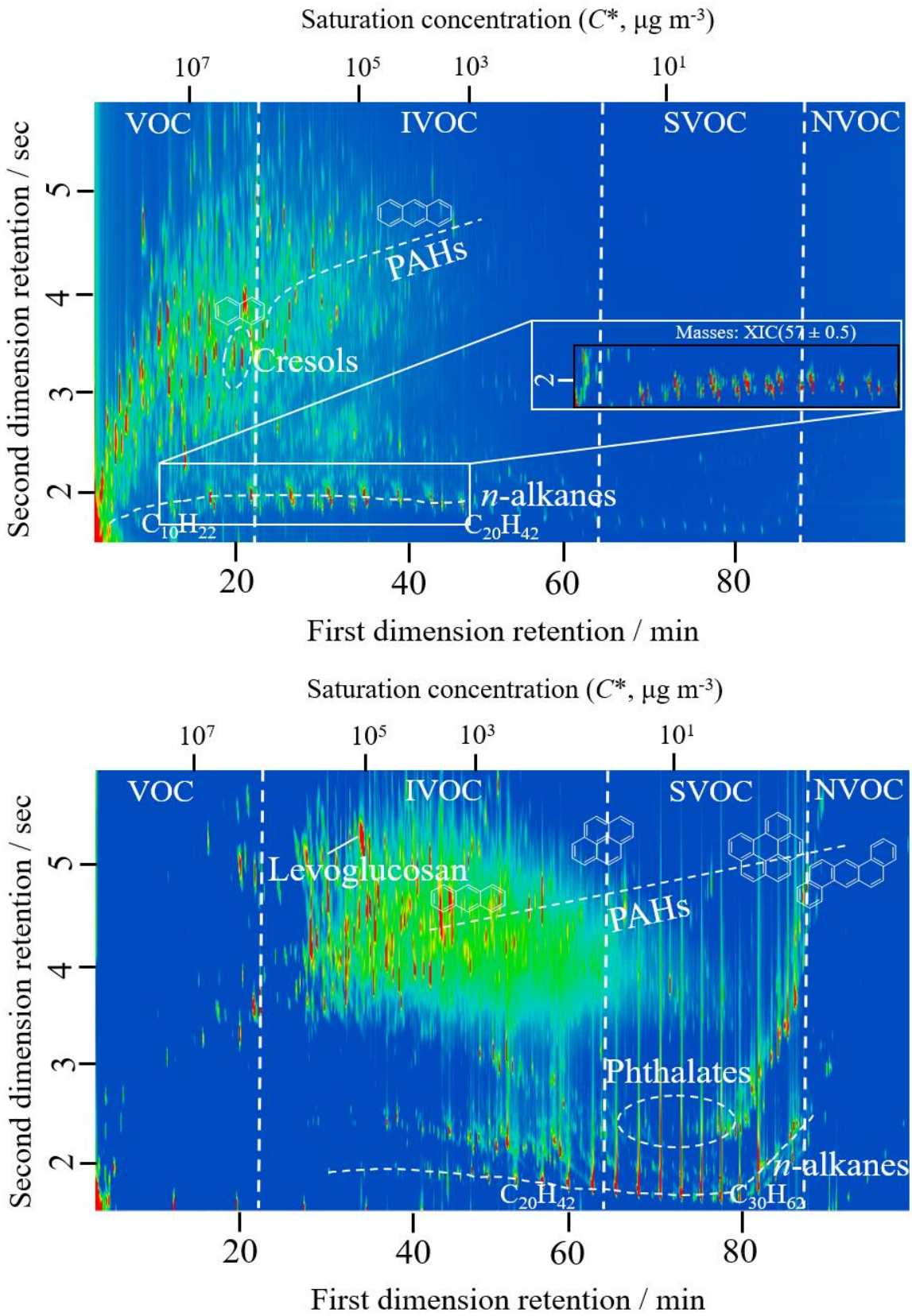

Figure 3.4. Chromatograms of extracted samples from entire burn of cow dung cake from SPE disk (top) and PTFE filter (bottom). *n*-Alkane and PAH series are marked on the chromatograms. The saturation concentration scale matches the *n*-alkane series. See the Supplementary Information 8.10 for a detailed compositional breakdown by functionality and phase.

The SPE disks showed 1297 peaks with unique mass spectra and captured gaseous NMVOCs and I/VOCs with C^* ~ 1×10^8 - 5×10^2 μg m^{-3} at 298 K. The largest peaks were from alkanes, 1-alkenes, limonene, phenolics, substituted naphthalenes, furans and substituted pyridines. The PTFE filters captured 1617 I/SVOCs and low- and extremely low-volatility NMVOCs (L/ELVOCs) with unique mass spectra present in the aerosol phase from C^* ~ 5×10^6-1×10^{-5} μg m^{-3} at 298 K. A transition can be seen in the two chromatograms from the gas to the aerosol phase. Species with a saturation vapour concentration less than 5×10^4 μg m^{-3} at 298 K were predominantly in the aerosol phase after passing though the dilution chamber. A large region of more polar components was present in the I/SVOC region from C^* 5×10^4-5×10^0 μg m^{-3} at 298 K and contained sugar pyrolysis products and highly substituted aromatics such as those with ketone, ether and di and trisubstituted phenol substituents. Many alkanes, from *n*-octadecane to *n*-triatriacontane were present, mainly in the SVOC region. The LVOC region was dominated by a series of sterols and stanols. GC×GC provided extremely high resolution to allow deconvolution of complex samples. The insert in Figure 3.4 shows how the complexity of the SPE chromatogram can be further resolved by looking at a single ion chromatogram, for example m/z = 57, which highlighted aliphatic non-polar peaks, with large peaks for alkanes from *n*-nonane to *n*-nonadecane.

Figure 3.5 shows that the complexity of emissions was vast, with almost 400 PAHs forming a group towards the top centre to right of the chromatogram. The most abundant calibrated PAH in the gas phase was naphthalene, followed by methyl and dimethyl naphthalene isomers. A range of methyl, dimethyl, tri and tetramethyl naphthalenes as well as ethyl, propyl, butyl and methyl propyl isomers were detected. Naphthalene isomers substituted with aldehydes, carboxylic acids and nitriles were also released. Biphenyl and a range of methyl, dimethyl and ethyl biphenyls were also released. A range of other PAHs such as acenaphthylene, fluorene, azulene, quinoline, chamazulene, benzophenone, stilbene and benzofurans along with their alkyl substituted isomers were also in the gas phase. A large amount of highly substituted, larger PAHs with more than 3 aromatics rings in their structure were present in the aerosol phase.

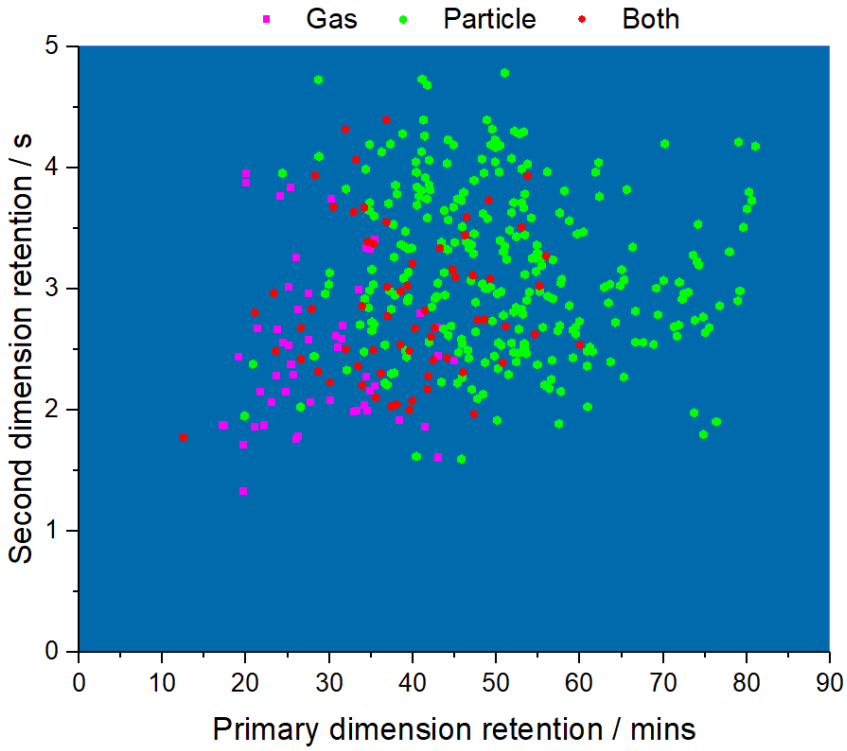

Figure 3.5. Gas and particle phase PAH emissions from burning cow dung cake.

Other peaks present on SPE disks and PTFE filters (SPE/PTFE) included alkenes (84/43), mostly towards the bottom of the chromatogram, along with a row of non-cyclic aliphatic (23/35) and cyclic aliphatic species (25/6). Above was a row of substituted aromatics (103/35), carboxylic acids (68/118) and sterols/stanols (1/63) as well as oxygenated hydrocarbons containing a range of ether, alcohol and aldehyde functionalities (229/234). Peaks were also present from oxygenated aromatics (106/145), phenols (54/122), substituted benzoic acids (15/27), furanic species (72/42), monoterpenes (2/1) and sulphur containing species (13/4).

A wide array of nitrogen containing NMVOCs were present in the cow dung cake samples, with peaks on SPE disks and PTFE filters (SPE/PTFE) from pyridines and pyrazines (43/35), amines (47/28), amides (38/37), nitriles (42/31), 6-membered heterocycles (13/14), 5-membered heterocycles including aromatics such as pyrroles as well as pyrazolines and pyrrolidines (50/45), 4-membered heterocycles (3/3), 3-membered heterocycles (4/1), nitrogen containing PAHs (14/24), imidazoles (9/12), imines (3/1) and azoles (23/10). Previous studies have measured the nitrogen content of cow dung cake to be as high as 1.9% (Stockwell et al., 2014) in comparison to other fuel types such as fuel woods (0.14-

0.35%), rice straws (0.4%) and coal (0.6%). The large amount of nitrogen containing NMVOCs are likely formed from the volatilisation and decomposition of nitrogen-containing compounds within the cow dung cake, such as free amino acids, pyrroline, pyridine and chlorophyll (Leppalahti and Koljonen, 1995; Burling et al., 2010; Ren and Zhao, 2015). Nitrogen containing NMVOCs are of concern because they can be extremely toxic (Ramírez et al., 2014; Farren et al., 2015) and amines in particular can change the hydrological cycle by leading to the creation of new particles (Smith et al., 2008; Kirkby et al., 2011; Yu and Luo, 2014) which act as cloud condensation nuclei (Kerminen et al., 2005; Laaksonen et al., 2005; Sotiropoulou et al., 2006).

Figure 3.6 shows a comparison of organic aerosol composition observed from different fuel types (LPG, fuel wood, sawdust and municipal solid waste). The measured emissions had very different compositions, reflecting the variability of organic components produced from different fuel types. Sawdust, municipal solid waste and cow dung cake (shown in Figure 3.4) emitted a wide range and complexity of species. Particle phase emissions from LPG burning were minimal, with most peaks from the internal standard or contaminants in the solvent. Fuel wood combustion released more organic components into the aerosol phase, with the majority of IVOCs with $C^* \sim 1.2\times10^{5}$-7×10^{1} μg m^{-3} at 298 K. The largest peak belonged to levoglucosan, with other peaks from monoaromatics with several polar substituents such as ethers and phenols, for example dimethoxyhydrotoluene and syringyl acetone. These were likely from the depolymerisation of lignin (Simoneit et al., 1993; Sekimoto et al., 2018), an amorphous polymer constituting about 25% of fuel woods (Sjöström, 1993) and formed of randomly linked, high-molecular weight phenolic compounds (Shafizadeh, 1982).

Sawdust, not a widely used fuel source, released many I/S/L/ELVOC components in the aerosol phase over a much wider range ($C^* \sim 5.8\times10^{5} – 1\times10^{-3}$ μg m^{-3} at 298 K). The largest peak was from levoglucosan, with another large peak from squalene. Many peaks were from polar substituted aromatics as well as many PAHs and their substituents, such as 2-methyl-9,10-anthracenedione. The largest peak from municipal solid waste burning was also levoglucosan, but this fuel type released fewer of the polar substituted monoaromatics than other fuels. Municipal solid waste released alkanes and SVOC species such as terphenyls, alkanes and many PAHs.

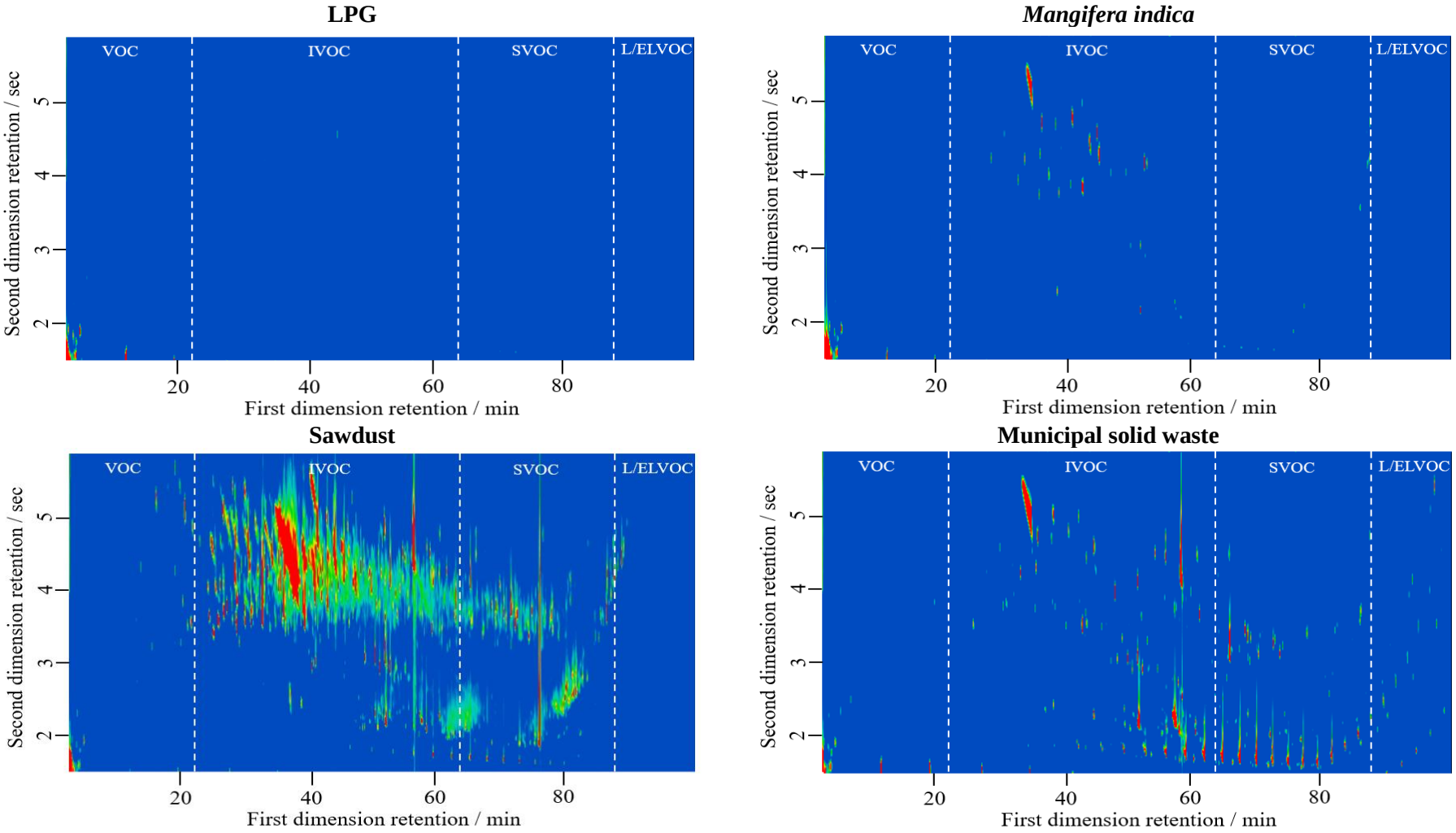

Figure 3.6. Measurements of organic aerosol from a range of different fuel types, with the contrast at the same scale.

3.3.2. Molecular markers for domestic fuels

Cow dung cake combustion emitted a range of sterols/stanols, which have been reported previously. Sheesley et al. (2003) suggested that 5β-stigmastanol, coprostanol and cholestanol could be used as tracers for emissions from cow dung cake burning. This is because in higher animals, anaerobic microbial reduction of sitosterol and cholesterol forms the distinctive β configuration of the C-5 proton of 5β-stigmastanol and coprostanol. This contrasts with the α C-5 proton caused by aerobic digestion in aquatic environments. Jayarathne et al. (2018) reported 5β-stigmastanol emissions from hardwood, and Fine et al. (2001) reported 5α- stigmastanol emissions from hardwood. Four fuel wood combustion experiments in our study showed emissions of an isomer of stigmastanol, a result similar to Jayarathne et al. (2018) that 5β-stigmastanol was not unique to cow dung cake burning or the MS measurement method used was unable to distinguish between 5α- and 5β-stigmastanol. Cholestanol and coprostanol were found uniquely during cow dung cake combustion in our study and suggested that these are unique tracers of this source.

Fuel wood combustion generally released fewer organic components into the aerosol phase than fuels such as cow dung cake, MSW and sawdust. Levoglucosan has been traditionally suggested as a tracer for biomass burning emissions, however, emissions of levoglucosan from a range of sources mean that this is of limited use as a unique tracer of woodsmoke emissions in regions with multiple burning sources. This could be resolved in future studies by examining the ratio of levoglucosan to other sugar pyrolysis products as the chemical composition of different sources should determine the emission ratio of levoglucosan to these pyrolysis products (Sheesley et al., 2003).

The presence of a wide range of terphenyls from municipal solid waste combustion in this study was not unique. Jayarathne et al. (2018) suggested triphenyl benzene to be a unique tracer of waste burning emissions. Whilst this study found triphenyl benzene present in one cow dung cake sample and in municipal solid waste samples, the waste combustion emitted on average 19 terphenyls, many more than from cow dung cake combustion (2). Terphenyls have been previously reported from incineration of waste (Tong et al., 1984) and our study suggests that these compounds are good indicators of municipal solid waste burning.

3.3.3. Total identification

Figures 3.7A and 3.7B show a comparison of the relative abundance of peaks identified, defined here as the sum of peak areas identified and calibrated using genuine standards for compounds present in the SPE and PTFE samples compared to the total observed peak area (using the blank subtracted total ion current, TIC).

Figure 3.7A shows that between 15 and 100% of the peak area of the TIC in the SPE chromatogram could be identified. The highest proportion of species that could be identified was from fuel wood (67%), followed by crop residue (57%), charcoal (48%), municipal solid waste (46%), cow dung cake (39%) and sawdust (16%). Lower total identification in samples such as cow dung cake was due to increased complexity of emissions, which were not covered by the standards used.

Figure 3.7B shows that between 7 – 100% of the organic composition of aerosol released from burning was identified. Generally, a much lower proportion of organic matter within aerosol samples was identified due to a lack of genuine standards available, particularly in complex samples. The lowest mean relative contribution identified from samples was sawdust (9%), followed by cow dung cake (11%) and municipal solid waste (16%). A larger relative contribution was identified from fuel woods (34%) and charcoal (39%) due to less complex emissions. A large relative contribution of some fuel woods was identified from *Saraca indica* (91%) and *Pithecellobium spp* (82%), due to a low amount of organic matter released from these samples. This also influenced the percentage identification from crop residue which achieved 46% identification, due to only 3 samples with 98% identification from *Solanum melongena* but only 26% from *Cocos nucifera* and 13% from *Brassica spp*. 100% of the aerosol released from LPG was quantified due to little being released into the aerosol phase and this was principally composed of PAHs. These low levels of identification of organic aerosol are in line with those reported by Jen et al. (2019) where unknown chemical species represented 35-90% of the observed organic aerosol mass from biomass burning samples.

3.3.4. Composition

Figure 3.7C provides an indication of I/SVOC composition on SPE disks by mass of quantified species, assuming no compound breakthrough. Phenolic and furanic compounds were the most abundant I/SVOC species released from all fuel types, except for LPG. As a proportion of the total mass of species quantified with genuine standards on SPE disks, phenols released from fuel woods (22-80%) represented the largest range, with large amounts released from municipal solid waste (24-37%), cow dung cake (32-36%), crop residue (32-57%) and sawdust (46%). High emissions of phenolic compounds were of significance because phenolics contribute significantly to SOA production from biomass-burning emissions (Yee et al., 2013; Lauraguais et al., 2014; Gilman et al., 2015; Finewax et al., 2018).

Large emissions of furanic species were measured from fuel wood (6-59%), municipal solid waste (35-45%), cow dung cake (39-42%), crop residue (25-44%) and sawdust (43%). These were important as furanics can be toxic and mutagenic (Ravindranath et al., 1984; Peterson, 2006; Monien et al., 2011; WHO, 2016) and have been shown to be some of the species with the highest OH reactivity from biomass burning emissions (Hartikainen et al., 2018; Coggon et al., 2019). Furanics have also been shown to result in SOA production (Gómez Alvarez et al., 2009; Strollo and Ziemann, 2013) with 8-15% of SOA produced from combustion of black spruce, cut grass, Indonesian peat and ponderosa pine estimated to originate from furanics and 28-50% of SOA from rice straw and wiregrass (Hatch et al., 2015). Furanics from biomass burning emissions are thought to come from low temperature depolymerisation of hemi-cellulose (Sekimoto et al., 2018) and from large alcohols and enols in high-temperature regions of hydrocarbon flames (Johansson et al., 2016).

Emissions of alkanes were most important from combustion of cow dung cake and municipal solid waste (4-9%), with only small quantities released from combustion of various fuel woods (< 2%) and crop residues (< 1%). This reinforced previous studies which found emissions of C_{12}-C_{39} *n*-alkanes from municipal waste incinerators (Karasek and Tong, 1985). PAH emissions represented (3 – 15%) of the total quantified emission by mass for fuel types other than LPG and have carcinogenic and mutagenic properties (IARC, 1983,

1984; Nisbet and LaGoy, 1992; Lewtas, 2007; Zhang and Tao, 2009; Jia et al., 2011). They can damage cells through the formation of adducts with DNA in many organs such as the kidneys, liver and lungs (Vineis and Husgafvel-Pursiainen, 2005; Xue and Warshawsky, 2005).

Figure 3.7D shows the quantified aerosol mass was largely dominated by levoglucosan, with a particularly significant contribution in the fuel wood samples (13-98%). This was similar to a previous study of fuel wood samples from Bangladesh, where levoglucosan was the largest contributor to aerosol mass (Sheesley et al., 2003). Levoglucosan emissions were also large from cow dung cake (30-58%), which contrasted with the findings of Sheesley et al. (2003). This could be due to differences in the feeding of cows leading to differences in residual undigested organic matter in cow dung cake fuel as well as differences in preparation between samples collected in Bangladesh and those in this study, which had additional dried biogenic material, such as straw, mixed into samples. Levoglucosan emissions were also high from sawdust (91%), crop residue (19-85%) and municipal solid waste (58-75%), with municipal solid waste emissions likely from cellulosic material collected with the fuel.

Levoglucosan emissions from charcoal (76%) were significant as a proportion of emissions. Emissions from charcoal were low, which meant that a small emission of levoglucosan represented a large proportion of total emissions. It was likely that the fuel collected here may have contained small amounts of cellulosic organic matter that led to the emission of levoglucosan.

Emissions of alkanes in the gas and particle phases were similar by source type, with particulate alkanes emitted principally during the combustion of cow dung cake and municipal solid waste fuels. Emissions of particulate phenolics were large as a proportion of total quantified mass with genuine standards when the total emission of other components was low. For example, phenolics represented a large proportion of emissions from the fuel wood species *Morus spp* and *Pithecellobium spp* with the mass principally from dimethoxyphenols. Emissions from LPG were mainly PAHs and very low.

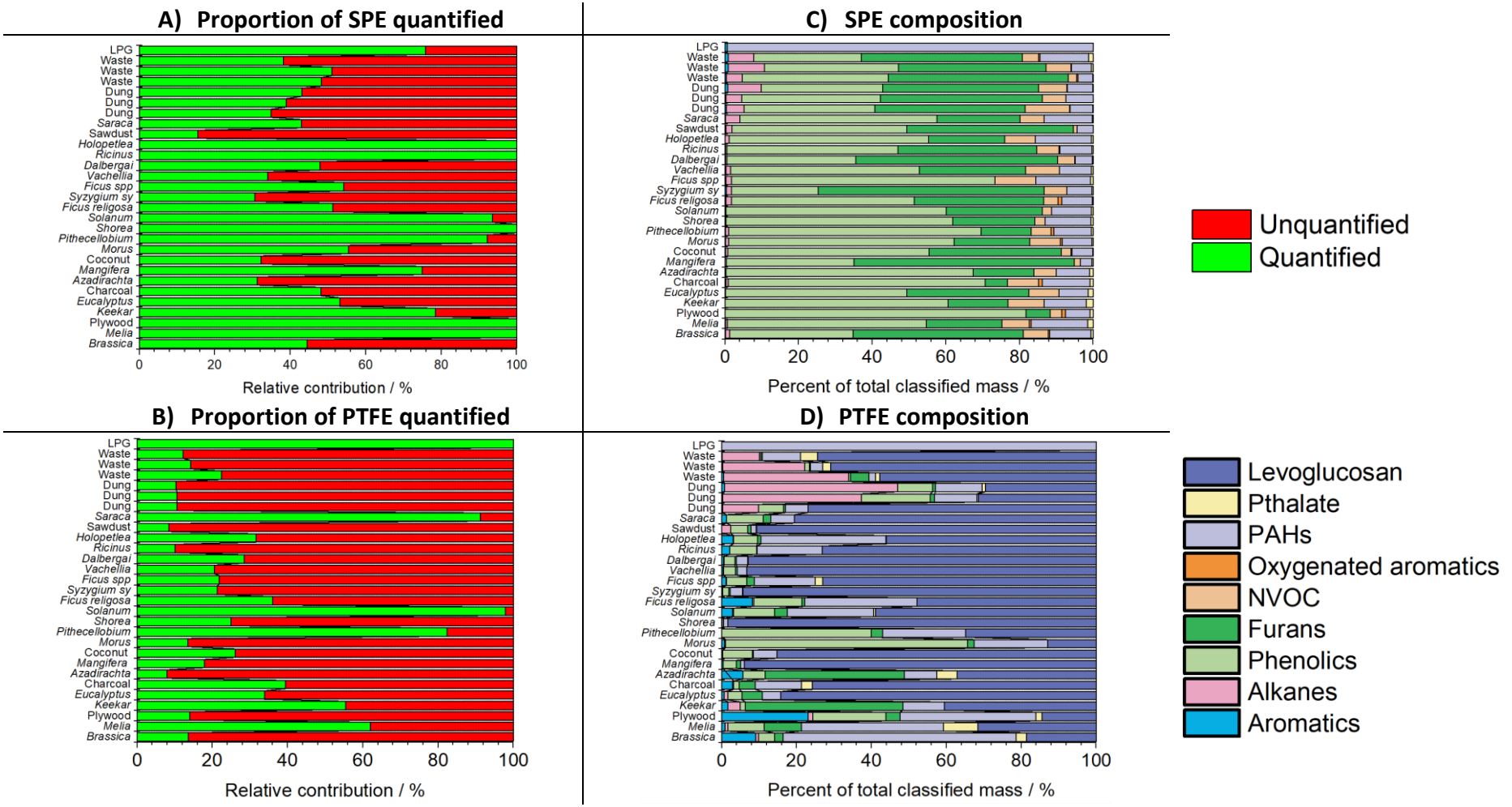

Figure 3.7. Area of organic matter quantified with genuine standards, as a fraction of total ion current (TIC) (3.7A and 3.7B, left panel). Semi-quantitative/quantitative analysis of SPE/PTFE fraction (3.7C and 3.7D, right panel).

Whilst SPE samples for these compounds remained semi-quantitative due to slight breakthrough, the detection of high emissions of phenolics and furanics in the gas phase from burning was in line with recently published studies (Hatch et al., 2015; Stockwell et al., 2015; Koss et al., 2018). Relatively low levels of total quantified material within the aerosol phase was in line with the current literature (Jen et al., 2019), but meant that this analysis was not entirely reflective of the organic fraction for complex samples. It is likely that this study overemphasises the contribution of levoglucosan in complex aerosol samples, relative to other components present at lower levels (Sheesley et al., 2003; Jen et al., 2019). Future instrument development could allow better quantification of complex burning and ambient samples by splitting the eluent between a -MS and -FID. This study suggests that future research uses lower sample volumes, thicker SPE disks and studies the adsorption characteristics of NMVOCs to the surfaces of these disks.

3.3.5. Development of emission factors

Emission factors have been developed for PAHs (see Figure 3.8) by calculating the total volume of air convectively drawn up the flue, using measurements of gas velocity up the sample hood from partners at CSIR-NPL, and relating this to the mass of fuel burnt (see the Supplementary Information 8.11 for details of calculation). Emission factors for sawdust (1240 mg kg^{-1}), municipal solid waste (1020 mg kg^{-1}), crop residue (747 mg kg^{-1}) and cow dung cake (615 mg kg^{-1}) were generally larger than for fuel wood (247 mg kg^{-1}), charcoal (151 mg kg^{-1}) and LPG (56 mg kg^{-1}). The measurement of higher emission factors for cow dung cake than fuel wood was similar to that reported previously (Bhargava et al., 2004; Gadi et al., 2012). A wide range of emission factors were measured from combustion of fuel woods from 50 mg kg^{-1} for *Prosopis* to 907 mg kg^{-1} for *Ficus religosa*. For most fuel types, PAH emissions in the gas phase were dominated by naphthalene, methylnaphthalenes and dimethylnaphthalenes with gas-phase PAHs observed up to pyrene. For fuel wood, crop residue, municipal solid waste and cow dung cake the percentage of PAHs in the gas phase decreased from 97%, 96%, 91% to 89%. PAHs from LPG showed the largest fraction in the gas phase (99.9%) compared to the aerosol phase (0.1%). Figure 3.9 shows gas and particle phase PAH emissions by individual fuel type, excluding naphthalene as well as C_1- and C_2-substituted naphthalenes. PAHs were present in the aerosol phase from dibenzofuran ($C_{12}H_8O$) to benzo(ghi)perylene ($C_{22}H_{12}$).

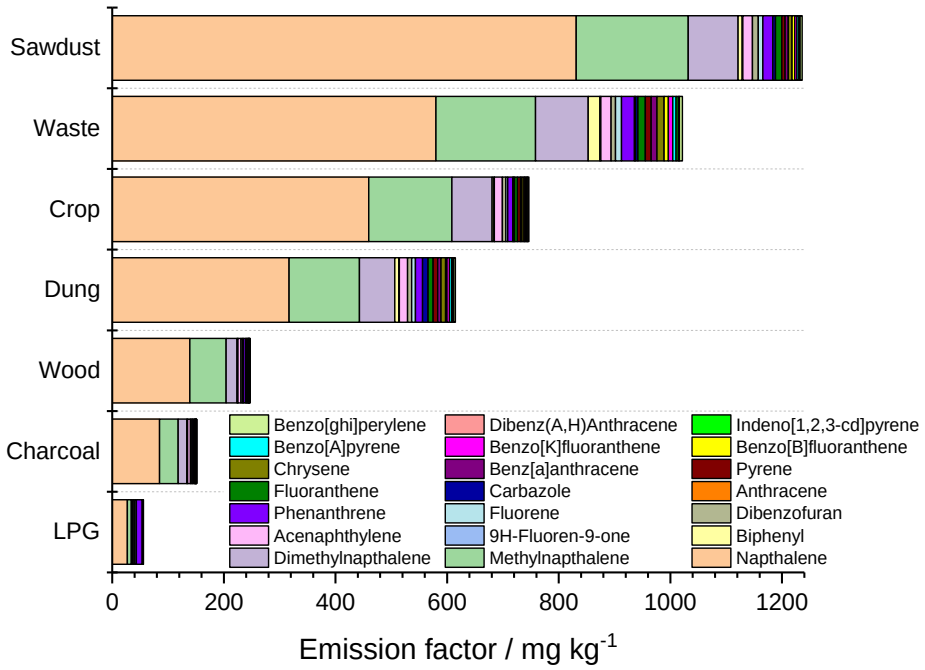

Figure 3.8. Mean PAH emission factors by fuel type.

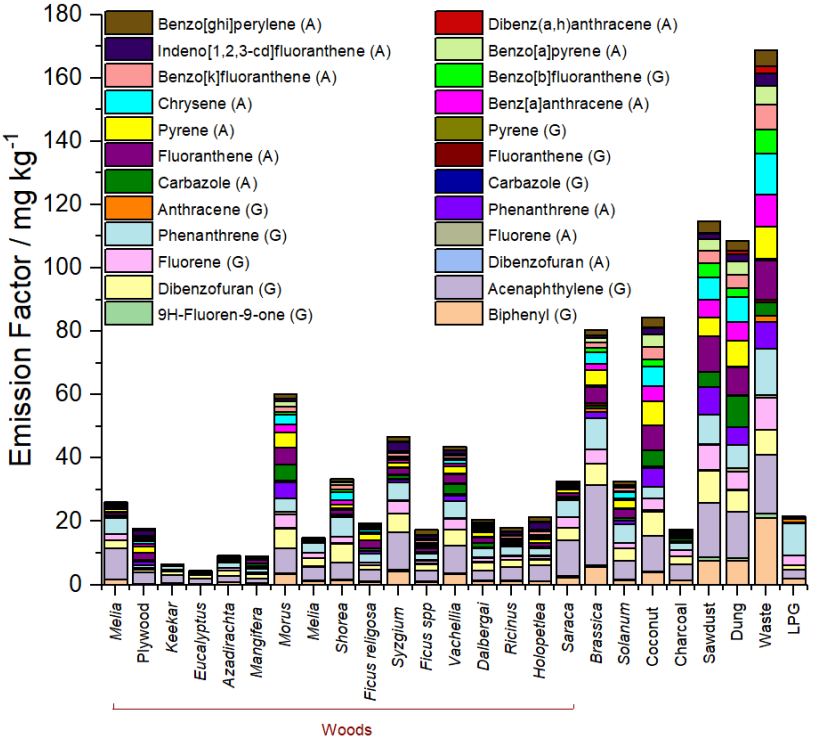

Figure 3.9. Emission factors of PAHs measured from SPE/PTFE where G and A represent gas- and aerosol-phase samples, respectively, excluding naphthalene as well as naphthalenes with C_1 and C_2 substituents.

Table 3.3 shows a comparison of the mean emission factors measured in our study with previous studies. The mean fuel wood total PAH emission factor measured in our study (247 mg kg^{-1}) was a factor 4.7-5.6 larger than those measured by Gadi et al. (2012) and Singh et al. (2013) of 44 and 53 mg kg^{-1}, respectively, for similar fuel woods collected across New Delhi and the Indo-Gangetic Plain. The PAH emission factor measured for cow dung cake (615 mg kg^{-1}) was around a factor of 10 larger than those previously measured (60 mg kg^{-1}). The larger total emission factors for fuel wood and cow dung cake were a result of high emissions of gas-phase PAHs measured using PTR-ToF-MS (51-896 mg kg^{-1} for fuel wood and 446-660 mg kg^{-1} for cow dung cake) compared with previous measurements made using PUF plugs (7 mg kg^{-1}). This indicated that either the PTR-ToF-MS was able to better detect and characterise gas-phase emissions than previous methods and suggested either breakthrough or off gassing of smaller gas-phase PAHs from PUF plugs or measurement of significant quantities of other $C_{10}H_8$ isomers on the PTR-ToF-MS. This may highlight an underestimation of 2-ring gas-phase PAH emissions in previous burning studies. Gadi et al. (2012) measured PAH emissions in the particle phase, with the mean emission for fuel wood (44 mg kg^{-1}) greater than our study (9 mg kg^{-1}). Particulate phase emissions of PAHs measured by Singh et al. (2013) from fuel wood (45 mg kg^{-1}) were also larger than our study. By contrast, particle phase PAH emissions from cow dung cake in our study (66 mg kg^{-1}) were comparable to those measured previously of 57-60 mg kg^{-1} (Gadi et al., 2012; Singh et al., 2013). Variability in emission of particulate-phase PAHs in our study compared to literature was likely to be influenced by the efficiency of combustion of different fuel types. Although not measured in our study, differences in moisture content between fuel types in our study and literature were likely have a large influence on the total amount of PAHs emitted and may explain the differences in particle-phase emissions.

The particulate phase PAH emission factors from municipal solid waste combustion in our study (14-181 mg kg^{-1}) were much smaller than those of previous studies (1910-8486 mg kg^{-1}), but the number of samples was limited. Emissions from coconut shell have not been well studied, making comparisons difficult (Gulyurtlu et al., 2003). The emission of particulate phase PAHs from sawdust in our study (62 mg kg^{-1}) was less than that previously reported 259 mg kg^{-1}, but our study found large gas phase PAH emissions (1175 mg kg^{-1}). Particulate PAH emissions from the crop residue burnt in our study (13-53 mg kg^{-1}) fell

within the range reported by Kim Oanh et al. (2015) of 0.34-34 mg kg^{-1} for rice straw. Those reported by Wiriya et al. (2016) were smaller (0.47 mg kg^{-1}), but were from fuel dried in an oven at 80 ^{o}C for 24 hours and ignited by an LPG burner and were likely to represent more complete combustion conditions. Emissions of PAHs from charcoal in our study (151 mg kg^{-1}) were larger than those measured for South Asian fuels (25 mg kg^{-1}), caused principally by larger measurement of gas-phase species by PTR-ToF-MS. Both our study, and that of Kim Onah et al. (1999) showed charcoal released the least amount of PAH per kg burnt for biofuels. LPG combustion released less particulate PAHs (0.1 mg kg^{-1}) than previous studies (0.8 mg kg^{-1}), but also included a small gas-phase emission (56 mg kg^{-1}). Differences in the distribution of PAHs found in the gas and aerosol phases between our study and literature were also likely to be influenced by the different sample dilutions and gas-to-aerosol partitioning prior to measurement.

Table 3.3. PAH emission factors measured in our study compared to literature.

Fuel	**PAH (mg kg^{-1})**			
	Gas	**Particle**	**Total**	**Ref**
Wood	51-896	0.4-34	51-907	Our study
		1-12		(Hosseini et al., 2013)
	22-111	0.4-6	24-114	(Kim Oanh et al., 2005)
	-	44	44	(Gadi et al., 2012)
	7	45	52	(Singh et al., 2013)
		805-7294		(Kakareka et al., 2005)
			43	(Lee et al., 2005)
	66	0.8	67	(Kim Oanh et al., 2002)
	105	4	105	(Kim Oanh et al., 1999)
Dung	446-660	48-98	493-710	Our study
	-	59	-	(Gadi et al., 2012)
	3	57	60	(Singh et al., 2013)
Waste	696-1233	14-181	776-1414	Our study
	-	8486	8486	(Kakareka et al., 2005)
	-	1910	1910	(Young Koo et al., 2013)
Crop	205-1231	13-53	219-1255	Our study
	-	-	5-683	(Jenkins et al., 1996)
	-	-	3-50	(Lu et al., 2009)
	-	-	129-569	(Wei et al., 2014)
	5-230	0.3-34	5-264	(Kim Oanh et al., 2015)
	-	0.47	-	(Wiriya et al., 2016)
Sawdust	1175	62	1236	Our study
		259	261	(Kim Oanh et al., 2002)
Charcoal	147	4	151	Our study
	25	0.1	25	(Kim Oanh et al., 1999)
LPG	56	0.1	56	Our study
Coal	-	0.8	-	(Geng et al., 2014)

3.4. Conclusions

This study demonstrated an extraction technique for analysis of I/SVOCs collected onto SPE disks and PTFE filters from combustion of biofuels, which was well suited to the analysis of non-polar species. A range of fuels relevant to burning in India were combusted with organic components collected and analysed, which showed large differences in the composition of organic matter released. The separation power of GC×GC has been used to identify an extensive range of I/SVOCs in both gas and particle phases with 15-100% of gas-phase emissions and 7-100% of particle-phase emissions characterised.

The ability to quantify species on SPE disks was assessed and scope for future studies which should assess the adsorption characteristics of IVOCs onto SPE disks has been provided. It is recommended that breakthrough of IVOCs collected onto SPE disks at lower sample volumes is evaluated, and better methods for quantification of complex samples are developed. Further fuel types from a wider range of sources would enable a better understanding of the drivers of poor air quality in the developing world, such as crop residue burning. This study found that cholestanol and coprostanol were unique to cow dung cake burning samples and these species were therefore suggested as tracers for emissions from cow dung cake burning. Similarly, municipal solid waste burning released many terphenyls, which could act as good indicators of this source. This study found that phenolic and furanic species were the most important gas-phase emissions by mass of I/SVOCs from biomass burning. New emission factors were developed for US EPA criteria PAHs present in gas and aerosol phases from a large range of fuel types. This suggested that many sources important to air quality in the developing world are larger sources of PAHs than conventional fuel wood burning.

Chapter 4

Emissions of non-methane volatile organic compounds from combustion of domestic fuels in Delhi, India

The majority of this chapter has been published as a manuscript under the same name:

Gareth J. Stewart, W. Joe F. Acton, Beth S. Nelson, Adam R. Vaughan, James R. Hopkins, Rahul Arya, Arnab Mondal, Ritu Jangirh, Sakshi Ahlawat, Lokesh Yadav, Sudhir K. Sharma, Rachel E. Dunmore, Siti S. M. Yunus, C. Nicholas Hewitt, Eiko Nemitz, Neil Mullinger, Ranu Gadi, Lokesh. K. Sahu, Nidhi Tripathi, Andrew R. Rickard, James D Lee, Tuhin K. Mandal and Jacqueline F. Hamilton. *Atmos. Chem. Phys.,* 21, 2383–2406, 2021.
https://doi.org/10.5194/acp-21-2383-2021

4.1. Introduction

Biomass burning is the second largest source of trace gases to the troposphere, releasing around a half of global CO, ~ 20% of NO and ~ 8% of CO_2 emissions (Olivier et al., 2005; Wiedinmyer et al., 2011; Andreae, 2019). Biomass burning releases an estimated 62 Tg yr^{-1} of non-methane volatile organic compounds (NMVOCs) (Andreae, 2019) and is the dominant source of both black carbon (BC) and primary organic aerosol (POA), representing 59% and 85% of global emissions respectively (Bond et al., 2013). Biomass burning includes open vegetation fires in forests, savannahs, agricultural burning and peatlands (Chen et al., 2017) as well as the biofuels used by approximately 3 billion people to meet their daily cooking and heating energy requirements worldwide (World Bank, 2020). A wide range of trace gases are released from biomass burning, in different amounts depending on the fuel type and the combustion conditions, meaning that detailed studies at the point of emission are required to accurately characterise emissions. The gases released lead to soil-nutrient redistribution (Ponette-Gonzalez et al., 2016; N'Dri et al., 2019), can themselves be toxic (Naeher et al., 2007) and can significantly degrade local, regional and global air quality through the photochemical formation of secondary pollutants such as ozone (O_3) (Pfister et al., 2008; Jaffe and Wigder, 2012) and secondary organic aerosol (SOA) (Alvarado et al., 2015; Kroll and Seinfeld, 2008). They can also lead to indoor air quality issues (Fullerton et al., 2008).

Emissions from biomass burning and their spatial distribution remain uncertain and estimates by satellite retrieval vary by over a factor of three (Andreae, 2019). Bottom-up approaches use information about emission factors and fuel usage. However, information for many developing countries, where solid fuels are a primary energy source, is particularly sparse. Toxic pollution from burning has been linked to chronic bronchitis (Akhtar et al., 2007; Moran-Mendoza et al., 2008), chronic obstructive pulmonary disease (Dennis et al., 1996; Orozco-Levi et al., 2006; Rinne et al., 2006; Ramirez-Venegas et al., 2006; Liu et al., 2007; PerezPadilla et al., 1996), lung cancer (Liu et al., 1993; Ko et al., 1997), childhood pneumonia (Smith et al., 2011), acute lower respiratory infections (Bautista et al., 2009; Mishra, 2003) and low birth weight of children (Boy et al., 2002; Yucra et al., 2011). Smoke from inefficient combustion of domestic solid fuels is the leading cause of conjunctivitis in developing countries (West et al., 2013). The harmful emissions from burning also resulted

in an estimated 2.8-3.9 million premature deaths due to household air pollution (Kodros et al., 2018; World Health Organization, 2018b; Smith et al., 2014), of which 27% originated from pneumonia, 18% from strokes, 27% from ischaemic heart disease, 20% from chronic obstructive pulmonary disease and 8% from lung cancer, with hazardous indoor air pollution responsible for 45% of pneumonia deaths in children less than 5 years old (World Health Organization, 2018b). For this reason, hazardous indoor air pollution from the combustion of solid fuels has been calculated to be the most important risk factor for the burden of disease in South Asia from a range of 67 environmental and lifestyle risks (Lim et al., 2012; Smith et al., 2014).

The emissions from biomass burning fires are complex and can contain many hundreds to thousands of chemical species (Crutzen et al., 1979; McDonald et al., 2000; Hays et al., 2002; Hatch et al., 2018). Measurements of emissions by gas chromatography (GC) have been made (EPA, 2000; Wang et al., 2014; Gilman et al., 2015; Stockwell et al., 2016; Fleming et al., 2018), as it has the potential to provide isomeric speciation of emissions. However, it is of limited use in untargeted measurements from burning due to the complexity of emissions, leading to large amounts of NMVOCs released not being observed. Some of the main issues are that GC does not provide high time resolution measurements and several instruments with different column configurations and detectors are required to provide information on different chemical classes. Samples can also be collected into canisters or sample bags and then analysed off-line (Wang et al., 2014; Sirithian et al., 2018; Barabad et al., 2018), which can increase time resolution, but can also lead to artefacts (Lerner et al., 2017).

Recent developments have allowed the application of proton-transfer-reaction mass spectrometry (PTR-MS) to study the emissions from biomass burning (Warneke et al., 2011; Yokelson et al., 2013; Brilli et al., 2014; Stockwell et al., 2015; Bruns et al., 2016; Koss et al., 2018). PTR-MS uses proton transfer from the hydronium ion (H_3O^+) to ionise and simultaneously detect most polar and unsaturated NMVOCs including aromatics, oxygenated aromatics, alkenes, furanics and nitrogen containing volatile organic compounds in gas samples. PTR-MS can measure at fast acquisition rates of up to 10 Hz over a mass range of 10 – 500 Th with very low detection limits of tens to hundreds of pptv (Yuan et al., 2016). The more recently-developed technique of proton-transfer-reaction

time-of-flight mass spectrometry (PTR-ToF-MS) has allowed around 90% of total measured NMVOC emissions in terms of mixing ratio from burning experiments to be speciated (Koss et al., 2018) and has also been used to study the formation of SOA (Bruns et al., 2016). The main disadvantages of the PTR-ToF-MS technique are its inability to speciate isomers, significant fragmentation of parent ions, only being able to detect species with a proton affinity greater than water and the formation of water clusters needing to be considered (Stockwell et al., 2015; Yuan et al., 2017). More recently, measurements have also been made using iodide chemical ionization time-of-flight mass spectrometry (I^--CIMS), which is well suited to measuring acids and multifunctional oxygenates (Lee et al., 2014) as well as isocyanates, amides and organo-nitrate species released from biomass burning (Priestley et al., 2018). Multiple measurement techniques used in concert are therefore complementary, with the use of PTR-ToF-MS and simultaneous gas chromatography often alleviating some of the difficulties highlighted above.

Since the start of the century, rapid growth has resulted in India becoming the second largest contributor to NMVOC emissions in Asia (Kurokawa et al., 2013; Kurokawa and Ohara, 2020). However, effective understanding of the relative strength of different sources and subsequent mitigation has been limited by a deficiency of suitably detailed, spatially disaggregated emission inventories (Garaga et al., 2018). One study estimated that approximately 60% of total NMVOC emissions from India in 2010 were due to solid fuel combustion (Sharma et al., 2015). However, a need has been identified to measure local source profiles to allow evaluation with activity data to better understand the impact of unaccounted and unregulated local sources (Pant and Harrison, 2012).

Approximately 25% of worldwide residential solid fuel use takes place in India (World Bank, 2020), with approximately 25% of ambient particulate matter in South Asia attributed to cooking emissions (Chafe et al., 2014). Despite large government schemes, traditional solid fuel cookstoves remain popular in India because they are cheaper than ones that use liquefied petroleum gas (LPG) and the meals cooked on them are perceived to be tastier (Mukhopadhyay et al., 2012). The total number of biofuel users has been sustained by an increasing population, despite the percentage use of biofuels decreasing as a proportion of overall fuel use due to increased LPG uptake (Pandey et al., 2014). Cow dung cakes remain prevalent as a fuel because they are cheap, readily available, sustainable and ease pressure

on local fuel wood resources. Few studies have reported emissions data from cow dung cake (Venkataraman et al., 2010; Stockwell et al., 2016; Koss et al., 2018; Fleming et al., 2018), leaving considerable uncertainty over the impact that cow dung cake combustion has on air quality. LPG usage has increased to around 500 million users, but only reflects around 10% of current rural fuel consumption (Gould and Urpelainen, 2018).

India-specific inventories which include residential burning indicate a considerable emission source of total NMVOCs of around 6000-7000 kt yr^{-1} (Pandey et al., 2014; Sharma et al., 2015). Burning is likely to have a large impact on air quality in India, but considerable uncertainties exist over the total amount of NMVOCs released owing to a lack of India specific emission factors and information related to the spatial distribution of emissions.

Few studies exist measuring highly speciated NMVOC emission factors from fuels specific to India. Recent studies using PTR-ToF-MS to develop emission factors, which are more reflective of the range of species emitted from burning, have focussed largely on grasses, crop residues and peat (Stockwell et al., 2015) as well as fuels characteristic of the western U.S. (Koss et al., 2018). A previous study measured emission factors of NMVOCs from cow dung cake using gas chromatography with flame ionisation detection (GC-FID) of 8-32 g kg^{-1} (EPA, 2000). Fleming et al. (2018) quantified 76 NMVOCs from fuel wood and cow dung cake combustion using *chulha* and *angithi* stoves by collecting samples into Kynar bags, transferring their contents into canisters and off-line analysis using GC-FID, GC-ECD (electron capture detector) and GC-MS. The emission factors measured from these 76 NMVOCs were 14 g kg^{-1} for cow dung cake burnt in *chulha* stoves, 27 g kg^{-1} for cow dung cake burnt in *angithi* stoves and 6 g kg^{-1} for fuel wood burnt in *angithi* stoves. An emission factor from one single dung burn measured using PTR-ToF-MS was considerably larger at around 66 g kg^{-1} (Koss et al., 2018). Emissions from dung in Nepal have also been measured (Stockwell et al., 2016) by sampling into whole air sample canisters followed by off-line analysis with GC-FID/ECD/MS and Fourier-transform infrared spectroscopy (FTIR). However, very few speciated NMVOC measurements were made and the emission factors were similar to those measured using just GC (Fleming et al., 2018). Studies have also focussed on making detailed measurements, using a range of techniques, from the burning of municipal solid waste (Christian et al., 2010; Yokelson et al., 2011; Yokelson et al., 2013;

Stockwell et al., 2015; Stockwell et al., 2016; Sharma et al., 2019) and crop residues (Stockwell et al., 2015; Koss et al., 2018; Kumar et al., 2018).

Detailed chemical characterisation of NMVOC emissions from fuel types widely used in the developing world is much needed to resolve uncertainties in emission inventories used in regional policy models and global chemical transport models. A greater understanding of the key sources is required to characterise and hence understand air quality issues to allow the development of effective mitigation strategies. In this study we measure emission factors of NMVOCs from a range solid fuels characteristic to northern India.

4.2. Methods

4.2.1. Fuel collection and burning facility

A total of 76 fuels, reflecting the range of fuel types used in northern India, were collected from across Delhi (see Figure 4.1 and Table 4.1). Cow dung cake usage was prominent in the north and west regions, whereas fuel wood use was more evenly spread across the state. Municipal solid waste was collected from Bhalaswa, Ghazipur and Okhla landfill sites. Collection also included less used local fuel types which were found being burnt including crop residues, sawdust and charcoal. A low-cost LPG stove, widely promoted across India as a cleaner fuel through government initiatives such as the Pradhan Mantri Ujjwala Yojana scheme, was used for direct emission comparison with other local fuel types.

Fuels were burnt at the CSIR-National Physical Laboratory (NPL), New Delhi, under controlled conditions utilizing a combustion chamber based on the design of Venkataraman and Rao, (2001), with a schematic given in the Supplementary Information 8.12 alongside additional information about sample collection. Several previous studies have been based on this chamber design (Venkataraman and Rao, 2001; Venkataraman et al., 2002; Saud et al., 2011; Saud et al., 2012; Singh et al., 2013), which was designed to simulate the convection-driven conditions of real-world combustion. The burn-cycle used in this study was adapted from the VITA water-boiling test, which was designed to simulate emissions from cooking and included emissions from both low- and high-temperature burning conditions. Fuels were collected and stored in the same manner as local customs using expert local judgement. This was designed to ensure that the moisture content of fuel wood samples was like those being burnt locally and that the combustion replicated real-

world burning conditions encountered in local cooking practices to give a more realistic NMVOC emission factor.

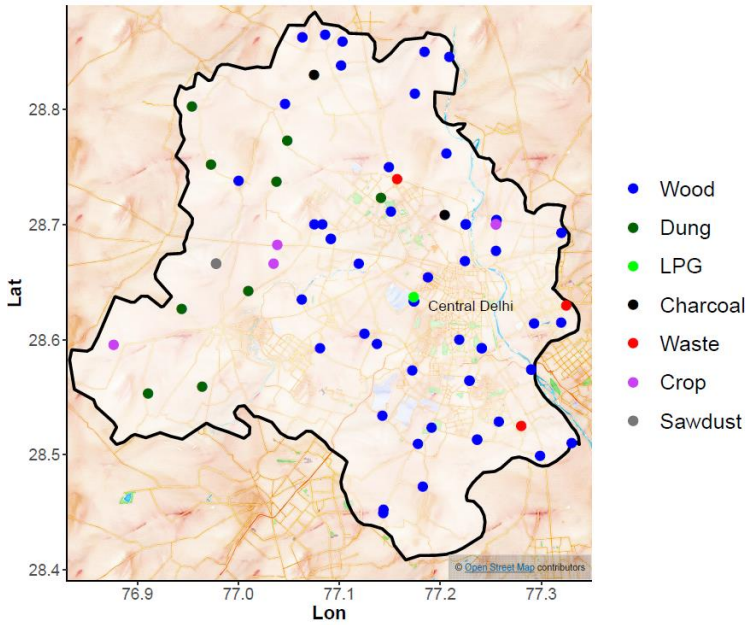

Figure 4.1. Locations across Delhi used for the local surveys into fuel use and collection of representative biomass fuels. Map tiles by Stamen Design. Data by © OpenStreetMap contributors 2020. Distributed under a Creative Commons BY-SA License.

Table 4.1. Types and numbers of fuels burnt, the mean emission factor of total NMVOCs (TVOC) in g kg^{-1} measured and standard deviation (SD) from all available burns. Discussion of TVOC calculation is given in the text.

Fuel woods	***n***	**TVOC**	**SD**	**Other**	***n***	**TVOC**	**SD**
Azadirachta indica	3	18.6	7.9	Cow dung cake	8	61.9	18.4
Morus spp	4	27.4	21.1	*Cocos nucifera*	2	57.4	23.3
Melia azedarach	2	23.7	13.1	Charcoal	2	5.1	3.9
Shorea spp	2	9.8	2.2	Sawdust	2	71.3	60.8
Ficus religiosa	2	51.9	63.4	Waste	3	87.3	31.4
Syzygium spp	2	8.9	4.9	LPG	3	5.8	5.6
Ficus spp	2	7.1	1.2	Cow dung cake mix	1	34.7	-
Vachellia spp	2	13.5	9.7	*Solanum melongena*	2	13.6	6.5
Dalbergia sissoo	2	17.9	8.8	*Brassica spp*	2	41.0	45.5
Ricinus spp	2	8.5	2.5				
Holoptelea spp	2	6.0	0.8				
Mixed woods	1	6.1	-				
Saraca indica	2	12.9	5.2				
Populus spp	1	8.5	-				
Pithecellobium spp	2	19.5	5.4				
Eucalyptus spp	2	6.9	1.9				
Prosopis spp	6	14.5	10.4				
Mangifera indica	2	12.4	3.4				
Plywood	8	26.6	24.3				
Processed wood	2	33.7	17.2				

Fuel (200 g) was placed 45 cm from the top of the hood and rapidly heated to spontaneous ignition, with emissions convectively driven into a hood and up a flue to allow enough dilution, cooling, and residence time to achieve the quenching typically observed in indoor environments. These conditions have been previously optimised to ensure that emissions entrainment into the hood did not exert a draft which altered combustion conditions. The mid-point velocity of gases driven up the flue by convection was measured by a platinum hot-wire sensor, calibrated for total flow rate using a standard orifice calibrator. Samples were drawn down a sample line at 4.4 L min^{-1} (Swagelok, ¼" PFA, < 2.2 s residence time) from the top of the flue, passed through a pre-conditioned quartz filter (ø = 47 mm, conditioned at 550 °C for 6 hours and changed between samples) held in a filter holder (Cole-Parmer, PFA) which was subsampled for analysis by PTR-ToF-MS, GC×GC-FID and DC-GC-FID instruments at a distance no greater than 5 m from the top of the flue.

Measurements of *n*-alkanes from *n*-tridecane (C_{13}) to eicosane (C_{20}) were made from a subset of 29 burns using solid phase extraction disks, as detailed in chapter 3.

4.2.2. PTR-ToF-MS

The PTR-ToF-MS (PTR 8000; Ionicon Analytik, Innsbruck) instrument from Physical Research Laboratory (PRL), Ahmedabad, was operated by Joe Acton at the University of Lancaster and used to quantify 107 masses and subsampled the common inlet line using ¼ inch PFA. Additional details of the PTR-ToF-MS system used in this study are given in previous papers (Sahu and Saxena, 2015; Sahu et al., 2016). The sample air was diluted into zero air, generated by passing ambient air (1 L min^{-1}) through a heated platinum filament at 550 °C, before entering the instrument with an inlet flow of 250 ml min^{-1}. Samples were diluted by either 5 or 6.25 times (50 ml min^{-1} in 200 ml min^{-1} zero air or 40 ml min^{-1} in 210 ml min^{-1} zero air). The instrument was operated with an electric field strength (E/N, where N is the buffer gas density and E is the electric field strength) of 120 Td. The drift tube temperature was 60 °C with a pressure of 2.3 mbar and 560 V applied across it.

Calibrations were performed twice a week using a gas calibration unit (Ionicon Analytik, Innsbruck). The calibration gas (Apel-Riemer Environmental Inc., Miami) contained 18 compounds: methanol, acetonitrile, acetaldehyde, acetone, dimethyl sulphide, isoprene, methacrolein, methyl vinyl ketone, 2-butanol, benzene, toluene, 2-hexanone, *m*-xylene,

heptanal, α-pinene, 3-octanone and 3-octanol at 1000 ppbv (± 5%) and β-caryophyllene at 500 ppbv (± 5%). This standard was dynamically diluted into zero air to provide a 6-point calibration. The normalised sensitivity (ncps/ppbv) was then determined for each mass using a transmission curve (Taipale et al., 2008). The maximum error in this calibration approach has been shown to be 21%. Peak assignment was assisted with results reported by previous burning studies and references therein (Brilli et al., 2014; Stockwell et al., 2015; Koss et al., 2018), but the results may also contain other indistinguishable structural isomers not mentioned here.

Mass calibration and peak fitting of PTR-ToF-MS data were performed using PTRwid software (Holzinger, 2015). Count rates (cps) of each mass spectral peak were normalised to the primary ion (H_3O^+) and water cluster ($H_3O.H_2O)^+$ peaks, and mixing ratios were then determined for each mass using the normalised sensitivity. Where compounds known to fragment in the PTR-ToF-MS were identified, the mixing ratio of these species was calculated by summing parent ion and fragment ion mixing ratios. Before each burn, ambient air was sampled to provide a background for the measurement.

Petrol and diesel fuel samples were collected from an Indian Oil fuel station in Pusa, New Delhi and the headspace analysed to allow comparison with benzene/toluene ratios. This was designed to analyse the ratios in evaporative emissions, as these have been shown to be an important source of atmospheric NMVOCs (Srivastava et al., 2005b; Rubin et al., 2006; Yamada et al., 2015), which for example represented ~ 15% of anthropogenic UK NMVOC emissions in 2018 (Lewis et al., 2020). Fuel samples were placed in a small metal container (¼" Swagelok cap) which was connected to a two-way tap (¼" Swagelok) which could be opened and closed. The tap was connected to a t-piece (¼" Swagelok) which had a flow of zero air (250 ml min^{-1}) passed through it and could be sampled by the PTR-ToF-MS. The tap was opened and closed which allowed the headspace of fuels to be analysed.

4.2.3. DC-GC-FID

Gas chromatography was used to analyse entire burns to provide an integrated picture of emissions from fuel types. The DC-GC-FID was operated by Beth Nelson at the University of York and sampled 51 burns to measure 19 C_2-C_7 non-methane hydrocarbons (NMHCs) and C_2-C_5 oxygenated NMVOCs (OVOCs) (Hopkins et al., 2003). A 500 ml sample (1.5 L pre-

purge of 100 ml min^{-1} for 15 mins, sample at 17 mL min^{-1} for 30 mins) was collected (Markes International CIA Advantage), passed through a glass finger at -30 ^{o}C to remove water and adsorbed onto a dual-bed sorbent trap (Markes International ozone precursors trap) at -20 ^{o}C (Markes International Unity 2). The sample was thermally desorbed (250 ^{o}C for 3 mins) then split 50:50 and injected into two separate columns for analysis of NMHCs (50 m × 0.53 mm Al_2O_3 PLOT) and OVOCs (10 m × 0.53 mm LOWOX with 50 µm restrictor to balance flow). The oven was held at 40 ^{o}C for 5 mins, then heated at 13 ^{o}C min^{-1} to 110 ^{o}C, then finally at 8 ^{o}C min^{-1} to 200 ^{o}C with a 30-min hold.

4.2.4. GC×GC-FID

The GC×GC-FID was used to measure 58 C_7-C_{12} hydrocarbons (C_7-C_{12} alkanes, monoterpenes and monoaromatics) and collected 3 L samples (100 ml min^{-1} for 30 mins) using an adsorption-thermal desorption system (Markes International Unity 2). NMVOCs were trapped onto a sorbent (Markes International U-T15ATA-2S) at -20 ^{o}C with water removed in a glass cold finger at -30 ^{o}C, removed and heated to ~ 100 ^{o}C after each sample to prevent carryover of unanalysed, polar interfering compounds. The sample was thermally desorbed (250 ^{o}C for 5 mins) and injected splitless down a transfer line. Analytes were refocussed for 60 s using liquid CO_2 at the head of a non-polar BPX5 held at 50 psi (SGE Analytical 15m × 0.15 µm × 0.25 mm) which was connected to a polar BPX50 at 30 psi (SGE Analytical 2 m × 0.25 µm × 0.25 mm) via. a modulator held at 180 ^{o}C (5 s modulation, Analytical Flow Products ELDV2-MT). The oven was held for 2 mins at 35 ^{o}C, then ramped at 2.5 ^{o}C min^{-1} to 130 ^{o}C and held for 1 min with a final ramp of 10 ^{o}C min^{-1} to 180 ^{o}C and hold of 8 mins. Calibration was carried out using a 4 ppbv gas standard containing alkanes and aromatics (NPL UK) and through the relative response of liquid standard injections to toluene for components not in this gas standard, as detailed in Dunmore et al. (2015) and chapter 2. Integration of peak areas was performed in Zoex GC image software (Zoex, USA). Peaks were individually checked and where peaks were split in the software, they were manually joined. The areas corresponding to alkane isomers were manually joined within the GC image software and calibration performed by comparing the areas to the corresponding *n*-alkane. For both GC instruments, blanks of ambient air were made at the beginning, middle and end of the day and the mean subtracted from samples.

4.2.5. GC×GC-ToF-MS

Measurements were made of a subset of 29 burns of C_{13}-C_{20} alkanes, as well as other gas-phase species to assist with qualification of mases measured by PTR-ToF-MS, by adsorbing samples to the surface of SPE disks with analysis by GC×GC-ToF-MS, as detailed in chapter 3. An 8-point calibration was performed for *n*-alkanes using a commercial standard (C_7-C_{40} saturated alkane standard, certified 1000 μg mL^{-1} in hexane, Sigma Aldrich 49452-U) diluted in the range 0.25 – 10 μg ml^{-1}.

4.3. Results

4.3.1. Chromatography

Figure 4.2 shows GC×GC-FID chromatograms obtained from collecting the emissions during the combustion of LPG (Figure 4.2A), *Saraca indica* fuel wood (Figure 4.2B), cow dung cake (Figure 4.2C) and municipal solid waste (Figure 4.2D). Figure 4.2D is labelled to show the position of NMVOCs measured and displays a homologous series of *n*-alkanes from *n*-heptane (C_7) to *n*-tetradecane (C_{14}) along the bottom, with the 1-alkenes positioned to the left. Above are more polar species such as monoterpenes, aromatics from benzene to substituted monoaromatics with up to 5 carbon substituents, and at a higher second dimension retention time even more polar species, such as styrene.

Many peaks were present in the chromatograms for cow dung cake and municipal solid waste, and these fuels released significantly more NMVOCs per unit mass than fuel wood and LPG (see Table 4.1). Cow dung cake and municipal solid waste released a range of NMVOCs including *n*-alkanes, alkenes, and aromatics. The municipal solid waste (Figure 4.2D) showed a particularly large and tailing peak 22 owing to large emissions of styrene. Several unidentified peaks were observed in these complex samples which were broad in the second dimension. These were assumed to be from polar, oxygenated species formed during burning such as phenol. These species could not be identified and were not analysed using the GC×GC-FID, and peaks have been omitted if they were found to interfere with these significantly. Analysis has only been carried out using the DC-GC-FID from ethane (C_2) to *n*-hexane (C_6) owing to the significant presence of coeluting peaks. The large peak in the LPG chromatogram (Figure 4.2, 1^o ~ 6 min, 2^o ~ 0.5 s) was from unresolved propane and butane because of the high concentrations from this fuel source.

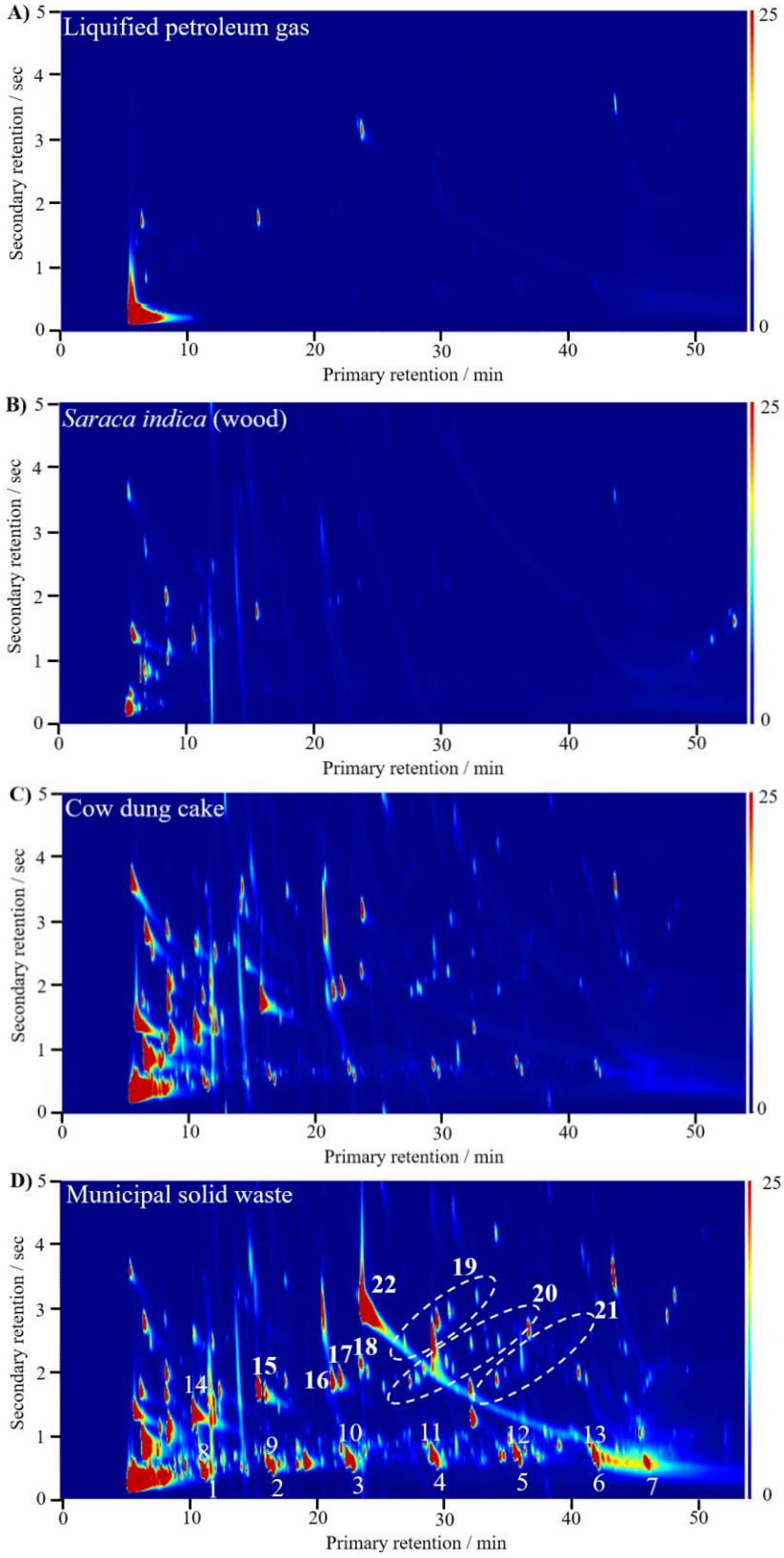

Figure 4.2. GC×GC-FID chromatograms from burning A = LPG, B = Saraca indica (fuel wood), C = cow dung cake and D = municipal solid waste samples where 1-7 = *n*-octane – *n*-tetradecane, 8-13 1-octadecene – 1-tridecene, 14 = benzene, 15 = toluene, 16 = ethylbenzene, 17 = *m*/*p*-xylene, 18 = *o*-xylene, 19 = C_3 substituted monoaromatics, 20 = C_4 substituted monoaromatics, 21 = C_5 substituted monoaromatics and 22 = styrene.

4.3.2. PTR-ToF-MS

Figure 4.3 shows an example concentration-time series measured by the PTR-ToF-MS for a cow dung cake burn. A sharp rise in NMVOC emissions was seen from the start of the burn which decreased as the fuel was combusted. Emissions of small oxygenated species as well as phenolics and furanics were dominant throughout most of the burn. At the beginning, a greater proportion of lower mass species were released, as shown in the binned mass spectrum of region A in Figure 4.3. At the end in the smouldering phase, emissions were dominated by heavier and lower volatility species (Figure 4.3., Region B). A previous study indicated larger molecular weight phenolics were from low temperature pyrolysis (Sekimoto et al., 2018).

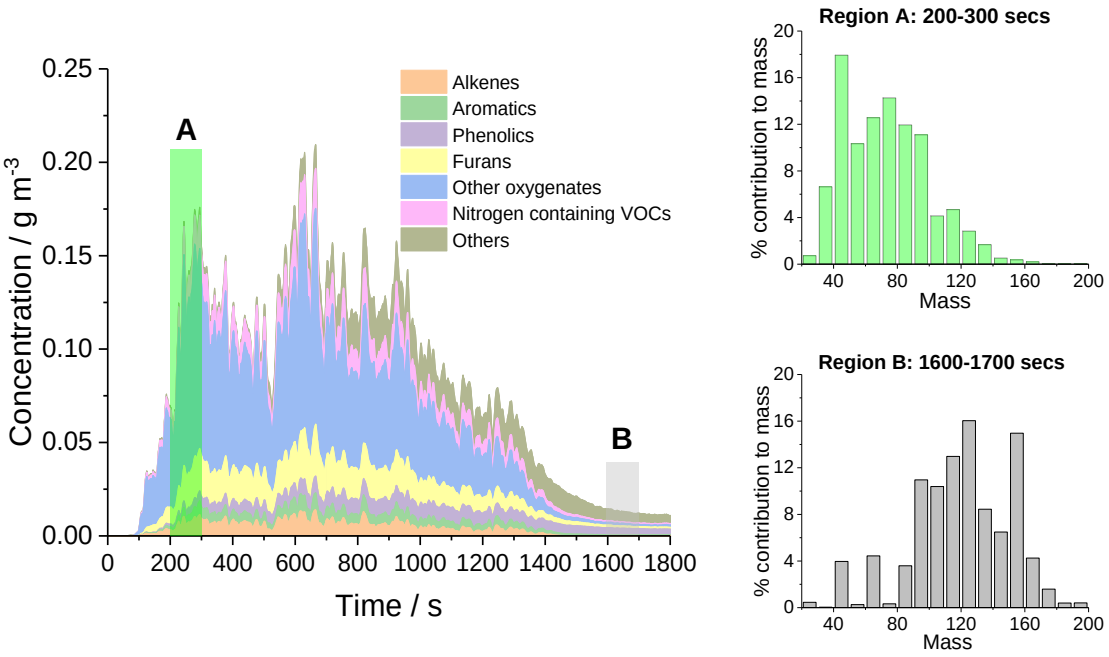

Figure 4.3. PTR-ToF-MS concentration-time series during the first 30 minutes of a cow dung cake burn coloured by functionality with regions A and B displaying mass spectra placed into m/z bins of 10 Th. Fuel collected from Pitam Pura, Delhi.

Figure 4.4 shows the cumulative mass of species measured from burns of fuel wood, cow dung cake, municipal solid waste and charcoal as a proportion of the total mass of NMVOCs quantified using PTR-ToF-MS. The results were similar to those reported by Brilli et al. (2014) and Koss et al. (2018): 65-90% of the mass of NMVOCs at emission originated from around 40 NMVOCs, with around 70-90% identification by mass when quantifying around 100 NMVOCs. The largest contributors to the NMVOC mass from burning of fuel wood and

cow dung cake were methanol (*m/z* 33.034), acetic acid (*m/z* 61.028) and a peak that reflected the sum of hydroxyacetone, methyl acetate and ethyl formate (*m/z* 75.043). For municipal solid waste samples around 28% of total mass was from methyl methacrylate (*m/z* 101.059) and styrene (*m/z* 105.068), and two of the three municipal solid waste samples released significant quantities of styrene, most likely the result of degradation of polystyrene in the samples.

Figure 4.5 shows a time series for phenolics and furanics from the burning of an example fuel wood. Most species of similar functionality tracked each other. Stockwell et al. (2015) demonstrated that benzene, phenol and furan could act as tracers for aromatic, phenolic and furanic species released from biomass burning. Figure 4.5A shows that heavier, more substituted phenolics appeared to be released at cooler temperatures. Guaiacol (dark blue) was released at the start of the flaming phase before the temperature increased and more phenol (red) was released at higher burn temperatures. Later in the burn, a larger proportion of vinyl guaiacol (pink) and syringol (yellow) were emitted. This agreed well with previous results which showed that species emitted from lower temperature depolymerisation had a larger proportion of low-volatility compounds compared to higher temperature processes during flaming (Sekimoto et al., 2018; Koss et al., 2018). Figure 4.5B shows timeseries of furanic species, with most species showing similar characteristics throughout the burn. The only species to peak later in the burn was 2-hydroxymethyl-2-furan.

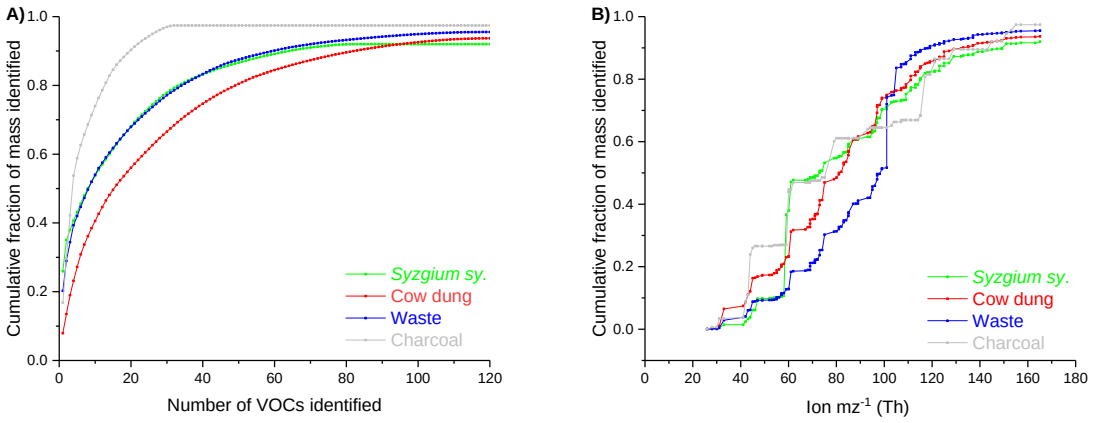

Figure 4.4. Cumulative NMVOC mass identified from PTR-ToF-MS compared with total NMVOC signal from PTR-ToF-MS with A ordered by decreasing NMVOC mass contribution and B ordered by ion mass. High quantification from charcoal was due to a low emission factor (2.4 g kg^{-1}).

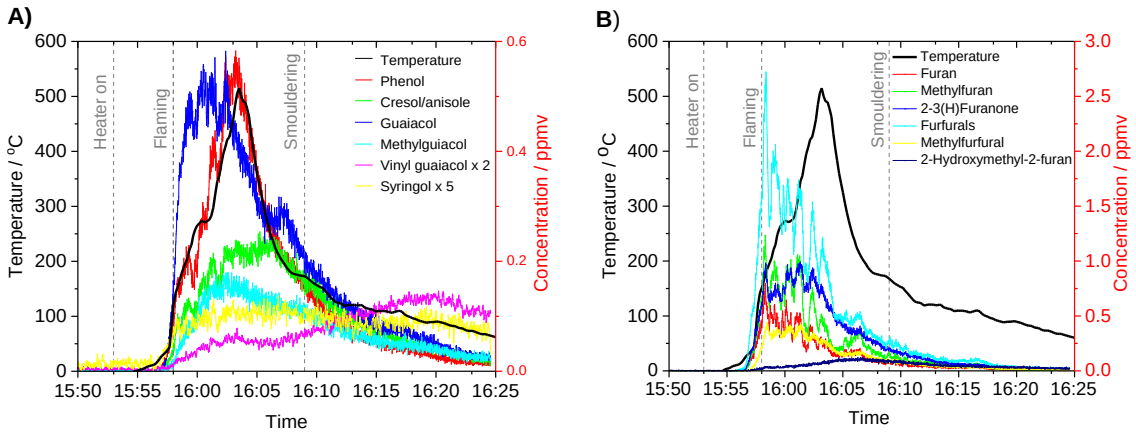

Figure 4.5. Timeseries analysis of phenolic and furanic compounds released from burning of *Azadirachta indica* which released 27.0 g kg^{-1} of NMVOCs. Temperature corresponds to the increase in temperature above ambient measured in the flame directly above the combustion experiment.

4.3.3. Comparison of data obtained with different instruments

Previous instrument inter-comparisons from biomass burning samples were between PTR-MS, GC-MS and open path FTIR (Gilman et al., 2015) and between PTR-ToF-MS, FTIR, aircraft cavity-enhanced spectroscopy (ACES) and I^--CIMS (Koss et al., 2018). Gilman et al. (2015) showed generally good agreement of slopes of measured emission factors between benzene, ethyne, furan, ethene, propene, methanol, toluene, isoprene and acetonitrile using different instruments/techniques with slopes of ~ 1 ± 30% and correlation coefficients > 0.9. Koss et al. (2018) showed mean measured values of most NMVOCs from all burns with other instruments compared to the PTR-ToF-MS which agreed within a factor of two and had correlation coefficients > 0.8 for most species except butadienes, furan, hydroxyacetone, furfural, phenol and glyoxal. These previous comparisons underline the challenges faced with quantitative NMVOC measurements from burning experiments.

Figure 4.6 shows a comparison of measurements made using the DC-GC-FID, GC×GC-FID and PTR-ToF-MS techniques. Bar plots show that the mean and lower/upper quartiles of all measurements agreed within a factor of two. The correlation coefficient between different instruments is given by blue circles, with all > 0.8. Generally, the mean values measured for the PTR-ToF-MS were slightly larger than using the GC instruments, which was attributed to the presence of other undistinguishable structural isomers measured by the PTR-ToF-MS. Comparison between DC-GC-FID and GC×GC-FID measurements were also complicated by high levels of coelution of additional NMVOC species released from combustion with

similar retention times (R_t) to benzene/toluene (R_t = 21/25 mins) on the DC-GC-FID instrument. Generally, the smallest values were measured with the GC×GC-FID instrument, consistent with the greatest ability to speciate isomers and limit the impacts of coelution. Significant efforts were made to synchronise the sample periods for the three instruments as best as possible; however, slight uncertainty existed over the exact time each instrument started measuring when calculating mean sample windows (± 30 s). These factors combined, may help to explain the slight differences observed between different instruments during this study. When multiple instruments have measured the same NMVOC in this study, preference was given to the data from the GC×GC-FID due to the ability of this instrument to resolve coeluting peaks, followed by the DC-GC-FID and then the PTR-ToF-MS.

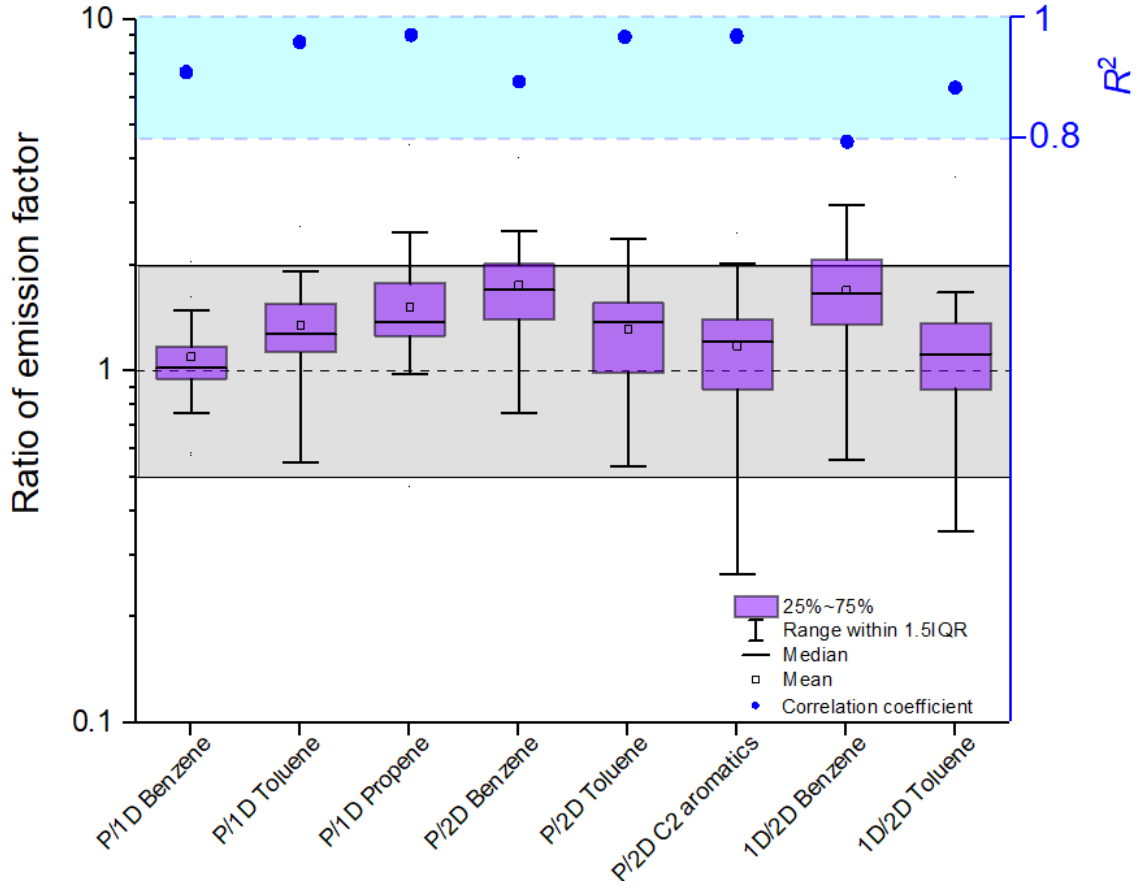

Figure 4.6. Comparison of PTR-ToF-MS to DC-GC-FID and GC×GC-FID with the black dashed line representing slopes equal to one, grey shaded region = slopes agreeing within a factor of two, shaded blue region indicating correlation coefficients > 0.8 and P = PTR-ToF-MS, 1D = DC-GC-FID and 2D = GC×GC-FID.

4.3.4. NMVOC emission factors from different fuels

Figure 4.7 shows a detailed breakdown of the mean NMVOC emission factors by fuel type measured for all 76 burns. The data is split by functionality to show trends for different chemical types. This shows that burning released a large amount of different NMVOCs, across a wide range of functionalities, molecular weights, and volatilities. The large variety of NMVOCs are likely to have different influences on ozone formation, SOA production and the toxicity of emissions.

Figure 4.7A shows very large emissions of smaller oxygenated species which were driven by methanol, acetic acid and the unresolved combined peak for hydroxy acetone, methyl acetate and ethyl formate. For the fuel wood samples, acetic acid/glycolaldehyde (2.6 g kg^{-1}), methanol (1.8 g kg^{-1}) and acetaldehyde (0.6 g kg^{-1}) compared well with mean values reported by Koss et al. (2018) for pines, firs and spruces (2.7/1.3/1.2 g kg^{-1}) and the mean values measured by Stockwell et al. (2015) mainly from crop residues, grasses and spruces (1.6/1.3/0.94 g kg^{-1}). The emission factor from this study for the unresolved peak of hydroxy acetone, methyl acetate and ethyl formate (1.4 g kg^{-1}) was larger than those previously reported by Koss et al. (2018) and Stockwell et al. (2015) of 0.55 and 0.25 g kg^{-1}, respectively.

Figure 4.7B shows that there were large emissions of furans and furanones from combustion, mainly from methyl furans, furfurals, 2-(3H)-furanone, methyl furfurals and 2-methanol furanone. The World Health Organisation consider furan a carcinogenic species of high-priority (WHO, 2016) with furan and substituted furans, suspected to be toxic and mutagenic (Ravindranath et al., 1984; Peterson, 2006; Monien et al., 2011). Furan emissions originate from the low temperature depolymerisation of hemi-cellulose (Sekimoto et al., 2018) and from large alcohols and enols in high-temperature regions of hydrocarbon flames (Johansson et al., 2016). The OH chemistry of furans has been the subject of several studies (Bierbach et al., 1994; Bierbach et al., 1995; Tapia et al., 2011; Liljegren and Stevens, 2013; Strollo and Ziemann, 2013; Zhao and Wang, 2017; Coggon et al., 2019) and often produces more reactive products such as butenedial, 4-oxo-2-pentenal and 2-methylbutenedial (Bierbach et al., 1994; Gómez Alvarez et al., 2009; Aschmann et al., 2011, 2014). Oxidation can also occur by nitrate (Berndt et al., 1997; Colmenar et al., 2012) or chlorine radicals (Cabañas et al., 2005; Villanueva et al., 2007). As a result, furans

have recently been shown to be some of the species with highest OH reactivity from biomass burning, causing an estimated 10% of the O_3 produced by the combustion emissions in the first 4 hours after emission (Hartikainen et al., 2018; Coggon et al., 2019). Oxidation of furans can lead to SOA production (Gómez Alvarez et al., 2009; Strollo and Ziemann, 2013) with an estimated 8-15% of SOA caused by furans emitted by burning of black spruce, cut grass, Indonesian peat and ponderosa pine and 28-50% of SOA from rice straw and wiregrass (Hatch et al., 2015), although SOA yields are still uncertain for many species (Hatch et al., 2017).

Phenols are formed from the low-temperature depolymerisation of lignin (Simoneit et al., 1993; Sekimoto et al., 2018) which is a polymer of randomly linked, amorphous high-molecular weight phenolic compounds (Shafizadeh, 1982). Owing to their high emission factors and SOA formation potentials, phenolic compounds contribute significantly to SOA production from biomass-burning emissions (Yee et al., 2013; Lauraguais et al., 2014; Gilman et al., 2015; Finewax et al., 2018).

Figure 4.7C shows that the largest phenolic emissions from fuel wood in this study were methoxyphenols, with significant contributions from phenol, guaiacol, cresols and anisole. Phenolic emissions from sawdust were dominated by guaiacol and creosol. Phenolic emissions from coconut shell were greatest, most likely as a result of the lignin rich nature of coconut shell (Pandharipande et al., 2018). The larger mean emission of furans (3.2 g kg^{-1}) compared to phenols (1.1 g kg^{-1}) from fuel wood was consistent with wood being composed of around 75% cellulose/hemicellulose and 25% lignin (Sjöström, 1993).

Figure 4.7D shows that the largest alkene emission was styrene from burning municipal solid waste, likely caused by the presence of polystyrene in the fuel. Emissions of alkenes from fuel woods were dominated by ethene and propene, species with high photochemical ozone creation potentials (Cheng et al., 2010). Monoterpenes, which are extremely reactive with the OH radical (Atkinson and Arey, 2003), were emitted from sawdust, cow dung cake and municipal solid waste.

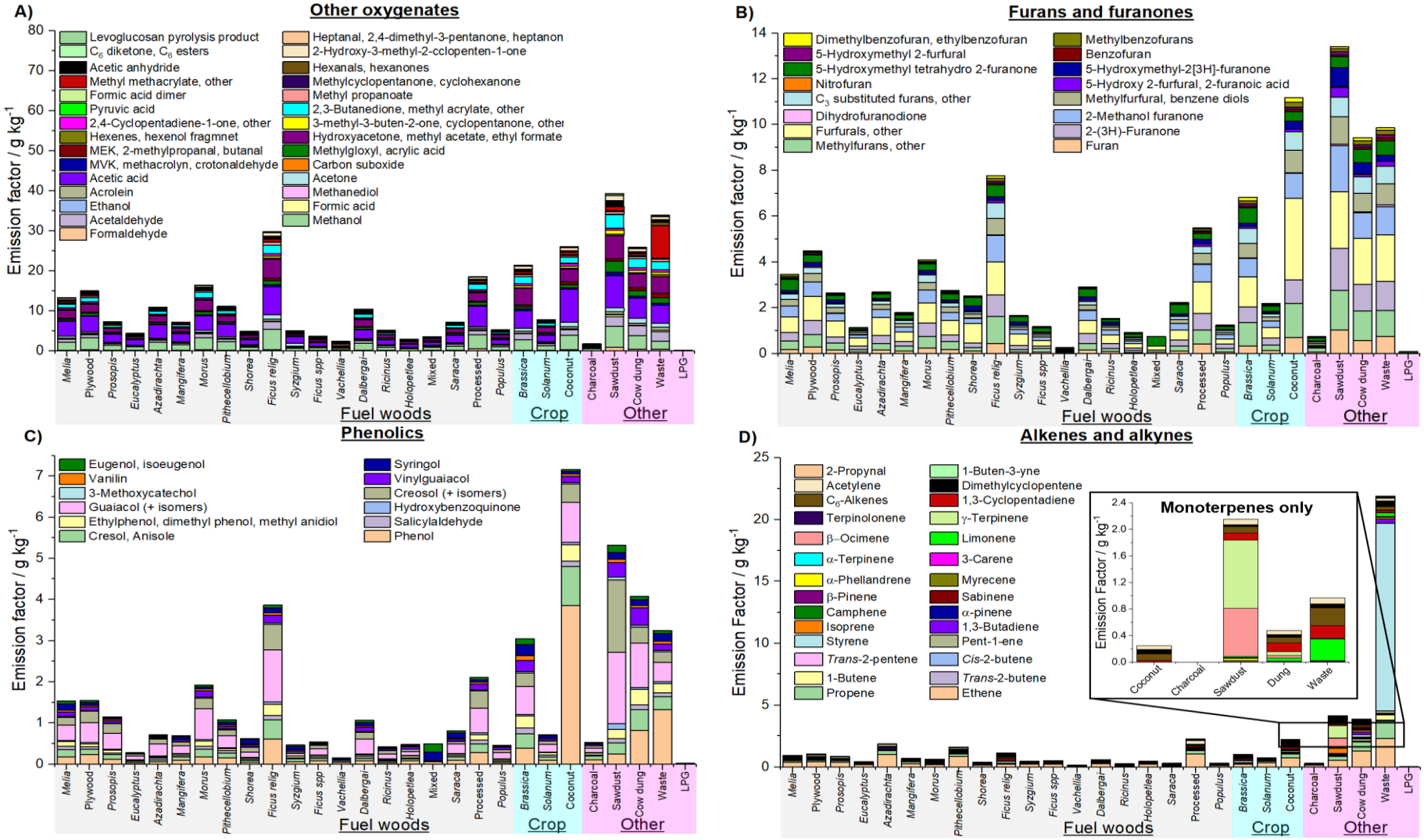

Figure 4.7. Measured emission factors grouped by functionality.

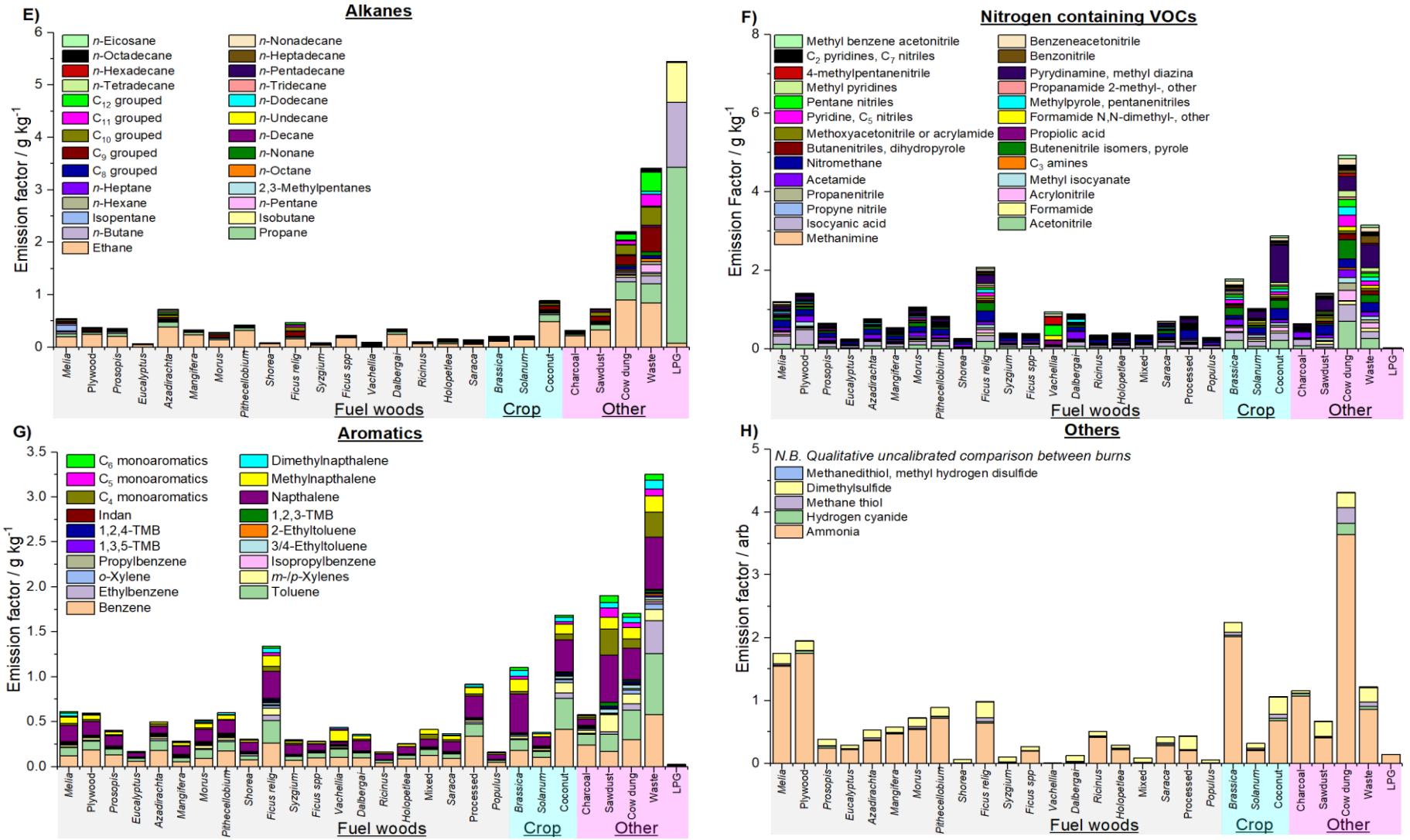

Figure 4.7. continued.

Ethane and propane dominated the alkane emissions for fuel wood samples (see Figure 4.7E). A wider range of alkanes from C_2-C_{20} were observed from combustion of coconut shell, cow dung cake and municipal solid waste. The largest alkane emission by mass was from LPG due to unburnt propane and butane.

Nitrogen containing NMVOCs are formed from the volatilisation and decomposition of nitrogen-containing compounds within the fuel, mainly from free amino acids but can also be from pyrroline, pyridine and chlorophyll (Leppalahti and Koljonen, 1995; Burling et al., 2010; Ren and Zhao, 2015). Nitrogen containing NMVOCs are of interest because nitrogen may be important in the development of new particles (Smith et al., 2008; Kirkby et al., 2011; Yu and Luo, 2014) which act as cloud condensation nuclei (Kerminen et al., 2005; Laaksonen et al., 2005; Sotiropoulou et al., 2006) and alter the hydrological cycle by forming new clouds and precipitation (Novakov and Penner, 1993). They can also contribute to light-absorbing brown carbon (BrC) aerosol formation, effecting climate (Laskin et al., 2015). Additionally, nitrogen containing NMVOCs can be extremely toxic (Ramírez et al., 2012, 2014; Farren et al., 2015). Figure 4.7F shows that cow dung cake was the largest emitter of nitrogen containing NMVOCs (4.9 g kg^{-1}), releasing large amounts of nitriles, which are likely to have a large impact on the toxicity and chemistry of emissions.

Figure 4.7G shows emissions of aromatics from fuel wood, cow dung cake and municipal solid waste were principally benzene, toluene and naphthalenes. Large emissions of benzene were unsurprising as biomass burning is the largest global benzene source (Andreae and Merlet, 2001). Emissions of benzene, toluene, ethylbenzene and xylenes (BTEX) from cow dung cake (0.5-1.7 g kg^{-1}) were in line with previous measurements of 1.3 g kg^{-1} (Koss et al., 2018) and 1.8 g kg^{-1} (Fleming et al., 2018) but lower than the 4.5 g kg^{-1} reported from cow dung cake combusted from Nepal (Stockwell et al., 2016). Emissions of BTEX from municipal solid waste burning (0.9– 2.6 g kg^{-1}) were comparable to that measured previously (3.5 g kg^{-1}) (Stockwell et al., 2016).

Figure 4.7H shows a qualitative comparison of species such as ammonia, HCN and dimethyl sulphide which were measured during experiments, but could not be accurately quantified

as their sensitivity was too different from the NMVOCs used to build the transmission curve. Cow dung cake emitted significantly more of these species than other fuel types.

Table 4.2 shows the total emission factors of NMVOCs for different fuel types. Emission factors have been calculated over a 30-minute period, in line with the GC sample time, with any small emissions after this sample window not included. The total emission factor has been calculated as the sum of the PTR-ToF-MS signal, excluding reagent ion peaks (< *m*/*z* 31 Th), water cluster peaks (*m*/*z* 37 Th) and isotope peaks identified for all masses (SIS, 2016). The emission factors for all alkanes measured were also included as alkanes up to *n*-hexane had proton affinities less than water and larger alkanes had proton affinities similar to water (Ellis and Mayhew, 2014; Wróblewski et al., 2006). This low sensitivity meant that no peaks were present in the PTR-ToF-MS spectra for these larger species.

Table 4.2. Mean total NMVOC emission factors (g kg^{-1}, including IVOC fraction) where high/low EF represent the largest/smallest emission factor measured for a given sample type (g kg^{-1}) and IVOC is the sum of emission factors of species with a mass greater than benzaldehyde (g kg^{-1}) where *n* = number of measurements made.

	Wood	**Dung**	**Waste**	**LPG**	**Charcoal**	**Sawdust**	**Crop**
NMVOC	18.7	62.0	87.3	5.7	5.4	72.4	37.9
High EF	96.7	83.0	119.1	9.8	7.9	114.0	73.8
Low EF	4.3	35.3	56.3	1.9	2.4	28.3	8.9
IVOC	3.5	12.6	13.2	0.2	1.4	16.9	8.0
n	51	8	3	3	2	2	6

Coconut shell, sawdust, cow dung cake and municipal solid waste released the greatest mass of NMVOC per kg of fuel burnt. The mean emission factor for all fuel woods (18.7 g kg^{-1}) was comparable to that for chaparral (16.6 g kg^{-1}) measured using PTR-ToF-MS by Stockwell et al. (2015). This may be due to similarities between north Indian fuel wood types with chaparral, which is characterised by hot dry summers, and mild wet winters. The mean fuel wood emission factor was smaller than Stockwell et al. (2015) reported for coniferous canopy (31.0 g kg^{-1}). The NMVOC emission measured for cow dung cake (62.0 g kg^{-1}) was comparable to that previously reported (66.3 g kg^{-1}) in literature using PTR-ToF-MS (Koss et al., 2018), but 2-3 times larger than that measured by GC-FID/ECD/MS likely due to those techniques missing significant amounts of emissions (Fleming et al., 2018). Whilst the total emissions reported by Fleming et al. (2018) might therefore be an

underestimate, it is noteworthy that the emission factors measured by Fleming et al. (2018) in *angithi* stoves for cow dung cake were ~ factor of 4 greater than fuel wood under the same conditions. This result was comparable to this study, which showed that cow dung cake emissions were ~ factor of 3 larger than fuel wood, however the techniques used here targeted a greater proportion of total emissions. Moreover, Fleming et al. (2018) reported emission factors from combustion of biomass fuels from a neighbouring state, Haryana, and there may be slight heterogeneity between the different fuels collected in both studies.

NMVOC emissions from municipal solid waste (87.3 g kg^{-1}) were significantly larger than the 7.1 g kg^{-1} (Stockwell et al., 2015) and 33.8 g kg^{-1} (Stockwell et al., 2016) previously reported. This was likely due to differences in composition and moisture content of the fuels collected from Indian landfill sites for the present study, compared with the daily mixed waste collected at the US fire services laboratory and plastic bags (Stockwell et al., 2015) and a variety of mixed waste and plastics collected from around Nepal (Stockwell et al., 2016). It seems noteworthy that combustion experiments of fuels collected from developing countries in Stockwell et al. (2016) had larger emission factors than those collected from, and burnt at a laboratory (Stockwell et al., 2015). The mean crop residue combustion emission factor (37.9 g kg^{-1}) was similar to that of Stockwell et al. (2015) (38.8 g kg^{-1}), despite the small number of samples in this study and compositional differences.

NMVOC emissions from charcoal combustion were low (5.4 g kg^{-1}). During charcoal production the fuel is heated in minimal oxygen which removes moisture and volatile components. This is likely to result in samples with low moisture content which combust efficiently and therefore do not result in large total emissions of NMVOCs. In addition, many volatile components are removed during the production process and this is likely to result in lower emissions during combustion. The lower NMVOC emission factor does not account for any additional volatile emissions during the production process.

Intermediate-volatility organic compounds (IVOCs) are defined as having effective saturation concentration, C^*, =300-3×10^6 µg m^{-3} (Donahue et al., 2012). The C^* of several species were estimated using a previously established approach (Lu et al., 2018), with the IVOC boundary defined in this study at benzaldehyde (m = 106.12) for which C^* was ~ 7×10^6 µg m^{-3}. Table 4.2 also shows an approximation for the mean amount of IVOCs released by fuel type. This approach was approximate as vapour pressures depend on both mass and

functionality. The fuels tested in this study showed that mean emissions of IVOC species represented approximately 18 – 27% of total measured emissions from all fuel types other than LPG. This demonstrated that domestic solid fuel combustion is potentially a large global source of IVOCs. In addition, this may represent an underestimate because the quartz filter placed on the sample line may remove IVOC species which have partitioned to the aerosol phase due to the high aerosol concentrations present during source testing. Further studies are required to better understand the contribution of IVOC emissions from biomass burning to SOA formation.

Figure 4.8A shows the distribution of total measured NMVOC emission factors for fuel wood, cow dung cake, crop residues and MSW. Boxplots show the mean, median, interquartile range and range within 1.5IQR. The solid circles display the spread of measured emission factors by fuel type. The zoomed green region given in Figure 4.8B specifically focuses on the variability in emission factors of individual species of fuel wood, which has been explored in detail due to the large number of samples. Repeat samples collected from the same location are shaded in grey. For fuel wood, measured NMVOC emission factors varied by over a factor of 20 between 4.3-96.7 g kg^{-1}. The NMVOC emission factors showed a right skewed distribution with a median of 11.7 g kg^{-1}, mean of 18.7 g kg^{-1} and an interquartile range of 15.3 g kg^{-1}. For repeat measurements of identical species of fuel wood collected at the same location, except for *Ficus religiosa*, measured emission factors from repeat experiments varied over a much smaller range, by up to a factor of 2.3. Variation between emissions from these samples were likely due to different moisture contents of actual samples measured and the specific combustion conditions of individual burns. The large variation observed for *Ficus religiosa* was likely due to the samples being significantly different in terms of composition. Despite the samples for *Holopetlea spp* and *Eucalyptus spp* coming from different locations, emission factors for these samples were quite reproducible and only varied by a factor of 1.2-1.5. For remaining identical species of fuel wood collected from different locations, emission factors varied over a much larger range by factors of ~ 2-9.

For the crop residue species studied here, NMVOC emissions were right skewed with a with a median of 29.5 g kg^{-1}, which was less than the mean of 37.9 g kg^{-1} and varied from 8.9-73.8 g kg^{-1} with an interquartile range of 53.9 g kg^{-1}. *Cocos nucifera* and *Solanum melongena*

were repeat measurements of fuel collected from the same location and varied by factors of 1.8-2. NMVOC emissions from *Brassica spp* fuel, which was collected from different locations, varied by a factor of ~ 8. Cow dung cake and MSW samples were all collected from different locations and varied by up to factors of up to 2.4 and 2.1, respectively.

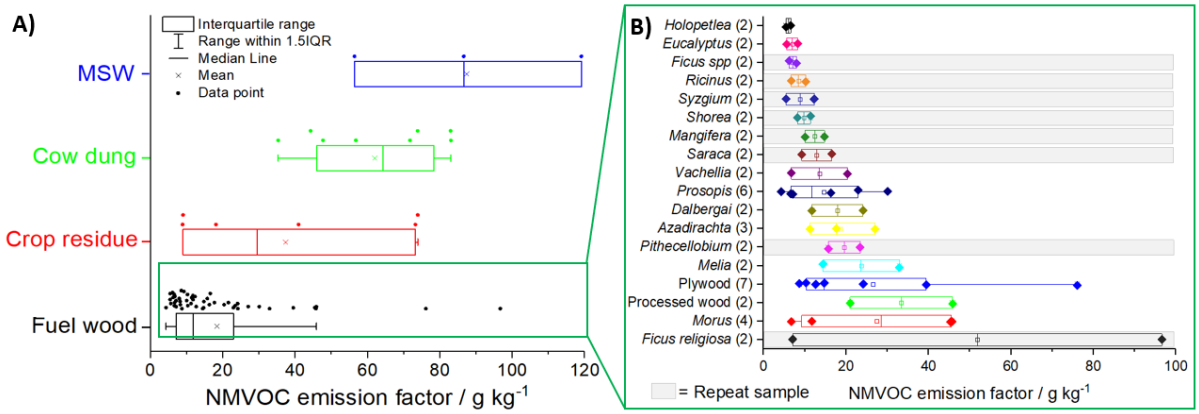

Figure 4.8. Variability in NMVOC emission factor by fuel type. A = Range of emission factors measured for fuel wood, cow dung cake, crop residue and municipal solid waste samples with box plots showing the mean, median, interquartile range, range within 1.5IQR and solid circles showing the spread of measured emission factors by fuel type. B = Zoomed green region displaying range of NMVOC emission factors measured for individual species of fuel wood, with grey shaded region indicating repeat samples from the same sample collection location and diamonds indicating the measured NMVOC emission factors.

Figure 4.9A shows the mean total emissions measured in this study for different fuel types split by functionality. Large variability in total emissions were observed for fuel woods, with emission factors from individual burns varying by ~ factor 20. Figure 4.9B shows the mean emissions by functionality as a proportion of total emissions averaged by overall fuel type. Oxygenates were the largest emission (33-55%), followed by furanic compounds (16-21%), phenolics (6-12%) and aromatics (2-9%) for all fuel types except LPG. LPG emissions were mainly alkanes, with a small emission of furanic species. These have previously been reported to be produced in hydrocarbon flames (Johansson et al., 2016).

Figure 4.9A-B also show the amount of NMVOC which remained unidentified (black). On average 94% of all measured NMVOCs across all burns were speciated. Quantification was greater than 90% for all sample types, except *Vachellia spp* due to several large unidentified peaks. Mean quantification by fuel type was between 93-96% for all other fuels, except LPG where quantification was > 99%.

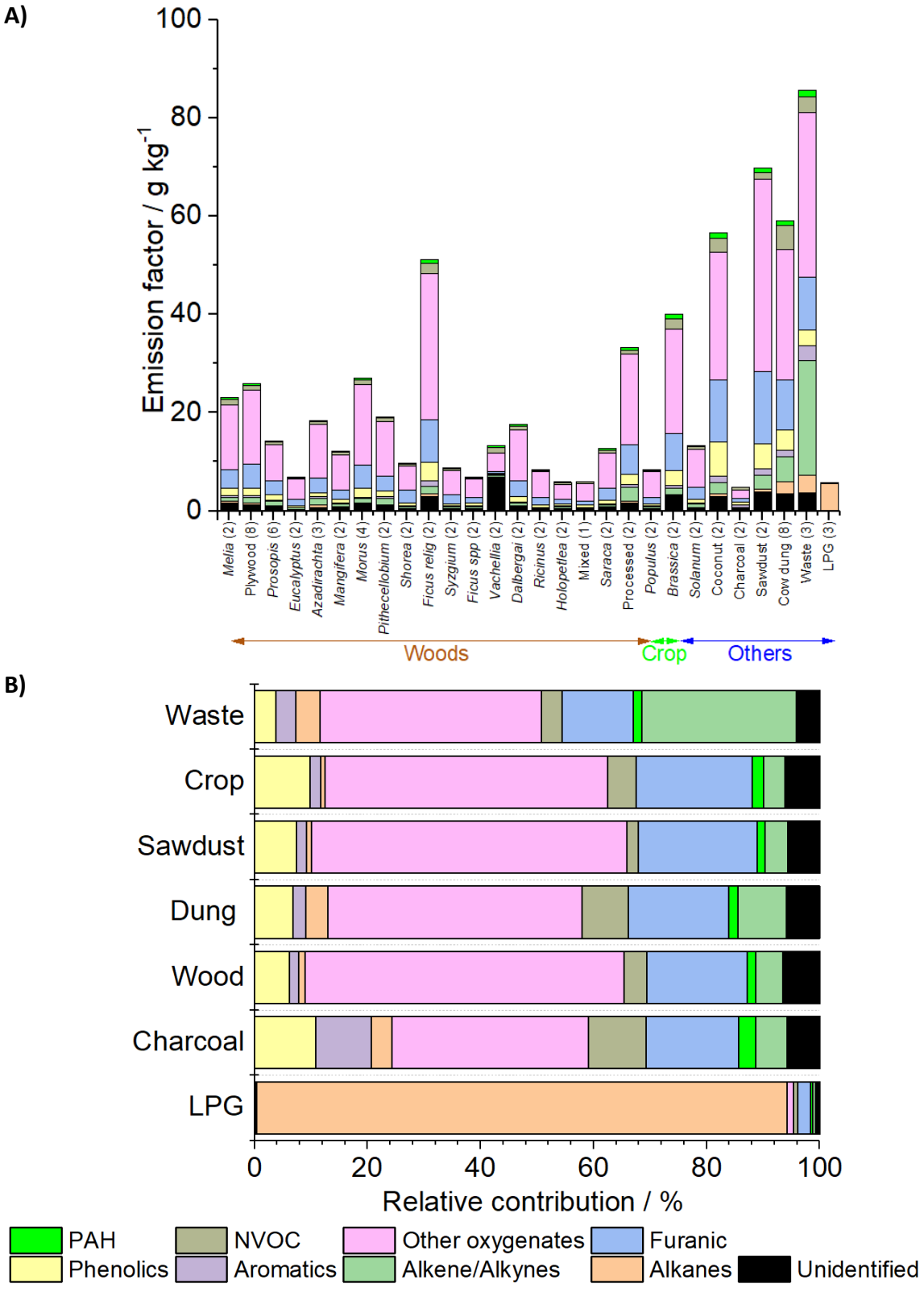

Figure 4.9. NMVOC emissions from burning sources in Delhi, India, grouped by functionality with unidentified emissions given by the total NMVOC signal measured by the PTR-ToF-MS minus the fraction quantified using DC-GC-FID, GC×GC-FID and PTR-ToF-MS instruments with A = all fuel types and B = mean values by type of fuel.

4.3.5. Emission ratios

The ratio of the mixing ratios of NMVOCs in the emitted gas can be a useful indicator of their source(s) in ambient air. Ratios can be specific to sources and can allow one source to be distinguished from another. The ratio of *i*-/*n*-pentane can be a useful indicator of whether emissions are anthropogenic or from biomass burning, with a ratio 2.2-3.8 indicative of vehicular emissions, 0.8-0.9 for natural gas drilling, 1.8-4.6 for evaporative fuel emissions and < 1 from burning (Li et al., 2019). Benzene/toluene ratios can also be useful and have been reported from traffic exhaust to be around 0.3 (Hedberg et al., 2002).

i-/*n*-Pentane indicator ratios have been evaluated for fuel wood sources, propane/butane ratios for LPG and benzene/toluene ratios for fuel wood and cow dung cake (see Figure 4.10). The range of values for multiple different burns have been evaluated rather than just reporting mean and median ratios. The median of *i*-/*n*-pentane ratios from biomass samples measured during this study was ~ 0.7 (see Figure 4.10). The mean ratio was ~ 1.0, with an interquartile range (IQR) ~ 0.5-1.5, which suggests caution is required when assigning burning sources based on emission ratios due to considerable variability. Despite this, the ratio from solid fuel combustion sources was often less than expected from petrol emissions. The mean ratio of propane/butane from LPG burning was measured to be 3.1. The ratios of benzene/toluene varied considerably between different sources and was measured for fuel wood combustion (2.3), cow dung cake combustion (0.94), petrol liquid fuel (0.40) and diesel liquid fuel (0.20). The range of benzene/toluene ratios for fuel wood was large, with an IQR of ~ 1.5 - 2.8 and the range within 1.5 IQR shown by the whiskers in Figure 4.10 from ~ 0.9 - 4.2. Despite the variability of ratios from specific source types, the considerable range of benzene/toluene ratios could potentially be a useful indicator of the origin of unaged (fresh) ambient emissions in Delhi. However, further study would be required to assess if these ratios were also true in the exhaust of petrol and diesel vehicles in India or just limited to fugitive emissions. These findings agree well with literature which report mean benzene/toluene ratios of 1.4-5.0 from fuel wood and 0.3 from automotive emissions (Hedberg et al., 2002), indicating that on average biomass burning releases a greater molar ratio of benzene than toluene when compared to automotive emissions.

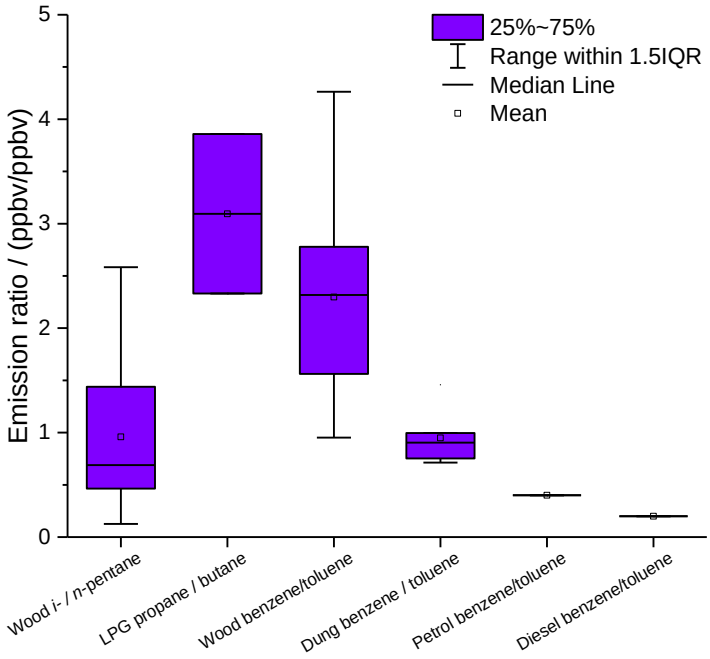

Figure 4.10. Summary of ratios of NMVOCs measured during this study from the burning of fuel wood, LPG and cow dung cake and from the headspace of liquid petrol and diesel fuels collected in India. The different mean and median values have been considered to evaluate the ratios at emission of specific sources.

4.4. Conclusions

This study was based on comprehensive measurements of NMVOC emissions using a range of detailed and complementary techniques across a large range of functionalities and volatilities. 29 different fuel types used in residential dwellings in northern India were collected from across Delhi and emission factors of a wide range of NMVOCs (192 compounds in total) were measured during controlled burning experiments. 94% speciation of total measured NMVOC emissions was achieved on average across all fuel types. The largest contributors to emissions from most fuel types were small non-aromatic oxygenated species, phenolics and furanics. The emission factors (in g kg^{-1}) for total gas-phase NMVOCs were fuel wood (18.7, 4.3-96.7), cow dung cake (62.0, 35.3-83.0), crop residue (37.9, 8.9-73.8), charcoal (5.4, 2.4-7.9), sawdust (72.4, 28.6-115.5), municipal solid waste (87.3, 56.6-119.1) and liquefied petroleum gas (5.7, 1.9-9.8). The emission factors measured in this study allow for better characterisation, evaluation and understanding of the air quality impacts of residential solid fuel combustion in India.

Chapter 5

Comprehensive organic emission profiles, secondary organic aerosol potential and OH reactivity of domestic fuel combustion in Delhi, India

The majority of this chapter has been published as a manuscript under the same name:

Gareth J. Stewart, Beth S. Nelson, W. Joe F. Acton, Adam R. Vaughan, James R. Hopkins, Siti S. M. Yunus, C. Nicholas Hewitt, Eiko Nemitz, Tuhin K. Mandal, Ranu Gadi, Lokesh. K. Sahu, Andrew R. Rickard, James D Lee and Jacqueline F. Hamilton. *Environmental Science*: *Atmospheres*, 1, 104-117, 2021. https://doi.org/10.1039/D0EA00009D

5.1. Introduction

Around 3 billion people globally use solid fuels to meet their daily cooking energy requirements (World Health Organization, 2018b). Emissions from residential solid fuel combustion are significant and have been shown to cause indoor air pollution which resulted in 2.8-3.9 million premature deaths globally, (Kodros et al., 2018; World Health Organization, 2018b; Smith et al., 2014) with around 25% of ambient particulate matter (PM) in South Asia related to cooking emissions (Chafe et al., 2014). Approximately a quarter of worldwide residential solid fuel use is in India, (World Bank, 2020) where cooking domestically over biomass remains popular because biomass fuel is cheaper than liquefied petroleum gas (LPG) and meals cooked with traditional methods perceived to be tastier (Mukhopadhyay et al., 2012). Recent studies have shown that 16% (Stewart et al., 2021) of non-methane hydrocarbons and 27% (Wang et al., 2020) of non-methane volatile organic compounds (NMVOCs) by mixing ratio at different urban sites in Delhi were from solid fuel combustion sources. Furthermore, Aerosol Mass Spectrometer measurements found that crop residue burning and solid fuel combustion jointly accounted for 24% (35.8 μg m^{-3}) of the PM_1 concentration during the post-monsoon in Delhi, with likely additional contributions to the SOA (Cash et al., 2020).

Studies focussed on organic emissions from both open biomass burning and domestic solid fuel combustion have shown that organic components are released over a range of volatilities (Stockwell et al., 2015; Hatch et al., 2018; Koss et al., 2018). These include non-methane volatile organic compounds (NMVOCs, effective saturation concentration, C^*, 3×10^6-10^{11} μg m^{-3}), intermediate-volatility organic compounds (IVOCs, C^* =300-3×10^6 μg m^{-3}), semi-volatile organic compounds (SVOCs, C^* = 0.3-300 μg m^{-3}) as well as low- and extremely low-volatility organic compounds (L/ELVOCs, where LVOC $C^* \leq 0.3$ μg m^{-3}) (Donahue et al., 2012). As a result, I/SVOCs from domestic solid fuel combustion potentially represent a large global source of SOA, however, the effect of I/SVOCs on OH reactivity, aging and SOA formation remains poorly understood (Liu et al., 2017; Decker et al., 2019; Sengupta et al., 2020).

The factors controlling SOA formation are complex. These include the oxidation of NMVOCs to less volatile products which partition into the particle phase, the heterogeneous oxidation of particle-phase SVOCs, and plume dilution with subsequent SVOC evaporation

followed by further gas-phase oxidation (Lim et al., 2019). Of 17 studies examining the enhancement factor of organic aerosol (OA) to CO from the aging of open biomass burning emissions, 10 found no increase in SOA, 4 found an increase and 3 reported a decrease (Shrivastava et al., 2017). Despite varied results, a recent lab study has shown SOA formation from combustion of fuels relevant to open biomass burning to be significant. Lim et al. (2019) showed a carbon yield of SOA from NMVOCs emitted from western U.S. fuels of 24 ± 4% when exposed to atmospheric aging equivalent to 6 hours, which increased to 56 ± 9% after aging equivalent to 6 days (Lim et al., 2019).

Formation of SOA from open biomass burning has been examined as part of several recent studies. Hatch et al. (2015) estimated that 8-15% of SOA from the combustion of black spruce, cut grass, Indonesian peat and ponderosa pine was because of furanic compounds. The contribution of furanic compounds to SOA was estimated to be greater still (28-50%) from rice straw and wiregrass (Hatch et al., 2015). Gilman et al. (2015) examined the relative contributors to SOA from U.S. fuels and found the main contributors to be polyunsaturated oxygenated NMVOCs (Gilman et al., 2015). High SOA formation potential was driven by benzene diols, benzaldehyde, and phenols. Ahern et al. (2019) showed that for coniferous fuels, which were dominated by the burning of biomass needles, biogenic NMVOCs were the most important class of SOA precursor (Ahern et al., 2019). Akherati et al. (2020) reported that oxygenated aromatic compounds resulted in just under 60% of the SOA from western U.S. fuels (Akherati et al., 2020). These studies have also shown that reactive chemical species such as furanics, oxygenated aromatics and aliphatics are important drivers of the OH reactivity of open biomass burning emissions (Gilman et al., 2015; Stockwell et al., 2015; Hartikainen et al., 2018). Recent model simulations by Coggon et al. (2019) focussed on modelling the OH radical chemistry in emissions from the combustion of fuels from the western U.S. showed that up to 10% of O_3 in the first 4 h after emission was a result of the oxidation of furanic compounds (Coggon et al., 2019).

Few studies have examined SOA formation from fuels used for domestic solid fuel combustion, with little known about the impact of the species released on the reactivity of emissions. Bruns et al. (2016) examined SOA formation from beech fuel wood and demonstrated that the main contributors were 22 compounds, and in some cases up to 80% of the SOA produced was estimated to be formed from phenol, naphthalene and

benzene (Bruns et al., 2016). A further study suggested that furanic and phenolic compounds were important precursors to SOA as a result of spruce combustion (Hartikainen et al., 2018).

The concentration of primary organic aerosol (POA) is determined by dynamic gas-to-particle partitioning of an extremely complex mixture of organics over a wide range of volatilities. Understanding the gas-to-particle partitioning represents one of the main difficulties in accurately characterising SOA formation, as measurements of organic emissions using multiple measurement techniques are required. As a result, gas-phase emissions are traditionally considered up to C_{12} (saturation vapour concentration, C^*, ~ 10^6 $\mu g\ m^{-3}$) and POA as non-volatile (Robinson et al., 2007; Fujitani et al., 2012; May et al., 2013; Lu et al., 2018). Consequently, many models neglect the importance of I/SVOCs as SOA precursors. The effect is a significant underestimation of SOA production and an overestimation of POA in chemical transport models (Hodzic et al., 2010; Woody et al., 2016; Shrivastava et al., 2017). The concentration of organic aerosol (OA) is determined by the volatility of species and ambient conditions, with many source tests occurring at unrealistically high OA concentrations. Laboratory-based source studies typically enhance the POA emission factor relative to more dilute ambient conditions (Lipsky and Robinson, 2006; Fujitani et al., 2012). The inclusion of I/SVOCs leads to better agreement between modelled and measured values (Ots et al., 2016; Woody et al., 2016; Murphy et al., 2017; Jathar et al., 2017). A range of studies have been conducted to comprehensively characterise organic emissions from mobile sources (May et al., 2014; Zhao et al., 2015; Zhao et al., 2016; Lu et al., 2018) and aircraft engines (Presto et al., 2011; Cross et al., 2013), however, a need has been highlighted to develop source profiles for both open and domestic biomass burning (Lu et al., 2018). These have the potential to result in a better understanding of the SOA formed from the I/SVOCs released. Comprehensive source profiles are far better suited to predicting SOA formation than traditional separated gas- and particle-phase emission factors developed at the point of emission. Comprehensive profiles can be adjusted to real-world dilutions, aerosol concentrations and temperatures. These parameters are all likely to have a large influence on the mass of SOA present.

This study develops comprehensive, model-ready organic emission profiles for solid fuels routinely burnt across the Delhi area of India. These profiles account for the full range of

volatilities of organic emissions to better constrain the impact of domestic biomass burning on SOA formation. This study also compares the relative impacts of different solid fuel combustion sources to SOA production potential and OH reactivity and examines the most important chemical contributors.

5.2. Methods

5.2.1. Datasets

The data used in this study come from a detailed field campaign designed to measure emissions of solid fuels widely used in India. 76 samples were collected from across Delhi in a manner designed to reflect the range and variability of solid fuels used across this region. Detailed descriptions of the analytical procedures, which are summarised below, are provided in chapters 3 and 4.

NMVOCs were sampled from the top of the flue down a ¼" PFA sample line which was subsampled by three separate online gas-phase instruments designed to target a wide range of NMVOCs of different functionality and volatility. A dual-channel gas chromatograph with flame ionisation detection (DC-GC-FID) was used to sample alkanes from ethane to *n*-hexane and a range of small alkenes of mass from ethene – isoprene. A two-dimensional gas chromatograph with flame ionisation detection (GC×GC-FID) was used to sample alkanes from *n*-heptane to *n*-dodecane, aromatic species from benzene to monoaromatics with up to 5 carbon substituents and up to 12 monoterpenes. A proton-transfer-reaction time-of-flight mass spectrometer (PTR-ToF-MS, PTR 8000; Ionicon Analytik, Innsbruck) was used to sample a range of small oxygenates, oxygenated aromatics, alkenes, furanic species and nitrogen-containing volatile organic compounds. Gas chromatographs (GCs) made a single integrated measurement of each burn lasting 30 minutes to provide a single speciated measurement from each experiment. The PTR-ToF-MS made time-resolved measurements at 1 s to evaluate the profiles of each burn and was averaged to the same 30-minute sample window of the GC instruments.

Aerosol phase organics were collected onto PTFE filters after passing through a dilution chamber at 46.7 L min^{-1}. This process was designed to replicate the immediate condensational processes that occur in smoke particles approximately 5-20 mins after emission, yet prior to photochemistry which may change composition (Akagi et al., 2011).

Residual low-volatility NMVOC gases were adsorbed to the surface of solid phase extraction disks (SPE) coated with C_{18} alkanes placed behind the PTFE filter. Filters were extracted using accelerated solvent extraction and analysed using two-dimensional gas chromatography with time-of-flight mass spectrometry (GC×GC-ToF-MS). The chromatographic analysis method for PTFE filters allowed well-resolved separation of hydrocarbons across a two-dimensional space from *n*-nonane to *n*-tetracontane. This overcame issues often arising from the conventional use of one-dimensional chromatography, as these components traditionally elute as an unresolved complex mixture.

Data which was collected using these 5 separate measurement techniques of organic emissions was combined from a range of fuel woods (*Melia azedarach, Prosopis spp, Eucalyptus spp, Azadirachta indica, Mangifera indica, Morus spp, Pithecellobium spp, Shorea spp, Ficus religosa, Syzgium spp, Ficus spp, Vachellia spp, Dalbergai sissoo, Ricinus spp, Holopetlea spp, Saraca indica* and plywood), cow dung cake, municipal solid waste (collected from 3 landfill sites: Ghazipur, Bhalswa and Okhla), crop residue (*Brassica spp, Solanum melongena and Cocos nucifera),* charcoal, sawdust and LPG. Emission factors of 192 speciated NMVOCs, which achieved on average 94% quantification, were combined from *n* fires sampled by the DC-GC-FID (*n* = 51), GC×GC-FID (*n* = 74), PTR-ToF-MS, (*n* = 75) and SPE-GC×GC-ToF-MS (*n* = 28) with information on organic aerosol composition given by PTFE-GC×GC-ToF-MS (*n* = 28). All measurements used the same procedures to characterise emissions to create a self-consistent dataset of speciated organic emissions spanning a large range of volatilities. Speciation profiles are based on a subset of tests which included SPE/PTFE samples from fuel wood (*n* = 16), cow dung cake (*n* = 3), municipal solid waste (*n* = 3), crop residue (*n* = 3), LPG (*n* = 1), charcoal (*n* = 1), sawdust (*n* = 1) and blank measurements (*n* = 8).

5.2.2. Mapping organics to volatility basis data set

The volatility-basis dataset (VBS) is designed to simulate the emission and evolution of I/SVOCs into the atmosphere (Donahue et al., 2006) and places NMVOCs into logarithmically spaced bins of saturation concentration, *C**, at 298 K. Emissions from fuel wood, cow dung cake, municipal solid waste and LPG have been mapped onto a VBS to visualise and compare emissions across the entire range of volatilities measured using data

collected by the DC-GC-FID, GC×GC-FID, PTR-ToF-MS, SPE-GC×GC-ToF-MS (> C_{12}) and PTFE-GC×GC-ToF-MS. *C** values have been calculated for individual NMVOCs measured online using DC-GC-FID, GC×GC-FID and PTR-ToF-MS. For SPE-GC×GC-ToF-MS and PTFE-ToF-MS analyses, organics have been lumped into groups of unspeciated compounds. These have been spaced between *n*-alkanes, with the volatility assigned as the mean volatility of the alkanes either side of the bin. For NMVOCs where insufficient data is available for a calculation of *C**, the volatility has been assigned as *C** of the *n*-alkane with the nearest boiling point. C_i^* for each NMVOC$_i$ has been calculated using E5.1:

$$C_i^* = \frac{M_i 10^6 \zeta_i P^o_{L,i}}{760RT} \quad \text{(E5.1)}$$

where M_i = molecular weight of NMVOC$_i$ (g mol^{-1}), ζ_i = activity coefficient of NMVOC$_i$ in the condensed phase (assumed to be 1), $P^o_{L,i}$ = liquid vapour pressure of NMVOC in Torr, R = gas constant (8.206 × 10^{-5} m^3 atm mol^{-1} K^{-1}) and T = temperature (K). The constant 760 has been used to convert between units of atm and Torr where 1 atm = 760 Torr. $P^o_{L,i}$ values have been taken from the EPA Estimation Programme Interface Suite data (EPA, 2012). Grouped regions of organics from SPE disks and PTFE filters have been calibrated to allow semi-quantification based on the mean total ion current (TIC) chromatogram of the two *n*-alkanes either side of the bin close to a concentration of ~ 1 μg ml^{-1}. The approach was uncertain and suggestions for better quantification of this complex organic material are provided in chapter 3.

Experimental and/or predicted vapour pressures of species, especially the *n*-alkanes used for assigning volatility bins, remain uncertain. We have adopted a similar approach to Lu et al. (2018), with the factor of 10 spacing of volatility bins to minimise the chance of volatility misassignment. IVOCs are in the *n*-alkane range ~ C_{12} to C_{22}, SVOCs from C_{23} to C_{32}, and L/ELVOCs from C_{33} to C_{40}. Care has been taken to avoid double counting of species measured using multiple techniques. Gas-phase species, which were possible to measure using either of the GC instruments or the PTR-ToF-MS, have been counted once only. In summary C_2-C_6 non-methane volatile organic compounds (alkanes/alkenes) were measured using the DC-GC-FID. C_7-C_{12} non-methane volatile organic compounds (alkanes and benzene-C_3 substituted monoaromatics) were measured using the GC×GC-FID. Remaining NMVOCs and gas-phase I/SVOCs were measured using the PTR-ToF-MS (C_4-C_5

substituted monoaromatics, phenolics, furanics, oxygenated aromatics, oxygenated aliphatics and nitrogen containing volatile organic compounds). The unidentified gaseous I/SVOC fraction was estimated using SPE-GC×GC-ToF-MS. The organic aerosol fraction was measured using the PTFE-GC×GC-ToF-MS. To allow incorporation of I/SVOCs species from SPE disks, species and their isomers measured using the PTR-ToF-MS have been removed from the SPE and PTFE analyses.

5.2.3. Comparison of EPA and fuel wood source profiles

Fuel wood source profiles were compared to those from the EPA SPECIATE 5.0 (2019) database. Notably profiles from the EPA for burning sources were split into either gas- or particle-phase measurements. All available profiles for residential combustion were considered from sets of experiments including fireplace wood combustion (4640-4642), residential combustion using wood and pellet stoves (95129-95138), residential wood stove combustion (95156-95159) and residential wood combustion (G95467-G95470). EPA profiles 95156-95159 for residential wood stove combustion were not directly compared due to the low number of organic species measured (*n*=37). Comparison was made to *Pinus ponderosa* (G95467), *Eucalyptus spp* (4640) and a wood stove (95133). This placed into context the VBS developed in this work, because the multiple techniques used here allowed simultaneous measurement of organics in both gas and aerosol phases.

EPA G95467 was a source profile derived from measurement of 179 organic species from combustion of *Pinus ponderosa* (McDonald et al., 2000). C_2-C_{12} compounds were collected into canisters and analysed by GC-FID/-MS, C_8-C_{20} compounds were collected onto Tenax tubes and analysed by GC-FID/-MS, carbonyls were collected onto 2,4-dinitrophenylhydrazine cartridges and analysed by HPLC and fine particles and SVOCs were collected onto filter/PUF/XAD/PUF cartridges and analysed by GC-MS. EPA 4640 was a source profile derived from measurement of 85 organic species from *Eucalyptus spp*. This profile was chosen as *Eucalyptus spp* was also measured as part of this study. Gas phase semi-volatile species were collected onto PUF cartridges, particles collected onto filters and carbonyls onto C_{18} cartridges impregnated with dinitrophenylhydrazine. Samples were then extracted and analysed by GC-MS (Schauer et al., 2001). EPA 95133 was developed by sampling VOCs into Tedlar gas sampling bags followed by GC-FID analysis and semi-volatile

PAHs were collected onto PUF plugs, extracted and analysed by GC-MS (Pettersson et al., 2011).

5.2.4. Estimation of the SOA formation potential

The overall yield of SOA, γ_{SOA}, from gas-phase emissions from biomass burning samples (mass of SOA produced/mass of NMOG emissions) was estimated using E5.2 (Lu et al., 2018):

$$\gamma_{SOA} = \sum_i f_{gas,\,i}\,\gamma_i \qquad \text{(E5.2)}$$

where $f_{gas,i}$ = the mass fraction of SOA precursor as a proportion of total mass of gas-phase emissions and γ_i = yield of SOA precursor *i* at a concentration of OA = 10 μg m^{-3}. SOA yields have been calculated from literature (see the Supplementary Information 8.13 using OA mass loadings as close to 10 μg m^{-3} under both high and low NO_x conditions, where supporting information from relevant literature was available), with gas-phase SVOCs assumed to have SOA mass yields of 1. The rate of reaction of chemical species with OH is not included in E5.2. IVOCs usually react faster than NMVOCs with OH, and so IVOCs and NMVOCs contribute differently to SOA with respect to time (Zhao et al., 2016). As a result, this approach estimates a lower-bound contribution of the ultimate yield of IVOCs to SOA (Lu et al., 2018). It also does not include species which may form SOA heterogeneously, which have not been assigned traditional SOA yield values.

5.2.5. Estimation of OH reactivity

The OH reactivity of emissions from different fuel types were examined to understand the largest contributors. The mean concentrations of NMVOCs from the DC-GC-FID, GC×GC-FID and PTR-ToF-MS were used to calculate OH reactivity, s^{-1}, using E5.3:

$$s^{-1} = \left([\text{NMVOC}](\text{ppbv}) \times 10^{-9} \times [\text{M}]\right) \times k_{OH}(298\ \text{K}) \qquad \text{(E5.3)}$$

where [M] is given by E5.4 and the rate constants for reaction with OH, k_{OH}, used in this study are given in the Supplementary Information 8.14.

$$[\text{M}] = \left(\frac{\text{Pressure (mbar)} \times 10^{-4}}{(8.314 \times (273.15 + \text{temperature}))}\right) \times 6.023\times10^{23} \qquad \text{(E5.4)}$$

5.2.6. Estimation of PAH toxicity

Toxicity equivalence factors (TEFs) have been used to assess the relative toxicity of emissions per kg of fuel burnt. TEFs indicate the relative toxicity of a PAH to benzo[a]pyrene (BaP), one of the most carcinogenic PAHs (OEHHA, 1994). The toxicity of a PAH is commonly expressed in BaP equivalents ($[BaP]_{eq}$), which is calculated in E5.5 by multiplying the concentration of PAH_i, in nanograms per cubic metre (ng m^{-3}), by the corresponding TEF for i, TEF_i, with values for TEF_i given in the Supplementary Information 8.15 (Ramírez et al., 2011; Tomaz et al., 2016; Elzein et al., 2019).

$$\sum [BaP]_{eq} = \sum_{i}^{n=1} (C_i \times TEF_i) \quad \text{(E5.5)}$$

5.3. Results and discussions

5.3.1. Volatility distribution

Figure 5.1 shows the mean volatility distribution of characterised organic emissions for (A) all fuel wood types studied (n=16) and (B) cow dung cake (n =3) classified by measurement technique: PTR-ToF-MS (orange), DC-GC-FID (green), GC×GC-FID (purple), SPE-GC×GC-ToF-MS (blue) and PTFE-GC×GC-ToF-MS (red). Figure 5.1 emphasises the importance of using multiple measurement techniques to measure organic emissions, and this study covers a volatility range of over 13 orders of magnitude. This allowed a comprehensive characterisation of emissions during domestic fuel burning. Cow dung cake samples released significantly more SVOC and L/ELVOC than fuel wood samples.

Figure 5.1 illustrates the particle fraction, X_p, which was calculated according to the method in Lu et al. (2018), assuming all the organic emissions formed a quasi-ideal solution when diluted to ambient conditions (Lu et al., 2018). The particle fraction demonstrated the gas-to-particle partitioning of organics at typical atmospheric conditions (T = 298 K and OA concentration = 10 μg m^{-3}). IVOCs were predominantly found in the gas phase and SVOCs were present in both phases. The predicted particle fraction suggested that there should have been more gas-phase contributions in the I/SVOC range. The amount of organic material in the gas and particle phase is dependent on multiple factors such as temperature and concentration of OA. It is likely that at the high concentrations (OA > 10 μg m^{-3}) during source testing, a larger fraction of I/SVOCs partitioned into the particle phase.

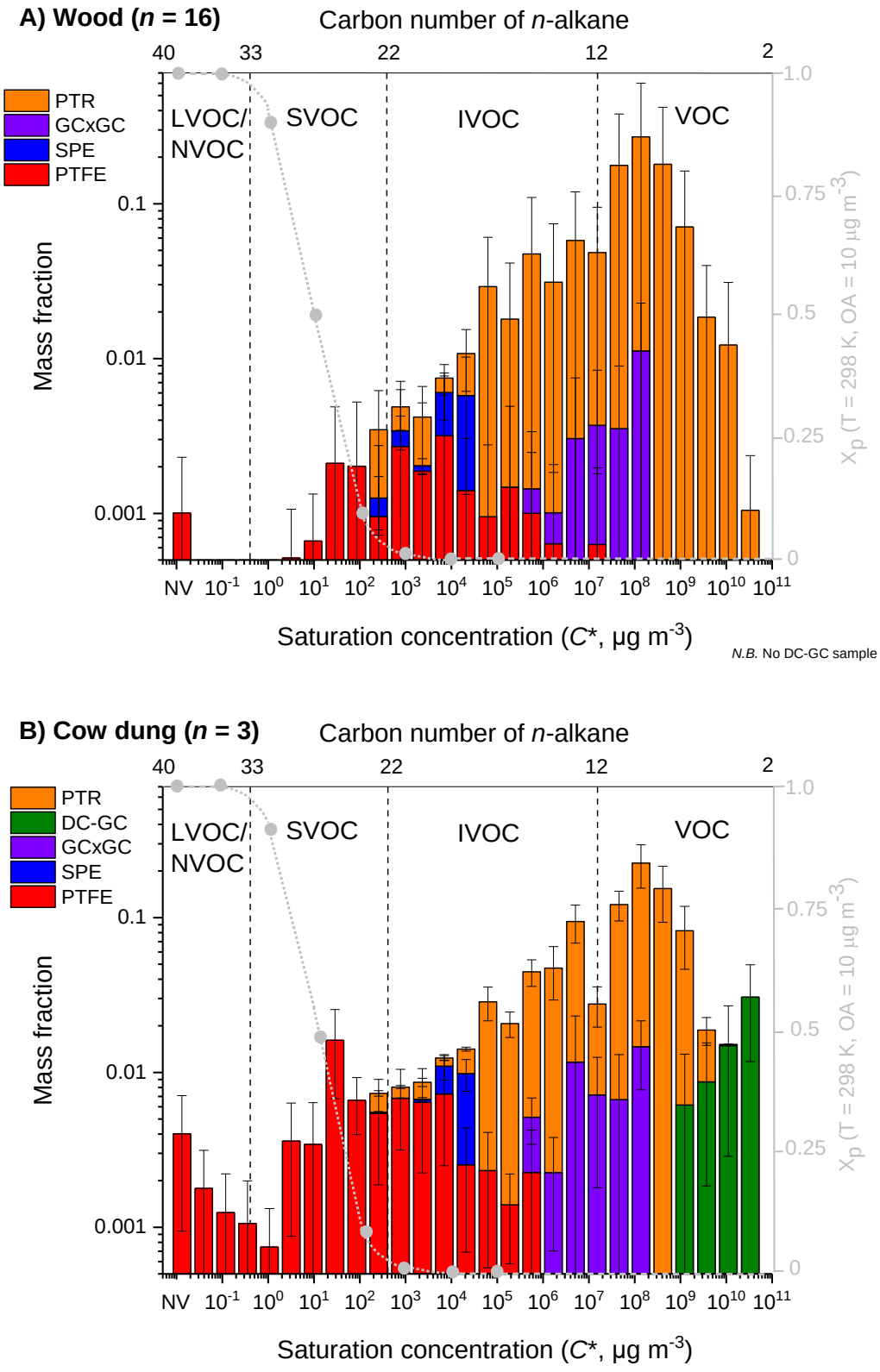

Figure 5.1. Mean volatility distribution of organics from fuel wood (top) and cow dung cake (bottom) collected from India. Emissions are classified by sampling technique with PTR-ToF-MS (orange), DC-GC-FID (green), GC×GC-FID (purple), SPE-GC×GC-ToF-MS (blue) and PTFE-GC×GC-ToF-MS (red). The grey dashed line indicates the particle fraction, assuming the emissions form a quasi-ideal solution at organic aerosol concentration = 10 µg m^{-3} and temperature = 298 K.

5.3.2. Chemical composition distribution

Figure 5.2 shows the mean volatility distributions of organic emissions from seven different source categories (A) fuel wood, (B) cow dung cake, (C) municipal solid waste, (D) crop residue, (E) charcoal, (F) sawdust and (G) LPG. The largest mass fraction at emission for all sources, expect LPG, was in the range $C^* \sim 10^7$-10^9 μg m^{-3} and a result of small oxygenated species. LPG emission was dominated by fugitive emissions of propane and butane from C^* 10^9-10^{10} μg m^{-3}. Figure 5.2 highlights how changes in the type of the source influenced emissions of I/S/L/ELVOCs. All sources, except LPG, have significant emissions of IVOCs.

Figure 5.2A also shows comparison to EPA source profiles G95467 for softwood (red circles) and 4640 (blue squares) for *Eucalyptus spp*. These profiles highlight the difficulties in using current source profiles to predict SOA from biomass burning plumes, due to significantly different predictions in the range $C^* \sim 10^2$-10^6 μg m^{-3}.

EPA 95133 reported essentially no IVOCs, EPA G95467 showed some IVOCs in the range $C^* \sim 10^5$-10^6 μg m^{-3} and EPA 4640 showed considerably higher IVOC emissions. EPA 95133 did not measure important I/SVOC species released from domestic biomass burning such as phenolics and furanics and therefore no organic matter was represented for $C^* < 5\times10^6$ μg m^{-3}. EPA G95467 was one of the best current source profiles, however, no organic matter was present in this profile for $C^* < 10^5$ μg m^{-3}. This may be due to lack of simultaneous gas- and particle-phase measurements of all organic species present. As a result, gas-phase organic species may have partitioned into the particle phase because of high organic aerosol concentrations during source testing and were therefore not represented. EPA 4640 measured more phenolic and furanic compounds. Despite this, the measurement of only 85 organic species in EPA 4640 overemphasised the importance of I/SVOCs as a mass fraction. This therefore still posed significant problems when using EPA 4640 to model SOA formation. These issues demonstrated the benefit of the VBS developed here, as simultaneous measurement of organics in both gas and aerosol phases should alleviate these problems. For some sources, such as the combustion of MSW, cow dung cake, crop residues and sawdust a greater mass fraction was released of I/SVOCs. The use of a VBS for these sources is likely even more important due the presence of large amounts of I/SVOC material.

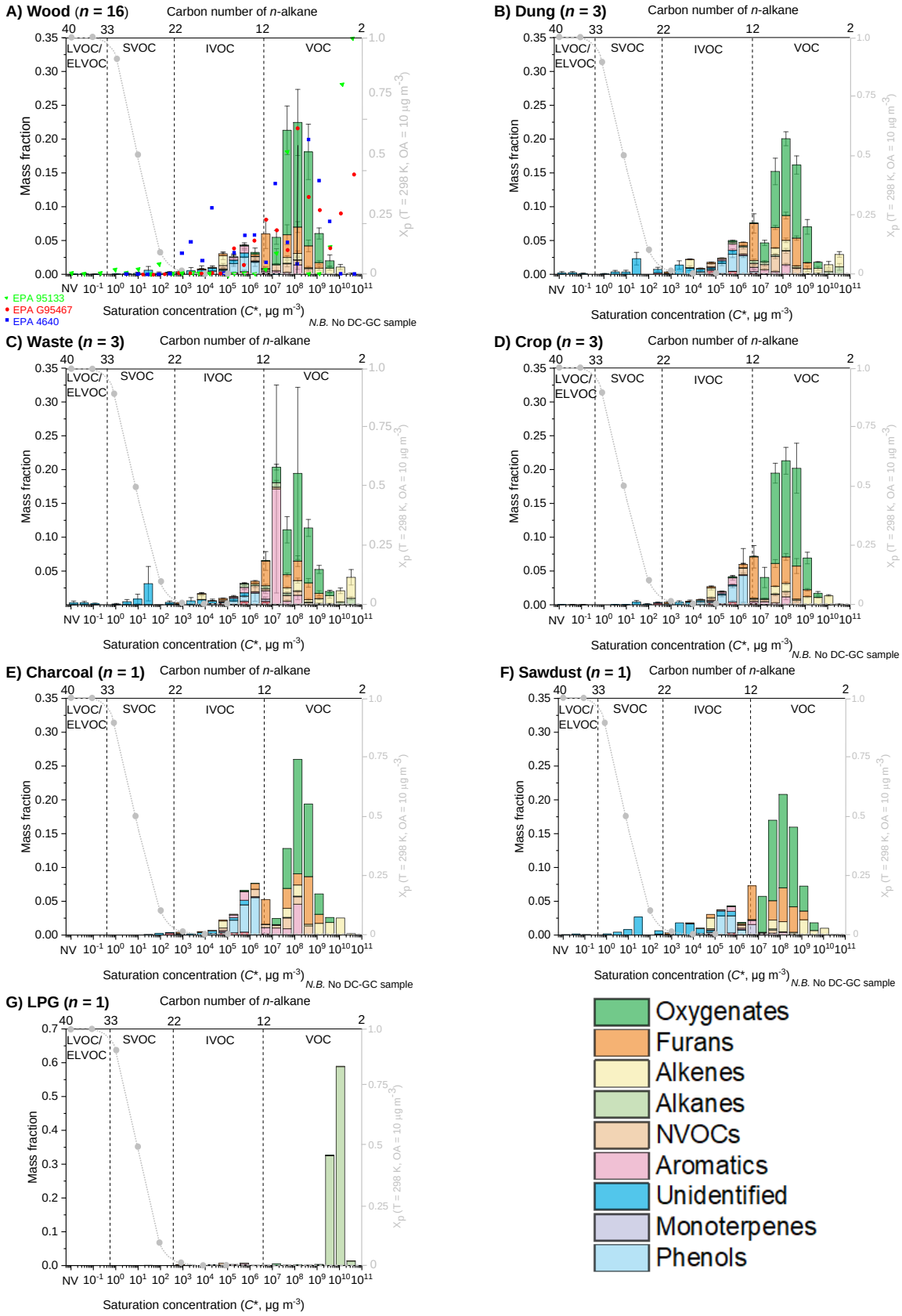

Figure 5.2. Mean volatility distribution of organic emissions for A = fuel wood, B = cow dung cake, C = municipal solid waste, D = crop residue, E = charcoal, F = sawdust and G = LPG with composition indicated by colour. Fuel wood profiles are compared to EPA inventories G95467 for softwood (red) and EPA 4640 for *Eucalyptus spp* (blue).

The comparison results suggested that the profile presented for Indian domestic fuel wood from this study was significantly lower than the data in EPA G95467 and 95133 in the two most volatile bins (C^* ~ 10^{10} – 10^{11} μg m^{-3}). However, this was an artefact due to the lack of measurements with the DC-GC-FID, which targeted the most volatile species. However, the underestimation of emissions from C^* ~ 10^{10}-10^{11} μg m^{-3} is unlikely to be significant when calculating SOA formation using the measured species and VBS presented.

Table 5.1 shows the mass fraction of organic material presented in Figure 5.2 from the 7 different sources studied here, presented in volatility bins spanning over 13 orders of magnitude. For certain sources, such as LPG and charcoal, only one sample was taken. The lack of repeat measurements significantly increased the uncertainty associated with the VBS presented. Despite this, multiple gas-phase NMVOC measurements were made. These showed similar results and therefore these VBS were included. The results in Table 5.1 should be used to better characterise SOA formation in chemical-transport models from domestic biomass combustion sources as the volatility distribution of organic emissions presented can be accurately adjusted to atmospheric dilutions, aerosol concentrations and temperatures.

Table 5.1. Mass fraction of organic material released from burning in logarithmic saturation vapour pressure C^* (μg m^{-3}) bins.

C^*	Range	Wood	Dung	Waste	Sawdust	LPG	Charcoal	Crop
NV	ELVOC	0.001	0.006	0.006	0.002	0.000	0.007	0.001
10^{-1}	SVOC	0.000	0.002	0.002	0.001	0.000	0.000	0.000
10^{0}	L/SVOC	0.001	0.008	0.012	0.014	0.000	0.000	0.000
10^{1}	SVOC	0.004	0.023	0.025	0.027	0.001	0.001	0.004
10^{2}	S/IVOC	0.008	0.015	0.006	0.017	0.001	0.009	0.008
10^{3}	IVOC	0.012	0.021	0.014	0.033	0.000	0.011	0.010
10^{4}	IVOC	0.040	0.043	0.027	0.047	0.000	0.036	0.038
10^{5}	IVOC	0.066	0.065	0.035	0.071	0.001	0.087	0.062
10^{6}	I/VOC	0.090	0.142	0.117	0.091	0.001	0.129	0.135
10^{7}	VOC	0.224	0.149	0.278	0.206	0.000	0.122	0.202
10^{8}	VOC	0.449	0.379	0.348	0.387	0.001	0.471	0.434
10^{9}	VOC	0.090	0.101	0.073	0.093	0.350	0.101	0.092
10^{10}	VOC	0.013	0.046	0.058	0.011	0.646	0.027	0.014

Figure 5.3 shows that the mean mass fractions of IVOCs emitted increased from municipal solid waste (0.12 ± 0.02) to fuel wood (0.15 ± 0.04) to crop residue (0.16 ± 0.04) to cow dung cake (0.18 ± 0.02). SVOC emissions for fuel wood and crop residue were the lowest mass fraction (0.01 ± 0.01) and larger for cow dung cake (0.04 ± 0.02) and municipal solid waste (0.05 ± 0.04). L/ELVOC emissions for crop residue (0.001 ± 0.001) and fuel wood (0.002 ± 0.002) were the lowest and larger for cow dung cake (0.006 ± 0.004) and municipal solid waste (0.009 ± 0.008). SVOC and L/ELVOC emissions from crop residue and charcoal were similarly low as fuel wood. This may be a result of the different fire conditions caused by the difference in composition of samples. Fires which are intense and flaming have been shown to have high black carbon emissions and those which are more towards the smouldering phase have high OA emissions (Radke et al., 1991; Yokelson et al., 2003; McMeeking et al., 2009; Kortelainen et al., 2018). It is likely that the higher emissions of OA from cow dung cake, municipal solid waste and sawdust are a result of the lower combustion efficiency of these samples.

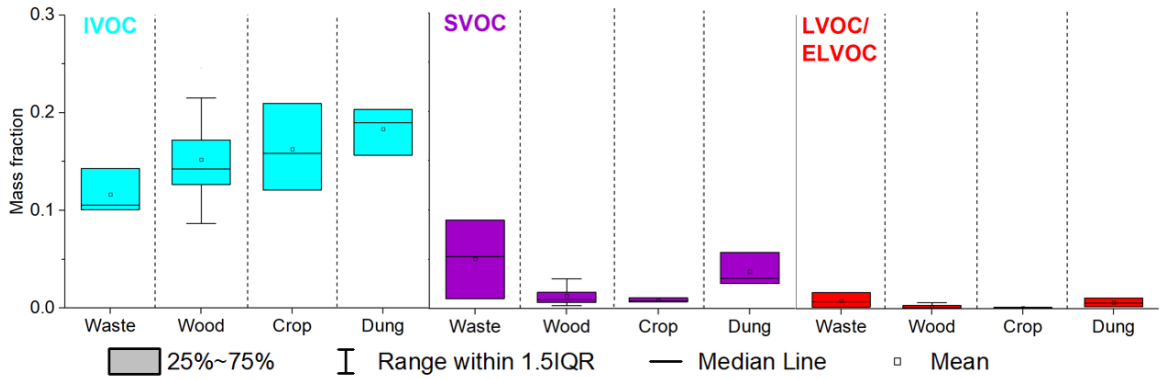

Figure 5.3. IVOC, SVOC and L/ELVOC mass fractions emitted from combustion of municipal solid waste, fuel wood and cow dung cake. SVOC and L/ELVOC material represented on average a smaller mass fraction from fuel wood and crop residue than from municipal solid waste and cow dung cake.

5.3.3. SOA formation potential

Figure 5.4 shows the sum of the mass fraction of NMVOCs released from domestic fuel burning in this study. Only the species identified as SOA precursors and assigned with SOA yields in the Supplementary Information 8.13 were included. The mass fraction of SOA precursors from fuel wood, crop residue and cow dung cake samples were from 0.3-0.5.

Compared to sources calculated using the same method (Lu et al., 2018), the mass fraction which resulted in SOA was less, with the exception of MSW burning, compared to gasoline (~ 0.65) and diesel (~ 0.7) engines. This was principally due to the large emission of smaller oxygenated species from burning samples. MSW burning samples released the largest mass fraction of SOA precursors (0.4-0.65).

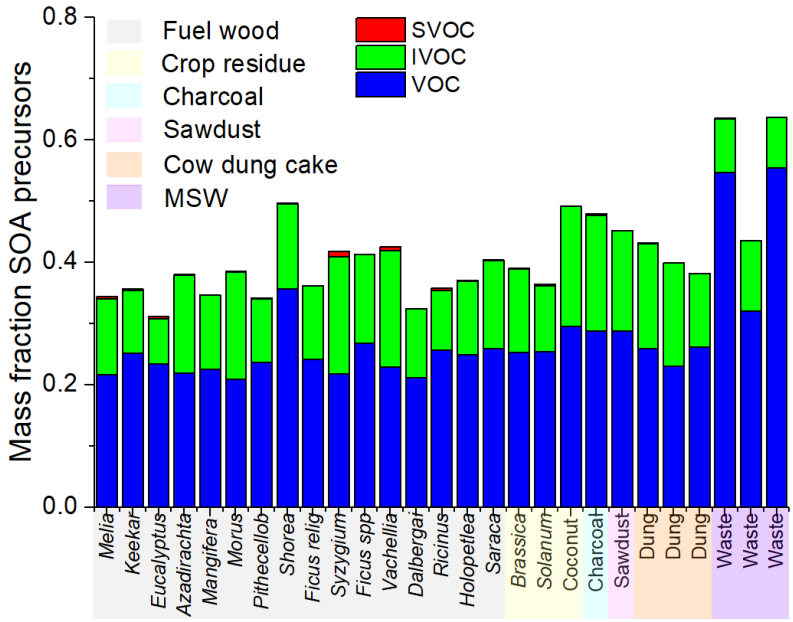

Figure 5.4. Mass fraction of NMVOCs from burning which were SOA precursors.

Figure 5.5A and Figure 5.5B show the estimated SOA yields from burning samples under high and low NO_x conditions. These are intended to represent idealised systems for photo-oxidation of SOA precursors. This is because generally the SOA yield decreases as NO_x levels increase (Ng et al., 2007a). This is due to competing reaction pathways of peroxy radicals between NO and HO_2. Under high NO_x conditions, RO_2 radicals react with NO_x and under low NO_x conditions, RO_2 radicals react with HO_2 (Yee et al., 2013). As a result, the low NO_x pathway generally leads to lower volatility reaction products than the high NO_x pathway. Whilst conditions vary between different experiments, SOA yield data (where possible) has been chosen from literature to best represent these two scenarios, with low NO_x conditions generally < 10 ppbv and high NO_x conditions ~ 100-1000s ppbv (Yee et al., 2013).

Consideration has been given to both cases since biomass burning in India impacts both urban high NO_x regions and rural lower NO_x regions. These scenarios are simplified and designed to understand the evolution of emissions once diluted into ambient air. More

complicated chemistry directly in the burning plume after emission is likely, due to the simultaneous emission of NO_x from nitrogen bonded into organic molecules in the fuel which is released as NO during combustion. This is called fuel NO_x and the nitrogen is mainly from pyridine and pyrrole groups in the organic matter which forms the fuel (Wendt et al., 1979). The amount of fuel NO_x formed is generally independent of the temperature. HCN is formed during combustion from the nitrogen in fuel samples, such as the nitrile group through R5.1 or R5.2 (Haynes et al., 1975).

$$CN + H_2 \rightleftharpoons HCN + H \quad \text{(R5.1)}$$

$$CN + H_2O \rightleftharpoons HCN + OH \quad \text{(R5.2)}$$

The HCN formed then reacts further through R5.3 - R5.5 (Miller and Fisk, 1987).

$$HCN + O \rightleftharpoons NCO + H \quad \text{(R5.3)}$$

$$NCO + H \rightleftharpoons NH + CO \quad \text{(R5.4)}$$

$$NH + H \rightleftharpoons N + H_2 \quad \text{(R5.5)}$$

NO is then formed via R5.6 or R5.7. Under high oxygen conditions, the more direct route is also possible through R5.8:

$$N + O_2 \rightleftharpoons NO + O \quad \text{(R5.6)}$$

$$N + OH \rightleftharpoons NO + H \quad \text{(R5.7)}$$

$$NH + O \rightleftharpoons NO + H \quad \text{(R5.8)}$$

where $k_{R5.6} = 1.16 \times 10^{-10}$ cm^3 molecule^{-1} s^{-1} (Cohen and Westberg, 1991). This will increase the amount of NO_x present during oxidation in the burning plume. In India, many cities are under high NO_x conditions and it is therefore likely that a lot of the initial chemistry occurs

under high NO_x conditions. Under high NO_x conditions, SOA yields are lower and IVOCs represent a larger proportion of the total SOA produced. Under low NO_x conditions, SOA yields are greater, and NMVOCs result in a greater proportion of the total SOA due to higher estimated SOA yields from aromatic and furanic species. Other studies examining emissions from burning have traditionally considered yields from only one of these regimes, but greater SOA production under low NO_x conditions has been well described previously (Ng et al., 2007b; Chan et al., 2009).

Figure 5.5C shows that high NO_x SOA yields from sawdust, charcoal, cow dung cake, fuel wood and crop residue were likely dominated by phenolics (light blue, 21-70%) with a significant contribution from furanics (orange, 9-33%) due to high emission factors of these species and high SOA yields. Other important SOA contributions were from aromatics (2-8%), oxygenated aromatics (2-8%), oxygenated aliphatic species (2-9%), monoterpenes (0-7%) and PAHs (2-16%). A larger proportion of SOA (40%) from municipal solid waste samples under high NO_x conditions was from aromatics due to a high emission factor of styrene from these samples.

Figure 5.5D shows that for sawdust, charcoal, cow dung cake and fuel wood samples, furanic species (17-58%) and aromatics (4-16%) were likely to provide a greater proportion of total SOA under low NO_x conditions. The contribution of phenolic compounds was less (10-43%) due to larger aromatic and estimated furanic SOA yields under these conditions. Contributions remained small from oxygenated aromatics (3-11%), aliphatic species (0-2%), oxygenated aliphatics (0-2%), nitrogen containing NMVOCs (0.5-3%), monoterpenes (0-2%) and PAHs (5-15%). The contribution of aromatics to SOA from municipal solid waste remained high (43%).

Bruns et al. (2016) showed that around 26% of SOA formed from the combustion of beech fuel wood was from phenols. This was notably higher than the 5-9% contribution of phenol from *Picea abies* (spruce) reported by Hartikainen et al. (2018), who reported that 12-14% of the total SOA was from phenolic compounds. The results of this study appear more like that of Bruns et al. (2016) with between 10-70% of the total SOA from biomass combustion a result of phenolic compounds.

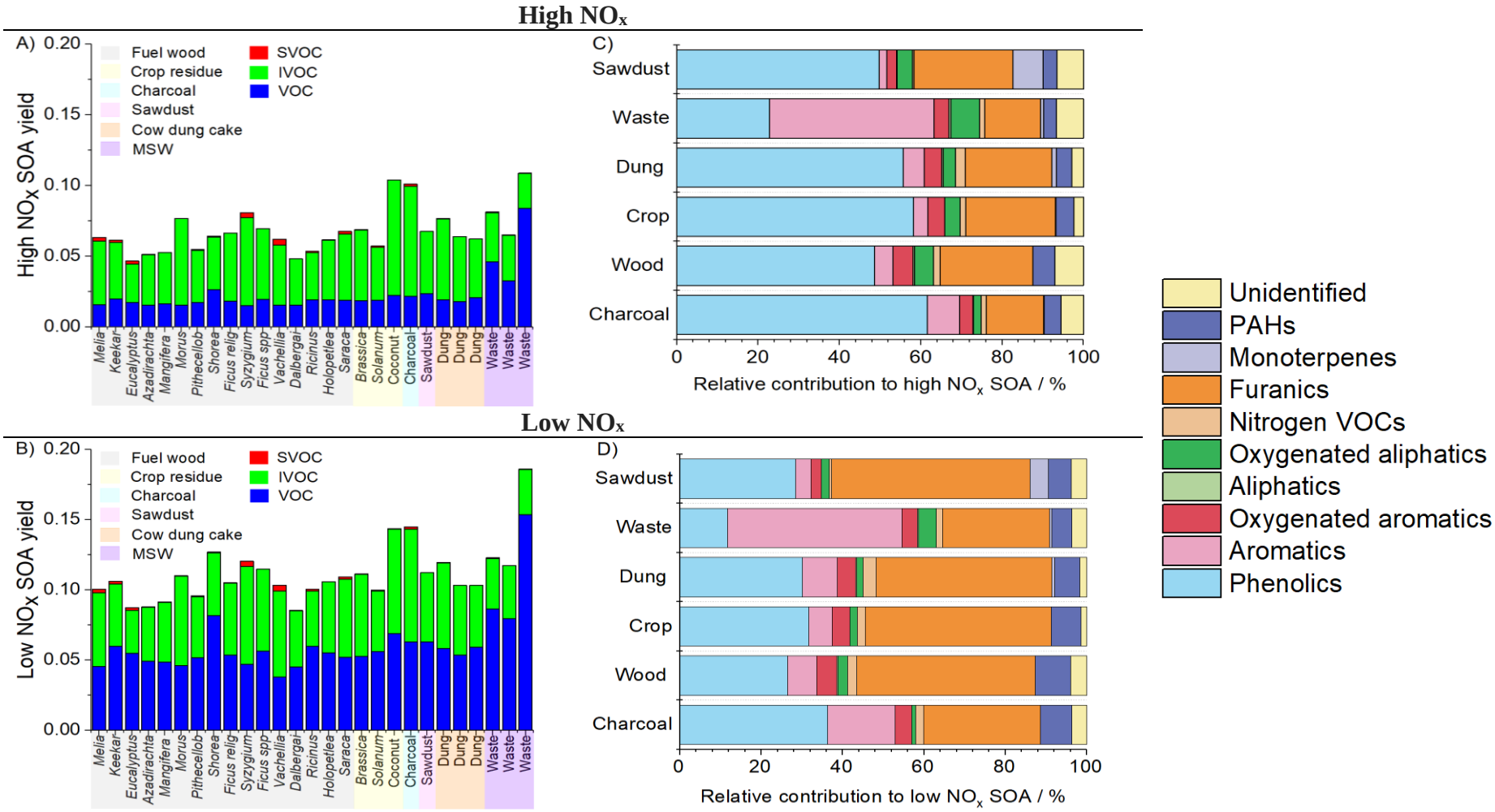

Figure 5.5. Results of SOA model with A = SOA yields as mass fraction of NMVOC released from biomass burning under high NO_x conditions, B = SOA yields as mass fraction of NMVOC released from biomass burning under low NO_x conditions, C = relative contributors to SOA formation under high NO_x conditions and D = relative contributions to SOA formation under low NO_x conditions. Unidentified corresponds to bulk material from SPE/PTFE filters.

The yields under high NO_x conditions for aromatics in this study (2-8%) were similarly low to those reported by Hartikainen et al. (2018) of 1.9-2.6% of the SOA from benzene and 1.9-3.3% from naphthalene, with low NO_x conditions in this study suggesting aromatics could result in greater SOA yields. This study found relatively low SOA yields from monoterpenes from biomass sources (0-7%), which is like Hartikainen et al. (2018) who found that monoterpenes contributed ~ 1-3% to SOA. This contrasts with Hatch et al. (2015) who showed that monoterpenes could result in 42-58% of the SOA from black spruce and ponderosa pine, however the fuel woods in that study were likely larger emitters of monoterpenes.

It remained difficult to accurately characterise SOA yields from furanic species, as there is a lack of chamber simulation studies. This study suggests that furanic compounds could act as a major SOA precursor source, similar to several other studies (Hatch et al., 2015; Hartikainen et al., 2018). In this study, the SOA yields of 2-methanol furanone, 2-(3H)-furanone, 5-hydroxymethyl-2[3H]-furanone, furfurals and methyl furfurals have been estimated using the toluene yield, as a previous study by Gilman et al. (2015) indicated they have similar secondary organic aerosol formation potentials (SOAP). This resulted in two different cases. Under high NO_x conditions, the SOA yield in this study of furanics was 0.08, which was similar to that of by Hatch et al. (2015) who used 0.10 based on the chemistry of 3-methyl furan measured from a previous study (Strollo and Ziemann, 2013). The low NO_x yield used in this study is 0.33, which is similar to Bruns et al. (2016), who used a furfural yield of 0.32 based on the average SOAP of all assigned ≥ C_6 compounds. The true SOA yields from furanic species from biomass burning samples remains uncertain and requires further chamber studies. This issue has been previously highlighted (Hatch et al., 2017). While following a different approach, this study arrives at similar estimated yields of furanic compounds as those used previously. It highlights that SOA formation from biomass burning smoke from solid fuels collected in India was predominantly driven by phenolic and furanic compounds as well as aromatics.

Table 5.2 shows the mass fraction of NMVOCs released which had been identified as SOA precursors from yield data, and the mass fraction of NMVOCs which resulted in SOA under high and low NO_x conditions. These are presented as mass fraction per mass of NMVOC released. Some sources, such as cow dung cake and municipal solid waste, released

significantly more NMVOCs per kg of fuel burnt than fuel wood (municipal solid waste ~ 88 g kg^{-1}, cow dung cake ~ 62 g kg^{-1} and fuel wood ~ 19 g kg^{-1}). Multiplying the emission factor by the mass fraction of NMVOC which will result in SOA highlighted interesting differences in SOA production between different source types. Table 5.2 shows this result, with the mass of SOA which would result per kg of fuel burnt under high NO_x (SOA_h g kg^{-1}) and low (SOA_l g kg^{-1}) conditions. The amount of SOA produced by each source has been considered relative to fuel wood, due to difficulties establishing SOA precursor from the chamber background for LPG. Emissions from cow dung cake and municipal solid waste resulted in ~ 3-4- and 6-7-times greater SOA per kg of fuel burnt than fuel wood, respectively. It is noteworthy that SOA estimated from chamber yield data and that observed experimentally have been shown to agree within a factor of 2 (Ahern et al., 2019).

The estimates of SOA formation should be considered relative to the heat output of specific fuels. Energy densities have been reported (EPA, 2000) for LPG (45,837 kJ kg^{-1}), charcoal (25,715 kJ kg^{-1}), acacia fuel wood (15,099 kJ kg^{-1}), eucalyptus fuel wood (15,333 kJ kg^{-1}), rice straw (13,027 kJ kg^{-1}), *Brassica spp* (11,763 kJ kg^{-1}) and dung cakes (11,763 kJ kg^{-1}). This highlights that whilst all sources are likely to result in SOA production, the burning of fuels such as cow dung cake is inadvisable due to the low calorific value and high emission factor. This means that more fuel is required to be burnt to achieve the same heat output, which will lead to greater levels of NMVOC emission. These will subsequently degrade local and regional air quality through the formation of a greater amount of secondary pollutants.

Table 5.2. Estimated contributions of gas-phase organic emissions to SOA where SOA_h = SOA formed under high NO_x conditions and SOA_l = SOA formed under low NO_x conditions.

Sample	Mass fraction			Mass formed (g kg^{-1} fuel)	
	SOA precursors	SOA_h	SOA_l	SOA_h	SOA_l
Wood	0.38	0.061	0.103	1.1 (0.3-5.9)	1.9 (0.4-10.0)
Dung	0.40	0.068	0.109	4.2 (2.4-5.6)	6.7 (3.8-9.0)
Waste	0.57	0.085	0.142	7.4 (4.8-10.1)	12.4 (8.0-16.9)
Charcoal	0.48	0.101	0.145	0.5 (0.2-0.8)	0.8 (0.3-1.1)
Sawdust	0.45	0.068	0.112	4.9 (1.9-7.7)	8.1 (3.2-12.8)
Crop	0.41	0.076	0.121	2.9 (0.7-5.6)	4.5 (1.1-8.9)

5.3.4. OH reactivity

Figure 5.6A shows that LPG OH reactivity was principally driven by alkanes (~ 75%). The contributions of other species were small and may have arisen from difficulties in background correction for this low emission fuel. For charcoal, the reactivity with OH was principally caused by furanic species (33%), phenolic species (19%) and oxygenates (15%). The reactivity of fuel wood emissions with OH was principally driven by furanic species (34%), oxygenated species (27%), phenolic species (13%) and alkenes (12%). Emissions from cow dung cake with OH were due to furanic species (32%), oxygenates (21%), alkenes (16%), phenolic species (12%) and nitrogen containing NMVOCs (11%). The OH reactivity from crop residue was from furanic species (38%), oxygenates (23%), phenolics (14%) and alkenes (11%). For sawdust, reactivity with OH was a result of furanic species (34%), oxygenates (24%), phenolic species (15%) and monoterpenes (9%). However, for charcoal and sawdust only 2 samples were measured. The OH reactivity from municipal solid waste samples was different and a result of aromatics (30%), followed by oxygenates (22%), furanic species (19%) and phenols (5%).

This study identified the species with the largest reactivity with the OH radical from Indian solid fuels. Ozone production from emissions when these fuels are combusted will be more complex and ultimately depend on NMVOC/NO_x ratios, meteorology and solar radiation (Coggon et al., 2019). Whilst the phenolic compounds here show relatively large contributions to OH reactivity (5-19%), these compounds will probably result in negative O_3 formation due to the formation of nitrophenols, which reduces the amount of NO_2 available for NMVOC oxidation (Lauraguais et al., 2014).

Gilman et al. (2015) calculated the relative contribution of different functionalities to the OH reactivity of fuel types from the U.S. The fuel types studied by Gilman et al. (2015) showed that alkenes contributed 25-29% of the OH reactivity, which was larger than found in this study (7-16%) for Indian fuels. The contribution to OH reactivity of OVOC for U.S. fuels (41-54%) was less than found in this study (45-76%). The contributions of monoterpenes for fuels from the U.S. were slightly larger (4-14%) than for those from India (0-7%). This was likely due to a greater contribution of monoterpene emitting fuel woods, such as pine, to fuels from the U.S. studied by Gilman et al. (2015). Both studies found a

small contribution from aromatics (<5%) and nitrogen containing NMVOCs (< 11%) to OH reactivity.

Figure 5.6B shows the OH reactivity of each source at the top of the combustion chamber relative to LPG. This has been calculated by multiplying the mean OH reactivity of flue gases by the volume of air sampled and normalising to the total reactivity of LPG. The OH reactivity of LPG was the lowest. Emissions from charcoal, fuel wood, crop residue, cow dung cake and sawdust were respectively ~ 8, 30, 90, 120 and 150 times more reactive with OH than those from LPG. The OH reactivity of emissions from municipal solid waste were the greatest and approximately 230 times greater than from LPG. Fuel wood, cow dung cake and municipal solid waste burning are large NMVOC sources in India (Wiedinmyer et al., 2014; Sharma et al., 2015). The significantly greater OH reactivity of emissions from these sources is likely to substantially deteriorate local and regional air quality compared to users cooking over LPG.

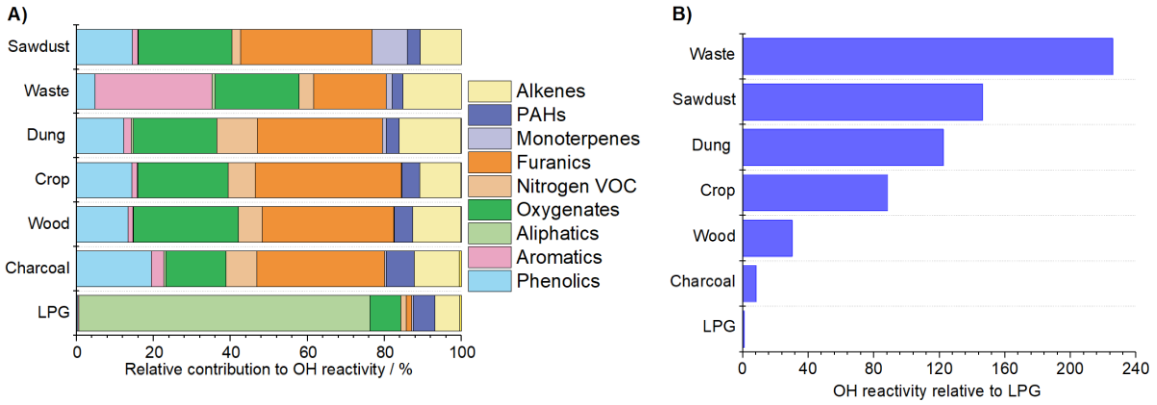

Figure 5.6. OH reactivity of emissions from different fuel types with A = relative contribution to OH reactivity and B = total OH reactivity of fuel types at top of flue relative to LPG which is set to 1.

5.3.5. PAH toxicity

A need has been identified to better understand the impact of PAHs from combustion sources in cities such as Delhi, where concentrations have been shown to be high and suggested to be enhanced by emissions from burning sources (Elzein et al., 2020). Figure 5.6 shows that when comparing the toxicity of 21 PAHs released, fuel wood, crop residue, cow dung cake and MSW were respectively 20, 60, 130 and 220 times more toxic than LPG

per kg of fuel burnt. Toxic emissions from these 21 PAHs released from LPG were small, and were principally driven by naphthalene (43%), fluoranthene (24%) and methylnaphthalenes (11%). The largest drivers for fuel wood/crop residue toxicity were benzo[a]pyrene (38%/48%), naphthalene (14%/11%) and benzo[b]fluoranthene (8%/8%), respectively. The contribution of naphthalene to the toxicity of cow dung cake and MSW was lower, with their toxicities driven by benzo[a]pyrene (49%/42%), dibenz(a,h)anthracene (13%/16%) and benzo[b]fluoranthene (8%/13%). The real-world effect of this toxicity would be significantly enhanced for fuel wood and cow dung cake, by around a further factor of 10. This is because significantly more fuel wood and cow dung cake fuel is used per user than LPG, due to the higher energy density of LPG and more efficient burning of this fuel (NSSO, 2014, 2015b). These results reinforced findings of other studies assessing the health benefits of LPG vs. solid fuels which suggested that to significantly reduce the impacts of combustion, a shift to cleaner cooking technologies was required (Simon et al., 2014; Pope et al., 2017; Sambandam et al., 2015).

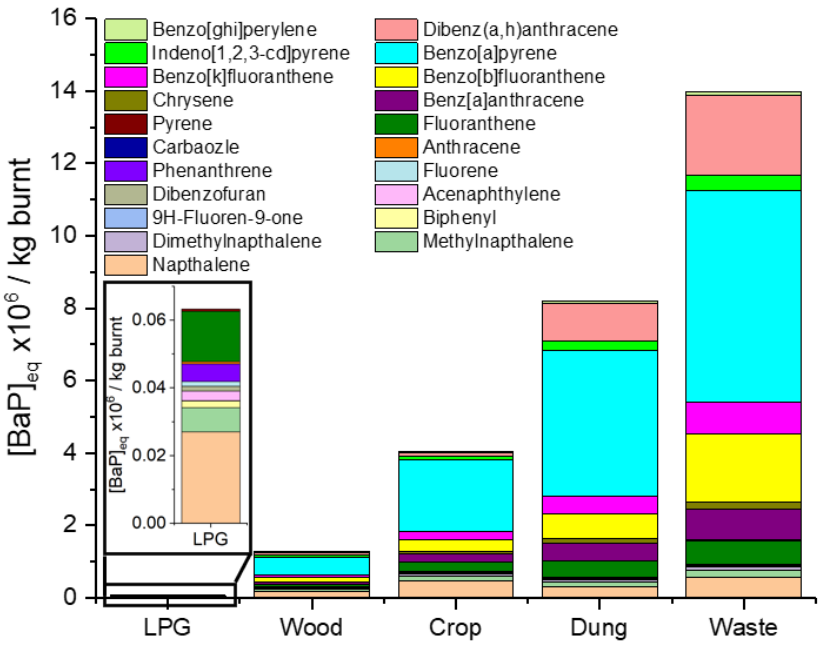

Figure 5.7. Comparison of equivalent toxicity of PAHs from different fuel types.

5.4. Conclusions

This study compiled comprehensive measurements of organic emissions from the combustion of a range of domestic fuels common to India. A range of detailed and complementary techniques allowed a VBS to be generated across a wide range of *C** values. This highlighted that IVOC emissions from burning should be better represented in models for an improved understanding of SOA production from burning emissions.

The results estimated that phenolics and furanics are important to both SOA production and OH reactivity, respectively accounting for 10-70% and 9-58% of the SOA and 5-22% and 9-48% of OH reactivity from biomass burning emissions. The contribution of smaller oxygenated species to OH reactivity was also significant at 15-42 %. Different combustion sources were compared which showed that emissions from fuel wood, crop residue, cow dung cake and municipal solid waste burning were 30, 90, 120 and 230 times more reactive with the OH radical and that PAH emissions were 20, 60, 130 and 220 times more toxic than LPG, respectively. This also showed that NMVOCs released from the combustion of cow dung cake and municipal solid waste samples in this study respectively resulted in ~ 3-4 and 6-7 times more SOA production per kg burnt than fuel wood. This demonstrated that reduction of emissions from these sources is important to improve local and regional air quality across India.

Few measurements were made from municipal solid waste, cow dung cake, crop residue and LPG samples and these emission profiles could be improved with future studies to better understand the effect of composition on emissions. The *C** of many species measured, including alkanes, remain uncertain and future studies are required to better understand the *C** of these species. In addition, there have only been a limited number of chamber studies to determine SOA formed during the oxidation of furanic species under high and low NO_x conditions. More studies of the oxidation and subsequent SOA formation from these important biomass burning emissions are required to better understand the impact of biomass burning and domestic solid fuel use on the atmosphere.

Chapter 6

Emission estimates and inventories of non-methane volatile organic compounds from anthropogenic burning sources in India

The majority of this chapter has been published as a manuscript under the same name:

Stewart, G. J., Nelson, B. S., Acton, W. J. F., Vaughan, A. R., Hopkins, J. R., Yunus, S. S. M., Hewitt, C. N., Wild, O., Nemitz, E., Gadi, R., Sahu, L. K., Mandal, T. K., Gurjar, B. R., Rickard, A. R., Lee, J. D., and Hamilton, J. F.: Emission estimates and inventories of non-methane volatile organic compounds from anthropogenic burning sources in India, Atmospheric Environment: X, 100115, 2021, https://doi.org/10.1016/j.aeaoa.2021.100115

6.1. Introduction

Biomass burning is the second largest global source of trace gases to the troposphere after biogenic emissions (Yokelson et al., 2008; Andreae, 2019). Major sources include wildfires, agricultural crop residue burning on fields and residential solid fuel combustion. Trace gases are released in varying amounts dependent on the combustion conditions and the material burned (Yokelson et al., 1996). Emission factors have been shown to vary significantly for different energy sources such as fuel wood, straw, grass, peat, and cow dung cake (Akagi et al., 2011; Andreae, 2019). Domestic biofuel burning has been estimated to release ~ 17 Tg yr^{-1} of non-methane volatile organic compounds (NMVOCs) globally (Andreae, 2019). NMVOCs have the potential to significantly reduce local, regional and global air quality though the formation of tropospheric ozone (Pfister et al., 2008; Jaffe and Wigder, 2012) and secondary organic aerosol (SOA) (Alvarado et al., 2015; Kroll and Seinfeld, 2008).

Emissions from biomass burning have been shown to be extremely complex, releasing a huge variety of chemical species (Crutzen et al., 1979; McDonald et al., 2000; Akagi et al., 2011; Koss et al., 2018). Recent developments in analytical techniques have allowed significantly improved understanding of the composition of emissions in both gas and particle phases. Application of the proton-transfer-reaction time-of-flight mass spectrometer (PTR-ToF-MS) to biomass burning emission experiments has allowed speciation of over 90% of measured NMVOC emissions (Stockwell et al., 2015; Koss et al., 2018). The use of PTR-ToF-MS in burning experiments has shown large emissions of small oxygenated species from burning and revealed the importance of intermediate-volatility and semi-volatile VOCs (I/SVOCs). IVOCs have been shown to represent a large fraction of total NMVOC emissions (Stockwell et al., 2015).

Emissions from domestic biofuel combustion pose significant health risks as approximately 3 billion people cook with solid fuels globally (World Health Organization, 2018b; World Bank, 2020). Emissions from burning have been linked to eye disease (Pokhrel et al., 2005; Karakoçak et al., 2019), chronic bronchitis (Akhtar et al., 2007; Moran-Mendoza et al., 2008), chronic obstructive pulmonary disease (Dennis et al., 1996; Orozco-Levi et al., 2006; Rinne et al., 2006; Ramirez-Venegas et al., 2006; Liu et al., 2007; PerezPadilla et al., 1996), lung cancer (Liu et al., 1993; Ko et al., 1997), childhood pneumonia (Smith et al., 2011),

acute lower respiratory infections (Bautista et al., 2009; Mishra, 2003) and low birth weight of children (Boy et al., 2002; Yucra et al., 2011). The detrimental impact of domestic biofuel combustion on indoor air pollution has been estimated to cause 2.8-3.9 million premature deaths annually (Smith et al., 2014; Kodros et al., 2018; World Health Organization, 2018b). In some regions of the world, such as South Asia, the impact is pronounced as widespread solid fuel use is coupled to extremely high population densities. Consequently, hazardous indoor air pollution because of the combustion of solid fuels has been determined to be the most important risk factor for the burden of disease in South Asia, from a range of 67 environmental and lifestyle risks (Lim et al., 2012; Smith et al., 2014).

Several studies have examined India-specific NMVOC sources (Kumari et al., 2019; Nagpure et al., 2015; Lal et al., 2016; Jain et al., 2014; Fleming et al., 2018), however, very few have used a range of sufficiently detailed, state-of-the-art analytical techniques to obtain full mass closure of gas-phase organic species emitted. This means that strategic improvement in Indian air quality with effective mitigation policies has been hindered by the lack of adequate, spatially disaggregated emission inventories created using local source profiles (Garaga et al., 2018). Recent top-down studies focussed on megacity Delhi have shown that 16% (Stewart et al., 2021) of non-methane hydrocarbons and 27% (Wang et al., 2020) of non-methane volatile organic compounds (NMVOCs) by mixing ratio at different urban sites were from solid fuel combustion sources. Bottom-up approaches have estimated the contribution of residential biofuel combustion to be greater at a national scale, representing approximately 60% of total anthropogenic NMVOC emissions (Sharma et al., 2015).

Several recent studies have focussed on understanding NMVOC emissions from solid fuel combustion sources specific to India. These measured emission factors for solid fuels using a range of state-of-the art techniques such as PTR-ToF-MS, gas chromatography (GC) and two-dimensional gas chromatography coupled to time-of-flight mass spectrometry (see chapters 3 and 4). These highlighted large differences in NMVOC emissions between different sources, with emission factors for cow dung cake and municipal solid waste (MSW) ~ 300% and 400% larger, respectively, than for conventional fuel wood combustion. The combustion of fuel wood, domestic crop residues, cow dung cake and MSW samples were also shown to contribute significantly to SOA formation. This meant that the burning

of cow dung cake fuel and MSW could have disproportionately large impacts on NMVOC emissions, and in turn air quality, in India.

Rapid growth has resulted in India being the second largest contributor to NMVOC emissions in Asia (Kurokawa et al., 2013; Kurokawa and Ohara, 2020). NMVOC emissions from India have been estimated in studies both focussed on Asia (Streets et al., 2003; Ohara et al., 2007; Zhang et al., 2009; Kurokawa et al., 2013; Crippa et al., 2019; Kurokawa and Ohara, 2020) or specifically on India (Varshney and Padhy, 1998; Pandey et al., 2014; Sharma et al., 2015). Lack of data and uncertainties in existing data complicate emission estimates and mean that considerable uncertainty exists over the size of NMVOC emissions from India, as shown in Table 6.1. Predicting emissions is complicated by a diverse range of sources such as older vehicle fleets, a high reliance on compressed natural gas (CNG), open crop burning on fields, MSW burning and solid biofuel combustion.

Table 6.1. Estimates of NMVOC emissions from India, with ( ) indicating estimated contribution from biomass burning.

Year	NMVOC / Tg yr^{-1}	Reference
1996	8.0 (6.6)	(Pandey et al., 2014; Sadavarte and Venkataraman, 2014)
1998	8.1 (4.7)	(Varshney and Padhy, 1998)
2000	8.0 (6.1)	(Pandey et al., 2014; Sadavarte and Venkataraman, 2014)
2000	10.8	(Streets et al., 2003)
2003	9.7	(Ohara et al., 2007)
2005	9.0 (6.5)	(Pandey et al., 2014; Sadavarte and Venkataraman, 2014)
2006	10.8	(Zhang et al., 2009)
2008	16.0	(Kurokawa et al., 2013)
2010	9.8 (6.9)	(Pandey et al., 2014; Sadavarte and Venkataraman, 2014)
2010	9.8 (6.5)	(Sharma et al., 2015)
2010	11.5	(Ohara et al., 2007)
2011	12.1 (6.0)	REAS 3.2 (Kurokawa and Ohara, 2020)
2015	12.0 (7.0)	(Pandey et al., 2014; Sadavarte and Venkataraman, 2014)
2015	13.5 (5.1)	EDGAR 5.0 (Crippa et al., 2019)

Traditional cook stoves represent a large pollution source in India due to their extensive use. Figure 6.1 shows an estimation of residential fuel use in India from fuel wood, cow dung cake, LPG, coal, charcoal, biogas, crop residues, kerosene and electricity (see the Supplementary Information 8.16 for details of calculation). Fuel wood and cow dung cake usage have been relatively constant over the last 25 years, with approximately three

quarters of a billion users (Pandey et al., 2014; World Health Organization, 2018b; World Bank, 2020). It has been forecast that solid fuel combustion sources will remain an important energy source to India in coming decades. Projections by the International Energy Agency show that with current policies, the proportion of the Indian population using biomass for cooking will reduce to a third of the population in 2030 and represent a quarter of the population by 2040 (IEA, 2020).

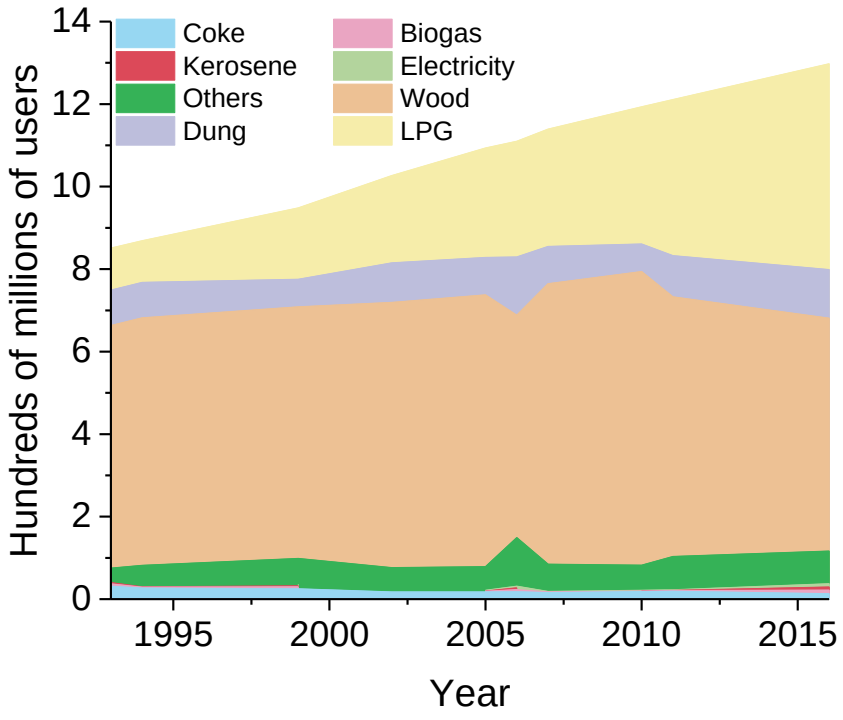

Figure 6.1. Approximate fuel use in India by number of users. See the Supplementary Information S8.16 for details of calculation. The peak in dung and other fuels in 2006 underlines one of the difficulties in accurately establishing fuel usage from surveys scaled up to India.

Biofuels such as fuel wood and cow dung cake are cheaper than modern cooking fuels, such as LPG and electricity. Traditional methods are also important to many local recipes, with the meals cooked using them considered to be tastier (Mukhopadhyay et al., 2012). Cow dung cakes are commonly used in the north of India because they are sustainable, reduce the demand on local fuel wood resources and are widely available. Despite this, the impact cow dung cake combustion has on air quality is poorly understood. This is because consumption estimates of dried cow dung cakes in India have been shown to vary by

around a factor of 3, in the range 35-128 Tg yr^{-1} for the years 2000-2001 (Habib et al., 2004). Emission estimates from cow dung cake combustion are also complicated by the varying moisture content of samples, which has a large influence on burn efficiency and in turn increases uncertainties in inventories.

The open burning of MSW is another poorly constrained, but likely important source of NMVOC pollution in India. This is a result of poor MSW management, as often not all of MSW in cities is collected and little MSW is collected rurally (Annepu et al., 2012). MSW is also used as a source of heating in cold seasons in low income areas (Nagpure et al., 2015). Fugitive methane emissions from decomposing organic matter in poorly managed landfill sites can result in fires, whilst burning often represents the only disposal method of MSW in rural regions. Nagpur et al. (2015) estimated that 90-1170 kg km^{-2} day^{-1} of MSW was burnt in winter and 13-1110 kg km^{-2} day^{-1} of MSW was burnt in summer in Delhi and that summer MSW burning in Agra was greater at 670-3485 kg km^{-2} day^{-1}. Previous studies have identified the open burning of MSW as a significant source of black carbon, hydrogen chloride, particulate matter, particulate chloride, NMVOCs and toxic emissions such as dioxins (McCulloch et al., 1999; Lemieux et al., 2000; Lemieux et al., 2003; Costner, 2005; Christian et al., 2010; Wiedinmyer et al., 2014; Stockwell et al., 2015; Stockwell et al., 2016; Kumari et al., 2019; Cash et al., 2020). Emission estimates from this source are complicated by lack of reliable data, as well as the variable composition of samples which are a mix of individual waste products and change with every sample. Official estimates of the amount of MSW produced in India were 49 Tg yr^{-1} in 2016 (CPCB, 2017), with other studies suggesting it to be larger (69-216 Tg yr^{-1}) (Annepu et al., 2012; Wiedinmyer et al., 2014; Sharma et al., 2019). This inevitably leads to differences in emissions and large uncertainty in the estimation of source strength. The result is hugely uncertain total NMVOC emission estimates from the burning of MSW in India, varying from 4-2060 Gg yr^{-1} (Sharma et al., 2019).

The burning of solid fuels is also a large source of polycyclic aromatic hydrocarbons (PAHs), with 57-61% of global PAH emissions (2950-3050 Gg yr^{-1}) estimated to be from the combustion of biofuels (Zhang and Tao, 2009; Shen et al., 2013). PAH concentrations in Indian cities have been reported to be 10-50 times higher than those measured internationally (Kulkarni and Venkataraman, 2000) and total emissions from India

calculated to be in the range 17-90 Gg yr^{-1} (Zhang and Tao, 2009; Shen et al., 2013; Gadi et al., 2012). PAHs are of interest because they are carcinogenic and mutagenic (IARC, 1983, 1984; Nisbet and LaGoy, 1992; Lewtas, 2007; Zhang and Tao, 2009; Jia et al., 2011) and damage cells through the formation of adducts with DNA in many organs such as the kidneys, the liver and lungs (Vineis and Husgafvel-Pursiainen, 2005; Xue and Warshawsky, 2005).

Uncertainty over data sources for Indian fuel consumption, the base year, emission factors and the spatial distribution of sources leads to large uncertainties in estimates of total emissions. In this study, we have developed comprehensive, spatially disaggregated emission inventories for NMVOCs released from burning sources in India. Inventories are produced for 10 different years from 1993-2016 and use recently published emission factors which far better reflect the full range of species released. This study then evaluates the relative contributions of individual sources to emissions to allow an assessment of the overall impact of emissions from burning sources to air quality in India. This is because recent studies have shown that NMVOC emission reduction is needed to accompany NO_x emission reduction to avoid increases in O_3 concentrations in cities like Delhi (Chen et al., 2020).

6.2. Methods

6.2.1. Emission factors

The emission factors used in this study come from a variety of recently published sources. All emission factors applied in this study included measurement by PTR-ToF-MS, a technique well suited to species released in significant quantities from solid fuel combustion such as small oxygenated species, phenolics and furanics. These species are often missed by GC measurement alone. Preference has been given to emission factors from studies which: (1) have many measurements (*n*), (2) use samples collected from India or (3) use samples collected from similar countries. For residential fuel combustion, the emission factors measured in chapter 4 were used for fuel wood, cow dung cake, LPG and MSW samples collected from around Delhi. This study was extremely detailed and measured online, gas-phase, speciated NMVOC emission factors for up to 192 chemical species using dual-channel gas chromatography with flame ionisation detection (DC-GC-

FID, *n* = 51), two-dimensional gas chromatography (GC×GC-FID, *n* = 74), proton-transfer-reaction time-of-flight mass spectrometry (PTR-ToF-MS, *n* = 75) and solid-phase extraction two-dimensional gas chromatography with time-of-flight mass spectrometry (SPE-GC×GC-ToF-MS, *n* = 28). Table 6.2 shows the emission factors applied in this study.

Emission factors for combustion of crop residues on fields were taken from measurements by Stockwell et al. (2015) made using PTR-ToF-MS of 115 NMVOCs (Stockwell et al., 2015) for wheat straw (*n* = 6), sugarcane (*n*=2), rice straw (*n*=7) and millet (*n*=2). This study also included the mean crop residue emission factor for 19 food crops, for use when no current emission factor had been comprehensively measured using PTR-ToF-MS. The emission factor applied (38.8 g kg^{-1}, see the Supplementary Information S8.17 for details of calculation) was evaluated against that for crop residues used for domestic combustion in Delhi (37.9 g kg^{-1}). Whilst the values measured by Stockwell et al. (2015) and in chapter 4 were comparable, the value from Stockwell et al. (2015) was used as the crop types were more reflective of the crop residues burnt on fields after harvest, compared to those burnt to meet residential energy requirements. The mean emission factor for crop residue combustion on fields was used for specific crop types with smaller levels of cultivation.

Emissions from coal burning were estimated using an emission factor from the combustion of bituminous coal from China (*n* = 14), a neighbouring Asian country, made using PTR-ToF-MS. Whilst the chemical composition of the coal may be more important than the development status of the country, there was overall a low level of reported residential coal use and this estimate was included for completeness. A total of 89 NMVOCs were identified, which represented 90-96% of the total mass spectra (Cai et al., 2019).

Indian specific PAH emission factors were recently measured in gas- and particle-phases using PTR-ToF-MS and GC×GC-ToF-MS (see chapter 3). This dataset provided PAH emission factors collected from combustion of fuel wood (*n* = 16), cow dung cake (*n* = 3), crop residue from domestic combustion (*n* = 3), MSW (*n* = 3), LPG (*n* = 1) and charcoal (*n* = 1) samples.

Table 6.2. NMVOC and PAH emission factors (g kg^{-1}) from combustion of different fuels

NMVOC emission factors / g kg^{-1}

	Wood	Dung	MSW	LPG	Charcoal	Rice	Wheat	Sugarcane	Millet	Crop	Coal
VOC	18.7	62.0	87.3	5.7	5.4	23.8	15.9	53.6	5.4	38.8	3.7
n	51	8	3	3	2	7	6	2	2	19	14
Ref	*a*	*a*	*a*	*a*	*a*	*b*	*b*	*b*	*b*	*b*	*d*

PAH emission factor / g kg^{-1}

	Wood	Dung	MSW	Crop	LPG	Charcoal
PAH	0.25	0.61	1.02	0.75	0.06	0.15
n	16	3	3	3	1	1
Ref	*c*	*c*	*c*	*c* *	*c*	*c*

References: [a] chapter 4, [b] Stockwell et al. (2015), [c] chapter 3, [d] Cai et al. (2019) and * crop types used for residential solid fuel combustion.

6.2.2. Spatial activity data

High resolution, gridded population data for India (WorldPop, 2017) was used at a resolution of 1 km^2. Officially, urban populations in India are defined as having (Chandramouli, 2011):

- population density > 400 people km^{-2}
- 75% of men employed in non-agricultural industries
- population of town > 5000 people.

Rural populations in India cannot be identified simply by having a population density of < 400 people km^{-2}, as some states such as Uttar Pradesh have an average population density of around 800 people km^{-2}. Rural grid squares were therefore identified by calculating the population density threshold in each state in which the sum of the 1km^2 grid squares below this threshold correctly reproduced the rural populations in these states from the 2001 and 2011 censuses (Government of India, 2014). Supplementary Information S8.18 shows that this resulted in good reproduction of rural and urban populations. Uncertainty existed over the exact population of India. The 2011 census calculated it to be 1.21 billion and the World Bank calculated 1.25 billion. Exit polls suggested the census would slightly underestimate the population. We used population statics indicated by the 2011 census.

NMVOC and PAH emissions from domestic solid fuel combustion were plotted against this high-resolution population data in the R statistical programming language at 1 km^2 for 2001

and 2011, with the population datasets scaled to the percentage changes in Indian population indicated by the World Bank for additional years of interest.

6.2.3. Fuel wood, LPG, charcoal and coal consumption

Preference has been given to large fuel usage surveys which included tens to hundreds of thousands of respondents. The Household Consumption of Goods and Services in India survey by the National Sample Survey Office (NSSO, 2007b, 2012b, 2014) gave state-wise kg capita^{-1} fuel wood, LPG, charcoal and coal burning statistics for rural and urban environments and was used for the years 2004-2005, 2009-2010 and 2011-2012. NMVOC emissions for these years were calculated though equation E6.1:

$$\mathrm{NMVOC}_{1\mathrm{km2,fuel}} = \mathrm{EF}_{\mathrm{fuel}} \times \mathrm{fuel\,use}_{\mathrm{capita}} \times \mathrm{pop}_{1\mathrm{km2}} \times \left(\frac{365}{30}\right) \quad \text{(E6.1)}$$

where $\mathrm{NMVOC}_{1\mathrm{km2,fuel}}$ = total NMVOC emission from respective fuel combustion per 1 km^2 grid (kg yr^{-1}), $\mathrm{EF}_{\mathrm{fuel}}$ = mean emission factor for fuel used, $\mathrm{fuel\,use}_{\mathrm{capita}}$ = per capita fuel consumption (kg 30 days^{-1}) converted from per 30 days to per year by multiplying by (365/30) and $\mathrm{population}_{1\mathrm{km2}}$ = population in 1km^2 grid. This calculation was performed separately for rural and urban grid cells to allow accurate incorporation of rural and urban per capita fuel consumption data.

Data were collected from additional large, previously conducted surveys. These surveys collected data in terms of the number of households using specific fuels per 1000 households in different Indian states in rural and urban environments. The Fifth Quinquennial Survey on Consumer Expenditure provided data for 1993-1994 (NSSO, 1997), the Energy Sources of Indian Households for Cooking and Lighting provided data for years 2004-2005, 2009-2010 and 2010-2011 (NSSO, 2007a, 2012a, 2015b) and the Household Consumer Expenditure and Employment-Unemployment Situation in India for 2002 and 2006-2007 (NSSO, 2003, 2008). The National Family Health Survey presented India-wide fuel use as a percentage of the population. To reflect spatial variation in fuel use, the raw data from these surveys were accessed (from the DHS Programme, U.S. Agency for International Development), extracted through the SPSS statistics software package and processed in the R programming language. This increased fuel usage data availability as the

number of households per 1000 households using specific fuels in Indian states and covered the years 1992-1993, 1998-1999, 2005-2006 and 2015-2016 (International Institute for Population Sciences, 1995, 2000, 2007, 2017). These were extensive datasets with 1992-1993, 1998-1999 and 2005-2006 surveying just under 100,000 households and 2015-2016 around 600,000 households.

To convert fuel use per 1000 households to a per capita consumption rate for these years a scaling factor was developed. It was possible to link the Household Consumption of Goods and Services in India and the Energy Sources of Indian Households for Cooking and Lighting surveys for the years 2005, 2010 and 2011. This was done using years where the number of users per 1000 and kg capita^{-1} fuel usage statistics were available, as it was possible to calculate the amount of fuel a primary user would use. This was achieved by multiplying the per capita usage for a particular fuel type by the inverse of the ratio of fuel usage in that state in rural or urban environments and is given in E6.2:

$$\text{Fuel use primary user} = \text{Fuel use}_{\text{capita}} \times \frac{1000}{\text{NHH}} \qquad \text{(E6.2)}$$

where Fuel use primary user = amount of a specific fuel type that that a person who just burns that fuel type uses (kg 30 days^{-1}), Fuel use$_{capita}$ = per capita fuel use per 30 days (kg capita^{-1} 30 days^{-1}) and NHH = number of households per 1000 households using a particular fuel type. This was calculated for urban and rural scenarios in Indian states in years where it was possible (2005, 2010, 2011).

The amount of fuel a primary user would use was then used to estimate the amount of fuel consumed per capita in years where only usage per 1000 household statistics were available (1993, 1994, 1999, 2002, 2006, 2007 and 2016) by rearranging E6.2. The amount of fuel per primary user was taken from the closest survey where data was available. In some earlier surveys, data were not collected for smaller states and these were either estimated by averages of neighbouring states, or from the nearest available usage values for other years for these states. NMVOC emissions for the years 1993, 1994, 1999, 2002, 2006, 2007 and 2016 were then determined using E6.1 with the newly calculated per capita consumption values.

6.2.4. Cow dung cake consumption

Cow dung cake consumption was only reported as number of households per 1000 in these surveys and the amount of cow dung cake burnt per primary user was determined based on the energy density compared to fuel wood. This was done using calorimetry data which showed that cow dung cake was 1.3-1.9 times less efficient than fuel wood (EPA, 2000; Gadi et al., 2012). For this reason, the amount of fuel per primary user for fuel wood in a state has been multiplied by 1.6 to give the equivalent amount of cow dung cake a user would need to burn for their cooking needs. Upper and lower estimates for cow dung cake consumption have been based on the range 1.3-1.9. This has been evaluated to validate this approach, which estimated Indian cow dung cake consumption to be in the range 25.7-79.7 Tg yr^{-1} from 1993-2016. This was generally towards the lower end of consumption values previously reported of 35-128 Tg yr^{-1} for the years 2000-2001 (Habib et al., 2004). This was then converted to fuel use per capita in kg per user per 30 days by rearranging E6.2.

6.2.5. Input to municipal solid waste

The input to MSW was one of the hardest inputs to calculate due to lack of reliable data and was consequently one of the most uncertain. An estimation of NMVOCs released from MSW burning was attempted as there was little information available for India, where MSW burning is potentially a very large pollution source. The amount of MSW burnt was estimated using an established approach (IPCC, 2006; Wiedinmyer et al., 2014) with revised inputs for India based on per capita MSW generation from over 300 Indian cities (Annepu et al., 2012), state wise MSW collection figures (CPCB, 2013) as well as estimates of the amount of urban (NEERI, 2010) and rural MSW burnt (World Bank, 2012).

Wiedinmyer et al. (2014) assessed worldwide emissions from MSW burning based on IPCC guidelines (IPCC, 2006). The approach used here was similar, with modifications to the input data which made them more specific to India. The approach split the amount of MSW burnt into the MSW burnt by rural and urban populations in the country. For rural populations this was given by:

$$W_{\text{Bres}} = \text{MSW}_{\text{pr}} \times P_{\text{rural}} \times B_{\text{frac,res}} \quad \text{(E6.3)}$$

where W_{res} = MSW burnt residentially, MSW_{pr} = per capita rural MSW generation, P_{rural} = population of rural grid cell and $B_{frac,res}$ = the fraction of MSW burnt residentially.

Per capita rural MSW generation was set at the lower limit indicated by the World Bank for South Asia of 0.12 kg capita^{-1} day^{-1} and evaluated in the range 0.08 kg capita^{-1} day^{-1} (Parmar and Pamnani, 2018) to 0.12 kg capita^{-1} day^{-1} (World Bank, 2012). The fraction of MSW burnt rurally was set to 0.6 which was the IPCC estimate (IPCC, 2006) and was further supported by a recent study which showed that only around 40% of rural MSW was collected in South Asia (Kaza et al., 2018).

The fraction of MSW burnt for an urban population was estimated by the sum of two calculations. The first is for street MSW burning:

$$W_{Bres} = MSW_{pu} \times P_{urban} \times f_{uncollected} \times B_{frac} \quad \text{(E6.4)}$$

where MSW_{pu} = per capita urban MSW generation, P_{urban} = population of urban grid cell and $f_{uncollected}$ = fraction of MSW which was not collected. The weighted per capita urban MSW generation was calculated by averaging per capita MSW generation statistics from 366 Indian cities by state (Annepu et al., 2012), with calculated values given in the Supplementary Information S8.19. The fraction of MSW which was uncollected was calculated from the Central Pollution Control Board (CPCB), as the difference in amount of MSW generated and collected (CPCB, 2013). Urban per capita MSW generation was scaled to its estimated change for different years of interest (see the Supplementary Information S8.19).

The second calculation was for the MSW burnt in landfill sites:

$$W_{Bdump} = MSW_{pu} \times P_{urban} \times f_{collected} \times B_{frac,dump} \quad \text{(E6.5)}$$

where W_{Bdump} = landfill MSW burnt and $f_{collected}$ = fraction of MSW collected. The fraction of MSW collected came from CPCB statistics, but was reduced by 17-50% due to the informal recycling sector, based on very limited data from studies focussed on MSW recovery by the informal sector which showed 17% recovery in Delhi (Talyan et al., 2008), 20% recovery at a landfill site in Pune (Annepu et al., 2012), 4% in Pondicherry (Rajamanikam et al., 2014) and up to 40-50% in Mohali (Nandy et al., 2015). This was due to the large contribution of the informal recycling sector to recycling in India, where waste

was collected by waste merchants, garbage collectors and waste pickers from highways, waste depots and landfill sites. This is an important consideration in India as studies have shown recovery of between 8.5-80 kg of material per picker per day and large cities such as Delhi having 80,000-100,000 pickers (Nandy et al., 2015). $B_{frac,dump}$ was given by NEERI who estimated that 10% of landfill MSW in Mumbai was burnt (NEERI, 2010). $B_{frac,dump}$ was notably lower here (0.1) than in Wiedinmyer et al. (2014) (0.6) and thus represents a conservative estimate of NMVOC emissions from landfill fires. Due to lack of reliable data in establishing $B_{frac,dump}$, and the associated uncertainty, the sensitivity of urban landfill burning emissions over the range 0.1-0.6 was evaluated as part of the range given in this study.

6.2.6. Input to crop residue burning

NMVOC emissions from crop residue burning in India were estimated to evaluate the relative importance of different burning sources using the most up-to-date input data currently available (see Table 6.2). A calculation was carried out for 2011, as NMVOC emissions from crop-residue burning showed little year-on-year variation from 1995-2009 (Jain et al., 2014). The residue generated from the cultivation of four main categories of crops was estimated. The amount of crop types produced in each state (Ministry of Agriculture, 2012) was collated for cereals (rice, wheat, coarse cereals, maize, jowar, bajra), oilseeds (ground nut, rapeseed, mustard, sun flower and 9 oilseeds), fibres (cotton, jute and mesta) and sugarcane. The amount burnt was calculated using India specific estimates of the residue to crop ratio, dry matter fraction and fraction burnt (Jain et al., 2014). Emissions were estimated using factors from recent studies of crop residue burning using PTR-ToF-MS (Stockwell et al., 2015). When the exact residue was measured (e.g. rice straw, wheat straw, sugarcane and millet) the correct emission factor was used. For cases where the exact residue was not measured, the average reported crop residue emission factor was used (see the Supplementary Information 8.20 for further details on inputs into crop residue estimate). The spatial distribution of croplands was then either indicated using agricultural land identified by the high-resolution 500 m NASA MODIS land use product reduced to 1 km^2 resolution or through croplands identified at 10 km^2 through evaluation of the distribution of agricultural lands (Ramankutty et al., 2008).

The total amount of crop residue burnt in a state was calculated by:

$$\text{Crop}_{\text{emission}} = \frac{\sum_0^n \text{CWG} \times \text{RTCR} \times \text{DMF} \times \text{FB} \times \text{EF}_{\text{crop},i}}{\text{area cultivated}} \quad \text{(E6.6)}$$

where $\text{Crop}_{\text{emission}}$ = NMVOC emitted in a state from crop residue burning (kg km^2) (Ministry of Agriculture, 2012), CWG = mass of crop produced in state, RTCR = residue to crop ratio (Jain et al., 2014), DMF = dry matter fraction (Jain et al., 2014), FB = fraction of crop residue burnt (Jain et al., 2014), $\text{EF}_{\text{crop},i}$ = emission factor for crop species *i* (g kg^{-1}), area cultivated = total agricultural area identified in a state from either MODIS (1 km^2) or Ramankutty et al. (2008) (10 km^2) and *n* = number of different crops produced in the state.

An overview of all emission model inputs is given in the Supplementary Information 8.21.

6.3. Results

6.3.1. Emission model

Figure 6.2 shows the calculated NMVOC emissions from the burning of fuel wood, cow dung cake, MSW, LPG, charcoal and crop residue for the year 2011. This year was chosen as the focus for this study, as this was a census year and had some of the best available fuel consumption data. In general, NMVOC emissions were lowest in the very north and north-east region of India around the Himalayas and in the north-west due to the Thar desert, both areas of low population density. Detailed NMVOC emission estimates by source and state are given in the Supplementary Information 8.22.

6.3.2. Fuel wood

NMVOC emissions from fuel wood burning were estimated as 4.3 (1.0-22.3) Tg and were the largest due to the high number of users (600 million) across India (see Figure 6.2A). Emissions were significant in many cities which appeared as red dots in Figure 6.2A, as well as across the Indo-Gangetic Plain. The greatest emissions were in West Bengal and Kerala due to high population densities (1028 and 860 people km^{-2} respectively) and high per capita fuel usage (West Bengal rural 18.0 kg $capita^{-1}$ per $30\ days^{-1}$ and urban 3.4 kg $capita^{-1}$ per $30\ days^{-1}$, Kerala rural 32.4 kg $capita^{-1}$ per $30\ days^{-1}$ urban 20.58 kg $capita^{-1}$ per $30\ days^{-1}$).

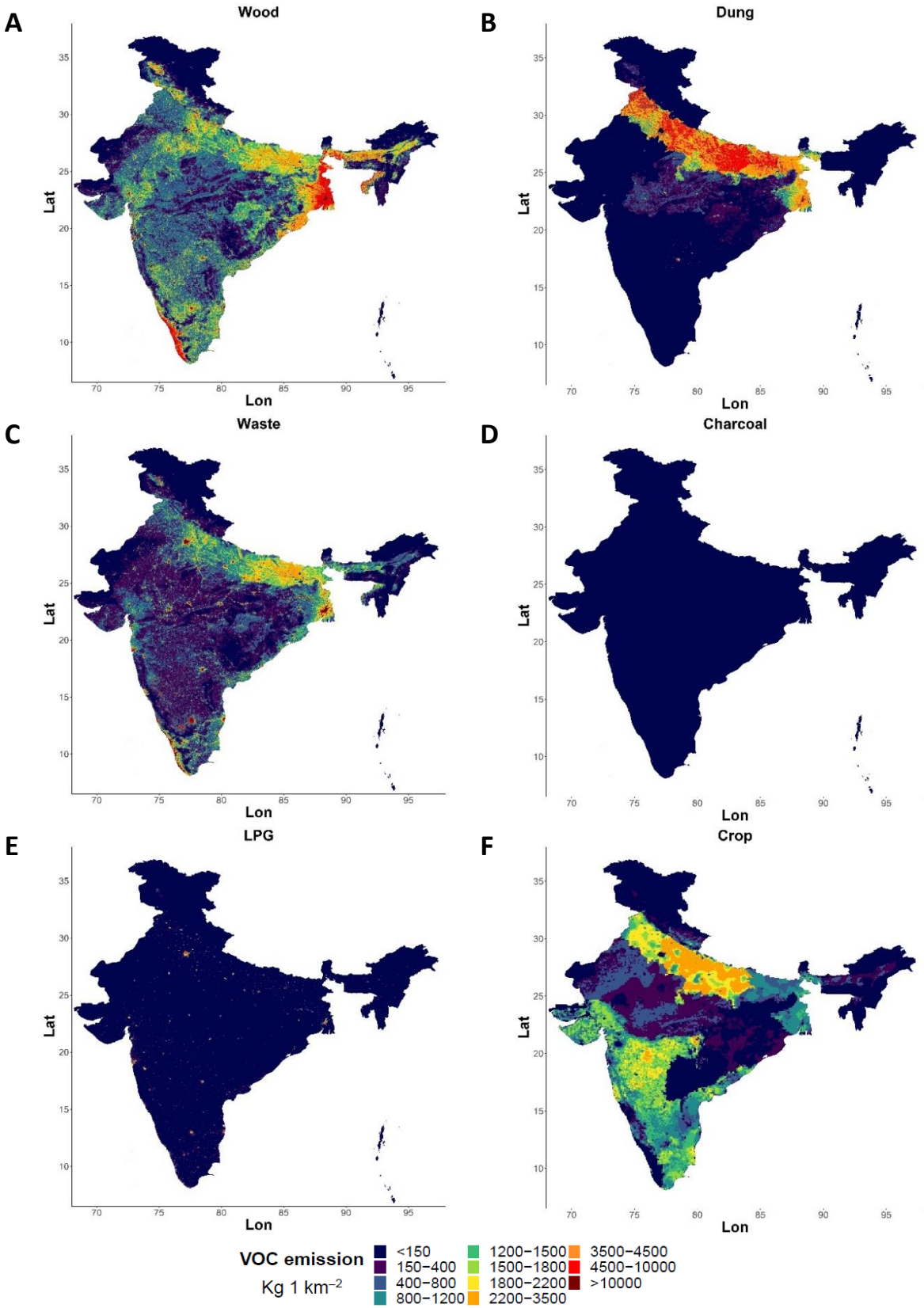

Figure 6.2. Spatial distribution and emission of NMVOCs in 2011 from various burning sources in India. The declination of international borders on this map are proximate and must not be considered authoritative.

6.3.3. Cow dung cake

Cow dung cake burning represented a significant NMVOC source, with emissions of 2.8 (1.3-4.4) Tg localised to the Indo-Gangetic Plain (see Figure 6.2B). Cow dung cakes are often considered as a co-product of cattle production (Gupta et al., 2016) and are used as a sustainable fuel in several regions, partly to alleviate demand on local fuel wood supplies. Cow dung cakes remained an important fuel source in northern states, with high per capita usage along the Indo-Gangetic plain in 2011 with 33.4% of rural households using cow dung cakes as a primary fuel source in Uttar Pradesh, 30.3% in Punjab, 24.4% in Haryana, 20.8% in Bihar and 10.6% in Madhya Pradesh (NSSO, 2015b).

6.3.4. Municipal solid waste

Figure 6.2C shows NMVOC emissions from the burning of MSW which were high from both rural and urban areas. In total, MSW burning in India was estimated to release 3.0 (1.6-6.9) Tg of NMVOCs in 2011. Emissions from combustion of MSW were significant, particularly to urban areas due to these being regions of high population density.

6.3.5. Charcoal/coal

NMVOC emissions from charcoal (0.9, 0.4-1.3 Gg) and coal (4.8, 1.7-5.9 Gg) remained low due to low per capita usage and a low emission factor. Figure 6.2D shows emissions from charcoal. Coal burning was only noticeable to West Bengal (see the Supplementary Information 8.23).

6.3.6. LPG

NMVOC emissions from LPG were low at 71 (24-123) Gg due to a low emission factor, high energy density and low per capita fuel usage (see Figure 6.2E). Emissions were principally in urban areas, such as New Delhi, which had higher per capita LPG usage. This source mainly released propane and butanes, which have been shown to be significantly less toxic and reactive with the OH radical than other solid fuel sources studied here (see chapter 5).

6.3.7. Crop residue

Crop residue burning was estimated to emit 3.0 (1.4-4.5) Tg of NMVOCs in 2011. Figure 6.2F shows emissions from crop residue burning visualised using the distribution of geographic lands (Ramankutty et al., 2008). Emissions from agricultural crop burning were

significant in the north of India and were driven by cereal production in Punjab and Haryana and sugarcane/cereal production in Uttar Pradesh and Bihar. The most significant emissions from Madhya Pradesh and Rajasthan were from the burning of oilseeds crops. Emissions from Maharashtra, Karnataka, Andhra Pradesh and Tamil Nadu were principally from burning of sugarcane residue.

6.3.8. PAHs

To better understand the scale and sources of PAH emissions in India, the emissions model was used to evaluate PAH emissions from burning sources. The spatial distribution of emissions by source type was similar to that displayed in Figure 6.2 for NMVOCs. Detailed PAH emission estimates by source and state are given in the Supplementary Information 8.25.

Figure 6.3 shows PAH emissions from the combustion of fuel wood, cow dung cake, MSW, charcoal and LPG in India in 2011. Total gas and particle phase PAH emissions were estimated to be 121 (52-326) Gg, from the burning of fuel wood (57 Gg, 12-209 Gg), cow dung cake (27 Gg, 18-38 Gg), LPG (0.7 Gg), charcoal (0.03 Gg) and MSW (36 Gg, 21-79 Gg). A previous estimate of PAH emissions from India in 2004 was 90 Gg yr^{-1} (Zhang and Tao, 2009), with ~ 80 Gg yr^{-1} from biofuel burning. This estimate was calculated based on fuel use indicated by the International Energy Agency (IEA), which listed the amount of biofuel used as a single category. The proportions of straw, cow dung cake and fuel wood were indicated by the Food and Agriculture organisation (FAO) of the UN and PAH emission factors were based on those for inventories in China, except for cow dung cake which was taken from relevant literature. A different study for 2007 estimated emissions of 67 Gg yr^{-1}, with 59 Gg yr^{-1} from residential combustion (Shen et al., 2013). This study followed a similar approach for biofuel consumption with fuel consumption from the IEA and the ratios of biofuel use from the FAO, with an updated PAH emission database using country/region specific PAH emission factors. The total PAH emission of fuel wood and cow dung cake in 2011 (85 Gg) was slightly larger than these two previous studies, partly explained by the inclusion of additional PAHs such as methyl and dimethylnaphthalene isomers and differences in fuel use between these years.

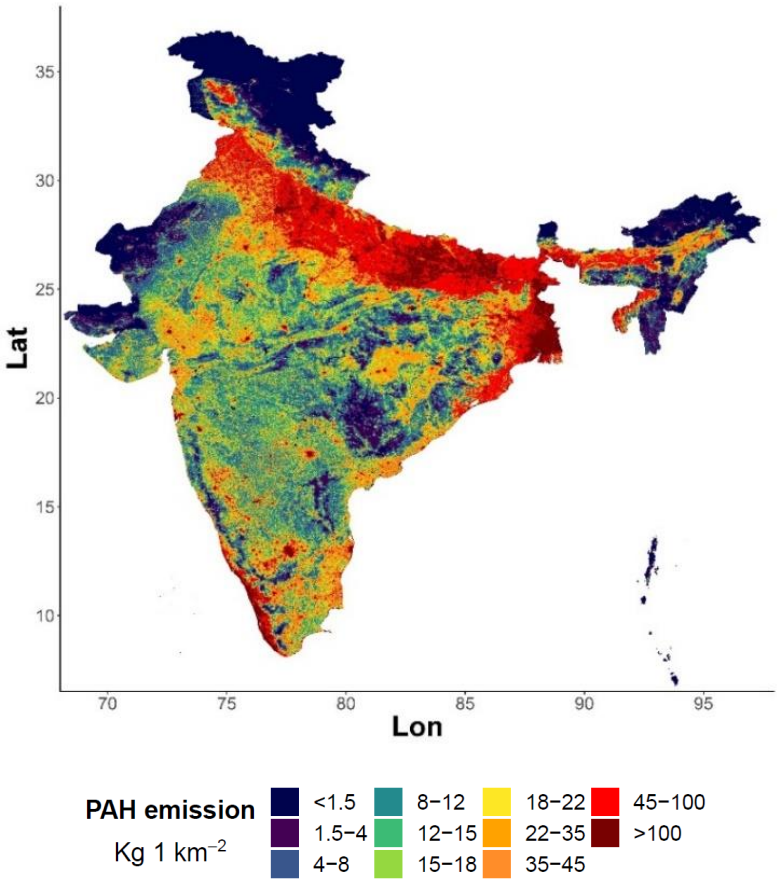

Figure 6.3. PAH emissions in India from combustion of fuel wood, cow dung cake, MSW, charcoal and LPG burning in 2011.

Total PAH emissions in this study, as well as from Zhang and Tao (2009) and Shen et al. (2013), were considerably larger than those estimated by Gadi et al. (2012) of 17.3 Gg yr^{-1} (12.3 Gg yr^{-1} from fuel wood and 3.7 Gg yr^{-1} from cow dung cake) and that estimated by Singh et al. (2013) of 23.8 Gg yr^{-1} (13.4 Gg yr^{-1} from fuel wood and 6.3 Gg yr^{-1} from cow dung cake). The inefficient combustion of MSW represented a considerable additional PAH source in India, which was likely to have significant impacts on human health.

Crop residue burning was also likely a large source of PAHs in India, which is not accounted for in this study. The mean emission factors of NMVOCs measured from the combustion of crop residues by Stockwell et al. (2015) and chapter 4 were comparable, despite the crop types being different. The emission factors of PAHs from wheat, rice and sugar cane were not measured in chapter 3, however, application of the emission factor for crop residues from this study would suggest that agricultural crop residue burning released an additional 67 (20-112) Gg of PAHs in 2011 across India.

6.4. Discussion of uncertainties

The generalisation of the laboratory combustion experiments in this study to the burning practices of a country with over 1 billion residents was likely to introduce significant uncertainties in the NMVOC emission estimates. Table 6.3 shows the fuel consumption values used in this study, the estimated NMVOC emissions and their uncertainties. Table 6.3 also compares fuel usage values from the limited available literature and previous NMVOC emission estimates from burning sources. Some general uncertainties existed due to the approach used here, as well as uncertainties which were specific to individual combustion sources. This significantly increased the uncertainties in emission estimates of specific combustion sources.

Table 6.3. Comparison of fuel consumption and NMVOC estimates in this study with literature.

	2011 fuel use this study/ Tg	2011 NMVOC estimate this study / Tg	Literature use / Tg	NMVOC estimate literature / Tg	Year	Reference
Fuel wood	230	4.3 (1.0-22.3)	220	-	1985	(Yevich and Logan, 2003)
			271	-	1990	(Streets and Waldhoff, 1998)
			169	-	1990	(Smith et al., 2000)
			302	-	1996	(Reddy and Venkataraman, 2002)
			265	-	1996	(Bond et al., 2004)
			281 (192-409)	-	2000	(Habib et al., 2004)
			316	-	2000	(Streets et al., 2003)
			154 [b]	1.1 (0.6-1.7)	2005	(Venkataraman et al., 2010)
			256	-	2007	TEDDY 2007 (Singh et al., 2013)
Cow dung cake	45 (36.3-53.4)	2.8 (1.3-4.4)	93	-	1985	Yevich and Logan, 2003)
			124	-	1990	(Streets and Waldhoff, 1998)
			54	-	1990	(Smith et al., 2000)
			121	-	1996	(Reddy and Venkataraman, 2002)
			128	-	1996	(Bond et al., 2004)
			62 (35-128)	-	2000	(Habib et al., 2004)
			105	-	2000	(Streets et al., 2003)
			-	1.8	2005	(Venkataraman et al., 2010)
			106	-	2007	TEDDY 2007 (Singh et al., 2013)
MSW	35 (28-56)	3.0 (1.6-6.9)	81.4	1.8	2010	(Wiedinmyer et al., 2014)
				0.1	2011	EDGAR 5.0
				0.01	2011	REAS 3.2
			68 (45-105)	1.7 (1.4-2.1)	2015	(Sharma et al., 2019)
Agricultural crop residue on fields	83.8	3.0 (1.4-4.5)	107.3	1.5	2008	(Jain et al., 2014)
				1.7 (0.6-4.0)	2010	(Pandey et al., 2014)
				0.7	2010	(Sharma et al., 2015)
				1.8 (0.6-4.1)	2015	(Pandey et al., 2014)
				0.3	1997-2009	(Pandey and Sahu, 2014)
			93		-	(Ministry of Agriculture, 2014)
				0.6	2011	EDGAR 5.0
LPG	12.5	71 (24-123) $\times 10^{-3}$	-	0.2	2005	(Venkataraman et al., 2010)
			-	0.2 (0.1-0.4) [a]	2010	(Pandey et al., 2014)
			-	0.3 (0.2-0.5) [a]	2015	(Pandey et al., 2014)
Coal	1.3	4.8 (1.7-5.9) $\times 10^{-3}$				
Charcoal	0.2	0.9 (0.4-1.3) $\times 10^{-3}$				
Solid fuel total	276.5 (267.8-284.6)	7.1 (2.3-26.7)		4.9 (1.6-11.6)	2010	(Pandey et al., 2014)
				4.9 (1.6-11.6)	2015	(Pandey et al., 2014)
			450	5.9	2010	(Sharma et al., 2015)
				4.2	2011	EDGAR 5.0
				5.9	2011	REAS 3.2

[a] Also includes estimate of kerosene use; [b] also includes charcoal use.

Uncertainties were likely to exist in the fuel consumption data utilised in this study, but these were not reported alongside official data and it was therefore not possible to account for this in the emission model. Furthermore, fuel consumption data was reported at a state-wide level, a lower resolution than used in this model. As a result, sharp distinctions were seen between neighbouring states which had very different reported levels of usage of a particular fuel type. This effect was particularly pronounced for emission estimates from cow dung cake and on-field crop residue combustion. The real distribution of emissions was likely to show a more gradual transition across state boundaries.

The representativeness of this initial laboratory data to real-world conditions potentially lead to large uncertainties in these emission estimates. The modified combustion efficiency was not measured in chapters 3 and 4, despite the likely large impact on NMVOC emission. A recent study suggested that emission factors from burning could vary by almost a factor of 2 if fuel was combusted in *chulha* or *angithi* stoves (Fleming et al., 2018). Little information was available about the spatial distribution of different types of cook stove used across India. Future fuel use statistics should include this, with studies examining the impact that this has on NMVOC emissions.

The emission factors measured in chapter 4 included speciation that on average represented 94% of the total measured NMVOC emissions. The total measured emission factor reflected the sum of gas-phase organic emissions detected using multiple gas-chromatography instruments and the PTR-ToF-MS. This also included the unspeciated fraction measured on the PTR-ToF-MS. It did not include organic emissions which were not measured by these techniques. For PAH emission estimates, only 21 species were measured. This highlights a more general uncertainty of bottom-up emission estimates as they may underestimate emissions as not all released species may be detected using the measurement techniques deployed. This also complicates comparisons between estimates from different emission inventories as they may not all include the same level of detail.

Varying climates in different regions of India, with different biomass varieties and moisture contents, also increased uncertainties in emission estimates at a countrywide level. This was because small variations, such as seasonal changes to humidity, may have large impacts on burning efficiency and in turn NMVOC emission. Despite this, the methods used in chapters 3 and 4 were designed to replicate local practices in Delhi for sample collection,

storage and combustion. Furthermore, municipal solid waste samples were collected from landfill sites, stored in sealed bags and combusted within 24 h. These approaches were designed to simulate real-world combustion conditions to ensure that the emission factors were reflective of local residential fuel use.

6.4.1. Fuel wood

The NMVOC emission factor used for fuel wood came from a large dataset based on 51 measurements. The large number of measurements should significantly increase the representativeness of the mean emission factor used for fuel wood emission estimates in India during this study. Despite this, the emission factors measured from fuel woods were highly variable, by over a factor of 20 from around 4-97 g kg^{-1}, even under repeatable laboratory conditions. The species of fuel wood and the composition of the sample burnt will vary considerably across India and will include species not measured here from different climatic conditions. This significantly increased the uncertainty in the NMVOC emission estimate, which was calculated for 2011 to be in the range 1.0-22.3 Tg.

6.4.2. Cow dung cake

The uncertainty in NMVOC emissions from cow dung cake combustion included uncertainty in the calorific conversion used to estimate fuel consumption, uncertainty in the emission factor and different reported levels of fuel usage. The uncertainty in the calorific conversion increased the uncertainty range by around 20%. This was reflected in the range of estimated cow dung cake consumption in India, which was 36.3-53.4 Tg in 2011.

Eight measurements were made of NMVOC emissions from cow dung cake combustion, with emission factors varying over a smaller range than for fuel wood from approximately 35-83 g kg^{-1}. The combined uncertainties in the calorific conversion and emission factor resulted in an uncertainty range of NMVOC emission estimates from 1.3-4.4 Tg in 2011, which was notably smaller than for fuel wood combustion.

One of the largest uncertainties in the NMVOC emission estimate from cow dung cake combustion was the different levels of fuel consumption reported by different surveys and was not accounted for in this study. Different studies report varying levels of cow dung cake usage in India between 5-15% of the population (EPA, 2000; International Institute for

Population Sciences, 2007; NSSO, 2012a). This study estimated cow dung cake fuel consumption from 1993-2016 to be in the range 25.7-79.7 Tg. This was smaller than many previous estimates of Indian dung consumption (see Table 6.3). The cow dung cake fuel usage inputs used in this study were generally closer to 5-10% of the population and thus represented a more conservative case study for NMVOC emissions from cow dung cake combustion across India. This study may therefore underestimate the potential impact of cow dung cake combustion in India and emphasised the need for better official reporting of cow dung cake fuel usage. The estimated emissions from cow dung cake combustion should be refined in future studies through collection of accurate per capita cow dung cake consumption data.

6.4.3. Municipal solid waste

The NMVOC emission estimate from MSW burning was one of the most uncertain, with large and potentially unquantifiable uncertainties in parts of the calculation. These included the low number of emission factor measurements, the high emission factor applied, uncertainty in the total mass of MSW generated in India, uncertainty in the amount of MSW recycled and uncertainty in the amount of MSW burnt in rural and urban environments. This emission estimate was presented as a discussion point, which should be treated with caution and could clearly be refined and improved as newer and better data becomes available.

The emission factors for MSW combustion used in this study varied from 56-119 g kg^{-1}. However, this was only measured from three MSW samples, leading to large uncertainty as domestic, commercial, and industrial wastes will vary largely in composition. However, this still represented one of the best available datasets for examining NMVOC emissions from MSW burning in India, as most current MSW burning datasets are modest and contain only a few samples. For comparison, Stockwell et al. (2015) measured an emission factor of ~ 9 g kg^{-1} from two combustion experiments of daily mixed waste and plastic bags collected at the US fire services laboratory using PTR-ToF-MS. A further study by Stockwell et al. (2016) measured a mean NMVOC emission factor of ~ 35 g kg^{-1} from 6 mixed waste fires and 3 segregated waste fires in Nepal using GC with -FID, -MS and electron capture detectors. A more recent study by Sharma et al. (2019) used an emission factor of ~ 25 g

kg^{-1} from measurements of 5 MSW fires measured in India in Mohali and a surrounding village which sampled fires from 2 landfill sites, household waste, horticultural and biomedical waste, and vegetable market waste. MSW combustion may occur under both flaming and smouldering conditions in backyards, landfill sites and incinerators. All of these are likely to have quite different combustion chemistry to the laboratory experiments and consequently lead to varying levels of emission, which were unaccounted for in this study. Jayarathne et al. (2018) suggested that emissions of particulate matter varied by around an order of magnitude and were dependent on the moisture content of samples. This may also be true for NMVOCs. Whilst the dataset used in this study for MSW only contained 3 measurements, all current MSW burning datasets contain few samples, which considerably increased the uncertainty and was one of the main present issues with NMVOC budget estimates from MSW combustion.

Lack of data and inconsistencies in existing data resulted in difficulties in establishing the amount of MSW generated in India and considerably increased the uncertainty in this estimate. Officially an average 46.5 Tg of MSW was generated yearly in India from 2009-2012 (CPCB, 2013). The estimate of MSW generated in 2011 in India for this study was 106 Tg, which was slightly less than the 144 Tg indicated by Wiedinmyer et al. (2014) for 2010 but approximately double the official estimate. Despite this, some studies have suggested that the amount of MSW produced was larger than this, with some estimates which indicated it to be over 200 Tg (Kaza et al., 2018; Sharma et al., 2019). This could potentially double the emission estimate given in this study and was not accounted for here.

The urban scenario in this study resulted in the generation of 69 Tg of MSW, which was similar to previous reports which estimated urban India to generate 61-62 Tg of MSW in 2010-2011 (Hanrahan et al., 2006; Planning Commission, 2014). It was estimated that 9-27 Tg of the urban MSW generated in 2011 was recycled, and this was comparable to that previously reported of 18-25 Tg (Nandy et al., 2015). It was estimated that 10-60% of the MSW which was collected and sent to landfill was burnt. This resulted in 13-34 Tg of MSW burnt and resulted in NMVOC emissions of 1.2-3.0 Tg in 2011. Further uncertainty existed in the spatial distribution of urban emissions, due to larger urban centres producing more MSW than smaller ones and MSW collection being more efficient in larger urban centres. Direct comparison was made for street waste burning in Delhi with the bottom-up estimate

reported by Nagpur et al. (2015) of 196-246 tons day^{-1} burnt. The approach used in this study estimated ~ factor 2 greater mass of street waste burnt at 511 tons day^{-1} for Delhi.

The rural scenario resulted in generation of 37 (25-37) Tg of MSW, of which 22 (15-22) Tg was burnt and released 2.0 Tg of NMVOCs. The fraction of MSW burnt in landfill remained very uncertain due to limited inputs, and the size of the NMVOC source from MSW combustion could be better assessed with new surveys conducted on the amount of MSW in landfill sites which was burnt and how this varied spatially across India. The approach used in this study had a lower amount of MSW burnt compared to Wiedinmyer et al. (2014) and Sharma et al. (2019), but the larger emission factor resulted in greater emissions of NMVOCs.

6.4.4. Crop residue

Uncertainty in the estimate of NMVOC emissions from crop residue burning on fields was related to the timing as well as spatial distribution of emissions, uncertainties in emission factors and the measurements not being from samples collected from fields in India.

The spatial distribution of emissions from crop residue burning on fields was like Jain et al. (2014) with emissions from cereals impacting the northern states, oilseeds to Rajasthan and Madhya Pradesh, fibre to Maharashtra, Gujarat and Andhra Pradesh and sugarcane to Uttar Pradesh, Karnataka and Tamil Nadu. Despite this, uncertainty existed in the timing and spatial distribution of emissions. Emissions from crop residue burning on fields will show large seasonality, which was not accounted for here and could potentially be inferred in future studies using satellite data (e.g., NASA VIIRS fire counts) to provide information on the timing of data. Emissions will be predominantly during the pre-monsoon season for rabi crops (Apr-May) and during the post-monsoon season for kharif crops (Oct-Nov) (Gopal, 2014). Agricultural land was identified using both MODIS land use data and through previously published data which evaluated the distribution of agricultural lands (Ramankutty et al., 2008). A better understanding of the true impact of emissions from crop residue burning on fields would require data about the relative distribution of fires on agricultural lands.

Jain et al. (2014) used the emission factors from a review (Andreae and Merlet, 2001). This study used recently measured emission factors using PTR-ToF-MS, a technique which has

been shown to measure a far greater amount of emissions from biomass burning than conventional techniques such as GC, due to measurement of additional species such as small oxygenates, phenolics and furanics. The emission factors used came from a dataset of 19 experiments and ranged from 4-69 g kg^{-1}. When the exact residue was measured (e.g., rice straw, wheat straw, sugarcane and millet) the emission factor was used, but for crops which were less widely produced, emission factors were not measured and the average crop value calculated by Stockwell et al. (2015) was used. This generalisation of emission factors measured by PTR-ToF-MS, and lack of measurements of some residues (e.g., sugarcane), led to uncertainty in the overall estimation. Notably these samples were not from India, with rice straw samples from China and Taiwan and millet from Ghana. Uncertainty was largest for generalised emission factors applied to crops with lower yields as well as millet and sugarcane, as these were only measured from two burns. However, high emissions from sugarcane were recorded previously using FTIR (Stockwell et al., 2014), which helped to validate the higher emission factor used in this study. Measurement of emission factors from combustion of crop residues collected from fields in India, as well as improved understanding of the quantity of crop residues burnt on fields, is required to better evaluate this source.

6.4.5. PAHs

The estimate of PAH emissions from cow dung cake and MSW combustion remained the most uncertain and requires further study to fully evaluate their impact. MSW and cow dung cake samples in chapter 3 had high emission factors, likely due to the low modified combustion efficiencies of the burns. The emission factor for MSW and cow dung cake combustion was based on only three samples and a better assessment is needed, as the effect of composition and moisture content of fuels on NMVOC emission was not accounted for in this study. In addition, this study quantified 21 major PAHs; however, the total was likely larger than predicted, as around 400 PAHs were shown to be released from cow dung cake in chapter 3.

6.5. Inventory comparison

Figure 6.4A shows the spatial distribution of the total NMVOC emissions estimated as part of this study from burning sources in India during 2011 (13.2 Tg). Residential combustion represented ~ 53% of total emissions with fuel wood and cow dung cake respectively contributing ~ 32% and ~ 21% of total NMVOC emissions (see Figure 6.5A). MSW and crop residue burning on fields each contributed ~ 23% to total NMVOC emissions.

The inventory developed for this study in Figure 6.4A was compared to inventories which were part of the Emission Database for Global Atmospheric Research (EDGAR 5.0, see Figure 6.4B) and the Regional Emission inventory in ASia (REAS 3.2, see Figure 6.4C). The estimated emissions from these inventories for residential combustion in the year 2011 (EDGAR 5.0 = 4.2 Tg, REAS 3.2 = 5.9 Tg, see Table 6.3) were of similar magnitude to this study of 7.1 (2.3-26.7) Tg. The larger emissions from residential combustion estimated in this study were likely driven by the larger NMVOC emission factors used as part of this study, which measured a greater number of gas-phase organic species. This study highlighted a potentially larger NMVOC source from the combustion of crop residue on fields of 3.0 (1.4-4.5) Tg when compared to EDGAR 5.0 of 0.6 Tg. It also highlighted that the waste sector (3.0 (1.6-6.9) Tg in 2011) may be responsible for a significantly greater NMVOC emission than estimated by EDGAR 5.0 (0.1 Tg) and REAS 3.2 (0.01 Tg).

One of the most detailed current India specific inventories focussed on the year 2010 and used a 36 km × 36 km grid. This estimated NMVOC emissions of 5.9 Tg yr^{-1} from residential combustion (Sharma et al., 2015). The emission factor for fuel wood (15.9 g kg^{-1}) used by Sharma et al. (2015) was comparable to our study (18.7 g kg^{-1}), however, that for cow dung cake (10.4 g kg^{-1}) was significantly lower compared to the present study (62.0 g kg^{-1}). Sharma et al. (2015) examined the percentage fuel use in urban and rural environments in India and used emission factors from comparable studies. Whilst the estimate was relatively close to that of this study (see Table 6.4, 6.2 Tg yr^{-1} from fuel wood and cow dung cake combustion in 2010), the scale of NMVOC emissions from cow dung cake and the countrywide spatial distribution of emissions were lost. Table 6.4 highlights how these NMVOC emission estimates may vary from year to year through the detailed use of different fuel use inputs.

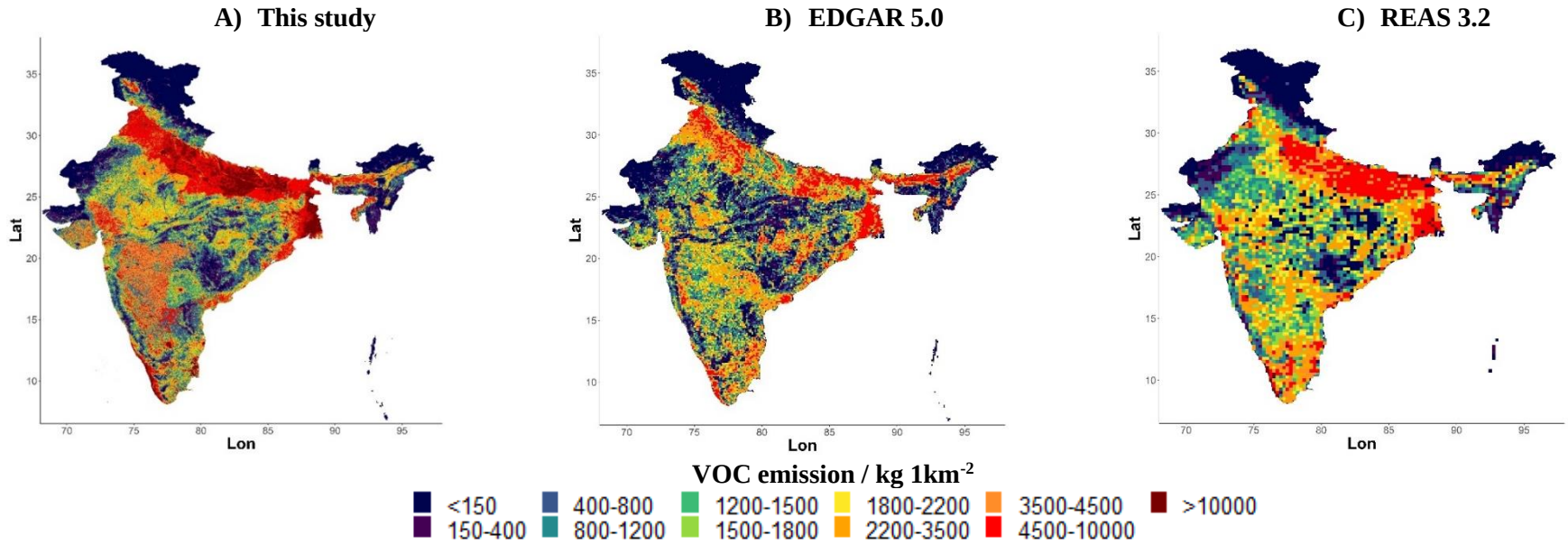

Figure 6.4. Comparison of NMVOC emissions from solid fuel combustion sources from 2011 in A = this study, B = EDGAR 5.0 and C = REAS 3.2, with data taken from Crippa et al, (2019) and Kurokawa and Ohara, (2020). Plots for EDGAR 3.2 and REAS 3.2 by individual source sector are given in the Supplementary Information S8.26. The declination of international borders on this map are proximate and must not be considered authoritative.

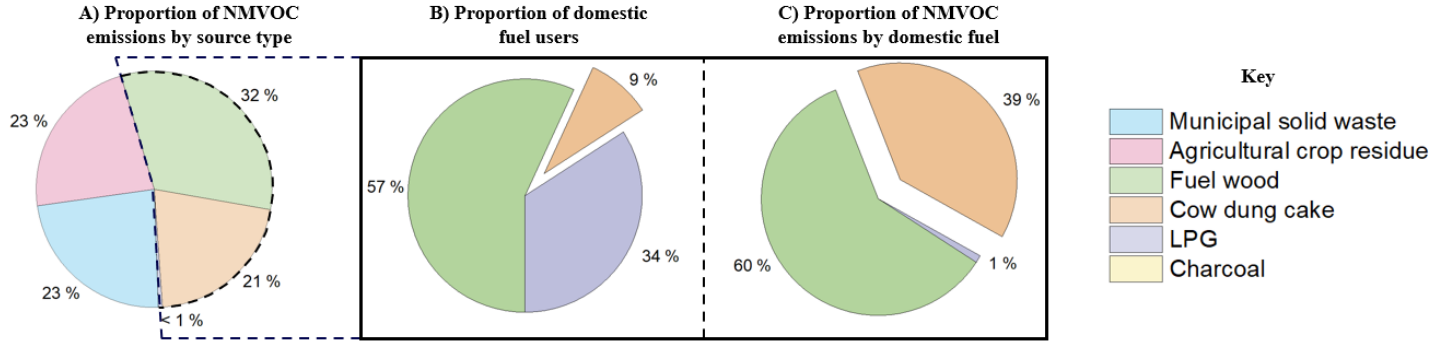

Figure 6.5. Breakdown of contributions of different burning sources to emissions in 2011 where A = relative contributions of different burning sources to total burning related NMVOC emissions, B = relative proportion of number of residential fuel users for fuel wood, cow dung cake and LPG and C = relative proportion of fuel wood, cow dung cake and LPG to residential combustion related NMVOC emissions.

Table 6.4. NMVOC pollution (Tg yr^{-1}) from various fuel types in India. NMVOC emissions from charcoal were omitted and are in the range 2-6×10^{-3} Tg yr^{-1}. NMVOC emissions from coal were omitted and decreased from 11×10^{-3} Tg in 1993 to 4×10^{-3} Tg in 2016.

Year	Wood	Dung	LPG	MSW	Crop	Total
1993	3.8 (0.9-19.9)	2.5 (0.9-3.2)	0.02 (0.006-0.03)	2.1 (1.0-4.6)	-	8.4 (2.8-27.7)
1994	3.9 (0.9-20.0)	2.5 (0.9-3.2)	0.02 (0.006-0.03)	2.1 (1.1-4.7)	-	8.5 (2.9-27.9)
1999	3.9 (0.9-20.4)	1.9 (0.7-2.4)	0.03 (0.01-0.06)	2.3 (1.2-5.3)	-	8.1 (2.8-28.2)
2002	4.0 (0.9-21.3)	2.6 (1.0-3.4)	0.04 (0.01-0.07)	2.4 (1.3-5.6)	-	9.0 (3.2-30.4)
2005	4.2 (1.0-21.6)	2.6 (1.2-4.1)	0.05 (0.02-0.09)	2.7 (1.4-6.2)	-	9.6 (3.6-32.0)
2006	3.6 (0.8-18.6)	4.1 (1.9-6.5)	0.05 (0.02-0.09)	2.8 (1.4-6.3)	-	10.6 (4.1-31.5)
2007	4.3 (1.0-22.3)	2.4 (1.1-3.8)	0.06 (0.02-0.09)	2.8 (1.4-6.4)	-	9.6 (3.5-32.6)
2010	4.4 (1.0-22.7)	1.9 (0.9-3.1)	0.07 (0.02-0.11)	3.0 (1.5-6.7)	-	9.4 (3.4-32.6)
2011	4.3 (0.9-22.3)	2.8 (1.3-4.4)	0.07 (0.02-0.12)	3.0 (1.6-6.9)	3.0 (1.4-4.5)	13.2 (3.8-33.7) [a]
2016	4.0 (0.9-20.5)	3.1 (1.4-4.9)	0.09 (0.03-0.16)	3.3 (1.7-7.5)	-	10.5 (4.0-33.1)

[a] Includes estimate from crop residue burning on fields in India in 2011.

This study also suggested a significant MSW burning source, often omitted from inventories, but which was calculated to represent ~ 23% of total NMVOC emissions from burning. The estimate of NMVOCs from burning in this study was larger than two previous estimates. Wiedinmyer et al. (2014) estimated NMVOC emissions of 1.8 Tg yr^{-1} from open MSW burning for 2010 and Sharma et al. (2019) estimated emissions of 1.4-2 Tg yr^{-1} for 59 NMVOCs in 2015. The larger NMVOC emission estimate in this study was due to measurement of a larger emission factor, partly driven by the inclusion of many additional NMVOCs. The NMVOC emission factor in this study was notably large and underlines the need for more detailed studies of NMVOC emissions from a greater number of MSW burning samples to truly understand the potential impact of this source.

The estimated total NMVOC emission from crop residue burning on fields for 2011 in this study was 3 Tg, around twice that estimated previously for 2008-2009 by Jain et al. (2014) of ~ 1.5 Tg. This was principally due to greater sugarcane production in this year and larger emission factors from PTR-ToF-MS studies of crop residue burning capturing a greater amount of NMVOC emissions. However, a need was identified for better characterisation of crop residues specifically burnt in India using these techniques.

Table 6.5 shows estimated emissions from transport, industry, solvents and power generation from various studies for 2008, 2010 and 2015. The emissions from domestic solid-fuel combustion estimated in this study were significantly larger than those at the countrywide level and thus underlined the significant role that solid-fuel combustion sources were likely to have on the high levels of ozone and SOA pollution observed in India.

Table 6.5. Estimated NMVOC emissions in India from literature for transport, industry, solvent and power generation (Tg yr^{-1}).

	Year	Transport	Industry	Solvent	Power
REAS 2.1 Kurokawa et al. (2013)	2008	5.6	2.1	1.1	-
Sharma et al. (2015)	2010	1.2	0.2	1.4	0.08
Sadavarte and Venkataraman (2014)	2015	2.8	1.8	-	0.10
EDGAR 5.0	2015	1.6	2.9	2.4	0.08

6.6. Impact of selective source reduction

Cow dung cake combustion represented only 6-14% of total fuel use in India by number of users when considering fuel wood, cow dung cake, LPG, coal and charcoal, but was responsible for ~ 27-53% of total NMVOC emissions from these residential combustion sources (see Figure 6.5A-C). This significantly increased NMVOC emissions across the Indo-Gangetic Plain. NMVOC emissions from cow dung cake combustion were highly sensitive to small changes in consumption. An interesting case was 2006, which had approximately 540 million fuel wood and 140 million cow dung cake users. Table 6.4 shows that the NMVOC emissions from cow dung cake (4.1 Tg) exceeded those of fuel wood (3.6 Tg) and demonstrated that a relatively small number of users burning cow dung cakes could have a disproportionately large impact on total NMVOC emission. Despite this, no factor in isolation could resolve the complex emissions of NMVOCs from burning sources in India, with multiple mitigation strategies required to target each of these different sources.

The emission model was used to evaluate the impact of potential emission reduction strategies. Two case studies were considered which aimed at 50% and 75% reductions in the total mass of NMVOCs released in 2011 (see Figure 6.6). Sources were carefully evaluated, with consideration given to their benefit to society as well as their emission factors. Combustion of cow dung cake was a highly polluting fuel source, with potentially large NMVOC emission reductions through widespread decrease in use. Burning of MSW and crop residues assisted in disposal, and crop residue combustion could help with soil fertility. Fuel wood provided the primary energy source for cooking and heating for around 600 million people and complete conversion to LPG may not be a viable NMVOC reduction strategy. For this reason, the 50% emission reduction strategy was focussed around preventing cow dung cake combustion and limiting the impacts of crop residue burning on

fields and MSW burning. It should be noted that policy interventions aimed at crop residue burning have already begun to be implemented (Bhuvaneshwari et al., 2019; Kaushal, 2020).

Figure 6.6A shows the impact of this 50% reduction in total NMVOC emissions, achieved through the complete conversion of cow dung cake users to LPG and a 65 % reduction in emissions from agricultural crop residue burning on fields and MSW waste combustion. This impact was significant, with NMVOC emissions from India in 2011 reduced to 6.5 (2.0-26.4) Tg, with only a small increase in LPG emissions to 90 (30-154) Gg.

The second case study required more significant reductions of 80% in agricultural crop residue burnt on fields and MSW burning, complete conversion of cow dung cake users to LPG and 55% conversion of residential fuel wood use to LPG (see Figure 6.6B). This resulted in NMVOC emissions of 3.3 (1.1-12.5) Tg in 2011, with LPG combustion emissions that only increased to 135 (45-233) Gg.

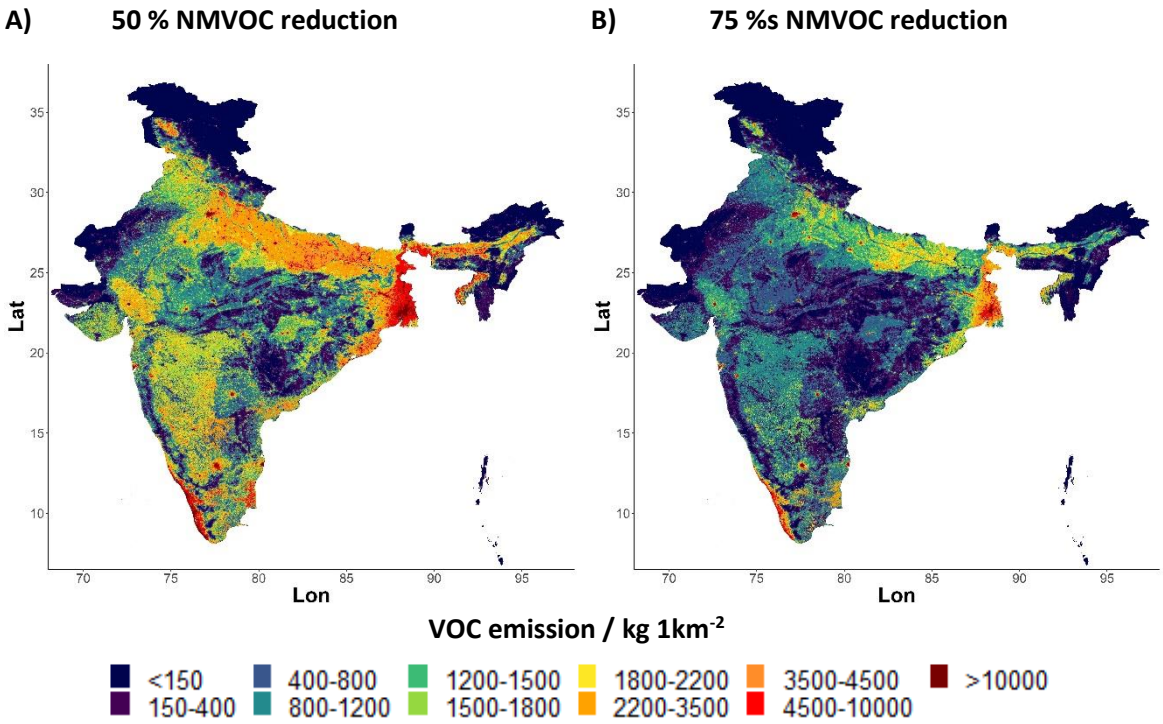

Figure 6.6. Effect of selective source control on total NMVOC emissions in 2011 with A = 50% reduction in NMVOC emissions achieved by complete replacement of cow dung cake burning with LPG and 65% reductions in the quantity of crop residues burnt on fields and MSW burnt and B = 75% reduction in NMVOC emissions achieved by complete replacement of cow dung cake burning with LPG, conversion of 55% of residential fuel wood use to LPG and 80 % reductions in the quantity of crop residues and MSW burnt. The declination of international borders on this map are proximate and must not be considered authoritative.

6.7. Evaluation of LPG uptake

Current NMVOC emission reduction policy in India is focussed on the replacement of solid fuels with LPG (Gould and Urpelainen, 2018). Recent government initiatives have included the Pradhan Mantri Ujjwala Yojana and Pratyaksh Hanstantrit Labh schemes (IEA, 2020). Figure 6.1 shows that from 1993 to 2016 there were around 400 million new Indian LPG users, whilst levels of other fuel usage remained relatively constant. This policy of increased LPG uptake was calculated to only increase NMVOC emissions from 19 Gg in 1993 to 94 Gg in 2016 (see Table 6.4).

The effect of this policy was evaluated within the emission model, compared to these 400 million new LPG users burning solid fuels. This was achieved by comparing total NMVOC emissions in 2016 to a scenario where the proportion of LPG usage had not increased from the 1993 level. Whilst total emissions from solid fuel combustion in India remained high due to the large numbers of users, the policy of increased LPG uptake was estimated to have prevented NMVOC emissions of 2.9 (0.7-14.7) Tg by 2016 compared to these new users burning solid fuels.

6.8. Conclusions

This study compiled recently measured emission factors and fuel consumption data to evaluate the magnitude and spatial distribution of NMVOC emissions from different solid fuel combustion sources across India. This was achieved by producing high-spatial resolution emission inventories, which addressed the yearly magnitude and spatial distribution of emissions. This showed the relative contributions of fuel wood (32%), cow dung cake (21%), municipal solid waste (23%), agricultural crop residue on fields (23%), charcoal (<1%), coal (<1%) and LPG (<1%) to burning related NMVOC emissions of 13 (5-38) Tg in 2011 in India. Certain sources, such as the combustion of fuel wood and cow dung cake for cooking, will remain relatively constant throughout the year. Combustion of fuel wood for heating and lighting will however be higher during winter months. Other burning sources, such as agricultural crop residue burning, will show large seasonality and occur predominantly during the kharif (Apr-May) and rabi (Oct-Nov) crop burning seasons. This was not accounted for in these emission inventories and means that these sources may have a disproportionally large impact on emissions during these seasons.

Small oxygenated, phenolic and furanic species represented half to three quarters of total emissions from the solid fuel combustion sources in this study. Better understanding of the chemistry of phenolic and furanic compounds is essential to further understand the impact of these reactive chemical species on air quality in developing regions, where burning is a large air-pollution source.

This study showed that cow dung cake was a disproportionally high NMVOC emission fuel and was responsible for a high proportion of total residential combustion related NMVOC emissions, particularly across the Indo-Gangetic Plain. This study also evaluated current emission reduction policies from 1993-2016, which incentivised LPG uptake, and were predicted to prevent emissions of almost 3 Tg of NMVOCs a year by 2016. Despite this, total NMVOC emissions were here calculated to increase by over 2 Tg over this period, highlighting the limits of this policy in the face of rapid population expansion.

For successful future net NMVOC emission reduction, policy should focus on replacement of solid fuels with LPG or other low emission fuels at a rate faster than the increase in population. Emission reduction from residential combustion can be accelerated by selectively replacing cow dung cake fuel use with LPG. This will lead to a three to four times greater reduction in NMVOC emissions per user compared to each fuel wood user replaced. In addition, countrywide measures are required to prevent the burning of agricultural crop residues on fields and of MSW to reduce the significant NMVOC emissions from these source categories.

Chapter 7

Conclusions and future work

7.1. Conclusions

This thesis examined the influence of different NMVOC sources in India. A detailed study of urban air quality in megacity Delhi was carried out through a suite of ambient NMVOC concentration measurements made during pre- and post-monsoon seasons in 2018. This was complemented by an extremely detailed dataset of NMVOC emission factors made of a range of north Indian solid fuel combustion sources. Results of the burning study were used to better understand the volatility distribution of organic emissions from biomass burning sources. They were also used to assess the implications of burning emissions across India, which potentially have a large impact on both rural and urban environments.

Measurements of a range of C_2-C_{14} NMVOCs were used to evaluate the relative contributions of different NMVOC sources to ambient concentrations in Delhi. Additional species were quantified, which were found to be present in ambient samples, such as 12 highly reactive monoterpenes. The results of this study are interesting, because despite biomass burning being a large NMVOC source in India, urban concentrations were still found to be predominantly from petrol, diesel, and LPG sources. The results of this study are well supported by recent literature and suggest that to achieve meaningful reduction of ambient concentrations of NMVOCs in Delhi, emissions reduction strategies must focus on limiting the impact of petrol and diesel sources. Whilst emission reduction strategies have targeted the impact of vehicular related emissions, they have failed to keep pace with the rapid growth in vehicle number in Delhi and emissions consequently remain high. Future policies will have to go further and be more wide reaching to achieve meaningful NMVOC emission reduction.

Extremely high NMVOC concentrations were measured at night during the post-monsoon campaign. It was questioned if this was due to a particularly large NMVOC source, such as widespread burning, or due to meteorological influences. Stagnant conditions, along with a very low boundary layer height, were found to be responsible for amplifying post-monsoon night-time concentrations. The impact of extremely high ground-level concentrations of pollutants, such as benzene, over many hours requires detailed evaluation though policy. The impact of prolonged exposure to elevated NMVOC concentrations at night is likely to have significant health impacts. Current mitigation policies limit heavy goods vehicles to the city at night, a policy which requires

comprehensive revaluation. Little can be done to alter meteorological influences, but limitations to night-time sources may help mitigate the impact of this effect.

A detailed study of north Indian solid fuel combustion sources allowed development of a new method for capturing I/SVOCs onto SPE disks and PTFE filters. This study complements current literature, where few studies provide comprehensive characterisation of complex mixtures of I/SVOCs from burning. The method mainly provided qualitative information on the range of I/SVOC species present in the gas phase from burning samples. Despite the quantification of gas-phase emissions in this study being limited, it found that by mass the most important I/SVOC emissions were from phenolic and furanic species, a finding confirmed by PTR-ToF-MS in chapter 4. This study provided a new chromatographic method to allow the compounds present in aerosol, which would typically elute as an unresolved complex mixture in conventional 1D chromatography, to be resolved. A case study was used of a cow dung cake sample, which showed a large variety of functionalities were released from burning samples and included many thousands of different compounds. This study measured emission factors of PAHs from Indian fuels and highlighted that better techniques are required for comprehensive quantification of complex mixtures of I/SVOCs.

Measurements were made under controlled laboratory conditions using three complementary instruments of a large variety of different gas-phase NMVOCs of many functionalities released from north Indian solid fuel sources. This included oxygenates, furanics, phenolics, alkenes, alkanes, nitrogen containing NMVOCs and aromatics. Experiments were made online to avoid potential artefacts caused by sampling into canisters or tedlar bags, particularly of I/SVOC species. Experiments involved a large variety of different fuel types, and whilst there was large variability between emissions of similar fuel types, fuel types such as cow dung cake and municipal solid waste released considerably more NMVOCs compared to fuel wood or LPG. A comprehensive dataset of emission factors was produced of solid fuels for a region where burning is an important fuel source, and likely large contributor to poor air quality.

The data collected from the SPE/PTFE measurements and using the three online gas-phase measurements were compiled and mapped onto a volatility-basis dataset to provide comprehensive, model-ready source profiles for the fuel types measured during controlled

laboratory experiments. This showed the fuel wood types tested only released a small mass fraction of S/L/ELVOC organics compared to fuel types, such as cow dung cake and municipal solid waste, which emitted a far greater variety of organic species into the aerosol phase. This study then directly compared the NMVOC emissions from sources for OH reactivity, SOA production potential and PAH toxicity which demonstrated that combustion of fuel wood, cow dung cake and municipal solid waste burning were likely to degrade local air quality significantly more than LPG.

The emission factors measured from the laboratory study, as well as relevant literature, were then used to estimate the quantity of NMVOCs and PAHs emitted from solid fuel combustion in India. A range of different fuel use surveys were used to estimate consumption. The major uncertainties of this study were due to lack of measurement of the quantity of cow dung cake and municipal solid waste burnt, a generalisation of fuel types from the north of India to the entire country, few measurements of municipal solid waste samples and lack of Indian agricultural emission factors measured in this study. This study estimated large emissions of NMVOCs from a range of sources and showed that emissions from burning cow dung cake per capita were greater than for fuel wood, and likely to significantly degrade air quality. It also showed very low NMVOC emissions from LPG, despite ~ 500 million users by 2016. This study also showed that total emissions of NMVOCs from burning remained relatively constant from 1993-2016, despite attempts to reduce total emissions, due to rapid population growth.

7.2. Future work

Future work is required to develop the GC×GC-FID instrument. Of the three campaigns it was deployed on, the valve-based modulator failed to work during two after shipping and storage. More robust solutions are required to allow routine and reliable deployment of this instrument to locations around the globe.

Prior to this project, the instrument was developed to allow measurement of up to C_{14} NMVOCs, however, detailed evaluation of how well the instrument measures these species is required. The instrument currently has a cold finger in line for water removal, which is required to stop water condensing onto the hydrocarbon trap which is held at – 20 ^{o}C. This causes a problem for analysis of less volatile species, as they will carry over or condense entirely in this glassware. During field studies, an inhouse standard containing *n*-dodecane

carried over between samples if the cold finger was at – 30°C. During burning studies, carryover was also observed between samples and it was necessary to change and heat the cold finger between samples to ensure that carryover was not observed. Lab studies showed that less carryover was observed in glassware which has a smaller volume, but this meant that with ambient samples the glass cold fingers were more prone to filling with ice and required defrosting entirely, resulting in increased instrumental downtime. This setup has been copied from instruments like the DC-GC-FID, which are required to trap at colder temperatures to capture more volatile species and is not necessarily required for the volatility of NMVOCs that the GC×GC-FID analyses. During this field study, the sterling cooler for the cold finger was shared with the DC-GC-FID instrument and so the temperature could not be reduced as trapping at – 20 °C was required to prevent breakthrough of more volatile species. The range of species measured by the GC×GC-FID instrument could potentially be improved in future by removing the cold finger entirely and using a dry purge technique. This would have the cold trap held at a temperature above 5 °C, meaning that water from ambient samples will not condense on the trap. It would also mean that more volatile species were not captured but should still allow trapping of less volatile species potentially beyond C_{14}. This would potentially be a good solution to carryover for this instrument but would require breakthrough testing to ensure that benzene/*n*-octane were still fully captured at the sample volumes used for the experiment.

Another final limitation of routine deployment of this instrument remains the manual nature of data workup. The use of Zoex software represents a significant improvement of manual integration of the 1D peaks from modulation, however, this approach is still not autonomous. The software routinely splits peaks incorrectly and means that all peaks of interest need to be manually checked, a process which quickly becomes overwhelming for large datasets. Better methods of automating the workup of data processing and integration from GC×GC instruments are still required.

Further work is required for better analyses using the GC×GC-ToF-MS instrument. Far better semi-quantification of complex samples could be achieved using a pre-detector split to an FID, as discussed in chapter 3. This would allow extremely novel and interesting analyses of complex aerosol samples, as a large amount of quantitative organic compositional data would be revealed.

This work shows that NMHC emissions near an urban site in Delhi were predominantly the result of traffic related emissions, however, the proximity of major roads and rail intersections close to the site likely had a large impact on the composition of measurements made. Future measurements are required in different areas of the city closer to other potential NMVOC sources, such as slum and landfill sites, to examine the influence these have on the composition of measurements. In addition, the diurnal profiles measured at the IGTDUW site were strongly influenced my meteorology and the measurement of direct NMVOC fluxes would allow the diurnal profile of emissions to be better examined. This would provide valuable information about the temporal profile of emissions and provide better information about NMVOC sources.

The study of emissions from solid fuel sources in northern India yielded many interesting results, however, many areas exist for future studies to exploit to further develop understanding in this area. Future studies need to include accurate measurements of CO/CO_2 and collect compositional information such as the moisture content of samples prior to analysis. This will allow an understanding of the differences in modified combustion efficiency between different types of burn and perhaps yield more useful emission factors potentially normalised to this. It is highly likely that the modified combustion efficiencies of dung and waste burns were very low, and this resulted in the high emission factors observed. This, alongside supporting information such as sample moisture content, should be explored in future studies.

Fuels in this study were collected and stored in a manner designed to be reflective of local practices to ensure that laboratory combustion conditions, and in turn emissions, reflected local burning practices. The impact of stove conditions on NMVOC emissions remains poorly understood. Experiments in this study were carried out using expert local judgment to attempt to ensure that laboratory conditions reflected real-world burning conditions. A range of stoves are used in India for combustion of local fuels such as *chulha* and *angithi* stoves, and an evaluation of the impact of these on emissions and their relative use and spatial distribution requires further study.

Nine measurements were made of NMVOCs from cow dung cake samples, and all were consistently high. It would be valuable to measure NMVOC emissions from cow dung cakes from different states across the Indo-Gangetic Plain to see the influence of different

preparation methods and mixtures on emission of NMVOCs. The impact of breaking up cow dung cake samples into smaller briquettes could also be explored as this may lead to better burning conditions, improve combustion efficiency, and reduce NMVOC emissions. Studies should also look at the influence of near-identical burns but using different stove conditions. For a country like India, the most effective mitigation strategies are likely those which require little change. If many repeat measurements showed that particular stoves, or particular methods of preparing cow dung cakes prior to combustion, resulted in more efficient combustion conditions and reduced NMVOC emissions, a public education policy could be undertaken. This may allow people to continue to burn cow dung cakes but reduce the worst of the NMVOC emissions.

Reviews of burning show different NMVOC emission factors from fuel wood collected from different environments such as savannahs, temperate forests and tropical forests. It is likely that across India fuel wood is collected and burnt from all these different environments, with the samples having different composition and moisture contents. The generalisation of fuel woods collected from the north of India to the whole country therefore has some uncertainty associated with the emission factor for the type of fuel wood being burnt.

Few measurements were made from domestic, commercial and industrial waste, and the emission factors measured in this study were higher than those observed in previous studies. The effect of moisture content on waste burning has been suggested to impact emissions of particulate matter by around an order of magnitude (Jayarathne et al., 2018). Furthermore, only one LPG stove was used to evaluate emissions from this fuel source, with emissions likely to vary by the type of burner used. Future studies should also make more measurements from waste burning to better understand the effect of composition on emissions. Comprehensive measurements should also be made of emissions from combustion of a range of additional crop residues, as these are an important NMVOC source in India (Jain et al., 2014).

Bottom-up emission inventories require both accurate emission factors and detailed spatial usage data to be reliable. This study generally meets these criteria for fuel wood samples and attention has been drawn to the need for a better understanding of the amount, location and composition of municipal solid waste being burnt across India as well as the

amount of cow dung cake burnt. This will lead to far more reliable estimations of NMVOC emissions from burning in India.

This thesis has looked in detail at the potential influence of different NMVOC sources in India. It is likely that as development and population growth continue across India, levels of air pollution remain high. The results of these studies show that to reduce NMHC concentrations in Delhi, emission reduction strategies which target vehicles are critical. This study also characterises the types of NMVOCs released from Indian burning samples in detail and examines the potential implications of different solid fuel combustion sources across India.

Chapter 8

Supplementary figures and tables

8.1. Mean, minimum and maximum NMHC mixing ratios

Calculated over sample periods where both DC-GC-FID and GC×GC-FID were measuring (29/05/18 20:00 to 05/06/18 11:00 and 11/10/2018 22:00 to 27/10/18 17:00). Instrumental limits of detection (LOD) are provided elsewhere (Dunmore et al., 2015).

Table S8.1. Mean, maximum and minimum mixing ratios (ppbv) of NMHC measured in Delhi during pre- and post-monsoon campaigns (based on hourly measurements with DC-GC-FID sample collection times of 20 minutes and GC×GC-FID sample collection times of 30 minutes).

NMHC	Pre	Pre max	Pre min	Post	Post max	Post min
		Alkanes				
Ethane	6.15	18.28	2.64	32.02	159.10	1.21
Propane	19.91	598.07	1.81	43.15	172.78	0.62
i-Butane	5.62	115.21	0.78	20.77	79.71	0.19
n-Butane	7.89	135.32	<LOD	39.74	153.99	<LOD
Cyclopentane	0.26	3.83	0.04	0.89	4.01	<LOD
i-Pentane	4.39	16.39	0.52	17.54	77.10	0.24
n-Pentane	1.55	5.94	0.21	6.76	28.78	0.10
n-Hexane	0.36	1.42	0.02	1.86	7.97	0.023
n-Heptane	0.25	0.92	0.05	1.36	6.57	0.02
n-Octane	0.14	0.53	<LOD	0.74	3.78	0.03
C_8 aliphatics	1.42	4.13	<LOD	5.79	29.36	0.54
n-Nonane	0.16	0.59	0.04	1.07	5.09	0.07
C_9 aliphatics	0.99	3.16	<LOD	3.74	15.76	0.38
n-Decane	0.15	0.60	0.04	0.87	4.17	0.10
C_{10} aliphatics	0.55	2.06	0.12	3.37	16.31	0.29
n-Undecane	0.11	0.51	0.01	0.45	2.14	0.05
C_{11} aliphatics	0.33	1.59	0.09	2.08	8.58	0.13
n-Dodecane	0.03	0.36	<LOD	0.93	3.59	0.05
C_{12} aliphatics	0.10	0.75	0.01	4.09	17.57	0.25
n-Tridecane	0.04	0.13	0.01	2.66	8.98	0.29
C_{13} aliphatics	0.08	0.67	0.01	3.89	14.86	0.27
n-Tetradecane	<LOD	<LOD	<LOD	1.28	3.17	0.15
C_{14} aliphatics	0.11	0.59	0.01	1.83	4.70	0.05
		Aromatics				
Benzene	1.36	5.13	0.35	6.67	41.24	0.51
Toluene	2.55	16.39	<LOD	18.38	120.89	1.02
Ethylbenzene	0.33	1.92	<LOD	2.64	14.52	0.21
m/*p*-Xylene	0.70	3.90	<LOD	4.93	29.92	0.31
o-Xylene	0.33	1.67	<LOD	2.42	13.93	0.08
Styrene	0.19	0.83	0.06	0.76	5.74	0.02
*i*Pr-benzene	0.02	0.11	<LOD	0.23	1.27	0.01

Table S8.1. continued.

NMHC	Pre	Pre max	Pre min	Post	Post max	Post min
Aromatics						
Pr-benzene	0.04	0.18	<LOD	0.32	1.58	0.02
3/4-Ethyltoluene	0.46	2.33	0.07	1.46	7.48	0.07
1,3,5-TMB	0.07	0.34	0.01	0.50	2.97	0.02
2-Ethyltoluene	0.08	0.39	0.01	0.53	2.70	0.03
1,2,4-TMB	0.27	1.40	0.05	1.53	8.13	0.06
*t*Bu-Benzene	<LOD	<LOD	<LOD	0.29	1.47	0.01
1,2,3-TMB	0.05	0.35	<LOD	0.51	2.84	0.02
Indan	0.01	0.08	<LOD	0.12	0.68	<LOD
C_4 aromatics	0.21	1.26	0.01	3.04	15.22	0.17
Indene	<LOD!	<LOD	<LOD	0.00	0.05	<LOD
2-Methylpropylbenzene	0.01	0.03	<LOD	0.12	0.64	<LOD
1-Methylpropylbenzene	0.01	0.05	<LOD	0.14	0.64	0.01
m/*p*-Cymene	0.03	0.22	0.01	0.42	2.10	0.02
o-Cymene	<LOD	<LOD	<LOD	0.02	0.26	<LOD
1-Methyl-3-propybenzene	0.01	0.03	<LOD	0.08	0.40	<LOD
1,3-Diethylbenzene	0.02	0.12	<LOD	0.16	0.85	<LOD
n-Butylbenzene/1,4-Diethylbenzene	0.04	0.20	<LOD	0.41	2.09	0.01
1,2-Diethylbenzene	0.01	0.07	<LOD	0.14	0.72	0.01
1-Methyl-4-propylbenzene	0.01	0.05	<LOD	0.11	0.61	<LOD
1-ethyl-2,4-dimethylbenzene	0.02	0.12	<LOD	0.14	0.73	0.01
4-Ethyl-1,2-dimethylbenzene	0.02	0.17	<LOD	0.27	1.51	0.01
1-Ethyl-2,3-dimethylbenzene	0.00	0.03	<LOD	0.07	0.42	<LOD
2-Ethyl-1,3-dimethylbenzene	0.00	0.02	<LOD	0.08	0.40	<LOD
1,2,4,5-Tetramethylbenzene	0.00	0.06	<LOD	0.13	0.55	<LOD
1,2,3,5-Tetramethylbenzene	0.01	0.13	<LOD	0.21	1.15	<LOD
1,1/1,3-Dimethylindan	<LOD	0.02	<LOD	0.03	0.17	<LOD
1,2,3,4-Tetramethylbenzene	0.01	0.09	<LOD	0.15	0.98	<LOD
1,1/1,3-Dimethylindan	<LOD	<LOD	<LOD	0.05	0.25	<LOD
1,2,3,4-Tetrahydronapthalene	0.00	0.01	<LOD	0.03	0.23	<LOD
C_5 aromatics	0.04	0.29	<LOD	0.83	3.95	<LOD
Monoterpenes						
α-Pinene	0.03	0.08	0.01	0.08	0.48	<LOD
Camphene	0.01	0.07	0.00	0.07	0.39	<LOD
Sabinene	<LOD	<LOD	<LOD	0.01	0.25	<LOD
β-pinene	0.01	0.05	<LOD	0.04	0.20	<LOD
Myrcene	<LOD	<LOD	<LOD	0.03	0.20	<LOD
α-Phellandrene	0.02	0.06	<LOD	0.07	0.35	<LOD
3-Carene	0.01	0.05	<LOD	0.06	0.39	<LOD
α-Terpinene	<LOD	<LOD	<LOD	0.02	0.12	<LOD

Table S8.1. continued.

NMHC	Pre	Pre max	Pre min	Post	Post max	Post min
Monoterpenes						
Limonene	0.01	0.19	<LOD	0.32	2.01	0.00
β-Ocimene	0.03	0.14	<LOD	0.22	1.71	<LOD
γ-Terpinene	<LOD	0.05	<LOD	0.02	0.14	<LOD
Terpinolene	<LOD	0.02	<LOD	0.04	0.29	<LOD
Sum monoterpenes	0.12	0.65	0.03	0.98	5.99	0.01
Alkenes						
Ethene	4.25	15.11	0.89	21.62	96.08	0.56
Propene	1.11	4.97	0.17	6.26	25.49	0.07
t-2-Butene	0.15	0.90	0.03	1.28	6.19	0.01
1-Butene	0.31	1.18	0.07	1.74	6.57	<LOD
i-Butene	0.47	1.72	0.15	2.59	10.05	0.02
c-2-Butene	0.16	0.77	0.04	1.21	5.42	0.01
1,3-Butadiene	0.12	0.67	<LOD	0.82	4.64	0.01
t-2-Pentene	0.14	0.60	0.01	0.60	3.20	0.01
1-Pentene	0.07	0.25	<LOD	0.39	1.83	0.01
Isoprene	1.10	4.62	0.01	0.90	3.92	0.05
1,2-Butadiene	0.13	0.39	0.06	0.31	1.09	0.01
Alkynes						
Acetylene	2.41	6.85	0.53	10.40	45.57	0.28
Propyne	0.08	0.31	0.01	0.45	1.91	0.013
Oxygenates						
Methanol	26.95	62.37	4.91	60.08	1187.81	13.75
Acetone	6.30	12.04	3.58	14.30	45.23	3.87
Ethanol	27.38	101.52	8.41	56.47	216.40	0.001

8.2. Zoomed pre-monsoon O_3, CO, NO, NO_2 and stacked NMHC timeseries

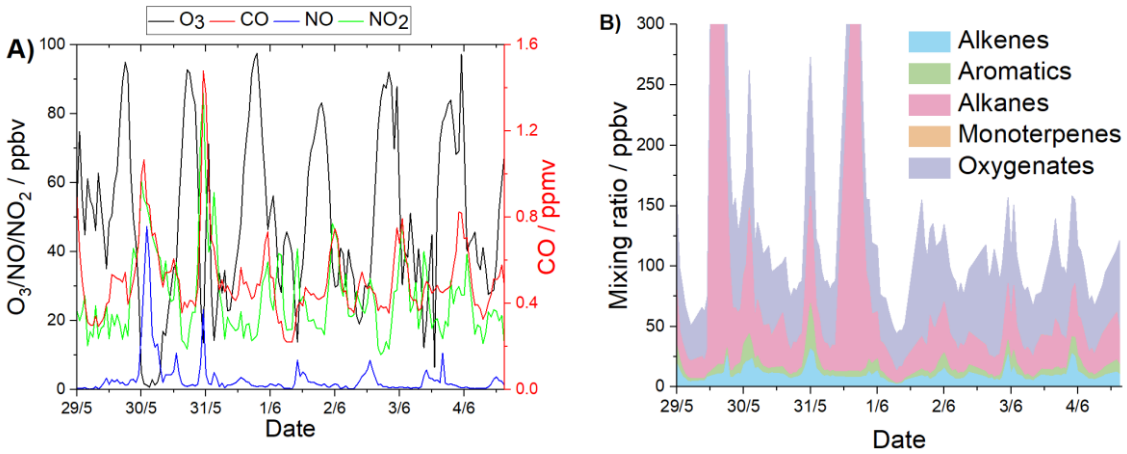

Figure S8.1. Zoomed-in pre-monsoon timeseries of NMHCs, O_3, NO, NO_2 and CO.

8.3. Pre- and post-monsoon diurnals for selected NMHCs

Pre monsoon

DC-GC-FID sample window 28/05/18 21:00 – 05/06/18 12:00.

GC×GC-FID sample window 29/05/18 16:00 – 05/06/18 11:00.

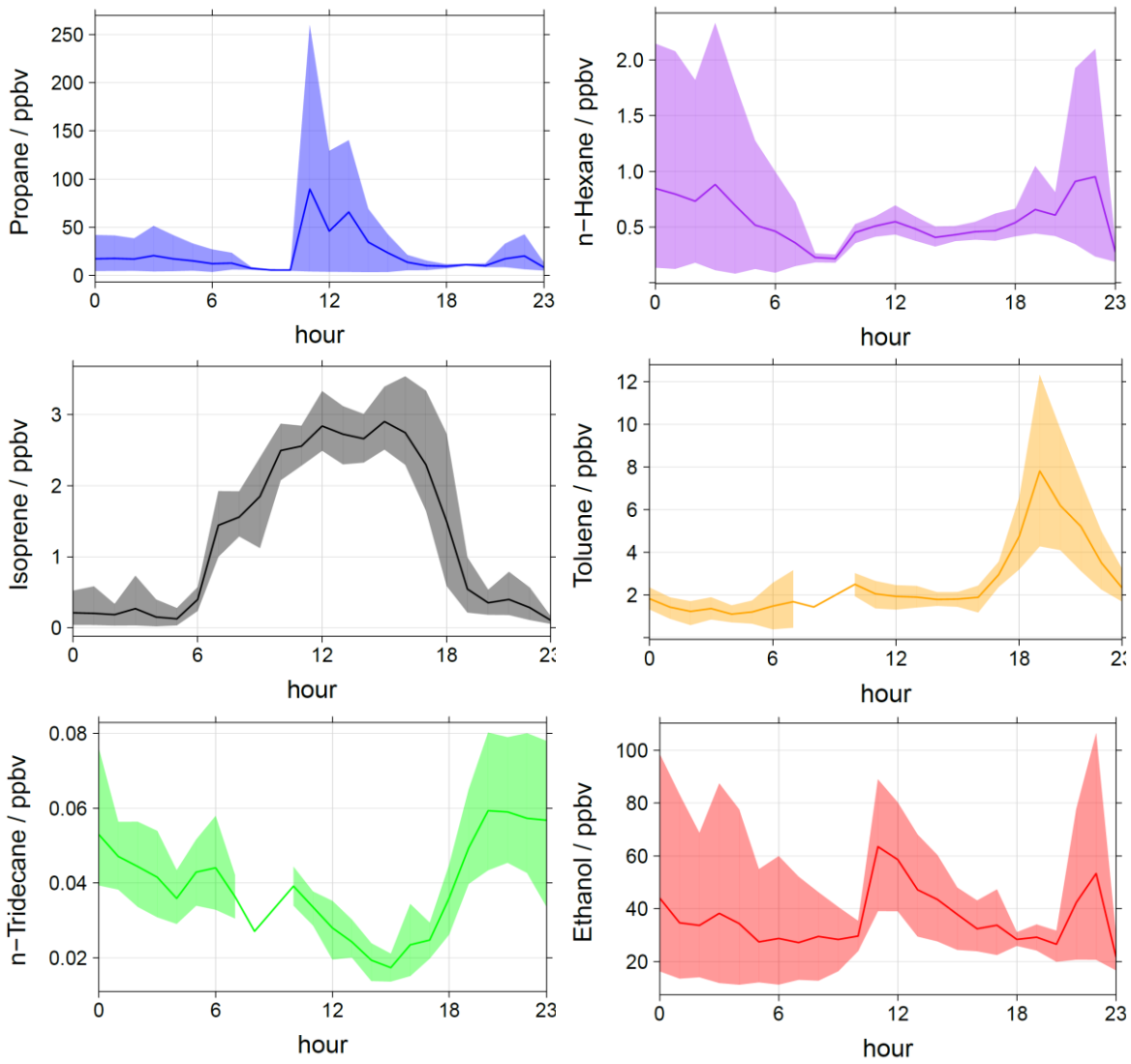

Figure S8.2. Diurnal NMHC profiles from the pre-monsoon campaign of propane, *n*-hexane, isoprene, toluene, *n*-tridecane and ethanol.

Post monsoon

DC-GC-FID sample window 05/10/18 00:00 – 27/10/18 17:00.

GC×GC-FID sample window 11/10/18 22:00 – 04/11/18 05:00.

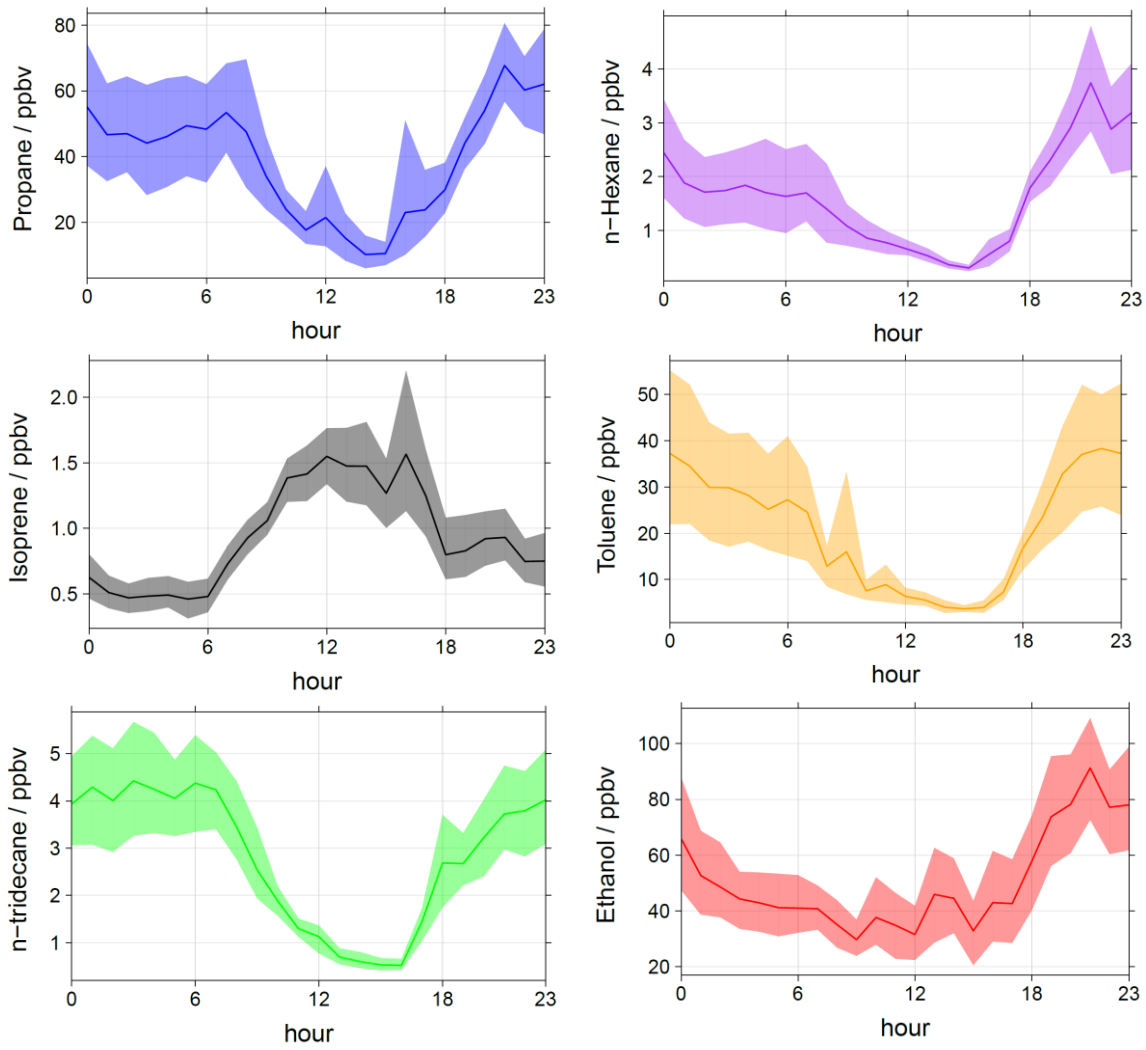

Figure S8.3. Diurnal profiles of NMHCs from the post-monsoon campaign of propane, *n*-hexane, isoprene, toluene, *n*-tridecane and ethanol.

8.4. Pre-monsoon stacked diurnals

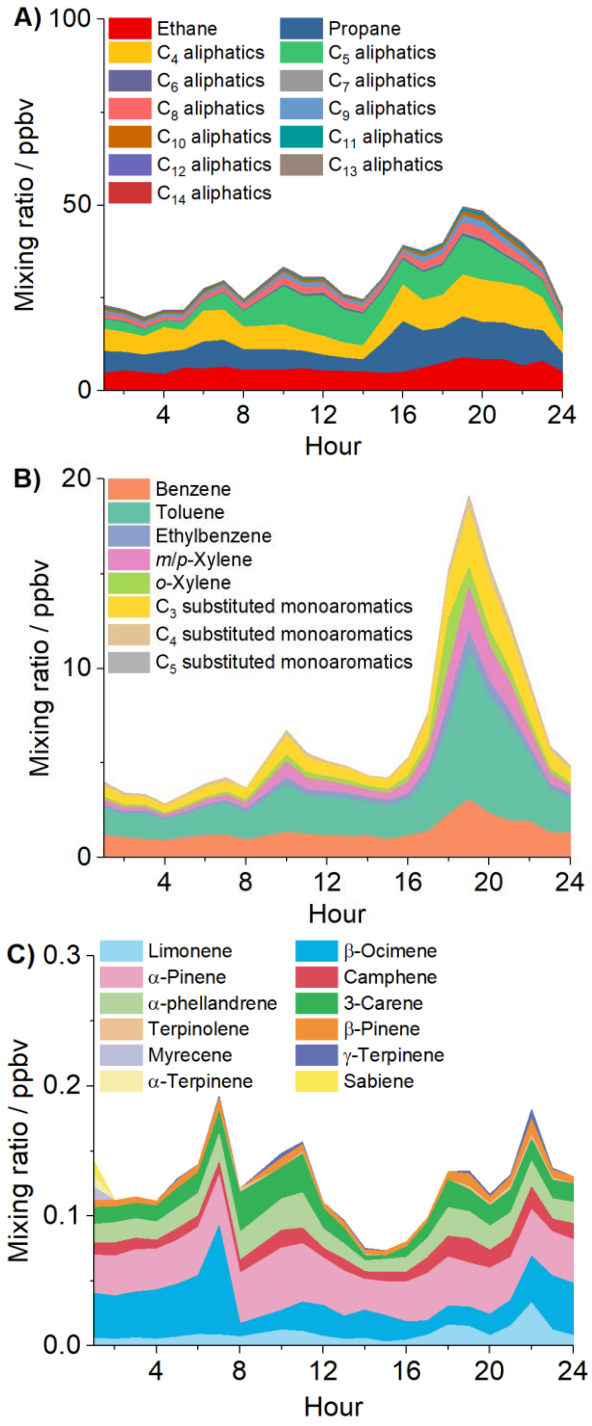

Figure S8.4. Zoomed stacked area diurnals from the pre-monsoon campaign of A = alkanes excluding LPG spikes, B = aromatics and C = monoterpenes.

8.5. PCA/APCS and EPA Unmix 6.0

Figure S8.5 and Figure S8.6 show the outputs of the Unmix 6.0 model and the combined mean output of PCA/APCS and Unmix 6.0 models. The results are relatively similar, but Unmix 6.0 showed slightly larger contributions of diesel to aromatics and heavier alkanes, and the differences between the two approaches may be caused by slight collinearity of sources.

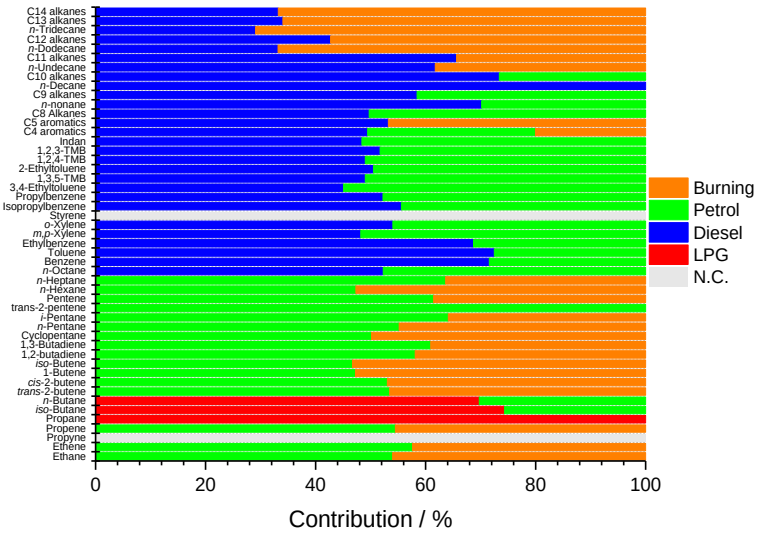

Figure S8.5. Mean Unmix 6.0 source contribution to NMHCs, where NC means that the model did not converge.

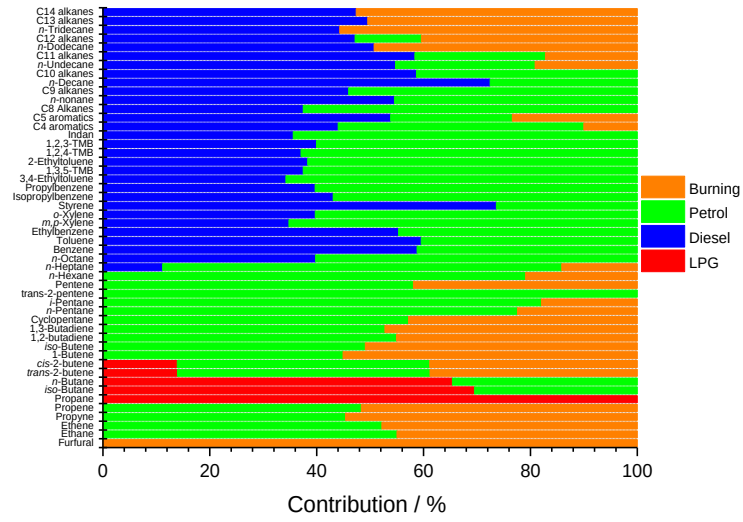

Figure S8.6. Mean Unmix 6.0 and PCA/APCS source contribution to NMHCs.

8.6. 4 factor PCA/APCS comparison

Comparison of EPA PMF 5.0 (see Figure S8.7) vs. PCA/APCS (see Figure S8.8) models using the combined dataset for a 4-factor solution for propane. Inclusion of additional factors into the PMF model did not resolve into an LPG factor and multiple factors from one source type.

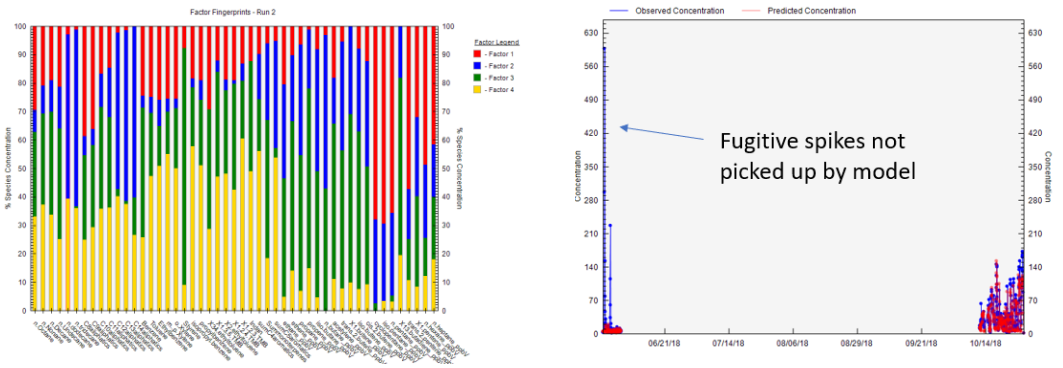

Figure S8.7. EPA PMF 5.0 4 factor solution on combined dataset.

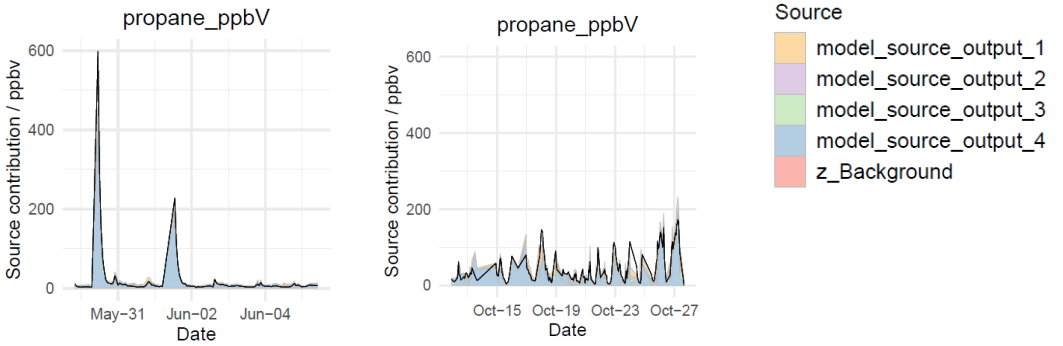

Figure S8.8. PCA/APCS 4 factor solution both datasets where model_source_output_4 = LPG source and the black line indicates the measured value.

8.7. SPE/PTFE sample collection

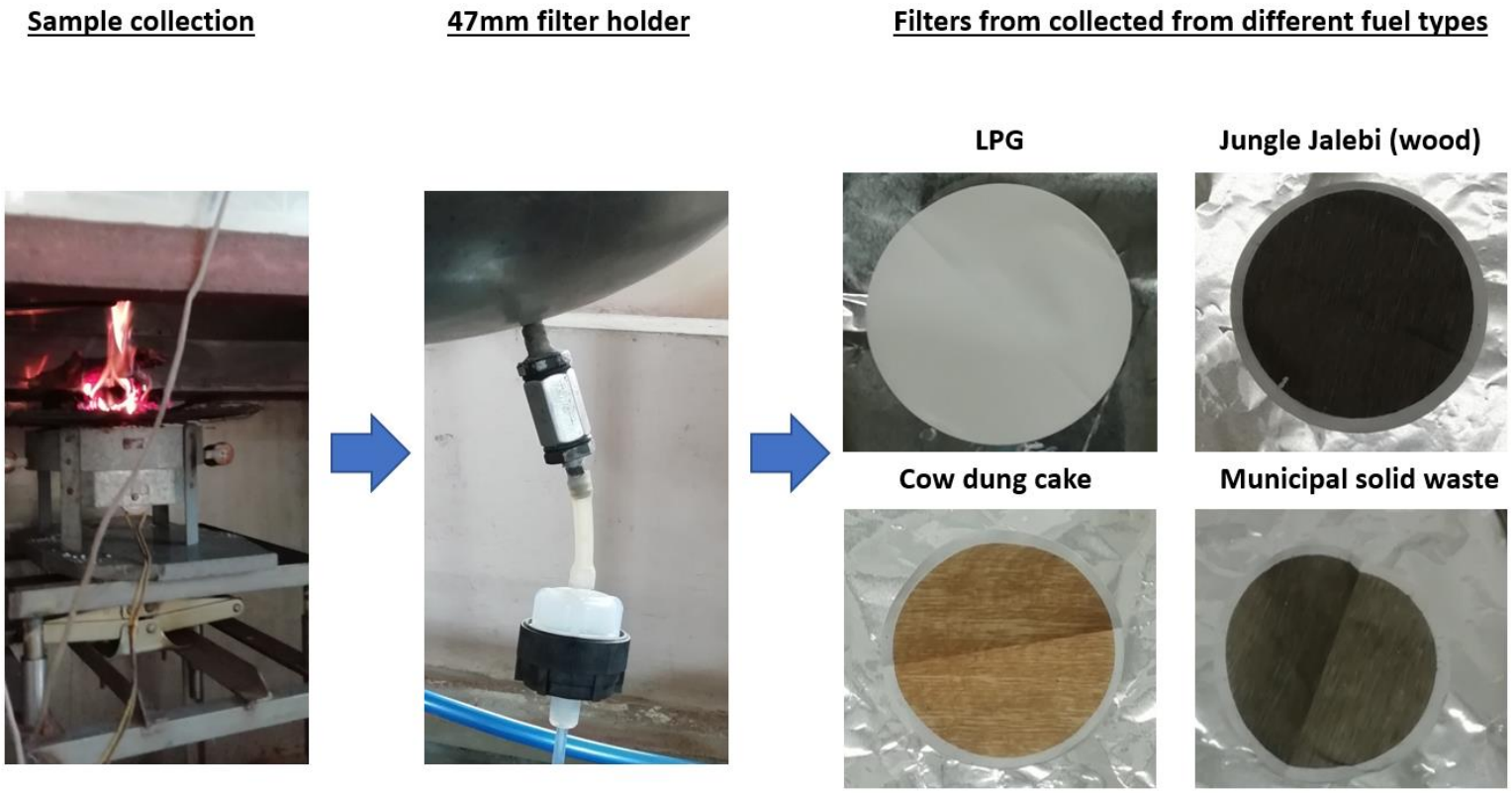

Figure S8.9. Figures showing sample burning in chamber (left), sample collection in 47mm PFA holder (middle) and examples of filters collected from different samples (right).

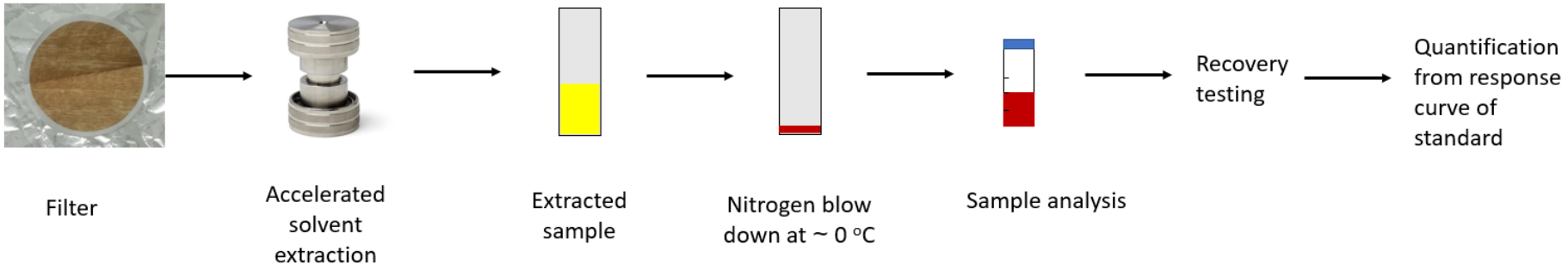

Figure S8.10. Flow diagram showing steps involved in quantification after sample collection.

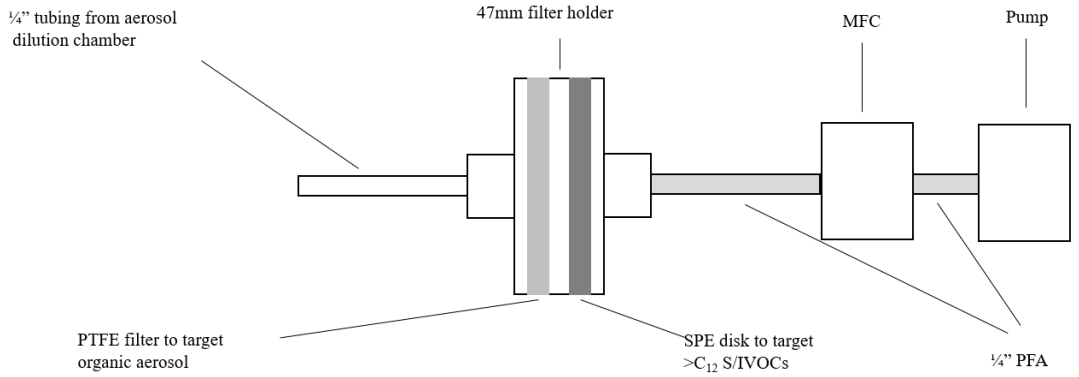

Figure S8.11. Schematic of SPE/PTFE filter collection setup.

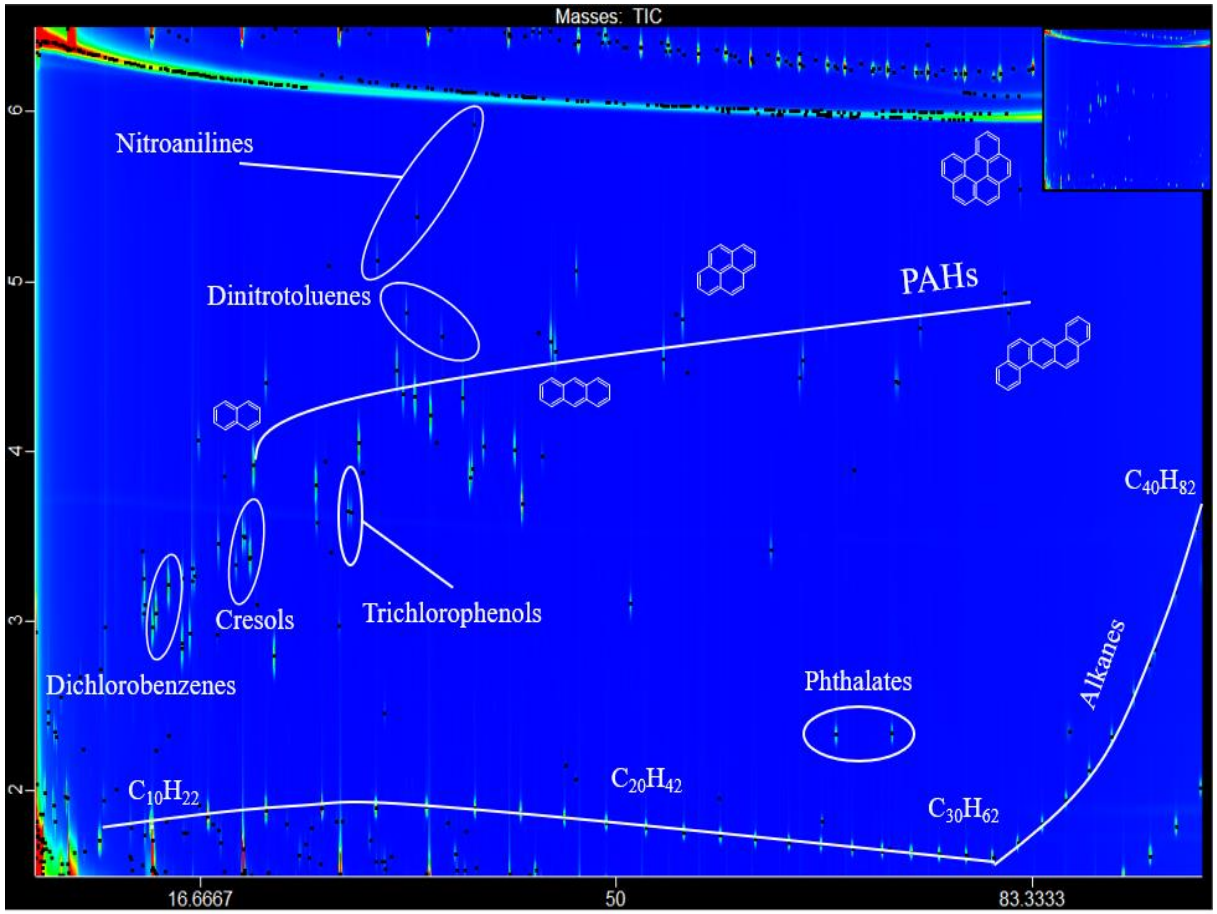

Figure S8.12. Example chromatogram from standard used with series of I/SVOCs labelled.

8.8. Results of breakthrough testing

Figure S8.13-Figure S8.19 show a comparison of the area from 6 spikes containing 136 compounds (50 µL at 20 µg mL^{-1}) directly into 0.95 mL of EtOAc to 6 separate PTFE filters (black) and SPE disks (red) spiked with the standard solution containing 136 compounds (50 µL at 20 µg mL^{-1}) extracted and analysed and SPE disks spiked with 96 compounds of interest (4 times, 50 µL at 20 µg mL^{-1}), subject to a purified air flow of 6 L min^{-1} for 30 mins then extracted and analysed (green).

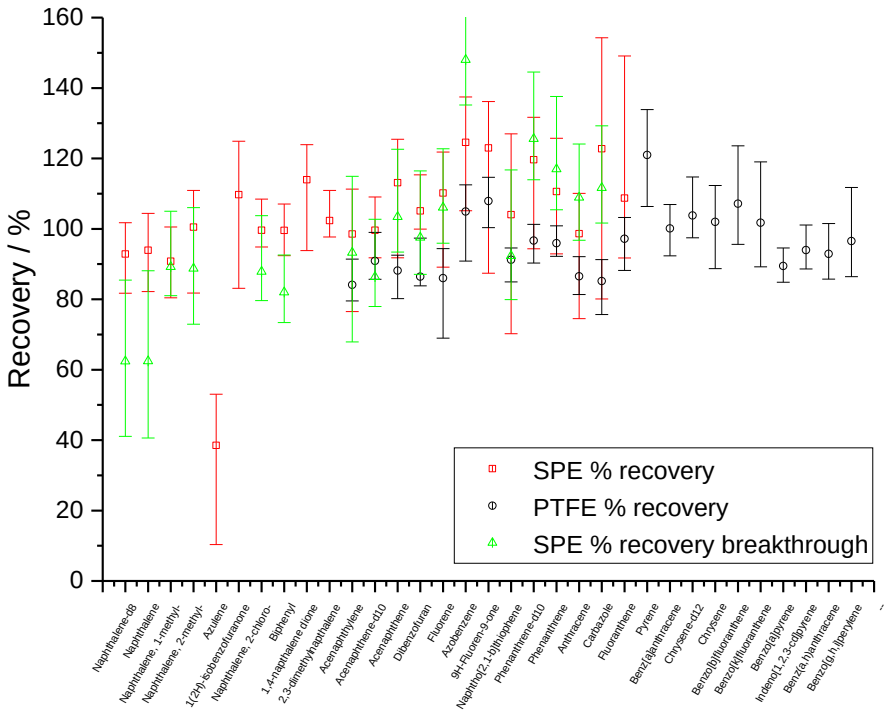

Figure S8.13. PAH breakthrough test.

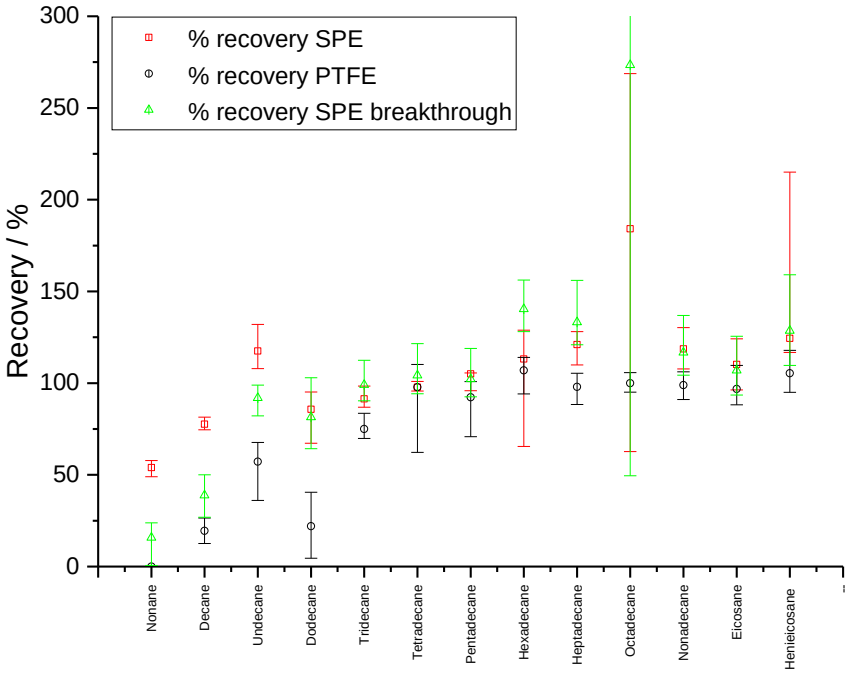

Figure S8.14. Alkane breakthrough test. The large over recovery of *n*-octadecane is assumed to be from the C_{18} coating on SPE disks.

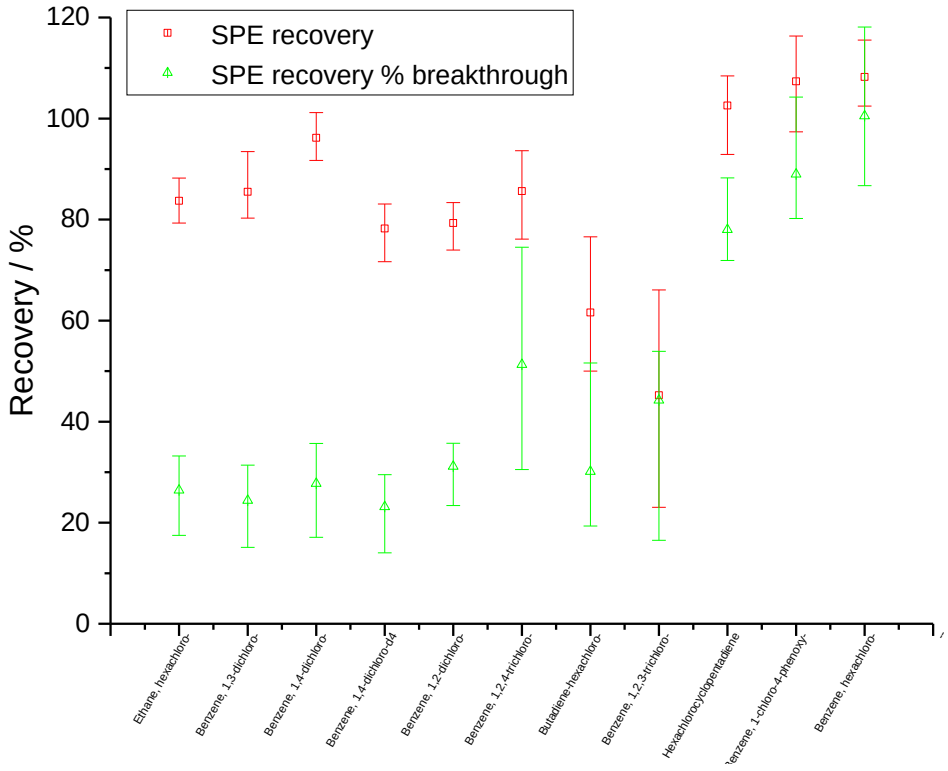

Figure S8.15. Chlorine containing species breakthrough test.

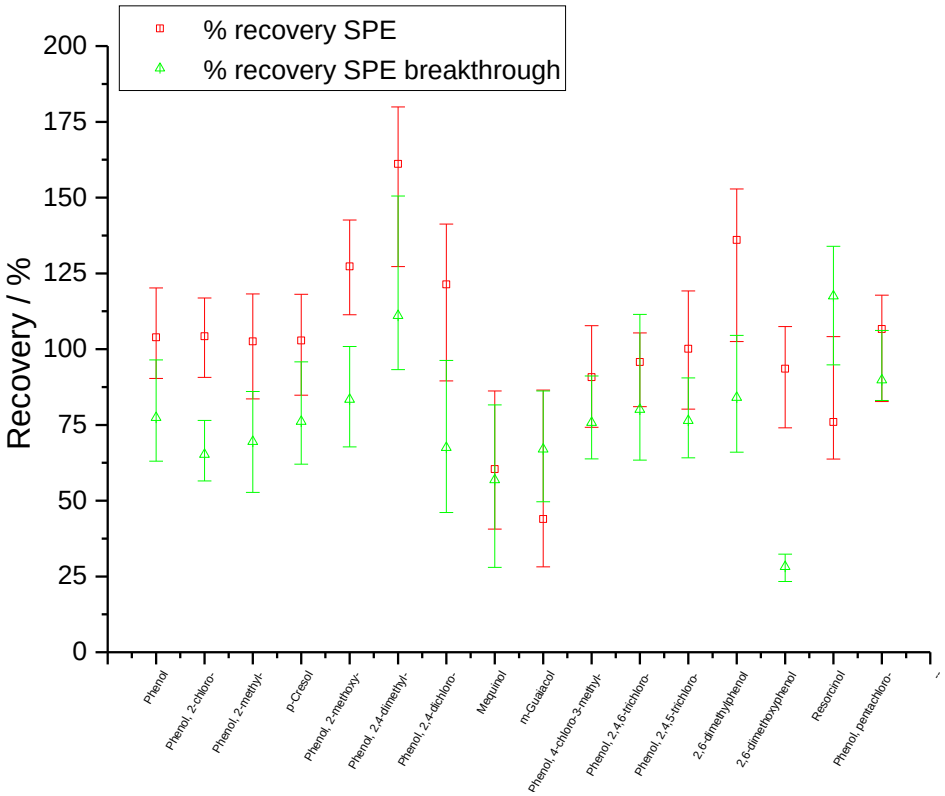

Figure S8.16. Phenols breakthrough test.

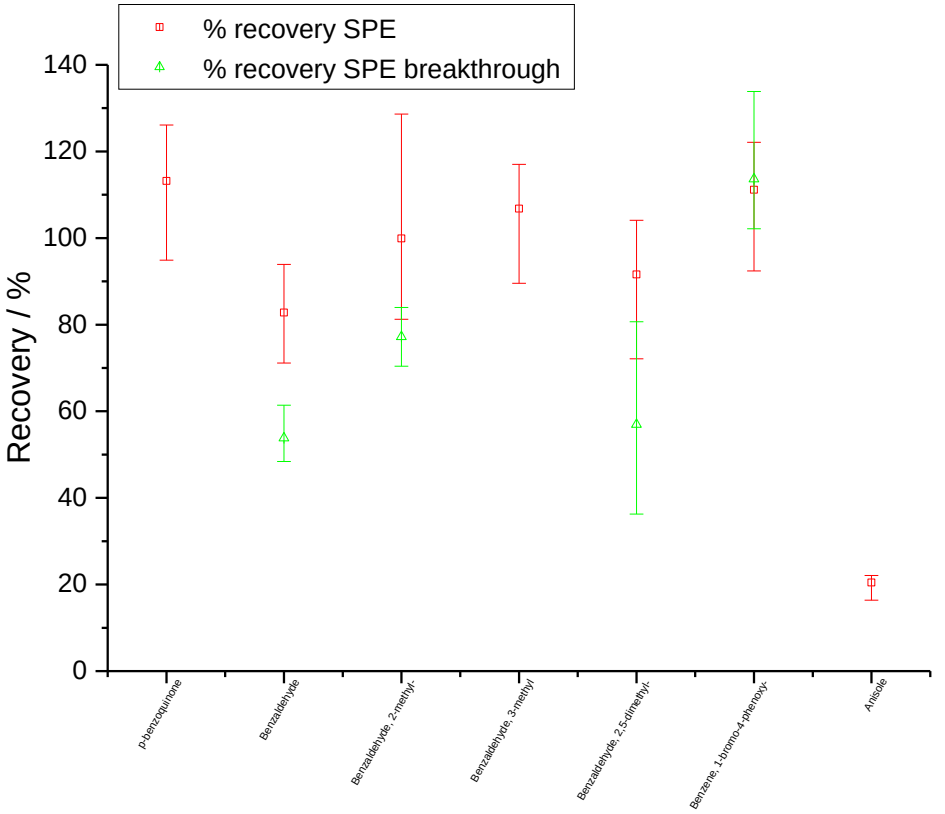

Figure S8.17. Oxygenated aromatics breakthrough test.

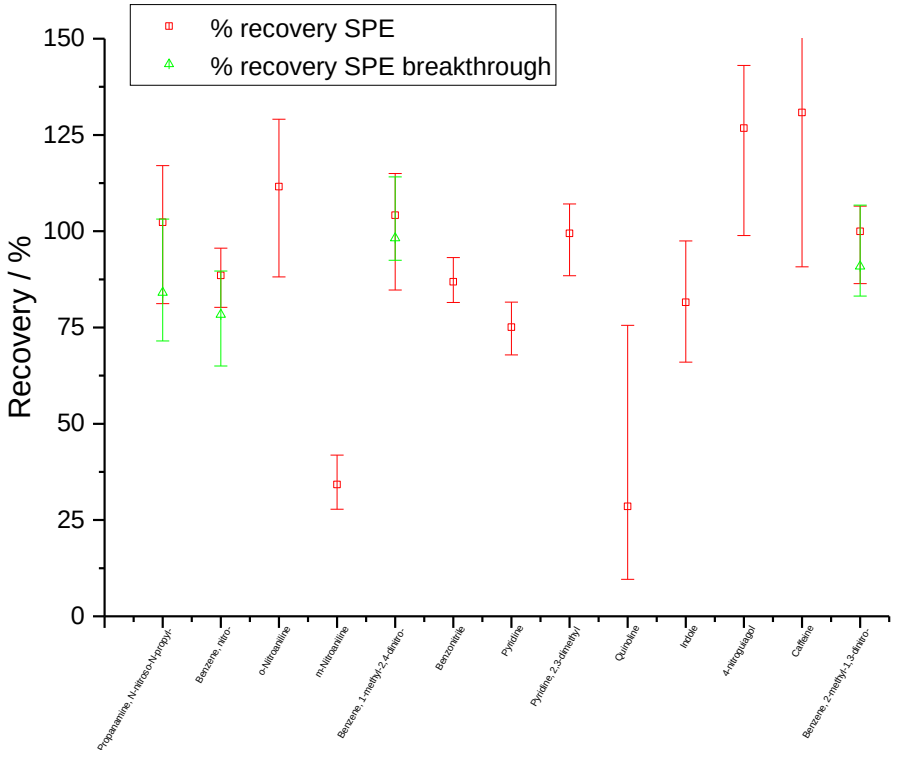

Figure S8.18. Nitrogen containing VOC breakthrough test.

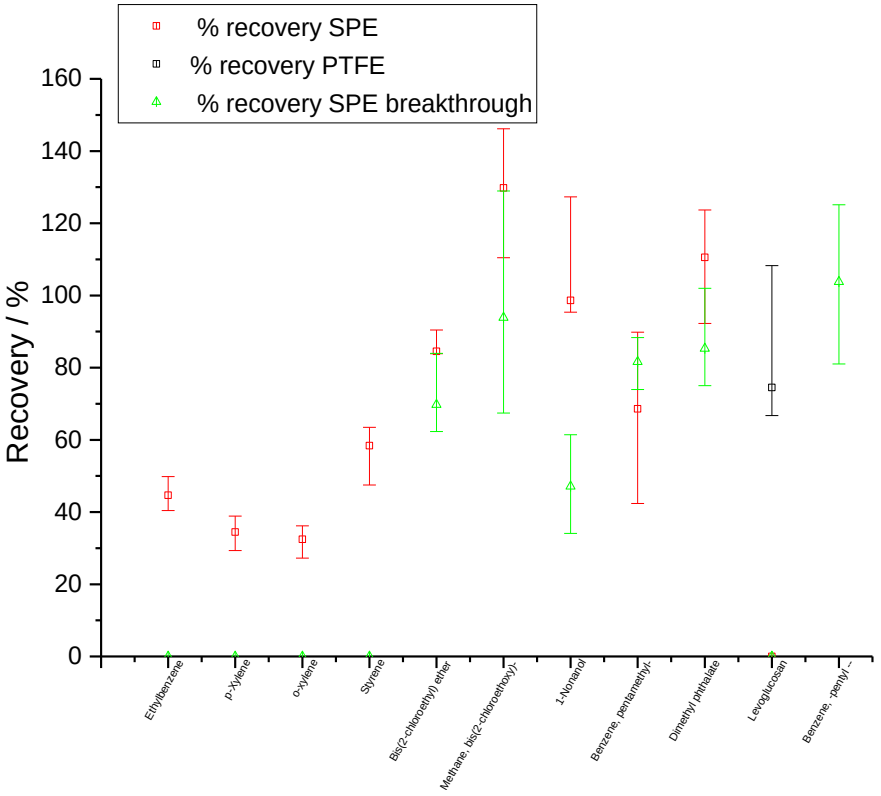

Figure S8.19. Aromatics and others breakthrough test. Levoglucosan PTFE recovery carried out from spiking stock solution in MeOH directly onto filter to give a final solution concentration of around 10 µg mL^{-1} due to low instrument sensitivity.

8.9. *n*-Alkane comparison to GC×GC-FID

Comparison to PTR-ToF-MS is complicated by more than one isomer being present at a mass and aerosol samples passing through a chamber stage with either losses to walls or off gassing of the more volatile components from the aerosol sample post acquisition.

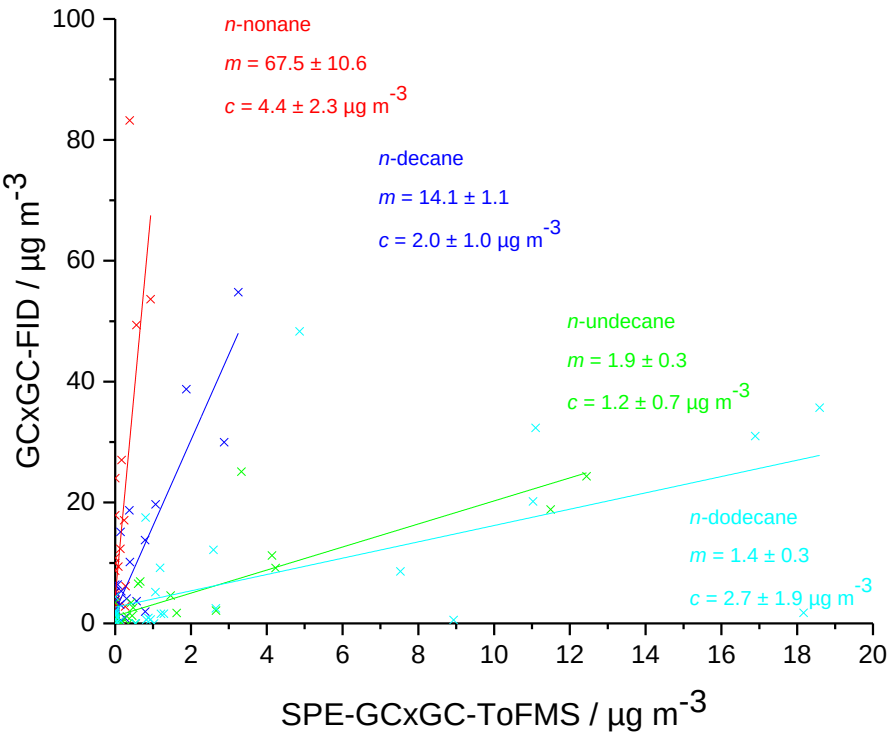

Figure S8.20. Comparison of GC×GC-FID to SPE-GC×GC-ToF-MS.

8.10. Gas and particle phase composition of I/SVOC emissionsfrom combustion of cow dung cake

Figure S8.21 shows the functionality and phase of peaks observed from a sample collected from the combustion of cow dung cake.

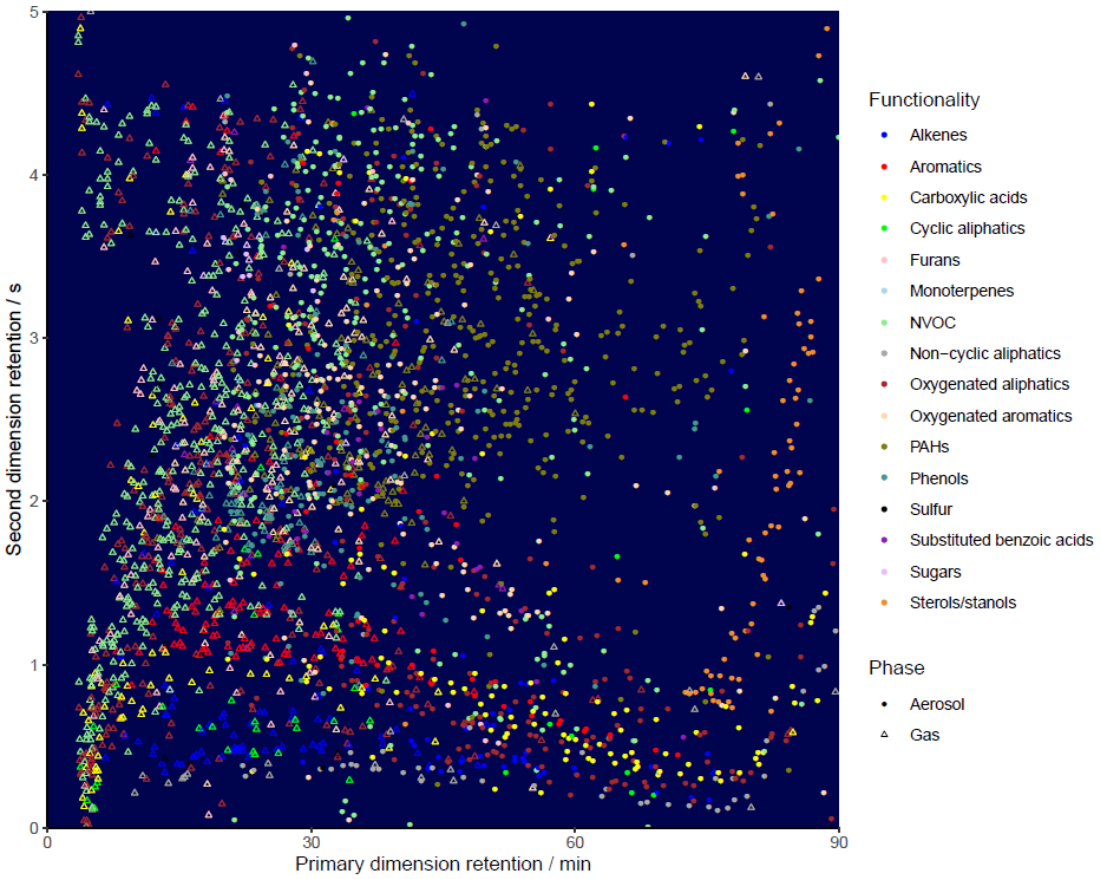

Figure S8.21. Gas and particle phase I/SVOCs from burning cow dung cake collected onto SPE disks and PTFE filters, split by functionality where empty triangles indicate peaks in the gas phase and solid circles show peaks in the aerosol phase.

8.11. Emission factors

The total volume of air convectively moving up the stack was determined from:

$$V_d = \sqrt{\frac{2gP_s}{D_s}}$$

where V_d = vertical displacement up the flue (ms^{-1}), g = 9.81 m^{-2}, P_s = average stack pressure (mmH_2O) and D_s is determined by:

$$D_s = \frac{TD_a}{T_s}$$

where T = ambient temperature (k), D_a = density of air (1.1455 kg m^{-3}), T_s = average stack temperature (^oK). The emission factor (EF) was calculated by:

$$EF = \frac{tCV_dA_d}{M}$$

where t = time burned (s), C = concentration (g m^3), A_d = area of flue, M = mass of fuel burnt (kg).

8.12. Sample collection details and schematic of combustion chamber

Sample collection was carried out by partners at CSIR-NPL Delhi and led by Arnab Mondal. This work will be published separately, with a summary provided here. The National Capital Territory was gridded into 66 grids of 25 km^2 area over which a ground survey of domestic fuels was conducted. 695 locations were sampled which included 636 slums and 59 villages and covered around 6500 households in total.

The combustion methodology was designed to replicate the convection-driven conditions of real-world combustion and was adapted from the VITA water-boiling test. A schematic of the combustion chamber is given in Figure S8.22. The fuel was placed 45 cm from the top of the hood. These conditions have been previously optimised (Venkataraman et al., 2002). This distance represented a balance so that the combustion experiment was not too close to the hood whereby entrainment into the hood could exert a draft which altered combustion conditions and not too far from the hood which would result in not all of the NMVOC emissions being captured by the hood. The dilution ratios in this setup have been studied in previous works (Saud et al., 2012). In summary, sample air was diluted 40-60 times in the duct and cooled to 2-3 ^oC above ambient temperatures at the top of the duct. A video supplement of a sample being burnt in the combustion chamber is available at https://doi.org/10.5446/50203 .

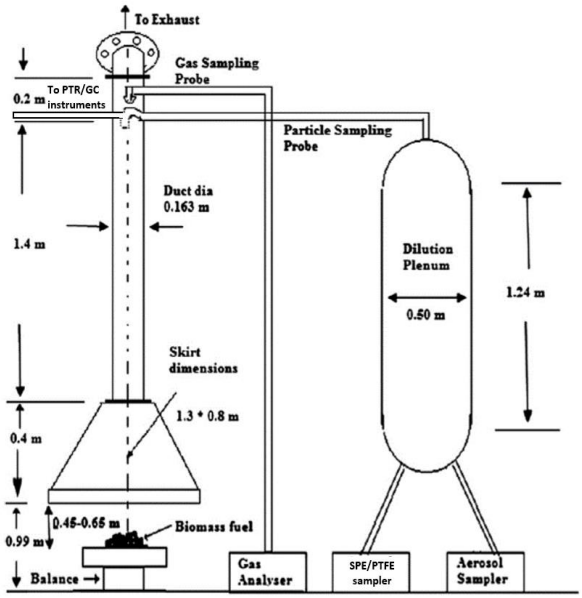

Figure S8.22. Schematic of combustion-dilution chamber with sampling locations for PTR-ToF-MS, DC-GC-FID and GC×GC-FID instruments and SPE/PTFE sample collection points.

Temperatures above combustion experiments were measured directly (see Table S8.2), with the hottest flame temperatures from LPG (721 ± 18 ^{o}C), followed by fuel wood (545 ± 122 ^{o}C), followed by crop residues (432 ± 143 ^{o}C), followed by sawdust (314 ± 163 ^{o}C), followed by cow dung cakes (303 ± 137 ^{o}C) and MSW (249 ± 161 ^{o}C).

Table S8.2. Mean maximum temperatures above different combustion experiments by fuel type.

Fuel	**Mean maximum flame temp ± σ / ^{o}C**
Fuel wood	545 ± 122
Cow dung cake	303 ± 137
Charcoal	251 ± 57
Crop residue	432 ± 143
Sawdust	314 ± 163
LPG	721 ± 18
MSW	249 ± 161

8.13. SOA yields

Table S8.3. SOA yields used for determining SOA from biomass burning NMVOC emissions.

Compound	High NO_x yield	High NO_x ref	Notes	Low NO_x yield	Low NO_x ref	Notes
Dodecane	0.08	(Zhao et al., 2016)		0.05	(Loza et al., 2014)	
Tridecane	0.21	(Zhao et al., 2016)		0.21 [b]	(Zhao et al., 2016)	Assumed same as low NO_x (Yuan et al., 2013)
Tetradecane	0.28	(Zhao et al., 2016)		0.28 [b]	(Zhao et al., 2016)	Assumed same as low NO_x (Yuan et al., 2013)
Pentadecane	0.34	(Zhao et al., 2016)		0.34 [b]	(Zhao et al., 2016)	Assumed same as low NO_x (Yuan et al., 2013)
Hexadecane	0.38	(Zhao et al., 2016)		0.38 [b]	(Zhao et al., 2016)	Assumed same as low NO_x (Yuan et al., 2013)
Heptadecane	0.42	(Zhao et al., 2016)		0.42 [b]	(Zhao et al., 2016)	Assumed same as low NO_x (Yuan et al., 2013)
Octadecane	0.42	(Zhao et al., 2016)		0.42 [b]	(Zhao et al., 2016)	Assumed same as low NO_x (Yuan et al., 2013)
Nonadecane	0.42	(Zhao et al., 2016)		0.42 [b]	(Zhao et al., 2016)	Assumed same as low NO_x (Yuan et al., 2013)
Eicosane	0.42	(Zhao et al., 2016)		0.42 [b]	(Zhao et al., 2016)	Assumed same as low NO_x (Yuan et al., 2013)
Naphthalene	0.21	(Zhao et al., 2016)		0.66	(Chan et al., 2009)	Assumed same as low NO_x (Yuan et al., 2013)
C1-Napthalene	0.27	(Zhao et al., 2016)		0.57	(Chan et al., 2009)	Average of 1-MN and 2-MN
C2-Napthalene	0.31	(Zhao et al., 2016)		0.57	(Chan et al., 2009)	Assumed same as C_1 napthalenes
Benzene	0.14	(Ng et al., 2007b)		0.34	(Ng et al., 2007b)	

Table S8.3. continued.

Compound	High NO_x yield	High NO_x ref	Notes	Low NO_x yield	Low NO_x ref	Notes
Toluene	0.083	(Ng et al., 2007b)		0.33	(Ng et al., 2007b)	
C_2-Benzenes	0.047	(Ng et al., 2007b)		0.27	(Ng et al., 2007b)	
C_3-Benzenes	0.047	(Ng et al., 2007b)	Assumed same as C_2 benzenes	0.27	(Ng et al., 2007b)	
C_4-Benzenes	0.04	(Zhao et al., 2016)		0.27	(Ng et al., 2007b)	Assumed same as C_2 benzenes
C_5-Benzenes	0.08	(Zhao et al., 2016)		0.27	(Ng et al., 2007b)	Assumed same as C_2 benzenes
Salicylaldehyde	0.18	[a]	Average	0.31	[a]	Average
Phenol	0.54	(Yee et al., 2013)	Assumed same as phenol	0.40	(Yee et al., 2013)	
Cresol/anisole	0.54	(Yee et al., 2013)	Assumed same as phenol	0.40	(Yee et al., 2013)	Assumed same as phenol
Ethyl phenol	0.54	(Yee et al., 2013)	Assumed same as phenol	0.40	(Yee et al., 2013)	Assumed same as phenol
Guaiacol	0.46	(Yee et al., 2013)		0.45	(Yee et al., 2013)	
Vinyl guaiacol	0.46	(Yee et al., 2013)	Assumed same as guaiacol	0.45	(Yee et al., 2013)	Assumed same as guaiacol
Methyl guaiacol	0.46	(Yee et al., 2013)	Assumed same as guaiacol	0.45	(Yee et al., 2013)	Assumed same as guaiacol
Eugenol, isoeugenol	0.3	(Yee et al., 2013)	Assumed same as syringol	0.32	(Yee et al., 2013)	Assumed same as syringol
Syringol	0.3	(Yee et al., 2013)		0.32	(Yee et al., 2013)	

Table S8.3. continued.

Compound	High NO_x yield	High NO_x ref	Notes	Low NO_x yield	Low NO_x ref	Notes
Vanillin	0.3	(Yee et al., 2013)	Assumed same as syringol	0.32	(Yee et al., 2013)	Assumed same as syringol
3-Methylcatechol	0.3	(Yee et al., 2013)	Assumed same as syringol	0.32	(Yee et al., 2013)	Assumed same as syringol
MVK, methacrolyn, crotonaldehyde	0.05	(Hatch et al., 2015; Liu et al., 2011)	Assumption of Hatch et al. (2015) applied to other oxygenated aliphatics > C_6	0.05	(Hatch et al., 2015; Liu et al., 2011)	Assumption of Hatch et al. (2015) applied to other oxygenated aliphatics > C_6.
Monoterpenes	0.15	(Lee et al., 2006; Hatch et al., 2015)		0.15	(Lee et al., 2006; Hatch et al., 2015)	Same as high NOx
Furan	0.05	(Bruns et al., 2016)		0.05	(Bruns et al., 2016)	
Methyl furans	0.09	(Strollo and Ziemann, 2013)	Based on 3-methylfuran	0.12	(Strollo and Ziemann, 2013)	Lower NO_x final, based on 3-methylfuran
Furfural	0.083	(Ng et al., 2007b; Gilman et al., 2015)	Based on same SOAP as toluene Gilman et al. (2015)	0.33	(Ng et al., 2007b; Gilman et al., 2015)	Based on same SOAP as toluene Gilman et al. (2015)
2-Methanol furanone	0.083	(Ng et al., 2007b; Gilman et al., 2015)	Based on same SOAP as toluene Gilman et al. (2015)	0.33	(Ng et al., 2007b; Gilman et al., 2015)	Based on same SOAP as toluene Gilman et al. (2015)
2-(3H)-furanone	0.083	(Ng et al., 2007b; Gilman et al., 2015)	Based on same SOAP as toluene Gilman et al. (2015)	0.33	(Ng et al., 2007b; Gilman et al., 2015)	Based on same SOAP as toluene Gilman et al. (2015)
5-hydroxymethyl-2[3H]-furanone	0.083	(Ng et al., 2007b; Gilman et al., 2015)	Based on same SOAP as toluene Gilman et al. (2015)	0.33	Based on same SOAP as toluene Gilman et al. (2015)	Based on same SOAP as toluene Gilman et al. (2015)

Table S8.3. continued.

Compound	High NO_x yield	High NO_x ref	Notes	Low NO_x yield	Low NO_x ref	Notes
C_2-furans	0.09	(Strollo and Ziemann, 2013)	Based on 3-methylfuran	0.12	(Strollo and Ziemann, 2013)	Lower NO_x final, based on 3-methylfuran
C_6-diketone isomers, C_6-esters	0.05	(Hatch et al., 2015; Liu et al., 2011)	Assumption of Hatch et al. (2015) applied to other oxygenated aliphatics > C_6	0.05	(Hatch et al., 2015; Liu et al., 2011)	Assumption of Hatch et al. (2015) applied to other oxygenated aliphatics > C_6
Methyl furfurals	0.083	(Ng et al., 2007b; Gilman et al., 2015)	Based on same SOAP as toluene Gilman et al. (2015)	0.33	(Ng et al., 2007b; Gilman et al., 2015)	Based on same SOAP as toluene Gilman et al. (2015)
C_2-pyroles	0.083	(Ng et al., 2007b; Gilman et al., 2015)	Based on same SOAP as toluene Gilman et al. (2015)	0.33	(Ng et al., 2007b; Gilman et al., 2015)	Based on same SOAP as toluene Gilman et al. (2015)
Structurally assigned ≥ C_6 compounds [a]	0.18	[a]		0.31	[a]	
structurally unassigned ≥ C_6 compounds [a]	0.18	[a]		0.31	[a]	

[a] Average of applied yields from NMVOCs in the table with at least 6 carbon atoms per molecule.

[b] Low NO_x alkane yields are poorly studied beyond *n*-dodecane, and alkane emission factors in this study are small. For *n*-dodecane, the low NO_x yield is comparable to the high NO_x yield of dodecane and high NO_x yields have been used for heavier alkanes.

8.14. Rate constants for reaction with OH

C_4 substituted monoaromatics have been taken from the PTR-ToF-MS as opposed to the speciated measurement with the GC×GC-FID, as these species have low emission factors and little influence on overall OH reactivity. Many OH rate constants have been taken from the Supplement of Koss et al. (2018).

Table S8.4. Rate constant used for calculation of OH reactivity.

No	VOC	Formula	Rate constant (10^{-12} cm^3 $molecule^{-1}$ s^{-1})	Reference
1	Ethane	C_2H_6	0.248	(Atkinson and Arey, 2003)
2	Ethene	C_2H_4	8.52	(Atkinson and Arey, 2003)
3	Propane	C_3H_8	1.09	(Atkinson and Arey, 2003)
4	Propene	C_3H_6H	30	NIST database
5	Isobutane	C_4H_{10}	2.12	(Atkinson and Arey, 2003)
6	*n*-Butane	C_4H_{10}	2.36	(Atkinson and Arey, 2003)
7	Acetylene	C_2H_2	0.7	NIST database
8	*Trans*-2-butene	C_4H_8	64	(Atkinson and Arey, 2003)
9	1-Butene	C_4H_8	31.4	(Atkinson and Arey, 2003)
10	Isobutene	C_4H_8	51.4	(Atkinson and Arey, 2003)
11	*Cis*-2-butene	C_4H_8	56.4	(Atkinson and Arey, 2003)
12	Cyclopentane	C_5H_{10}	4.97	(Atkinson and Arey, 2003)
13	*i*-Pentane	C_5H_{12}	3.6	(Atkinson and Arey, 2003)
14	*n*-Pentane	C_5H_{12}	3.8	(Atkinson and Arey, 2003)
15	1,3-Butadiene	C_4H_6	66.6	(Atkinson and Arey, 2003)
16	*Trans*-2-pentene	C_5H_{10}	67	(Atkinson and Arey, 2003)
17	*Cis*-2-pentene	C_5H_{10}	65	(Atkinson and Arey, 2003)

Table S8.4. continued.

No	VOC	Formula	Rate constant (10^{-12} cm^3 $molecule^{-1}$ s^{-1})	Reference
18	Pent-1-ene	C_5H_{10}	31.4	(Atkinson and Arey, 2003)
19	*n*-Heptane	C_7H_{16}	6.76	(Atkinson and Arey, 2003)
20	*n*-Octane	C_8H_{18}	8.11	(Atkinson and Arey, 2003)
21	*n*-Nonane	C_9H_{20}	9.7	(Atkinson and Arey, 2003)
22	*n*-Decane	$C_{10}H_{22}$	11	(Atkinson and Arey, 2003)
23	*n*-Undecane	$C_{11}H_{24}$	12.3	(Atkinson and Arey, 2003)
24	*n*-Dodecane	$C_{12}H_{26}$	13.2	(Atkinson and Arey, 2003)
25	*n*-Tridecane	$C_{13}H_{28}$	15.1	(Atkinson and Arey, 2003)
26	*n*-Tetradecane	$C_{14}H_{30}$	17.9	(Atkinson and Arey, 2003) *312K
27	C_8 grouped aliphatics	C_8H_{18}	8.11	(Atkinson and Arey, 2003)
28	C_9 grouped aliphatics	C_9H_{20}	9.7	(Atkinson and Arey, 2003)
29	C_{10} grouped aliphatics	$C_{10}H_{22}$	11	(Atkinson and Arey, 2003)
30	C_{11} grouped aliphatics	$C_{11}H_{24}$	12.3	(Atkinson and Arey, 2003)
31	C_{12} grouped aliphatics	$C_{12}H_{26}$	13.2	(Atkinson and Arey, 2003)
32	C_{13} grouped aliphatics	$C_{13}H_{28}$	15.1	(Atkinson and Arey, 2003)
33	C_{14} grouped aliphatics	$C_{14}H_{30}$	17.9	(Atkinson and Arey, 2003) *312K
34	Benzene	C_6H_6	1.22	(Atkinson and Arey, 2003)
35	Toluene	C_7H_8	5.6	(Atkinson and Arey, 2003)
36	Ethylbenzene	C_8H_{10}	7	(Atkinson and Arey, 2003)
37	*m*-/*p*-Xylene	C_8H_{10}	18.7	(Atkinson and Arey, 2003) *mean *m*/*p*-xylene

Table S8.4. continued.

No	VOC	Formula	Rate constant (10^{-12} cm^3 $molecule^{-1}$ s^{-1})	Reference
38	*o*-Xylene	C_8H_{10}	13.6	(Atkinson and Arey, 2003)
39	*i*-Propylbenzene	C_9H_{12}	6.3	(Atkinson and Arey, 2003)
40	*n*-Propylbenzene	C_9H_{12}	5.8	(Atkinson and Arey, 2003)
41	3/4-Ethyltoluene	C_9H_{12}	15.2	(Atkinson and Arey, 2003) *mean 3/4-ethyl toluene
42	1,3,5-TMB	C_9H_{12}	56.7	(Atkinson and Arey, 2003)
43	2-Ethyltoluene	C_9H_{12}	11.9	(Atkinson and Arey, 2003)
44	1,2,4-TMB	C_9H_{12}	32.5	(Atkinson and Arey, 2003)
45	*t*-Butylbenzene	$C_{10}H_{14}$	4.5	(Atkinson and Arey, 2003)
46	1,2,3-TMB	C_9H_{12}	32.7	(Atkinson and Arey, 2003)
47	Indan	C_9H_{10}	23.01429	(Atkinson and Arey, 2003) *mean C_3 substituted monoaromatic
48	α-Pinene	$C_{10}H_{16}$	52.3	(Atkinson and Arey, 2003)
49	Camphene	$C_{10}H_{16}$	53	(Atkinson and Arey, 2003)
50	Sabinene	$C_{10}H_{16}$	117	(Atkinson and Arey, 2003)
51	β-Pinene	$C_{10}H_{16}$	74.3	(Atkinson and Arey, 2003)
52	Myrcene	$C_{10}H_{16}$	215	(Atkinson and Arey, 2003)
53	α-Phellandrene	$C_{10}H_{16}$	313	(Atkinson and Arey, 2003)
54	3-Carene	$C_{10}H_{16}$	88	(Atkinson and Arey, 2003)
55	α-Terpinene	$C_{10}H_{16}$	363	(Atkinson and Arey, 2003)
56	Limonene	$C_{10}H_{16}$	164	(Atkinson and Arey, 2003)
57	β-Ocimene	$C_{10}H_{16}$	252	(Atkinson and Arey, 2003)

Table S8.4. continued.

No	VOC	Formula	Rate constant (10^{-12} cm^3 $molecule^{-1}$ s^{-1})	Reference
58	γ-Terpinene	$C_{10}H_{16}$	177	(Atkinson and Arey, 2003)
59	Terpinolonene	$C_{10}H_{16}$	225	(Atkinson and Arey, 2003)
60	Ammonia [a]	NH_3	0.2	(Gilman et al., 2015)
61	Acetylene	C_2H_2	0.7	NIST database
62	Hydrogen cyanide [a]	HCN	0.0	Cicerone 1983
63	Methanimine	CH_3N	0.2	*from ammonia
64	Formaldehyde	CH_2O	9.4	(Atkinson and Arey, 2003)
65	Methanol	CH_3OH	0.8	(Atkinson and Arey, 2003)
66	Acetonitrile	C_2H_3N	0.0	(Gilman et al., 2015)
67	Isocyanic acid	HNCO	0.0	(Gilman et al., 2015)
68	Acetaldehyde	C_2H_4O	15.0	(Atkinson and Arey, 2003)
69	Formamide	CH_3NO	1.5	NIST database: CH_2=NOH
70	Formic acid	CH_2O_2	0.4	NIST database
71	Ethanol	C_2H_5OH	3.2	(Atkinson and Arey, 2003)
72	Nitrous acid	HNO_2	6.0	(Gilman et al., 2015)
73	Methane thiol	CH_4S	33.0	NIST database
74	Methanediol	CH_4O_2	7.0	NIST database
75	Propyne nitrile	C_3HN	4.0	* From acrylonitrile
76	1-Buten-3-yne	C_4H_4	20.0	(Gilman et al., 2015)
77	Acrylonitrile	C_3H_3N	4.0	(Gilman et al., 2015)
78	2-Propynal	C_3H_2O	20.0	* From acrolein
79	Butadienes	C_4H_6	58.8	(Atkinson and Arey, 2003)
80	Propanenitrile	C_3H_5N	0.3	(Gilman et al., 2015)

Table S8.4. continued.

No	VOC	Formula	Rate constant (10^{-12} cm^3 $molecule^{-1}$ s^{-1})	Reference
81	Acrolein	C_3H_4O	20	(Gilman et al., 2015)
82	Butenes, other hydrocarbon	C_4H_8	31.8	(Atkinson and Arey, 2003)
83	Methyl isocyanate	C_2H_3NO	0.1	* From isocyanic acid, methanol (Koss et al., 2018)
84	Acetone	C_3H_6O	0.2	(Atkinson and Arey, 2003)
85	Acetamide	C_2H_5NO	8.6	NIST database
86	C_3 Amines	C_3H_9N	60.0	NIST database
87	Acetic acid	$C_2H_4O_2$	3.7	NIST database
88	Nitromethane	CH_3NO_2	0.0	(Gilman et al., 2015)
89	Dimethylsulfide [a]	CH_3NO_2	0.02	(Gilman et al., 2015)
90	1,3-Cyclopentadiene	C_5H_6	92.0	(Gilman et al., 2015)
91	Butenenitrile isomers, pyrole	C_4H_5N	111.4	(Gilman et al., 2015)
92	Carbon suboxide	C_3O_2	1.5	(Gilman et al., 2015)
93	Furan	C_4H_4O	40.0	(Gilman et al., 2015)
94	Isoprene	C_5H_8	100.0	(Atkinson and Arey, 2003)
95	Butane nitriles, dihydropyrole	C_4H_7N	7.7	SONGNEX PTR-ToF paper
96	Propiolic acid	$C_3H_2O_2$	26.0	* From acrylic acid
97	MVK, methacrolyn, crotonaldehyde	C_4H_6O	24.8	(Atkinson and Arey, 2003), NIST database

Table S8.4. continued.

No	VOC	Formula	Rate constant (10^{-12} cm^3 $molecule^{-1}$ s^{-1})	Reference
98	Methoxyacetonitrile or acrylamide	C_3H_5NO	0.02	From acetonitrile (Gilman et al., 2015)
99	Butene amines, tetrahydropyrole	C_4H_9N	25.0	* From butenes, ammonia see (Koss et al., 2018)
100	Methylglyoxal, acrylic acid	$C_3H_4O_2$	21.0962	Methylglyoxal (Atkinson and Arey, 2003), Acrylic acid (Gilman et al., 2015)
101	MEK	C_4H_8OH	5.46	(Atkinson and Arey, 2003) weighted average
102	Formamide N,N-dimethyl- or propanamide 2, ethyl or acetamide, N-methyl	C_3H_7NO	1.41	NIST Database
103	Hydroxyacetone, methyl acetate, ethyl formate	$C_3H_6O_2$	2.19763	NIST Database hydroxyacetone
104	Benzene	C_6H_6	1.22	(Atkinson and Arey, 2003)
105	Pyridine, C_5 nitriles	C_5H_5N	5.64607	NIST Database pyridine; *from pentane nitriles, pentyne nitrile
106	2,4-Cyclopentadiene-1-one, other hydrocarbon	C_5H_4O	19.9929	2-Methylfuran (Gilman et al., 2015)
107	Methyl cyclopentadiene	C_6H_8	91.0	Estimated as cyclopentadiene (Gilman et al., 2015)

Table S8.4. continued.

No	VOC	Formula	Rate constant (10^{-12} cm^3 $molecule^{-1}$ s^{-1})	Reference
108	Methylpyrole, pentanenitriles	C_5H_7N	62.6792	(Gilman et al., 2015)
109	Methylfurans, other hydrocarbon	C_5H_6O	37.0887	Cyclopentenone (Gilman et al., 2015)
110	Hexenol fragment or cyclohexene or hexenes or 1,3-hexadiene	C_6H_{10}	67.4	NIST database for cyclohexene
111	Pentane nitriles	C_5H_9N	0.5	* From butane nitriles
112	2-(3H)-Furanone	$C_4H_4O_2$	44.5	(Gilman et al., 2015)
113	3-Methyl-3-butene-2-one, cyclopentanone, other hydrocarbon	C_5H_8O	11.5	(Atkinson and Arey, 2003), NIST Database
114	1-Hexene, C_6-alkenes	C_6H_{12}	37.0	(Atkinson and Arey, 2003)
115	2,3-Butnaedione, methyl butanals, pentanones	$C_4H_6O_2$	0.8	(Gilman et al., 2015), NIST Database
116	Propanamide 2-methyl- or butanamide or acetamide N-ethyl-	C_4H_9NO	1.78	Estimated as propanamide, NIST database.
117	Pyruvic acid	$C_3H_4O_3$	0.1	(Gilman et al., 2015)
118	Methyl propanoate	$C_4H_8O_2$	0.9	NIST Database
119	Methyl pyridines	C_6H_7N	2.6	NIST Database methylpyridines average

Table S8.4. continued.

No	VOC	Formula	Rate constant (10^{-12} cm^3 $molecule^{-1}$ s^{-1})	Reference
120	Phenol	C_6H_5OH	28.0	(Gilman et al., 2015)
121	Pyrydinamine, methyl diazina	$C_5H_6N_2$	10	Average of 3 isomers, (Gilman et al., 2015)
122	C_2 substituted pyrroles	C_5H_7N	145	* From pyyrole (Koss et al., 2018)
123	Furfurals, other hydrocarbons	$C_5H_4O_2$	35.6	(Gilman et al., 2015)
124	C_2 substituted furans	C_6H_8O	132.0	2,5-Dimethylfuran (Gilman et al., 2015)
125	Cyclopentene dimethyl-1, methylcyclohexene	C_6H_{10}	67.4	NIST - considered same as cyclohexene
126	4-methylpentanenitrile	$C_6H_{11}N$	11.0	* From hexane (Koss et al., 2018)
127	2-Methanol furanone	$C_5H_6O_2$	13.6	* From furan
128	Methylcyclopentanone, cyclohexanone, hexanones	$C_6H_{10}O$	6.4	(Atkinson and Arey, 2003) cyclohexanone
129	Dihydrofuranodione	$C_4H_4O_3$	20.0	* From butadione, furan
130	Methyl methacrylate, other hydrocarbon	$C_5H_8O_2$	30.3	(Gilman et al., 2015)
131	Hexanals, hexanones	$C_6H_{12}O$	18.6	(Atkinson and Arey, 2003) average C_6 carbonyls
132	Acetic anhydride	$C_4H_6O_3$	43.0	* From methylmethacrylate
133	Benzonitrile	C_7H_5N	1.0	(Gilman et al., 2015)

Table S8.4. continued.

No	VOC	Formula	Rate constant (10^{-12} cm^3 $molecule^{-1}$ s^{-1})	Reference
134	Styrene	C_8H_8	58.0	(Atkinson and Arey, 2003)
135	Benzaldehyde	C_7H_6O	12.0	(Atkinson and Arey, 2003)
136	Dimethyl + ethyl pyridine, heptyl nitriles	C_7H_9N	3.2	NIST Database
137	Quinone	$C_6H_4O_2$	4.6	NIST Database
138	Cresol, anisole	C_7H_8O	26.2	NIST Database
139	Methyl furfural, benzene diols, 2-acetyl furan	$C_6H_6O_2$	80.1	NIST Database; *from furfural
140	C_3 Substituted furans, other compounds	$C_7H_{10}O$	23.3	* From furan
141	5-Hydroxy 2-furfural, 2-furanoic acid	$C_5H_4O_3$	49.0	* From 3-furfural
142	2-Hydroxy-3-methyl-2-cclopenten-1-one	$C_6H_8O_2$	57.0	* From methylfuran
143	Nitrofuran	$C_4H_3NO_3$	40.0	* From furan
144	5-Hydroxymethyl-2[3H]-furanone	$C_5H_6O_3$	100.0	* From furan, furanone
145	C_6 diketone isomers, C_6 esters	$C_6H_{10}O_2$	20.0	NIST Database average
146	Heptanal, 2,4-dimethyl-3-pentanone, heptanone	$C_7H_{14}O$	21.4	(Atkinson and Arey, 2003)

Table S8.4. continued.

No	VOC	Formula	Rate constant (10^{-12} cm^3 $molecule^{-1}$ s^{-1})	Reference
147	5-Hydroxymethyl tetrahydro 2-furanone, 5-hydroxy tetrahydro 2-furfural	$C_5H_8O_3$	5.0	* From dimethylfuran, cyclopentane, cyclopentadiene
148	Benzene acetonitrile	C_8H_7N	1.2	* From benzene
149	Benzofuran	C_8H_6O	37.0	NIST Database
150	Methyl styrene, propenyl benzene + methyl ethynyl benzene, indane	C_9H_{10}	50.4	(Atkinson and Arey, 2003)
151	Tolualdehyde	C_8H_8O	16.0	Atkinson 2003 average tolualdehydes
152	Salicylaldehyde	$C_7H_6O_2$	38.0	* From phenol, benzaldehyde
153	Ethylphenol + dimethyl phenol, methyl anidiol	$C_8H_{10}O$	46.6	NIST Database C_2 phenols, *anisol
154	Hydroxybenzoquinone	$C_6H_4O_3$	4.6	* From benzoquinone
155	Guaiacol	$C_7H_8O_2$	75.0	NIST Database
156	5-Hydroxymethyl 2-furfural	$C_6H_6O_3$	100.0	* From furfural, dimethylfuran
157	Naphthalene	$C_6H_8O_3$	132.0	* From dimethylfuran
158	Methyl benzene acetonitrile	C_9H_9N	5.6	* From toluene
159	Methylbenzofurans	C_9H_8O	37.0	(Gilman et al., 2015)
160	Methylacetephenone	$C_9H_{10}O$	4.5	NIST Database

Table S8.4. continued.

No	VOC	Formula	Rate constant (10^{-12} cm^3 $molecule^{-1}$ s^{-1})	Reference
161	C_{10} aromatics	$C_{10}H_{14}$	9.5	Atkinson 2003 average C_{10} aromatics
162	Methylbenzoic aicd	$C_8H_8O_2$	12.0	* From benzaldehyde
163	Methylguiacol	$C_8H_{10}O_2$	100.0	NIST Database
164	3-Methylcatechol	$C_7H_8O_3$	5	Estimated as same as benzene diols (Gilman et al., 2015)
165	Methylnaphthalene	$C_{11}H_{10}$	50.0	NIST Database
166	Levoglucosan pyrolysis product	$C_6H_8O_4$	4.6	* From benzoquinone
167	Dimethyl benzo furan, ethyl benzo furan	$C_{10}H_{10}O$	37.0	* From benzofuran
168	Estragole	$C_{10}H_{12}O$	50.0	NIST Database: 1-methoxy-4-(2-propenyl) benzene
169	C_{11} aromatics	$C_{11}H_{16}$	50.0	* From C_{10}, C_{12} aromatics
170	Vinyl guaiacol	$C_9H_{10}O_2$	100.0	* From methylguaiacol
171	Vanilin	C_8H8_{O3}	85.0	* From guaiacol, benzaldehyde
172	Syringol	$C_8H_{10}O_3$	100.0	* From methylguaiacol
173	Dimethylnaphthalene	$C_{12}H_{12}$	60.0	NIST Database
174	C_{12} aromatics	$C_{12}H_{18}$	113.0	Hexamethylbenzene (Atkinson and Arey, 2003)
175	Eugenol, isoeugenol	$C_{10}H_{12}O_2$	100.0	* From methylguaiacol

[a] Not included in final calculation due to sensitivity being too different from the NMVOCs used to build the transmission curve but included in table to show that low rate constant likely has little influence on OH reactivity.

8.15. Toxicity equivalence factors

Table S8.5. TEF values used for individual PAHs in calculation of fuel toxicity.

Compound	TEF	Ref
Naphthalene	0.001	(Nisbet and LaGoy, 1992)
Methylnaphthalene	0.001	(Nisbet and LaGoy, 1992)
Dimethylnapthalene	0.001	*
Biphenyl	0.001	*
9-Fluorenone	0.001	*
Acenaphthylene	0.001	(Nisbet and LaGoy, 1992)
Acenapthene	0.001	(Nisbet and LaGoy, 1992)
Dibenzofuran	0.001	
Fluorene	0.0005	(Larsen and Larsen, 1998)
Phenanthrene	0.0005	(Larsen and Larsen, 1998)
Anthracene	0.0005	(Larsen and Larsen, 1998)
Carbazole	0.001	*
Fluoranthene	0.05	(Larsen and Larsen, 1998)
Pyrene	0.001	(Larsen and Larsen, 1998)
Benzo[a]anthracene	0.082	(Larsen and Larsen, 1998)
Chrysene	0.017	(Larsen and Larsen, 1998)
Benzo[b]fluoranthene	0.25	(Larsen and Larsen, 1998)
Benzo[k]fluoranthene	0.11	(Larsen and Larsen, 1998)
Benzo[a]pyrene	1	(Larsen and Larsen, 1998)
Indeno[1,2,3-cd]pyrene	0.1	(Larsen and Larsen, 1998)
Dibenzo[a,h]anthracene	1.1	(Larsen and Larsen, 1998)
Benzo[g,h,i]perylene	0.02	(Larsen and Larsen, 1998)

* = lower limit value used equivalent to TEF for naphthalene as TEF values for these PAHs not found in literature.

8.16. Estimate of fuel use in India

Fuel use was estimated in India over a 24-year period by compiling the state wise number of users per 1000 in rural and urban environments for wood, dung, coke, charcoal, LPG, gobar gas, electricity and other fuel types and multiplying these by the rural and urban populations for the respective states. The variation in 2006 was likely driven by the difficulties in conducting a representative sample of fuel use of over 1 billion people and is assumed to not be a significant change in fuel use. The input was compiled from a range of sources and processed in R.

- The National Family Health Survey for 1992-1993, 1998-1999, 2005-2006 and 2015-2016 (International Institute for Population Sciences, 1995, 2000, 2007, 2017).
- Energy Sources of Indian Households for Cooking and Lighting 1993-1994, 2004-2005, 2009-2010 and 2011-2012 (NSSO, 1997, 2007a, 2012a, 2015a).
- Household Consumption of Goods and Services in India for 2004-2005, 2009-2010 and 2011-2012 (NSSO, 2007b, 2012b, 2014).
- Household Consumer Expenditure and Employment - Unemployment Situation in India for 2002 and 2006-2007 (NSSO, 2003, 2005, 2008).

8.17. Mean crop residue combustion total NMVOC emission factor

The total crop burning NMVOC emission factor was calculated as the sum of mean species measured from crop residues using OP-FTIR, the PTR-ToF-MS (n = 19) and the mean PTR-ToF-MS extended range analysis (n = 6) including unidentified peaks (Stockwell et al., 2015). Ketene fragments were removed and assumed to be an artifact of measurement by PTR-ToF-MS, and not formed from the fire. This approach was used as it was consistent with that in chapter 4.

Table S8.6. Calculation of total mean crop residue emission factor using masses from the Supplementary Table S3 in Stockwell et al. (2015).

m/z	Molecular formula	Identity	Mean / g kg^{-1}
	C_2H_2	Acetylene	0.331
	C2H4	Ethene	1.34
31.01784	HCHO	Formaldehyde	1.93
33.03349	CH_3OH	Methanol	1.87
43.05423	C_3H_6	Propene	0.576
47.01276	HCOOH	Formic acid	0.633
61.02841	CH_3COOH	Acetic Acid	3.88
	C_2H4O_2	Glycolaldehyde	2.29
69.03349	C_4H_4O	Furan	0.355
PTR-ToF-MS			
41.03858	C_3H_4	Propyne	0.34
42.03383	C_2H_3N	Acetonitirile	0.225
45.03349	C_2H_4O	Acetaldehyde	2.68
51.02293	C_4H_2	1,3-Butadiyne	0.00363
53.03858	C_4H_4	Butenyne	0.0559
55.01784	C_3H_2O	2-Propynal	0.0422
55.05423	C_4H_6	1,3-Butadiene	0.191
57.03349	C_3H_4O	Acrolein	0.875
57.06988	C_4H_8	1-Butene	0.134
59.04914	C_3H_6O	Acetone	0.884
67.05423	C_5H_6	1,3-Cyclopentadiene	0.0829
68.99711	C_3O_2	Carbon suboxide	0.00464
69.06988	C_5H_8	Isoprene	0.22
71.04914	C_4H_6O	Methyl Vinyl Ketone, Crotonaldehyde, Methacrolein (~50, 30, 20%)	0.607
73.02841	C_3H_4O2	Methylglyoxal	0.554
73.06479	C_4H_8O	Methyl Ethyl Ketone	0.29

Table S8.6. continued.

m/z	Molecular formula	Identity	Mean / g kg^{-1}
75.04406	$C_3H_6O_2$	Hydroxyacetone	1.69
79.05423	C_6H_6	Benzene	0.301
81.03349	C_5H_4O	2,4-Cyclopentadiene-1-one	0.303
83.04914	C_5H_6O	2-Methylfuran	0.532
83.08553	C_6H_{10}	Assorted HCs	0.0357
85.02841	$C_4H_4O_2$	2-Furanone	0.82
85.06479	C_5H_8O	Pentenone	0.186
87.04406	$C_4H_6O_2$	2,3-Butanedione	1.15
89.05971	$C_4H_8O_2$	Ethyl acetate	0.233
91.05423	C_7H_6	Unknown	0.0328
93.06988	C_7H_8	Toluene	0.296
95.04914	C_6H_6O	Phenol	0.494
97.02841	$C_5H_4O_2$	2-Furaldehyde (furfural)	1.03
99.04406	$C_5H_6O_2$	2-Furan Methanol (furfuryl alcohol)	1.02
101.0597	$C_5H_8O_2$	Unknown	0.295
103.0542	C_8H_6	Ethynyl Benzene (phenylacetylene)	0.254
105.0699	C_8H_8	Styrene	0.0563
107.0491	C_7H_6O	Benzaldehyde	0.0702
107.0855	C_8H_{10}	Xylenes/ethylbenzene	0.107
109.0284	$C_6H_4O_2$	Unknown	0.0698
111.0441	$C_6H_6O_2$	Catechol (Benzenediols); Methylfurfural	0.548
111.0804	$C_7H_{10}O$	Unknown	0.177
113.0233	$C_5H_4O_3$	Unknown	0.166
113.0597	$C_6H_8O_2$	2-Hydroxy-3-Methyl-2-Cyclopentenone	0.557
115.039	$C_5H_6O_3$	Unknown	0.041739
117.0699	C_9H_8	Unknown	0.014039
119.0491	C_8H_6O	Benzofuran	0.0435
119.0855	C_9H_{10}	Assorted HCs	0.0309
121.0648	C_8H_8O	Vinylphenol	0.574
121.1012	C_9H_{12}	Trimethylbenzene; Assorted HCs	0.0658
123.0441	$C_7H_6O_2$	Salicylaldehyde	0.106
123.0804	$C_8H_{10}O$	Xylenol (2,5-Dimethyl phenol)	0.275
125.0597	$C_7H_8O_2$	Guaiacol (2-Methoxyphenol)	0.578
127.039	$C_6H_6O_3$	Hydroxymethylfurfural	0.296
129.0699	$C_{10}H_8$	Naphthalene	0.164
131.0855	$C_{10}H_{10}$	Assorted HCs inc. Dihydronaphthalene	0.0401
137.1325	$C_{10}H_{16}$	Terpenes (α-Pinene)	0.0635

Table S8.6. continued.

m/z	Molecular formula	Identity	Mean / g kg^{-1}
143.0855	$C_{11}H_{10}$	Methyl-Naphthalenes	0.088
	PTR-ToF-MS Extended Analysis		
46.06513	C_2H_7N	Dimethylamine; Ethylamine	0.0844
60.04439	C_2H_5NO	Acetamide	
60.08078	C_3H_9N	Trimethylamine	0.0785
65.03858	C_5H_4	1,3-Pentadiyne	0.0129
71.08553	C_5H_{10}	Assorted HCs	0.0327
85.10118	C_6H_{12}	Assorted HCs	0.013
87.08044	$C_5H_{10}O$	Pentanone	
88.07569	C_4H_9NO	Assorted Amides	0.116
89.02332	$C_3H_4O_3$	Unknown	0.0157
90.09134	$C_4H_{11}NO$	Assorted Amines6	0.0394
93.03349	C_6H_4O	Unknown	0.0085
95.08553	C_7H_{10}	Unknown	0.741
97.06479	C_6H_8O	2,5-Dimethylfuran	0.0981
97.10118	C_7H_{12}	Assorted HCs	0.842
99.08044	$C_6H_{10}O$	Unknown	
101.0233	C_4H_4O3	Unknown	0.168
103.039	$C_4H_6O_3$	Methyl pyruvate	0.0708
103.0754	$C_5H_{10}O_2$	Unknown	0.0216
104.0495	C_7H_5N	Benzonitrile	
109.0648	C_7H_8O	Cresols (Methylphenols)	0.249
109.1012	C_8H_{12}	Unknown	
111.1168	C_8H_{14}	Unknown	0.00795
115.0754	$C_6H_{10}O_2$	Unknown	0.005923
117.0546	$C_5H_8O_3$	Unknown	0.011305
117.091	$C_6H_{12}O_2$	Unknown	
123.1168	C_9H_{14}	Unknown	0.0181
125.0233	$C_6H_4O_3$	Unknown	0.186
127.0754	$C_7H_{10}O_2$	Unknown	0.005792
133.0648	C_9H_8O	Assorted HCs inc. Methylbenzofurans	
135.0441	$C_8H_6O_2$	Unknown	0.0418
135.0804	$C_9H_{10}O$	Unknown	0.0521
135.1168	$C_{10}H_{14}$	*p*-Cymene	0.0172
137.0597	$C_8H_8O_2$	Unknown	0.159
137.0961	$C_9H_{12}O$	Unknown	
139.039	$C_7H_6O_3$	Unknown	0.113
139.0754	$C_8H_{10}O_2$	Creosol (4-Methylguaiacol)	0.138
141.0546	$C_7H_8O_3$	3-Methoxycatechol (3-Methoxy-1,2-Benzenediol)	0.573
141.091	$C_8H_{12}O_2$	Unknown	0.38

Table S8.6. continued.

m/z	Molecular formula	Identity	Mean / g kg^{-1}
145.0648	$C_{10}H_8O$	Unknown	0.131
145.1012	$C_{11}H_{13}$	Unknown	0.00808
147.0804	$C_{10}H_{10}O$	Unknown	0.0642
147.1168	$C_{11}H_{14}$	Unknown	
149.0597	$C_9H_8O_2$	Unknown	0.706
149.0961	$C_{10}H_{12}O$	Unknown	
149.1325	$C_{11}H_{16}$	Unknown	
151.0754	$C_9H_{10}O_2$	4-Vinylguaiacol (2-Methoxy-6-Vinylphenol)	0.306
151.1481	$C_{11}H_{18}$	Unknown	
155.0703	$C_8H_{10}O_3$	Syringol	0.121
165.091	$C_{10}H_{12}O_2$	Eugenol/ Isoeugenol	
Sum			**38.84**

8.18. Identification of rural and urban areas within the model

Table S8.7. Reproduction of rural and urban populations within model for 2011.

State	% Rural	% Urban	Rural model/real	Urban model/real
Andaman and Nicobar	62.3	37.7	1.00	1.00
Andhra Pradesh	66.6	33.4	1.00	1.00
Arunachal Pradesh	77.1	22.9	1.00	0.99
Assam	85.9	14.1	1.00	1.00
Bihar	88.7	11.3	1.00	1.00
Chandigarh	2.8	97.3	1.04	1.00
Chhattisgarh	76.8	23.2	1.00	1.00
Dadra and Nagar Haveli	53.3	46.7	1.00	1.00
Daman and Diu	24.8	75.2	1.01	1.00
Delhi	2.5	97.5	1.02	1.00
Goa	37.8	62.2	1.00	1.00
Gujarat	57.4	42.6	1.00	1.00
Haryana	65.1	34.9	1.00	1.00
Himachal Pradesh	90.0	10.0	1.00	1.00
Jammu and Kashmir	72.6	27.4	1.00	1.00
Jharkhand	76.0	24.1	1.00	1.00
Karnataka	61.3	38.7	1.00	1.00
Kerala	52.3	47.7	1.00	1.00
Lakshadweep	21.9	78.1	1.01	1.00
Madhya Pradesh	72.4	27.6	1.00	1.00
Maharashtra	54.8	45.2	1.00	1.00
Manipur	67.6	32.5	1.00	1.00
Meghalaya	79.9	20.1	1.00	1.00
Mizoram	47.9	52.1	1.00	1.00
Nagaland	71.1	28.9	1.00	0.99
Orissa	83.3	16.7	1.00	0.99
Puducherry	31.7	68.3	1.00	1.00
Punjab	62.5	37.5	1.00	1.00
Rajasthan	75.1	24.9	1.00	1.00
Sikkim	74.9	25.2	1.00	1.00
Tamil Nadu	51.6	48.4	1.00	1.00
Telangana	66.6	33.4	1.00	1.00
Tripura	73.8	26.2	1.00	1.00
Uttar Pradesh	77.7	22.3	1.00	1.00
Uttaranchal	69.8	30.2	1.00	1.00
West Bengal	68.1	31.9	1.00	1.00

8.19. Mean weighted urban per capita MSW generation

Table S8.8. Population weighted average urban MSW generation from Indian states, created from data taken from Annepu et al. (2012).

State	Per capita generation (kg day^{-1})
Andhra Pradesh	0.57
Assam	0.28
Bihar	0.41
Chandigarh	0.46
Chhattisgarh	0.48
Delhi	0.65
Gujarat	0.40
Haryana	0.46
Himachal Pradesh	0.31
Jammu and Kashmir	0.59
Jharkhand	0.37
Karnataka	0.49
Kerala	0.51
Madhya Pradesh	0.40
Maharashtra	0.46
Manipur	0.22
Meghalaya	0.39
Mizoram	0.29
Orissa	0.40
Puducherry	0.67
Punjab	0.49
Rajasthan	0.52
Tamil Nadu	0.60
Tripura	0.46
Uttar Pradesh	0.47
Uttaranchal	0.39
West Bengal	0.56
Arunachal Pradesh	0.28
Sikkim	0.28
Nagaland	0.28
Daman and Diu	0.46
Dadra and Nagar Haveli	0.46
Telangana	0.57
Goa	0.46
Andaman and Nicobar	0.44
Lakshadweep	0.44

Note: All rural environments treated as WorldBank lower limit of 0.12 kg capita^{-1} day^{-1}.

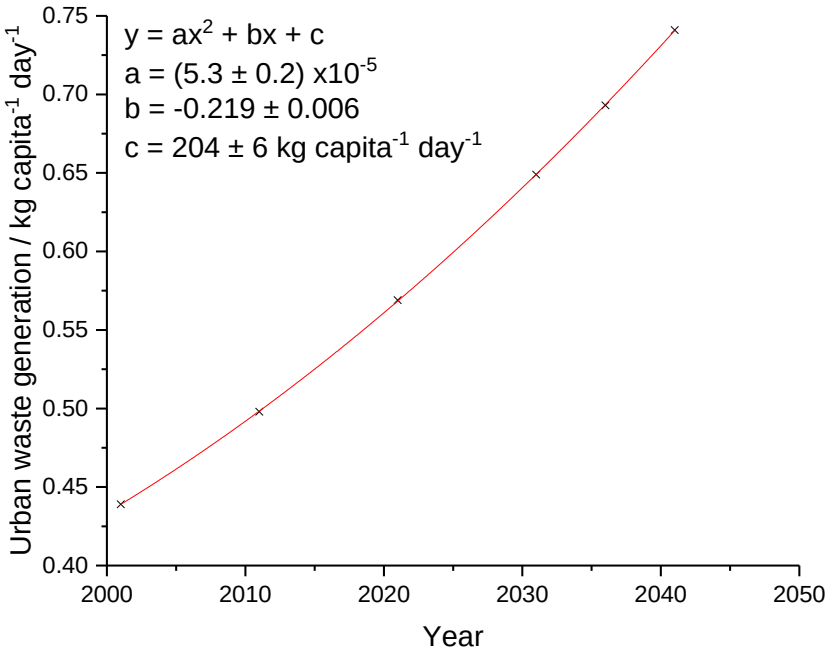

Figure S8.23. Estimated change in urban per capita waste generation in India, data from Annepu et al. (2012).

8.20. Inputs to crop residue NMVOC emission estimate

Table S8.9. Inputs used for estimation of NMVOC emissions from crop residue burning in 2011 in India.

	Cereals						Oilseeds				Fibres		Sugarcane
	Rice	Wheat	Cereals	Maize	Jowar	Bajra	9 oilseeds	Groundnut	Rapeseed and mustard	Sunflower	Cotton	Jute and mesta	Sugarcane
Residue to crop ratio	1.5	1.7	1.5	1.5	1.5	1.5	2.5	2	3	2.5	3	2.15	0.4
Dry matter fraction	0.86	0.88	0.88	0.88	0.88	0.88	0.8	0.8	0.8	0.8	0.8	0.8	0.88
Fraction burnt	0.08	0.1	0.1	0.1	0.1	0.1	0.1	0.1	0.1	0.1	0.1	0.1	0.25
Mean EF / g kg^{-1}	23.8	15.9	15.9	15.9	5.4	5.4	38.9	38.9	38.9	38.9	38.9	38.9	53.6
High EF/g kg^{-1}	57.3	23.5	23.5	23.5	5.9	5.9	69.3	69.3	69.3	69.3	69.3	69.3	69.3
Low EF/g kg^{-1}	7.6	4.9	4.9	4.9	4.2	4.2	4.2	4.2	4.2	4.2	4.2	4.2	36.5

State wise crop production / millions of tonnes

	Cereals						Oilseeds				Fibres		Sugarcane
Andaman and Nicobar													
Andhra Pradesh	14.42		4.44	3.96	0.31	0.1	2	1.46		0.16	5.3	0.22	14.96
Arunachal Pradesh													
Assam	4.74	0.05					0.15		0.14			0.65	1.08
Bihar	3.1	4.1	1.48	1.44			0.14		0.09	0.02		1.31	12.76
Chandigarh													
Chhattisgarh	6.16		0.23										

Table S8.9. continued.

State wise crop production / millions of tonnes

	Cereals						Oilseeds				Fibres		Sugarcane
Dadra and Nagar Haveli													
Daman + Diu													
Delhi													
Goa													
Gujarat	1.5	4.02	2.1	0.82	0.14	1.09	4.9	3.37	0.35		10.4		13.76
Haryana	3.47	11.63	1.37		0.04	1.19	0.96		0.94	0.02	1.75		6.04
Himachal Pradesh		0.55	0.7	0.67									
Jammu and Kashmir		0.45	0.55	0.53		0.01							
Jharkhand	1.11	0.16	0.28	0.26									
Karnataka	4.19	0.28	7.89	4.44	1.47	0.33	1.27	0.74		0.25	1.2		39.66
Kerala	0.52												
Lakshadweep													
Madhya Pradesh	1.77	7.63	2.17	1.05	0.62	0.31	8.04	0.3	0.86		2		2.67
Maharashtra	2.7	2.3	7.32	2.6	3.45	1.12	5.04	0.46		0.13	8.5	0.03	81.9
Manipur													
Meghalaya												0.05	
Mizoram													
Nagaland													
Orissa	6.83		0.36		0.01		0.18	0.09				0.11	0.9
Puducherry													

Table S8.9. continued.

State wise crop production / millions of tonnes													
	Cereals						Oilseeds				Fibres		Sugarcane
Punjab	10.84	16.47	0.54	0.49			0.7		0.04		2.1		4.17
Rajasthan		7.21	8.09	2.05	0.51	4.57	6.6	0.68	4.37		0.9		
Sikkim													
Tamil Nadu	5.79		1.56	1.03	0.25	0.08	0.93	0.9		0.01	0.45		34.25
Telangana													
Tripura													
Uttar Pradesh	11.99	30	3.22	1.11	0.21	1.56	0.92	0.08	0.72	0.01			120.55
Uttaranchal		0.88	0.34										6.5
West Bengal	13.05	0.87	0.37	0.35			0.7		0.42			8.21	1.13
Others	3.8	0.27	0.72	0.93	0.02	0.01	0.58	0.18	0.25	0.05	0.4	0.04	2.05
Total emission / kt													
Mean	235.8	206.6	91.8	45.6	5.0	7.3	257.2	51.3	76.3	5.0	307.6	70.9	1613.4
Low	74.9	64.2	28.5	14.2	3.9	5.7	27.8	5.6	8.2	0.5	33.3	7.7	1100.6
High	567.4	305.0	135.5	67.3	5.4	8.0	458.6	91.5	136.0	9.0	548.5	126.5	2086.8

8.21. Emission model inputs

Table S8.10 summaries fuel use statistics which have been collected and used to estimate emissions based on the emissions factors collated in this study.

Table S8.10. Summary of emission model inputs for 2011.

Abbreviation	Name	Value used	Ref
$Population_{1km2}$	Population per $1km^2$	-	(WorldPop, 2017)
% Rural	% Rural population in state	2.5-90.0%	(Government of India, 2014)
% Urban	% Urban population in state	10-97.5%	(Government of India, 2014)
EF_{wood}	Mean wood emission factor from this study	18.4 g kg^{-1}	This study
Wood consumption	Wood consumption = per capita wood consumption (kg $capita^{-1}$ 30 $days^{-1}$)	Rural 0.031-57.01 kg $capita^{-1}$ 30 $days^{-1}$ Urban 0.166-20.598 kg $capita^{-1}$ 30 $days^{-1}$	(NSSO, 2014)
Wood users	Number of wood users per 1000 people	Rural 3-932 Urban 3-365	(NSSO, 2015b)
Number of users	Number of users of a fuel type per 1000	-	-
EF_{LPG}	Mean LPG emission factor from this study	5.8 g kg^{-1}	This study
LPG consumption	LPG consumption = per capita LPG consumption (kg $capita^{-1}$ 30 $days^{-1}$)	Rural 0.046-2.492 kg $capita^{-1}$ 30 $days^{-1}$ Urban 0.937 – 3.056 kg $capita^{-1}$ 30 $days^{-1}$	(NSSO, 2014)
EF_{char}	Mean charcoal emission factor from this study	5.1 g kg^{-1}	This study
Char consumption	Charcoal consumption = per capita LPG consumption (kg $capita^{-1}$ 30 $days^{-1}$	Rural 0-0.576 kg $capita^{-1}$ 30 $days^{-1}$ Urban 0-0.716 kg $capita^{-1}$ 30 $days^{-1}$	(NSSO, 2014)
EF_{coal}	Mean coal emission factor	3.7 g kg^{-1}	(Cai et al., 2019)
Coal consumption	Per capita coal consumption (kg $capita^{-1}$ 30 $days^{-1}$)	Rural 0-0.513 kg $capita^{-1}$ 30 $days^{-1}$ Urban 0-0.917 kg $capita^{-1}$ 30 $days^{-1}$	(NSSO, 2014)
$Dung_{users}$	Number of dung users per 1000 people	Rural 0-334 per 1000 Urban 0 – 75 per 1000	(NSSO, 2015b)

Table S8.10. continued.

Abbreviation	Name	Value used	Ref
W_{res}	Waste burnt residentially	22421 kt	This study
MSW_{pr}	Per capita rural waste generation	0.12 kg capita^{-1} day^{-1}	(World Bank, 2012)
$B_{frac,res}$	Fraction of waste burnt residentially	0.6	(IPCC, 2006)
MSW_{pu}	Per capita urban waste generation	0.194-0.867	(Annepu et al., 2012)
$f_{uncollected}$	Fraction of waste which was not collected	3-58%	(CPCB, 2013)
W_{Bdump}	Landfill waste burnt	13252 kt	This study
$f_{collected}$	Fraction of urban waste collected	42-97%	(CPCB, 2013)
$B_{frac,dump}$	Fraction of urban waste burnt in landfill sites	10%	(NEERI, 2010)
$Crop_{emission}$	VOC emitted in a state from crop residue burning	-	This study
CWG	Mass of crop produced in state	8.29-342.38 Mt	(Jain et al., 2014)
RTCR	Residue to crop ratio	0.4-3.00	(Jain et al., 2014)
DMF	Dry matter fraction	0.80-0.88	(Jain et al., 2014)
FB	Fraction of crop residue burnt	0.08-0.25	(Jain et al., 2014)
$EF_{crop,i}$	Emissions factor for crop species *i*	5.6-57.5 g kg^{-1}	(Stockwell et al., 2015; Koss et al., 2018)
Area cultivated	Total agricultural area identified in a state from MODIS (km^2)	-	(NASA, 2011)
Wheat straw EF [a]		16.8 (5.2-25.0) g kg^{-1}	(Stockwell et al., 2015)
Sugarcane EF [b]		57.5 (39.35-74.33) g kg^{-1}	(Stockwell et al., 2015)
Rice straw EF		25.0 (7.8-60.1) g kg^{-1}	(Stockwell et al., 2015)
Millet EF		5.6 (4.4-6.2) g kg^{-1}	(Stockwell et al., 2015)
Crop average EF [c]		38.8 (4.3-74.3) g kg^{-1}	(Stockwell et al., 2015)

[a] Applied to coarse cereals, maize and jowar.
[b] Note slight difference in calculation (<1 g kg^{-1}) of mean from high/low measurements and mean reported in Stockwell et al. (2015).
[c] Applied to all oilseeds and fibres.

8.22. 2011 State wise NMVOC emission estimate by source

Table S8.11. State wise NMVOC emission estimates (kt) by source in 2011.

State	Wood	Dung	LPG	Coal	Charcoal	Waste	Crop
Andaman and Nicobar	1.4	0.0	0.0	0.0	0.0	0.9	0
Andhra Pradesh	153.8	2.2	3.7	0.1	0.0	112.0	200.6
Arunachal Pradesh	12.6	0.1	0.1	0.0	0.0	3.1	0
Assam	187.7	0.2	1.5	0.1	0.0	71.0	23.7
Bihar	219.3	420.1	2.3	0.7	0.0	225.0	94.5
Chandigarh	0.2	0.0	0.2	0.0	0.0	1.5	0
Chhattisgarh	117.8	24.1	0.5	0.4	0.0	56.3	15.6
Dadra & Nagar Haveli	1.3	0.0	0.0	0.0	0.0	0.6	0
Daman and Diu	0.2	0.0	0.0	0.0	0.0	0.4	0
Delhi	0.7	0.0	3.0	0.0	0.0	42.4	0
Goa	1.3	0.0	0.3	0.0	0.0	4.8	0
Gujarat	183.3	11.8	3.7	0.1	0.0	121.3	244.3
Haryana	46.8	144.2	2.4	0.0	0.0	55.0	101.1
Himachal Pradesh	50.8	0.7	0.5	0.0	0.0	15.1	4.2
Jammu and Kashmir	64.7	10.6	1.0	0.0	0.4	35.0	3.3
Jharkhand	121.2	25.2	1.1	0.2	0.0	89.1	4.2
Karnataka	274.0	0.0	3.9	0.0	0.0	248.6	252.6
Kerala	203.5	0.0	3.2	0.1	0.0	168.0	1.27
Lakshadweep	0.3	0.0	0.0	0.0	0.0	0.1	0
Madhya Pradesh	217.3	143.1	2.9	0.2	0.0	195.1	133.5
Maharashtra	257.9	4.1	10.1	0.0	0.0	201.5	544.6
Manipur	8.7	0.1	0.2	0.0	0.1	5.0	0
Meghalaya	17.5	0.1	0.1	0.0	0.0	6.7	0.3
Mizoram	6.6	0.0	0.2	0.0	0.0	2.6	0
Nagaland	14.9	0.0	0.1	0.0	0.0	4.2	0
Orissa	263.4	26.9	1.0	0.1	0.1	96.1	24.5
Puducherry	1.2	0.0	0.2	0.0	0.0	3.0	0
Punjab	53.1	267.7	3.2	0.0	0.0	61.7	113.0
Rajasthan	355.0	13.1	3.1	0.1	0.0	170.0	146.6
Sikkim	1.4	0.0	0.1	0.0	0.0	1.3	0
Tamil Nadu	192.5	0.0	7.7	0.0	0.0	164.0	198.4
Telangana	106.8	10.1	2.6	0.1	0.0	77.7	0
Tripura	39.5	0.0	0.2	0.0	0.0	9.7	0
Uttar Pradesh	461.8	1404.1	6.9	0.2	0.0	442.0	693.7
Uttaranchal	63.6	1.2	0.9	0.0	0.0	21.2	33.4
West Bengal	601.4	251.0	4.8	2.3	0.0	342.3	105.2
Other	-	-	-	-	-	-	35.5
Mean [a]	4303.7	2760.7	71.4	4.8	0.9	3054.5	2973.9
Low	989.6	1280.7	23.8	1.7	0.4	1550.1	1375.1
High	22255.0	4399.3	122.7	5.9	1.3	6885.0	4545.6

[a] Slight difference between sum of values in table and mean due to rounding errors.

This study estimated NMVOC emissions of 13.2 (5.2-38.2) Tg from burning sources in India in 2011.

8.23. Coal emission

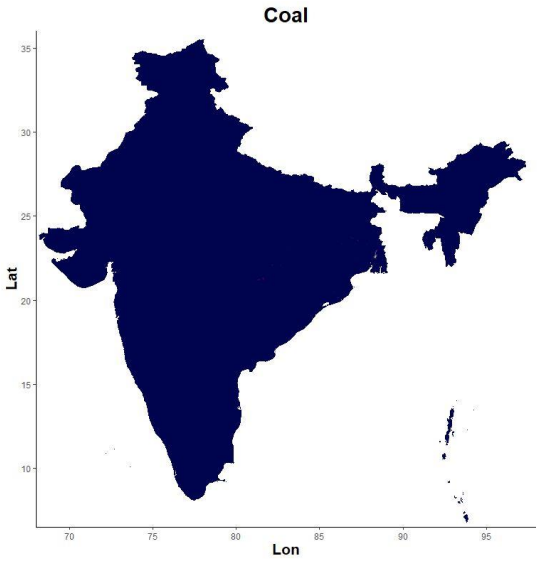

Figure S8.24. Estimated NMVOC emission from residential cooking coal combustion in India in 2011.

Table S8.12. Estimated NMVOC emission from residential coal combustion (kt yr^{-1}) from 1993-2016.

Year	Coal
1993	10.5
1994	10.2
1999	6.6
2002	4.8
2005	6.3
2006	4.1
2007	5.6
2010	5.4
2011	4.8
2016	4.1

8.24. LPG, coal and charcoal emission maps with different scale

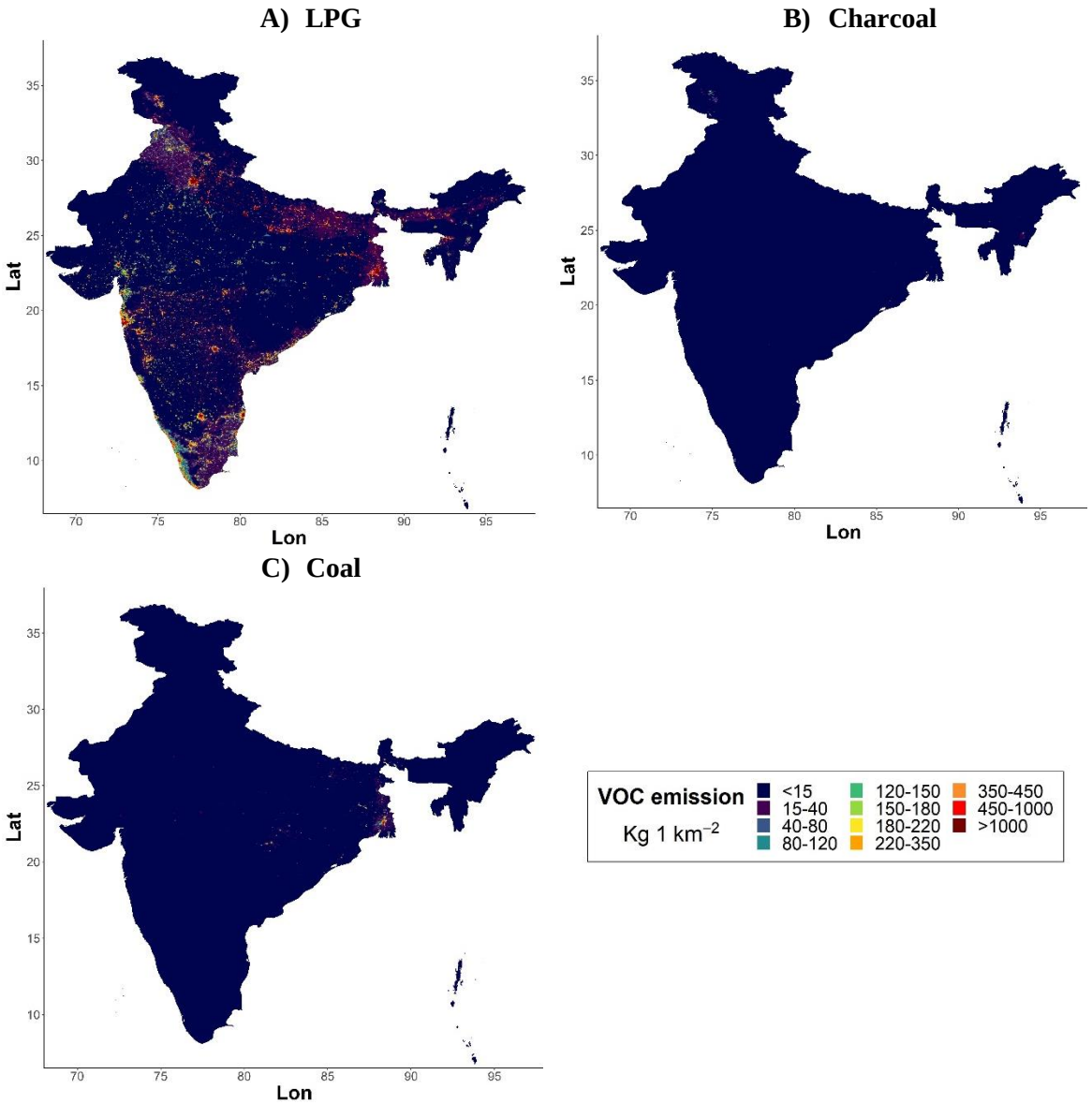

Figure S8.25. Spatial distribution and emission of NMVOCs in 2011 from A = LPG, B = Charcoal and C = Coal using a different scale to the main text. The declination of international borders on this map are proximate and must not be considered authoritative.

8.25. State wise PAH emission by source

Table S8.13. State wise emissions of PAHs (kt) from different fuel types in 2011.

State	Wood	Dung	LPG [a]	Charcoal [a]	Waste
Andaman and Nicobar	0.0	0.0	0.0	0.0	0.0
Andhra Pradesh	2.0	0.0	0.0	0.0	1.3
Arunachal Pradesh	0.2	0.0	0.0	0.0	0.0
Assam	2.5	0.0	0.0	0.0	0.8
Bihar	2.9	4.2	0.0	0.0	2.6
Chandigarh	0.0	0.0	0.0	0.0	0.0
Chhattisgarh	1.6	0.2	0.0	0.0	0.7
Dadra and Nagar Haveli	0.0	0.0	0.0	0.0	0.0
Daman and Diu	0.0	0.0	0.0	0.0	0.0
Delhi	0.0	0.0	0.0	0.0	0.5
Goa	0.0	0.0	0.0	0.0	0.1
Gujarat	2.4	0.1	0.0	0.0	1.4
Haryana	0.6	1.4	0.0	0.0	0.6
Himachal Pradesh	0.7	0.0	0.0	0.0	0.2
Jammu and Kashmir	0.9	0.1	0.0	0.0	0.4
Jharkhand	1.6	0.3	0.0	0.0	1.0
Karnataka	3.6	0.0	0.0	0.0	2.9
Kerala	2.7	0.0	0.0	0.0	2.0
Lakshadweep	0.0	0.0	0.0	0.0	0.0
Madhya Pradesh	2.9	1.4	0.0	0.0	2.3
Maharashtra	3.4	0.0	0.1	0.0	2.3
Manipur	0.1	0.0	0.0	0.0	0.1
Meghalaya	0.2	0.0	0.0	0.0	0.1
Mizoram	0.1	0.0	0.0	0.0	0.0
Nagaland	0.2	0.0	0.0	0.0	0.0
Orissa	3.5	0.3	0.0	0.0	1.1
Puducherry	0.0	0.0	0.0	0.0	0.0
Punjab	0.7	2.7	0.0	0.0	0.7
Rajasthan	4.7	0.1	0.0	0.0	2.0
Sikkim	0.0	0.0	0.0	0.0	0.0
Tamil Nadu	2.5	0.0	0.1	0.0	1.9
Telangana	1.4	0.1	0.0	0.0	0.9
Tripura	0.5	0.0	0.0	0.0	0.1
Uttar Pradesh	6.1	13.9	0.1	0.0	5.1
Uttaranchal	0.8	0.0	0.0	0.0	0.2
West Bengal	7.9	2.5	0.0	0.0	4.0
Mean	**56.8**	**27.4**	**0.7**	**0.0**	**35.5**
Low	**11.7**	**17.8**	**0.7**	**0.0**	**21.4**
High	**208.7**	**37.5**	**0.7**	**0.0**	**79.2**

[a] = only one sample of this fuel type.

8.26. EDGAR 5.0 and REAS 3.2 inventory comparison

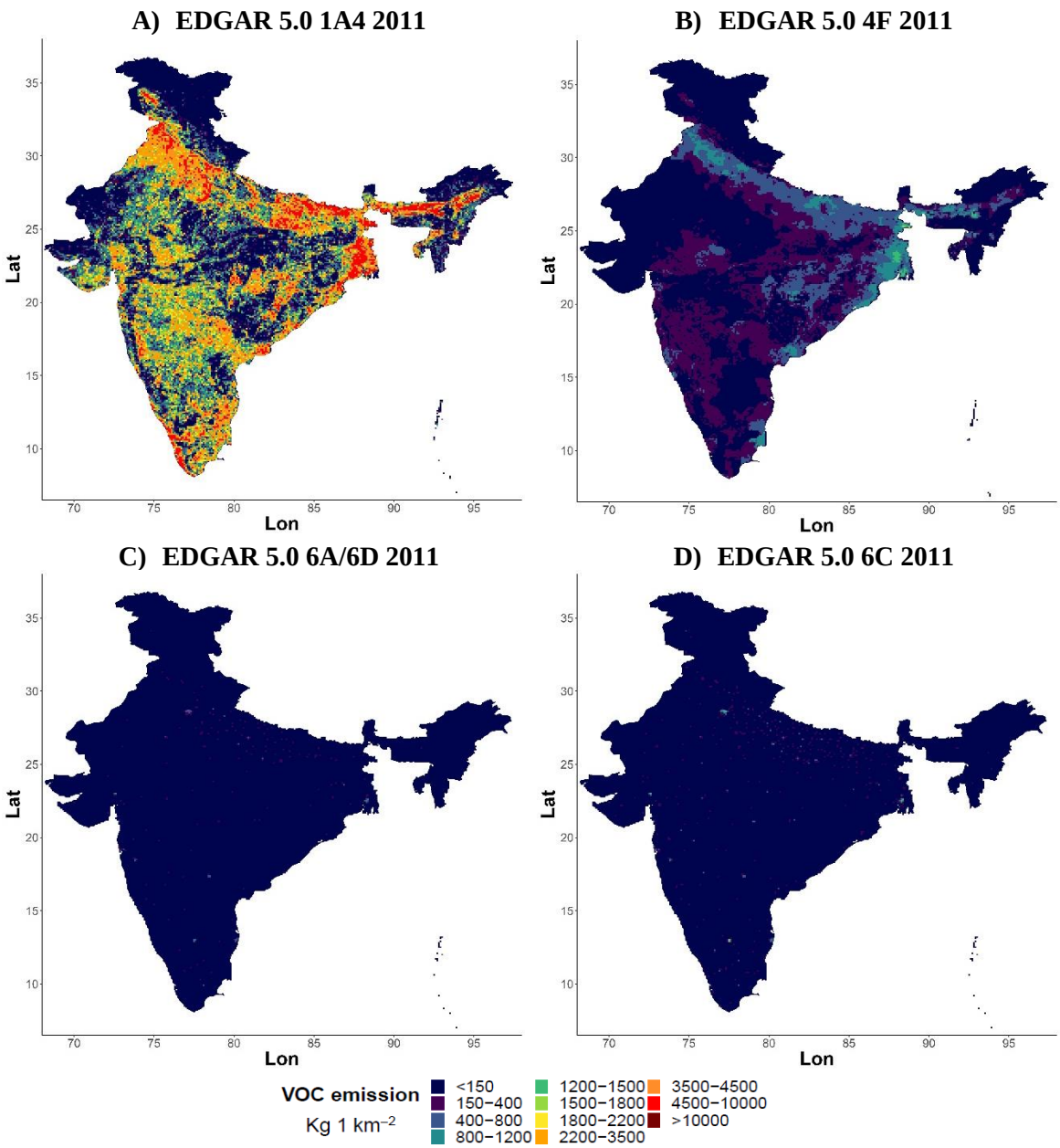

Figure S8.26. EDGAR 5.0 NMVOC emission inventories from 2011 for A = Energy for buildings (1A4), B = agricultural waste burning (4F), C = solid waste landfills (6A/6D) and D = solid waste incineration (6C) with data taken from Crippa et al. (2019).

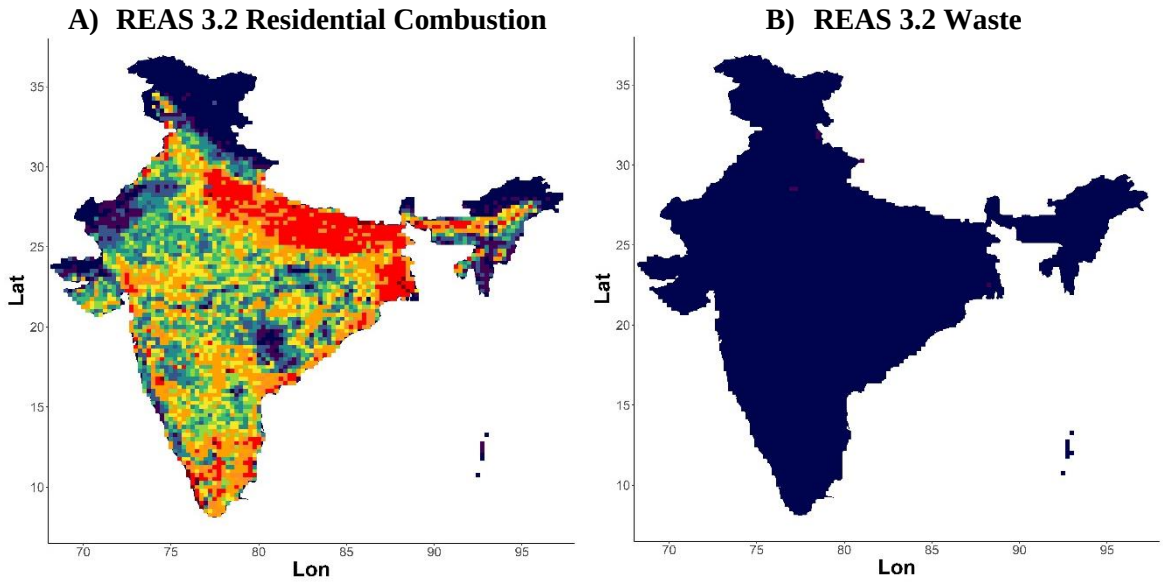

Figure S8.27. REAS 3.2 NMVOC emission inventories from 2011 for A = residential combustion and B = waste using data taken from Kurokawa and Ohara, (2020).

Abbreviations

ACES	Aircraft cavity-enhanced spectroscopy
APCS	Absolute principal component scores
ASE	Accelerated solvent extraction
BaP	Benzo[a]pyrene
BC	Black carbon
Bp	Boiling point
BTEX	Sum of benzene, toluene, ethylbenzene and xylenes
C_i^*	Saturation concentration of species i
$CH_3O_2^{\cdot}$	Methyl peroxy radical
CH_4	Methane
CNG	Compressed natural gas
CO	Carbon monoxide
CPCB	Central Pollution Control Board
Cps	PTR-ToF-MS count rates per second
CSIR	Council of Scientific and Industrial Research
d_c	Column diameter
DC-GC-FID	Dual-channel gas chromatography with flame ionisation detection
E/N	The ratio between electric field strength and buffer gas density in the PTR-ToF-MS drift tube
E_a	Activation energy
ECD	Electron capture detector
EI	Electron ionisation
EPA	Environmental Protection Agency
ERA5	Fifth-generation reanalysis from the European Centre for Medium-Range Weather Forecasts
EtOAc	Ethyl acetate
FAO	Food and Agriculture organisation of the UN
FID	Flame ionisation detector
FTIR	Fourier-transform infrared spectroscopy

GC	Gas chromatography
GC×GC-ToF-MS	Comprehensive two-dimensional gas chromatography with time-of-flight mass spectrometry
GC×GC-FID	Two-dimensional gas chromatography with flame ionisation detection
H	Height of a theoretical plate
HCH(O)	Formaldehyde
HYSPLIT	Hybrid Single Particle Lagrangian Integrated Trajectory
(I^-CIMS)	Iodine clustering chemical ionisation mass spectrometry
I	Kovats retention index
I/SVOCs	Intermediate-volatility and semi-volatile organic compounds
IC	Ion chromatography
IEA	International Energy Agency
IGTDUW	Indira Gandhi Delhi Technical University for Women
IPCC	Intergovernmental Panel on Climate Change
k_x	Rate constant for reaction of species with hydroxyl radical, unless otherwise specified
L	Column length
L/ELVOC	Low- and extremely low-volatility organic compounds
LPG	Liquefied petroleum gas
MeOH	Methanol
MS	Mass spectrometer
MSW	Municipal solid waste
N	Number of theoretical plates
n	Overall peak capacity
Ncps	Normalised PTR-ToF-MS sensitivity, normalised counts per second
NEERI	National Environmental Engineering Research Institute
N_h	Carbon number of n-alkane of higher boiling point than unidentified eluent
NIST	National Institute of Standards and Technology

n_I	Carbon number of n-alkane of lower boiling point than unidentified eluent
NMHCs	Non-methane hydrocarbons
NMVOCs	Non-methane volatile organic compounds
NO	Nitrogen monoxide
NO_2	Nitrogen dioxide
NOAA	National Oceanic and Atmospheric Administration
NO_x	Nitrogen oxides (= NO + NO2)
NPL	National Physical Laboratory
·OH	Hydroxyl radical
O_3	Ozone
OA	Organic aerosol
OC/EC	Organic/elemental carbon
OVOC	Oxygenated non-methane volatile organic compounds
PAHs	Polycyclic aromatic hydrocarbons
PBL	Planetary boundary layer
PBLH	Planetary Boundary Layer Height
PCA	Principal component analysis
PFA	Plastic made from Perfluoroalkoxy alkanes
PLOT	Porous Layer Open Tubular
PM	Particulate matter
PM_1	Particulate matter with a diameter < 1 µm
$PM_{2.5}$	Particulate matter with a diameter < 2.5 µm
PMF	Positive matrix factorisation
POA	Primary organic aerosol
PRL	Physical Research Laboratory, Ahmedabad, India
PTFE	Polytetrafluoroethylene / Teflon
PTR-ToF-MS	PTR-ToF-MS
PUF/XAD/PUF	Polyurethane styrene-divinylbenzene
R	Programming language for statistical computing and graphics
SD	Standard deviation

SOAP	Secondary organic aerosol formation potentials
SPE	Solid phase extraction
S_{rec}	% recovery observed on SPE disks
TIC	Total ion current
ToF	Time-of-flight
t_r	Retention time
TVOC	Total emission factor of NMVOCs
$\bar{u}$	Carrier gas flow velocity
VBS	Volatility-basis dataset
VOCs	Volatile organic compounds
WAS	Whole air samples
WCOT	Wall Coated Open Tubular
WHO	World Health Organisation
λ	Wavelength

References

Adahchour, M., Beens, J., Vreuls, R. J. J., and Brinkman, U. A. T.: Recent developments in comprehensive two-dimensional gas chromatography (GC×GC): IV. Further applications, conclusions and perspectives, TrAC Trends in Analytical Chemistry, 25, 821-840, https://doi.org/10.1016/j.trac.2006.03.003, 2006a.

Adahchour, M., Beens, J., Vreuls, R. J. J., and Brinkman, U. A. T.: Recent developments in comprehensive two-dimensional gas chromatography (GCxGC) II. Modulation and detection, Trends in Analytical Chemistry, 25, 540-553, 2006b.

Ahern, A. T., Robinson, E. S., Tkacik, D. S., Saleh, R., Hatch, L. E., Barsanti, K. C., Stockwell, C. E., Yokelson, R. J., Presto, A. A., Robinson, A. L., Sullivan, R. C., and Donahue, N. M.: Production of Secondary Organic Aerosol During Aging of Biomass Burning Smoke From Fresh Fuels and Its Relationship to VOC Precursors, Journal of Geophysical Research: Atmospheres, 124, 3583-3606, https://doi.org/10.1029/2018jd029068, 2019.

Akagi, S. K., Yokelson, R. J., Wiedinmyer, C., Alvarado, M. J., Reid, J. S., Karl, T., Crounse, J. D., and Wennberg, P. O.: Emission factors for open and domestic biomass burning for use in atmospheric models, Atmos. Chem. Phys., 11, 4039-4072, https://doi.org/10.5194/acp-11-4039-2011, 2011.

Akherati, A., He, Y., Coggon, M. M., Koss, A. R., Hodshire, A. L., Sekimoto, K., Warneke, C., de Gouw, J., Yee, L., Seinfeld, J. H., Onasch, T. B., Herndon, S. C., Knighton, W. B., Cappa, C. D., Kleeman, M. J., Lim, C. Y., Kroll, J. H., Pierce, J. R., and Jathar, S. H.: Oxygenated Aromatic Compounds are Important Precursors of Secondary Organic Aerosol in Biomass-Burning Emissions, Environmental Science & Technology, 54, 8568-8579, https://doi.org/10.1021/acs.est.0c01345, 2020.

Akhtar, T., Uah, Z., Khan, M. H., and Nazli, R.: Chronic bronchitis in women using solid biomass fuel in rural peshawar, Pakistan, Chest, 132, 1472-1475, https://doi.org/10.1378/chest.06-2529, 2007.

Alvarado, M. J., Lonsdale, C. R., Yokelson, R. J., Akagi, S. K., Coe, H., Craven, J. S., Fischer, E. V., McMeeking, G. R., Seinfeld, J. H., Soni, T., Taylor, J. W., Weise, D. R., and Wold, C. E.: Investigating the links between ozone and organic aerosol chemistry in a biomass burning plume from a prescribed fire in California chaparral, Atmos. Chem. Phys., 15, 6667-6688, https://doi.org/10.5194/acp-15-6667-2015, 2015.

Andreae, M. O., and Merlet, P.: Emission of trace gases and aerosols from biomass burning, Global Biogeochemical Cycles, 15, 955-966, https://doi.org/10.1029/2000GB001382, 2001.

Andreae, M. O.: Emission of trace gases and aerosols from biomass burning – an updated assessment, Atmos. Chem. Phys., 19, 8523-8546, https://doi.org/10.5194/acp-19-8523-2019, 2019.

Annepu, R. K., Themelis, N. J., and thompson, S.: Sustainable Solid Waste Management in India, Columbia University New York, 2012.

Aschmann, S. M., Nishino, N., Arey, J., and Atkinson, R.: Kinetics of the Reactions of OH Radicals with 2- and 3-Methylfuran, 2,3- and 2,5-Dimethylfuran, and E- and Z-3-Hexene-2,5-dione, and Products of OH + 2,5-Dimethylfuran, Environmental Science & Technology, 45, 1859-1865, https://doi.org/10.1021/es103207k, 2011.

Aschmann, S. M., Nishino, N., Arey, J., and Atkinson, R.: Products of the OH Radical-Initiated Reactions of Furan, 2- and 3-Methylfuran, and 2,3- and 2,5-Dimethylfuran in the Presence of NO, The Journal of Physical Chemistry A, 118, 457-466, https://doi.org/10.1021/jp410345k, 2014.

Atkinson, R., Baulch, D. L., Cox, R. A., Hampson, R. F., Kerr, J. A., Rossi, M. J., and Troe, J.: Evaluated kinetic and photochemical data for atmospheric chemistry: Supplement VI - IUPAC subcommittee on gas kinetic data evaluation for atmospheric chemistry, Journal of Physical and Chemical Reference Data, 26, 1329-1499, 1997.

Atkinson, R.: Gas-phase tropospheric chemistry of volatile organic compounds .1. Alkanes and alkenes, Journal of Physical and Chemical Reference Data, 26, 215-290, https://doi.org/10.1063/1.556012, 1997.

Atkinson, R., and Arey, J.: Atmospheric Degradation of Volatile Organic Compounds, Chemical Reviews, 103, 4605-4638, https://doi.org/10.1021/cr0206420, 2003.

Barabad, M. L. M., Jung, W., Versoza, M. E., Kim, M., Ko, S., Park, D., and Lee, K.: Emission Characteristics of Particulate Matter, Volatile Organic Compounds, and Trace Elements from the Combustion of Coals in Mongolia, International Journal of Environmental Research and Public Health, 15, 1706, https://doi.org/10.3390/ijerph15081706, 2018.

Barboni, T., Cannac, M., Pasqualini, V., Simeoni, A., Leoni, E., and Chiaramonti, N.: Volatile and semi-volatile organic compounds in smoke exposure of firefighters during prescribed burning in the Mediterranean region, International Journal of Wildland Fire, 19, 606-612, https://doi.org/10.1071/WF08121, 2010.

Bautista, L. E., Correa, A., Baumgartner, J., Breysse, P., and Matanoski, G. M.: Indoor Charcoal Smoke and Acute Respiratory Infections in Young Children in the Dominican Republic, American Journal of Epidemiology, 169, 572-580, https://doi.org/10.1093/aje/kwn372, 2009.

Beens, J., Adahchour, M., Vreuls, R. J. J., van Altena, K., and Th. Brinkman, U. A.: Simple, non-moving modulation interface for comprehensive two-dimensional gas chromatography, Journal of Chromatography A, 919, 127-132, https://doi.org/10.1016/S0021-9673(01)00785-3, 2001.

Berndt, T., Böge, O., and Rolle, W.: Products of the Gas-Phase Reactions of NO_3 Radicals with Furan and Tetramethylfuran, Environmental Science & Technology, 31, 1157-1162, https://doi.org/10.1021/es960669z, 1997.

Bhargava, A., Khanna, R. N., Bhargava, S. K., and Kumar, S.: Exposure risk to carcinogenic PAHs in indoor-air during biomass combustion whilst cooking in rural India, Atmospheric Environment, 38, 4761-4767, https://doi.org/10.1016/j.atmosenv.2004.05.012, 2004.

Bhuvaneshwari, S., Hettiarachchi, H., and Meegoda, J. N.: Crop Residue Burning in India: Policy Challenges and Potential Solutions, International Journal of Environmental Research and Public Health, 16, https://doi.org/10.3390/ijerph16050832, 2019.

Bierbach, A., Barnes, I., Becker, K. H., and Wiesen, E.: Atmospheric chemistry of unsaturated carbonyls - butenedial, 4-oxo-2-pentenal, 3-hexene-2,5-diome, maleic-anhydride, 3H-furan-2-one and 5-methyl-3H-furan-2-one, Environmental Science & Technology, 28, 715-729, https://doi.org/10.1021/es00053a028, 1994.

Bierbach, A., Barnes, I., and Becker, K. H.: Product and kinetic study of the oh-initiated gas-phase oxidation of Furan, 2-methylfuran and furanaldehydes at ≈ 300 K, Atmospheric Environment, 29, 2651-2660, https://doi.org/10.1016/1352-2310(95)00096-H, 1995.

Blake, R. S., Monks, P. S., and Ellis, A. M.: Proton-Transfer Reaction Mass Spectrometry, Chemical Reviews, 109, 861-896, https://doi.org/10.1021/cr800364q, 2009.

Bloss, W. J., Evans, M. J., Lee, J. D., Sommariva, R., Heard, D. E., and Pilling, M. J.: The oxidative capacity of the troposphere: Coupling of field measurements of OH and a global chemistry transport model, Faraday Discussions, 130, 425-436, https://doi.org/10.1039/b419090d, 2005.

Bon, D. M., Ulbrich, I. M., de Gouw, J. A., Warneke, C., Kuster, W. C., Alexander, M. L., Baker, A., Beyersdorf, A. J., Blake, D., Fall, R., Jimenez, J. L., Herndon, S. C., Huey, L. G., Knighton,

W. B., Ortega, J., Springston, S., and Vargas, O.: Measurements of volatile organic compounds at a suburban ground site (T1) in Mexico City during the MILAGRO 2006 campaign: measurement comparison, emission ratios, and source attribution, Atmos. Chem. Phys., 11, 2399-2421, https://doi.org/10.5194/acp-11-2399-2011, 2011.

Bond, T. C., Streets, D. G., Yarber, K. F., Nelson, S. M., Woo, J.-H., and Klimont, Z.: A technology-based global inventory of black and organic carbon emissions from combustion, Journal of Geophysical Research: Atmospheres, 109, https://doi.org/10.1029/2003JD003697, 2004.

Bond, T. C., Doherty, S. J., Fahey, D. W., Forster, P. M., Berntsen, T., DeAngelo, B. J., Flanner, M. G., Ghan, S., Kärcher, B., Koch, D., Kinne, S., Kondo, Y., Quinn, P. K., Sarofim, M. C., Schultz, M. G., Schulz, M., Venkataraman, C., Zhang, H., Zhang, S., Bellouin, N., Guttikunda, S. K., Hopke, P. K., Jacobson, M. Z., Kaiser, J. W., Klimont, Z., Lohmann, U., Schwarz, J. P., Shindell, D., Storelvmo, T., Warren, S. G., and Zender, C. S.: Bounding the role of black carbon in the climate system: A scientific assessment, Journal of Geophysical Research: Atmospheres, 118, 5380-5552, https://doi.org/10.1002/jgrd.50171, 2013.

Borbon, A., Fontaine, H., Veillerot, M., Locoge, N., Galloo, J. C., and Guillermo, R.: An investigation into the traffic-related fraction of isoprene at an urban location, Atmospheric Environment, 35, 3749-3760, https://doi.org/10.1016/S1352-2310(01)00170-4, 2001.

Bose, R. K., and Anandalingam, G.: Sustainable urban energy-environment management with multiple objectives, Energy, 21, 305-318, https://doi.org/10.1016/0360-5442(95)00098-4, 1996.

Boy, E., Bruce, N., and Delgado, H.: Birth weight and exposure to kitchen wood smoke during pregnancy in rural Guatemala, Environmental Health Perspectives, 110, 109-114, https://doi.org/10.1289/ehp.02110109, 2002.

Brilli, F., Gioli, B., Ciccioli, P., Zona, D., Loreto, F., Janssens, I. A., and Ceulemans, R.: Proton Transfer Reaction Time-of-Flight Mass Spectrometric (PTR-TOF-MS) determination of volatile organic compounds (VOCs) emitted from a biomass fire developed under stable nocturnal conditions, Atmospheric Environment, 97, 54-67, https://doi.org/10.1016/j.atmosenv.2014.08.007, 2014.

Bruckner, C. A., Prazen, B. J., and Synovec, R. E.: Comprehensive Two-Dimensional High-Speed Gas Chromatography with Chemometric Analysis, Analytical Chemistry, 70, 2796-2804, https://doi.org/10.1021/ac980164m, 1998.

Brunekreef, B., and Holgate, S. T.: Air pollution and health, The Lancet, 360, 1233-1242, https://doi.org/10.1016/S0140-6736(02)11274-8, 2002.

Bruno, P., Caselli, M., de Gennaro, G., and Traini, A.: Source apportionment of gaseous atmospheric pollutants by means of an absolute principal component scores (APCS) receptor model, Fresenius' Journal of Analytical Chemistry, 371, 1119-1123, https://doi.org/10.1007/s002160101084, 2001.

Bruns, E. A., El Haddad, I., Slowik, J. G., Kilic, D., Klein, F., Baltensperger, U., and Prévôt, A. S. H.: Identification of significant precursor gases of secondary organic aerosols from residential wood combustion, Scientific Reports, 6, 27881, 10.1038/srep27881, 2016.

Bueno, P. A., and Seeley, J. V.: Flow-switching device for comprehensive two-dimensional gas chromatography, Journal of Chromatography A, 1027, 3-10, https://doi.org/10.1016/j.chroma.2003.10.033, 2004.

Burling, I. R., Yokelson, R. J., Griffith, D. W. T., Johnson, T. J., Veres, P., Roberts, J. M., Warneke, C., Urbanski, S. P., Reardon, J., Weise, D. R., Hao, W. M., and de Gouw, J.: Laboratory measurements of trace gas emissions from biomass burning of fuel types from the southeastern and southwestern United States, Atmospheric Chemistry and Physics, 10, 11115-11130, https://doi.org/10.5194/acp-10-11115-2010, 2010.

Cabañas, B., Villanueva, F., Martín, P., Baeza, M. T., Salgado, S., and Jiménez, E.: Study of reaction processes of furan and some furan derivatives initiated by Cl atoms, Atmospheric Environment, 39, 1935-1944, https://doi.org/10.1016/j.atmosenv.2004.12.013, 2005.

Cai, S., Zhu, L., Wang, S., Wisthaler, A., Li, Q., Jiang, J., and Hao, J.: Time-Resolved Intermediate-Volatility and Semivolatile Organic Compound Emissions from Household Coal Combustion in Northern China, Environmental Science & Technology, 53, 9269-9278, https://doi.org/10.1021/acs.est.9b00734, 2019.

Cao, X., Yao, Z., Shen, X., Ye, Y., and Jiang, X.: On-road emission characteristics of VOCs from light-duty gasoline vehicles in Beijing, China, Atmospheric Environment, 124, 146-155, https://doi.org/10.1016/j.atmosenv.2015.06.019, 2016.

Carslaw, D. C., and Ropkins, K.: openair — An R package for air quality data analysis, Environmental Modelling & Software, 27–28, 52–61, https://doi.org/10.1016/j.envsoft.2011.09.008, 2012.

Cash, J. M., Langford, B., Marco, C. D., Mullinger, N., Allan, J., Reyes-Villegas, E., Joshi, R., Heal, M. R., Acton, W. J. F., Hewitt, N., Misztal, P. K., Drysdale, W., Mandal, T. K., Shivani,

Gadi, R., and Nemitz, E.: Seasonal analysis of submicron aerosol in Old Delhi using high resolution aerosol mass spectrometry: Chemical characterisation, source apportionment and new marker identification, Atmos. Chem. Phys. Discuss., https://doi.org/10.5194/acp-2020-1009, 2020.

Chafe, Z. A., Brauer, M., Klimont, Z., Van Dingenen, R., Mehta, S., Rao, S., Riahi, K., Dentener, F., and Smith, K. R.: Household Cooking with Solid Fuels Contributes to Ambient $PM_{2.5}$ Air Pollution and the Burden of Disease, Environmental Health Perspectives, 122, 1314-1320, https://doi.org/10.1289/ehp.1206340, 2014.

Chan, A. W. H., Kautzman, K. E., Chhabra, P. S., Surratt, J. D., Chan, M. N., Crounse, J. D., Kürten, A., Wennberg, P. O., Flagan, R. C., and Seinfeld, J. H.: Secondary organic aerosol formation from photooxidation of naphthalene and alkylnaphthalenes: implications for oxidation of intermediate volatility organic compounds (IVOCs), Atmos. Chem. Phys., 9, 3049-3060, https://doi.org/10.5194/acp-9-3049-2009, 2009.

Chandramouli, C.: Census of India 2011: Rural Urban distribution of Population, India, 2011.

Charles, B., Guinaudeau, H., Ferreira, M. E., Rojas de Arias, A., and Fournet, A.: Essential Oils from Zanthoxylum chiloperone and Z. riedelianum Growing in Paraguay AU - Guy, Isabelle, Pharmaceutical Biology, 39, 152-154, https://doi.org/10.1076/phbi.39.2.152.6255, 2001.

Chen, J., Li, C., Ristovski, Z., Milic, A., Gu, Y., Islam, M. S., Wang, S., Hao, J., Zhang, H., He, C., Guo, H., Fu, H., Miljevic, B., Morawska, L., Thai, P., Lam, Y. F., Pereira, G., Ding, A., Huang, X., and Dumka, U. C.: A review of biomass burning: Emissions and impacts on air quality, health and climate in China, Science of The Total Environment, 579, 1000-1034, https://doi.org/10.1016/j.scitotenv.2016.11.025, 2017.

Chen, Y., Beig, G., Archer-Nicholls, S., Drysdale, W., Acton, W. J. F., Lowe, D., Nelson, B., Lee, J., Ran, L., Wang, Y., Wu, Z., Sahu, S. K., Sokhi, R. S., Singh, V., Gadi, R., Hewitt, C. N., Nemitz, E. N., Archibald, A., McFiggan, G., and Wild, O.: Avoiding high ozone pollution in Delhi, India, Faraday Discussions, https://doi.org/10.1039/D0FD00079E, 2020.

Cheng, H. R., Guo, H., Saunders, S. M., Lam, S. H. M., Jiang, F., Wang, X. M., Simpson, I. J., Blake, D. R., Louie, P. K. K., and Wang, T. J.: Assessing photochemical ozone formation in the Pearl River Delta with a photochemical trajectory model, Atmospheric Environment, 44, 4199-4208, https://doi.org/10.1016/j.atmosenv.2010.07.019, 2010.

Christian, T. J., Yokelson, R. J., Cárdenas, B., Molina, L. T., Engling, G., and Hsu, S. C.: Trace gas and particle emissions from domestic and industrial biofuel use and garbage burning in central Mexico, Atmos. Chem. Phys., 10, 565-584, https://doi.org/10.5194/acp-10-565-2010, 2010.

Coggon, M. M., Veres, P. R., Yuan, B., Koss, A., Warneke, C., Gilman, J. B., Lerner, B. M., Peischl, J., Aikin, K. C., Stockwell, C. E., Hatch, L. E., Ryerson, T. B., Roberts, J. M., Yokelson, R. J., and de Gouw, J. A.: Emissions of nitrogen-containing organic compounds from the burning of herbaceous and arboraceous biomass: Fuel composition dependence and the variability of commonly used nitrile tracers, Geophysical Research Letters, 43, 9903-9912, https://doi.org/10.1002/2016gl070562, 2016.

Coggon, M. M., Lim, C. Y., Koss, A. R., Sekimoto, K., Yuan, B., Gilman, J. B., Hagan, D. H., Selimovic, V., Zarzana, K. J., Brown, S. S., Roberts, J. M., Müller, M., Yokelson, R., Wisthaler, A., Krechmer, J. E., Jimenez, J. L., Cappa, C., Kroll, J. H., de Gouw, J., and Warneke, C.: OH chemistry of non-methane organic gases (NMOGs) emitted from laboratory and ambient biomass burning smoke: evaluating the influence of furans and oxygenated aromatics on ozone and secondary NMOG formation, Atmos. Chem. Phys., 19, 14875-14899, https://doi.org/10.5194/acp-19-14875-2019, 2019.

Cohen, A. J., Ross Anderson, H., Ostro, B., Pandey, K. D., Krzyzanowski, M., Künzli, N., Gutschmidt, K., Pope, A., Romieu, I., Samet, J. M., and Smith, K.: The Global Burden of Disease Due to Outdoor Air Pollution, Journal of Toxicology and Environmental Health, Part A, 68, 1301-1307, https://doi.org/10.1080/15287390590936166, 2005.

Cohen, N., and Westberg, K. R.: Chemical kinetic data sheets for high-temperature reactions. Part II, J. Phys. Chem. Ref. Data, 20, 1211 - 1311, 1991.

Colmenar, I., Cabañas, B., Martínez, E., Salgado, M. S., and Martín, P.: Atmospheric fate of a series of furanaldehydes by their NO_3 reactions, Atmospheric Environment, 54, 177-184, https://doi.org/10.1016/j.atmosenv.2012.02.087, 2012.

Cortes, H. J., Winniford, B., Luong, J., and Pursch, M.: Comprehensive two dimensional gas chromatography review, Journal of Separation Science, 32, 883–904, 2009.

Costner, P.: Estimating Releases and Prioritizing Sources in the Context of the Stockholm Convention: Dioxin Emission Factors for Forest Fires, Grassland and Moor Fires, Open Burning of Agricultural Residues, Open Burning of Domestic Waste, Landfill and Dump Fires, The International POPs Elimination Project, Mexico, 1-40, 2005.

CPCB: Air quality assesment: National Air Quality Monitoring Programme (NAMP), 2006.

CPCB: Air Quality Monitoring, Emission Inventory and Source Apportionment Study for Indian Cities. , Central Pollution Control Board, 2010.

CPCB: National Ambient Air Quality Status 2009. Accessed 20/04/2018. Available from: http://cpcb.nic.in/cpcbold/upload/Publications/Publication_514_airqualitystatus2009.pdf , 2011.

CPCB: Status report on municipal solid waste managment, Delhi, India, 2013.

CPCB: Consolidated Annual Review Report on Implementation of Solid Waste Management Rules 2016, in, East Arjun Nagar, Delhi, 2017.

CPCB: Central Control Room for Air Quality Management - All India -Average Report Criteria. Accessed 22 March 2018. Available from: https://app.cpcbccr.com/ccr/#/caaqm-dashboard-all/caaqm-landing, 2018.

Crippa, M., Oreggioni, G., Guizzardi, D., Muntean, M., Schaaf, E., Lo Vullo, E., Solazzo, E., Monforti-Ferrario, F., Olivier, J. G. J., and Vignati, E.: EDGARv5.0 air pollutant website https://data.europa.eu/doi/10.2904/JRC_DATASET_EDGAR, 2019.

Cross, E. S., Hunter, J. F., Carrasquillo, A. J., Franklin, J. P., Herndon, S. C., Jayne, J. T., Worsnop, D. R., Miake-Lye, R. C., and Kroll, J. H.: Online measurements of the emissions of intermediate-volatility and semi-volatile organic compounds from aircraft, Atmos. Chem. Phys., 13, 7845-7858, https://doi.org/10.5194/acp-13-7845-2013, 2013.

Crutzen, P. J., Heidt, L. E., Krasnec, J. P., Pollock, W. H., and Seiler, W.: Biomass burning as a source of atmospheric gases CO, H_2, N_2O, NO, CH_3Cl and COS, Nature, 282, 253-256, https://doi.org/10.1038/282253a0, 1979.

Cubison, M. J., Ortega, A. M., Hayes, P. L., Farmer, D. K., Day, D., Lechner, M. J., Brune, W. H., Apel, E., Diskin, G. S., Fisher, J. A., Fuelberg, H. E., Hecobian, A., Knapp, D. J., Mikoviny, T., Riemer, D., Sachse, G. W., Sessions, W., Weber, R. J., Weinheimer, A. J., Wisthaler, A., and Jimenez, J. L.: Effects of aging on organic aerosol from open biomass burning smoke in aircraft and laboratory studies, Atmos. Chem. Phys., 11, 12049-12064, https://doi.org/10.5194/acp-11-12049-2011, 2011.

D. Flatt, V., Campos, C., P. Kraemer, M., Bailey, B., Satyal, P., and Setzer, W.: Compositional Variation and Bioactivity of the Leaf Essential Oil of Montanoa guatemalensis from Monteverde, Costa Rica: A Preliminary Investigation, 331-339 pp., 2015.

Dahiya, K. K.: No. 1135-1161/TE(D-II). Reg.Amended Notification of Transport Department, GNCT of Delhi regarding No Entry Timing for Goods Vehicles., in, edited by: Delhi Traffic Police, New Delhi, India. Available from: https://delhitrafficpolice.nic.in/about-us/notifications/, 2016.

de Gouw, J. A., Middlebrook, A. M., Warneke, C., Goldan, P. D., Kuster, W. C., Roberts, J. M., Fehsenfeld, F. C., Worsnop, D. R., Canagaratna, M. R., Pszenny, A. A. P., Keene, W. C., Marchewka, M., Bertman, S. B., and Bates, T. S.: Budget of organic carbon in a polluted atmosphere: Results from the New England Air Quality Study in 2002, Journal of Geophysical Research-Atmospheres, 110, https://doi.org/10.1029/2004jd005623, 2005.

Dechapanya, W., Russell, M., and Allen, D. T.: Estimates of Anthropogenic Secondary Organic Aerosol Formation in Houston, Texas Special Issue of Aerosol Science and Technology on Findings from the Fine Particulate Matter Supersites Program, Aerosol Science and Technology, 38, 156-166, https://doi.org/10.1080/02786820390229462, 2004.

Decker, Z. C. J., Zarzana, K. J., Coggon, M., Min, K.-E., Pollack, I., Ryerson, T. B., Peischl, J., Edwards, P., Dubé, W. P., Markovic, M. Z., Roberts, J. M., Veres, P. R., Graus, M., Warneke, C., de Gouw, J., Hatch, L. E., Barsanti, K. C., and Brown, S. S.: Nighttime Chemical Transformation in Biomass Burning Plumes: A Box Model Analysis Initialized with Aircraft Observations, Environmental Science & Technology, 53, 2529-2538, https://doi.org/10.1021/acs.est.8b05359, 2019.

Delhi Tourism: Seasons of Delhi. Accessed 15 March 2018. Available from: http://www.delhitourism.gov.in/delhitourism/aboutus/seasons_of_delhi.jsp 2016.

Dennis, R. J., Maldonado, D., Norman, S., Baena, E., and Martinez, G.: Woodsmoke Exposure and Risk for Obstructive Airways Disease Among Women, Chest, 109, 115-119, https://doi.org/10.1378/chest.109.1.115, 1996.

Dentener, F., Derwent, R., Dlugokencky, E., Holland, E., Isaksen, I., Katima, J., Kirchhoff, V., Matson, P., Midgley, P., and Wang, M.: Volatile organic compounds (VOC), in: IPCC Third Assessment Report: Climate Change 2001 (TAR). Working Group I: The Scientific Basis, edited by: Joos, F., and McFarlan, M., Intergovernmental Panel on Climate Change, Geneva, Switzerland, 241-287, 2001.

Department of Economics and Statistics: Statistics of Delhi at a glance: Population of Delhi as per Census 2011. Accessed:16 March 2018. Avalible from:

http://www.delhi.gov.in/wps/wcm/connect/doit_des/DES/Home/Statistics+of+Delhi+at+a+glance/, 2011.

Dettmer-Wilde, K., and Engewald, W.: Theory of Gas Chromatography, in: Practical Gas Chromatography: A Comprehensive Reference, 1 ed., edited by: Dettmer-Wilde, K., and Engewald, W., Springer Heidelburg, Germany, 21-57, 2014.

Dhital, N. B., Yang, H.-H., Wang, L.-C., Hsu, Y.-T., Zhang, H.-Y., Young, L.-H., and Lu, J.-H.: VOCs emission characteristics in motorcycle exhaust with different emission control devices, Atmospheric Pollution Research, 10, 1498-1506, https://doi.org/10.1016/j.apr.2019.04.007, 2019.

Directorate of Census Operations, D.: District census handbook of all the nine districts, 2011.

Donahue, N. M., Robinson, A. L., Stanier, C. O., and Pandis, S. N.: Coupled partitioning, dilution, and chemical aging of semivolatile organics, Environmental Science & Technology, 40, 2635-2643, https://doi.org/10.1021/es052297c, 2006.

Donahue, N. M., Kroll, J. H., Pandis, S. N., and Robinson, A. L.: A two-dimensional volatility basis set – Part 2: Diagnostics of organic-aerosol evolution, Atmos. Chem. Phys., 12, 615-634, https://doi.org/10.5194/acp-12-615-2012, 2012.

Dunmore, R. E., Hopkins, J. R., Lidster, R. T., Lee, J. D., Evans, M. J., Rickard, A. R., Lewis, A. C., and Hamilton, J. F.: Diesel-related hydrocarbons can dominate gas phase reactive carbon in megacities, Atmospheric Chemistry and Physics, 15, 9983-9996, https://doi.org/10.5194/acp-15-9983-2015, 2015.

Ehhalt, D. H.: Gas Phase Chemistry of the Trophosphere, in: Global Aspects of Atmospheric Chemistry, edited by: Zellner, R., Steinkopff, Heidelberg, Germany, 21-24, 1999.

Eiserbeck, C., Nelson, R., Reddy, C., and Grice, K.: Advances in Comprehensive Two-dimensional Gas Chromatography(GCxGC), 324 pp., 2014.

Ellis, A. M., and Mayhew, C. A.: Proton Transfer Reaction Mass Spectrometry: Principles and Applications, Wiley, Chichester, UK, 2014.

Elzein, A., Dunmore, R. E., Ward, M. W., Hamilton, J. F., and Lewis, A. C.: Variability of polycyclic aromatic hydrocarbons and their oxidative derivatives in wintertime Beijing, China, Atmos. Chem. Phys., 19, 8741-8758, https://doi.org/10.5194/acp-19-8741-2019, 2019.

Elzein, A., Stewart, G. J., Swift, S. J., Nelson, B. S., Crilley, L. R., Alam, M. S., Reyes-Villegas, E., Gadi, R., Harrison, R. M., Hamilton, J. F., and Lewis, A. C.: A comparison of $PM_{2.5}$-bound polycyclic aromatic hydrocarbons in summer Beijing (China) and Delhi (India), Atmos. Chem. Phys., 14303–14319, https://doi.org/10.5194/acp-20-14303-2020, 2020.

EPA: Greenhouse gases from small-scale combustion devices in devloping countries: phase IIA household stoves in India, 2000.

USEPA: Estimation Programs Interface Suite™ for Microsoft® Windows v 4.11: https://www.epa.gov/tsca-screening-tools/epi-suitetm-estimation-program-interface, 2012.

ERA5 hourly data on single levels from 1979 to present: https://cds.climate.copernicus.eu/cdsapp#!/dataset/reanalysis-era5-single-levels?tab=form, 2019.

Farren, N. J., Ramírez, N., Lee, J. D., Finessi, E., Lewis, A. C., and Hamilton, J. F.: Estimated Exposure Risks from Carcinogenic Nitrosamines in Urban Airborne Particulate Matter, Environmental Science & Technology, 49, 9648-9656, https://doi.org/10.1021/acs.est.5b01620, 2015.

Finewax, Z., de Gouw, J. A., and Ziemann, P. J.: Identification and Quantification of 4-Nitrocatechol Formed from OH and NO_3 Radical-Initiated Reactions of Catechol in Air in the Presence of NO_x: Implications for Secondary Organic Aerosol Formation from Biomass Burning, Environmental Science & Technology, 52, 1981-1989, https://doi.org/10.1021/acs.est.7b05864, 2018.

Fleming, L. T., Weltman, R., Yadav, A., Edwards, R. D., Arora, N. K., Pillarisetti, A., Meinardi, S., Smith, K. R., Blake, D. R., and Nizkorodov, S. A.: Emissions from village cookstoves in Haryana, India, and their potential impacts on air quality, Atmos. Chem. Phys., 18, 15169-15182, https://doi.org/10.5194/acp-18-15169-2018, 2018.

Fujitani, Y., Saitoh, K., Fushimi, A., Takahashi, K., Hasegawa, S., Tanabe, K., Kobayashi, S., Furuyama, A., Hirano, S., and Takami, A.: Effect of isothermal dilution on emission factors of organic carbon and *n*-alkanes in the particle and gas phases of diesel exhaust, Atmospheric Environment, 59, 389-397, https://doi.org/10.1016/j.atmosenv.2012.06.010, 2012.

Fullerton, D. G., Bruce, N., and Gordon, S. B.: Indoor air pollution from biomass fuel smoke is a major health concern in the developing world, Trans R Soc Trop Med Hyg, 102, 843-851, https://doi.org/10.1016/j.trstmh.2008.05.028, 2008.

Gadi, R., Singh, D. P., Saud, T., Mandal, T. K., and Saxena, M.: Emission Estimates of Particulate PAHs from Biomass Fuels Used in Delhi, India, Human and Ecological Risk Assessment: An International Journal, 18, 871-887, https://doi.org/10.1080/10807039.2012.688714, 2012.

Gamas, E. D., Magdaleno, M., Diaz, L., Schifter, I., Ontiveros, L., and Alvarez-Cansino, G.: Contribution of Liquefied Petroleum Gas to Air Pollution in the Metropolitan Area of Mexico City, Journal of the Air & Waste Management Association, 50, 188-198, https://doi.org/10.1080/10473289.2000.10464012, 2000.

Gani, S., Bhandari, S., Seraj, S., Wang, D. S., Patel, K., Soni, P., Arub, Z., Habib, G., Hildebrandt Ruiz, L., and Apte, J. S.: Submicron aerosol composition in the world's most polluted megacity: the Delhi Aerosol Supersite study, Atmos. Chem. Phys., 19, 6843-6859, https://doi.org/10.5194/acp-19-6843-2019, 2019.

Garaga, R., Sahu, S. K., and Kota, S. H.: A Review of Air Quality Modeling Studies in India: Local and Regional Scale, Current Pollution Reports, 4, 59-73, https://doi.org/10.1007/s40726-018-0081-0, 2018.

Geng, C., Chen, J., Yang, X., Ren, L., Yin, B., Liu, X., and Bai, Z.: Emission factors of polycyclic aromatic hydrocarbons from domestic coal combustion in China, Journal of Environmental Sciences, 26, 160-166, https://doi.org/10.1016/S1001-0742(13)60393-9, 2014.

Gilman, J. B., Lerner, B. M., Kuster, W. C., Goldan, P. D., Warneke, C., Veres, P. R., Roberts, J. M., de Gouw, J. A., Burling, I. R., and Yokelson, R. J.: Biomass burning emissions and potential air quality impacts of volatile organic compounds and other trace gases from fuels common in the US, Atmos. Chem. Phys., 15, 13915-13938, https://doi.org/10.5194/acp-15-13915-2015, 2015.

Goel, R., and Guttikunda, S. K.: Evolution of on-road vehicle exhaust emissions in Delhi, Atmospheric Environment, 105, 78-90, https://doi.org/10.1016/j.atmosenv.2015.01.045, 2015.

Goldstein, A. H., and Galbally, I. E.: Known and Unexplored Organic Constituents in the Earth's Atmosphere, Environmental Science & Technology, 41, 1514-1521, https://doi.org/10.1021/es072476p, 2007.

Gómez Alvarez, E., Borrás, E., Viidanoja, J., and Hjorth, J.: Unsaturated dicarbonyl products from the OH-initiated photo-oxidation of furan, 2-methylfuran and 3-methylfuran, Atmospheric Environment, 43, 1603-1612, https://doi.org/10.1016/j.atmosenv.2008.12.019, 2009.

Gopal, L.: History of Agriculture in India from c. AD 1947 to the Present: 5 (History of Science, Philosophy and Culture in Indian Civilization), Centre for Studies in Civilisations 2014.

Gordon, T., Balakrishnan, K., Dey, S., Rajagopalan, S., Thornburg, J., Thurston, G., Agrawal, A., Collman, G., Guleria, R., Limaye, S., Salvi, S., Kilaru, V., and Nadadur, S.: Air pollution health research priorities for India: Perspectives of the Indo-US Communities of Researchers, Environment International, 119, 100-108, https://doi.org/10.1016/j.envint.2018.06.013, 2018.

Gould, C. F., and Urpelainen, J.: LPG as a clean cooking fuel: Adoption, use, and impact in rural India, Energy Policy, 122, 395-408, 10.1016/j.enpol.2018.07.042, 2018.

Government of India: Rural Urban Distribution of Population - India, Census of India 2011 (PCA Final Data), India, 307-329, 2014.

Government of NCT Delhi: The Central Motor Vehicle Rules, in: 115(2), 24 November, New Delhi, 1989.

Gu, Q., David, F., Lynen, F., Rumpel, K., Xu, G., De Vos, P., and Sandra, P.: Analysis of bacterial fatty acids by flow modulated comprehensive two-dimensional gas chromatography with parallel flame ionization detector/mass spectrometry, Journal of Chromatography A, 1217, 4448-4453, https://doi.org/10.1016/j.chroma.2010.04.057, 2010.

Guar, M., Singh, R., and Shukla, A.: Variability in the Levels of BTEX at a Pollution Hotspot in New Delhi, India, Journal of Environmental Protection, 7, 1245-1258, 2016.

Gulyurtlu, I., Karunaratne, D. G. G. P., and Cabrita, I.: The study of the effect of operating parameters on the PAH formation during the combustion of coconut shell in a fluidised bed, Fuel, 82, 215-223, https://doi.org/10.1016/S0016-2361(02)00224-7, 2003.

Guo, H., Wang, T., and Louie, P. K. K.: Source apportionment of ambient non-methane hydrocarbons in Hong Kong: Application of a principal component analysis/absolute principal component scores (PCA/APCS) receptor model, Environmental Pollution, 129, 489-498, https://doi.org/10.1016/j.envpol.2003.11.006, 2004.

Gupta, K. K., Aneja, K. R., and Rana, D.: Current status of cow dung as a bioresource for sustainable development, Bioresources and Bioprocessing, 3, 28, https://doi.org/10.1186/s40643-016-0105-9, 2016.

Gurjar, B. R., van Aardenne, J. A., Lelieveld, J., and Mohan, M.: Emission estimates and trends (1990–2000) for megacity Delhi and implications, Atmospheric Environment, 38, 5663-5681, https://doi.org/10.1016/j.atmosenv.2004.05.057, 2004.

Guttikunda, S. K., and Calori, G.: A GIS based emissions inventory at 1 km × 1 km spatial resolution for air pollution analysis in Delhi, India, Atmospheric Environment, 67, 101-111, https://doi.org/10.1016/j.atmosenv.2012.10.040, 2013.

Guy, I., Charles, B., Guinaudeau, H., de Arias, A. R., and Fournet, A.: Chemical Composition and Insecticidal Activity of Hedeoma mandoniana Essential Oils AU - Vilaseca, Antonio, Journal of Essential Oil Research, 16, 380-383, https://doi.org/10.1080/10412905.2004.9698749, 2004.

Habib, G., Venkataraman, C., Shrivastava, M., Banerjee, R., Stehr, J. W., and Dickerson, R. R.: New methodology for estimating biofuel consumption for cooking: Atmospheric emissions of black carbon and sulfur dioxide from India, Global Biogeochemical Cycles, 18, GB3007, https://doi.org/10.1029/2003GB002157, 2004.

Hamilton, J. F., Webb, P. J., Lewis, A. C., Hopkins, J. R., Smith, S., and Davy, P.: Partially oxidised organic components in urban aerosol using GCXGC-TOF/MS, Atmos. Chem. Phys., 4, 1279-1290, https://doi.org/10.5194/acp-4-1279-2004, 2004.

Hamilton, J. F., and Lewis, A. C.: Comprehensive Two-Dimensional Gas Chromatography, in: Volatile Organic Compounds in the Atmosphere, Blackwell, London. UK, 467-488, 2007.

Hanrahan, D., Srivastava, S., and Ramakrishna, A. S.: Improving managment of municipal solid waste in India: Overview and challenges, Environment and Social Development Unit, South Asia Region. The World Bank, New Delhi, India 2006.

Hartikainen, A., Yli-Pirilä, P., Tiitta, P., Leskinen, A., Kortelainen, M., Orasche, J., Schnelle-Kreis, J., Lehtinen, K. E. J., Zimmermann, R., Jokiniemi, J., and Sippula, O.: Volatile Organic Compounds from Logwood Combustion: Emissions and Transformation under Dark and Photochemical Aging Conditions in a Smog Chamber, Environmental Science & Technology, 52, 4979-4988, https://doi.org/10.1021/acs.est.7b06269, 2018.

Hatch, L. E., Luo, W., Pankow, J. F., Yokelson, R. J., Stockwell, C. E., and Barsanti, K. C.: Identification and quantification of gaseous organic compounds emitted from biomass

burning using two-dimensional gas chromatography–time-of-flight mass spectrometry, Atmos. Chem. Phys., 15, 1865-1899, https://doi.org/10.5194/acp-15-1865-2015, 2015.

Hatch, L. E., Yokelson, R. J., Stockwell, C. E., Veres, P. R., Simpson, I. J., Blake, D. R., Orlando, J. J., and Barsanti, K. C.: Multi-instrument comparison and compilation of non-methane organic gas emissions from biomass burning and implications for smoke-derived secondary organic aerosol precursors, Atmos. Chem. Phys., 17, 1471-1489, https://doi.org/10.5194/acp-17-1471-2017, 2017.

Hatch, L. E., Rivas-Ubach, A., Jen, C. N., Lipton, M., Goldstein, A. H., and Barsanti, K. C.: Measurements of I/SVOCs in biomass-burning smoke using solid-phase extraction disks and two-dimensional gas chromatography, Atmos. Chem. Phys., 18, 17801-17817, https://doi.org/10.5194/acp-18-17801-2018, 2018.

Haynes, B. S., Iverach, D., and Kirov, N. Y.: The behaviour of nitrogen species in fuel rich hydrocarbon flames, Symposium (International) on Combustion, 15, 1103-1112, 1975.

Hays, M. D., Geron, C. D., Linna, K. J., Smith, N. D., and Schauer, J. J.: Speciation of Gas-Phase and Fine Particle Emissions from Burning of Foliar Fuels, Environmental Science & Technology, 36, 2281-2295, https://doi.org/10.1021/es0111683, 2002.

Health Effects Institute: State of global air: A special report on global exposire to air pollution and its diseased burden, Health Effects Institute, Boston, MA, 2019.

Hedberg, E., Kristensson, A., Ohlsson, M., Johansson, C., Johansson, P.-Å., Swietlicki, E., Vesely, V., Wideqvist, U., and Westerholm, R.: Chemical and physical characterization of emissions from birch wood combustion in a wood stove, Atmospheric Environment, 36, 4823-4837, https://doi.org/10.1016/S1352-2310(02)00417-X, 2002.

Henry, C. R.: EPA Unmix 6.0 Fundamentals & User Guide 2007.

Hodzic, A., Jimenez, J. L., Madronich, S., Canagaratna, M. R., DeCarlo, P. F., Kleinman, L., and Fast, J.: Modeling organic aerosols in a megacity: potential contribution of semi-volatile and intermediate volatility primary organic compounds to secondary organic aerosol formation, Atmos. Chem. Phys., 10, 5491-5514, 10.5194/acp-10-5491-2010, 2010.

Hodzic, A., Kasibhatla, P. S., Jo, D. S., Cappa, C. D., Jimenez, J. L., Madronich, S., and Park, R. J.: Rethinking the global secondary organic aerosol (SOA) budget: stronger production, faster removal, shorter lifetime, Atmos. Chem. Phys., 16, 7917-7941, https://doi.org/10.5194/acp-16-7917-2016, 2016.

Holloway, A. M., and Wayne, R. P.: Chemistry in the Troposphere, in: Atmospheric Chemistry, 1st ed., RSC, Oxford, UK, 99-136, 2010.

Holzinger, R.: PTRwid: A new widget tool for processing PTR-TOF-MS data, Atmos. Meas. Tech., 8, 3903-3922, https://doi.org/10.5194/amt-8-3903-2015, 2015.

Hopke, P.: A Review of Receptor Modeling Methods for Source Apportionment, 2016.

Hopkins, J., Lewis, A., and Read, K.: A two-column method for long-term monitoring of non-methane hydrocarbons (NMHCs) and oxygenated volatile organic compounds (o-VOCs), Journal of environmental monitoring : JEM, 5, 8-13, https://doi.org/10.1039/b202798d, 2003.

Hoque, R. R., Khillare, P. S., Agarwal, T., Shridhar, V., and Balachandran, S.: Spatial and temporal variation of BTEX in the urban atmosphere of Delhi, India, Science of The Total Environment, 392, 30-40, https://doi.org/10.1016/j.scitotenv.2007.08.036, 2008.

Hosseini, S., Urbanski, S. P., Dixit, P., Qi, L., Burling, I. R., Yokelson, R. J., Johnson, T. J., Shrivastava, M., Jung, H. S., Weise, D. R., Miller, J. W., and Cocker Iii, D. R.: Laboratory characterization of PM emissions from combustion of wildland biomass fuels, Journal of Geophysical Research: Atmospheres, 118, 9914-9929, https://doi.org/10.1002/jgrd.50481, 2013.

Huang, G., Brook, R., Crippa, M., Janssens-Maenhout, G., Schieberle, C., Dore, C., Guizzardi, D., Muntean, M., Schaaf, E., and Friedrich, R.: Speciation of anthropogenic emissions of non-methane volatile organic compounds: a global gridded data set for 1970–2012, Atmos. Chem. Phys., 17, 7683-7701, https://doi.org/10.5194/acp-17-7683-2017, 2017.

Huff, J.: Benzene-induced Cancers: Abridged History and Occupational Health Impact AU - Huff, James, International Journal of Occupational and Environmental Health, 13, 213-221, https://doi.org/10.1179/oeh.2007.13.2.213, 2007.

IARC: Polynuclear aromatic compounds, part 1: chemical, environmental, and experimental data. Monographs on the Evaluation of the Carcinogenic Risk of Chemicals to Humans International Agency for Research on Cancer, Lyon, France, 1983.

IARC: Polynuclear aromatic compounds, part 2: carbon blacks, mineral oils, and some nitroarenes. Monographs on the Evaluation of the Carcinogenic Risk of Chemicals to Humans, International Agency for Research on Cancer, Lyon, France, 1984.

IEA: India 2020 Energy Policy Review, 2020.

Indian Meteorological Office: Climate of Delhi at a Glance – A Tourist Guide. Accessed 15 March 2018. Available from: http://amssdelhi.gov.in/forecast/Climate.pdf, 2018.

International Institute for Population Sciences: National Family Health Survey India 1992-1993, Bombay, India, 1995.

International Institute for Population Sciences: National Family Health Survey (NFHS-2) 1998-1999, Mumbai, India, 2000.

International Institute for Population Sciences: National Family Health Survey (NFHS-3) 2005-2006, Mumbai, India, 2007.

International Institute for Population Sciences: National Family Health Survey (NFHS-4) 2015-2016, Mumbai, India, 2017.

IPCC: IPCC Guidelines for National Greenhouse Gas Inventories: Chapter 5 Incineration and open burning of waste, Geneva, Switzerland, 2006.

IPCC: Technical summary, in: The Physical Science Basis. Intergovernmental Panel on Climate Change, edited by: Solomon, S., Qin, D., Manning, M., Chen, Z., Marquis, M., Averyt, K. B., Tignor, M., and Miller, H. L., Cambridge University Press, Cambridge, UK, 19-93, 2007.

Jaffe, D. A., and Wigder, N. L.: Ozone production from wildfires: A critical review, Atmospheric Environment, 51, 1-10, https://doi.org/10.1016/j.atmosenv.2011.11.063, 2012.

Jain, N., Bhatia, A., and Pathak, H.: Emission of Air Pollutants from Crop Residue Burning in India, Aerosol Air Qual. Res., 14, 422-430, https://doi.org/10.4209/aaqr.2013.01.0031, 2014.

Jathar, S. H., Woody, M., Pye, H. O. T., Baker, K. R., and Robinson, A. L.: Chemical transport model simulations of organic aerosol in southern California: model evaluation and gasoline and diesel source contributions, Atmos. Chem. Phys., 17, 4305-4318, https://doi.org/10.5194/acp-17-4305-2017, 2017.

Jayarathne, T., Stockwell, C. E., Bhave, P. V., Praveen, P. S., Rathnayake, C. M., Islam, M. R., Panday, A. K., Adhikari, S., Maharjan, R., Goetz, J. D., DeCarlo, P. F., Saikawa, E., Yokelson, R. J., and Stone, E. A.: Nepal Ambient Monitoring and Source Testing Experiment (NAMaSTE): emissions of particulate matter from wood- and dung-fueled cooking fires, garbage and crop residue burning, brick kilns, and other sources, Atmos. Chem. Phys., 18, 2259-2286, https://doi.org/10.5194/acp-18-2259-2018, 2018.

Jen, C. N., Hatch, L. E., Selimovic, V., Yokelson, R. J., Weber, R., Fernandez, A. E., Kreisberg, N. M., Barsanti, K. C., and Goldstein, A. H.: Speciated and total emission factors of particulate organics from burning western US wildland fuels and their dependence on combustion efficiency, Atmos. Chem. Phys., 19, 1013-1026, https://doi.org/10.5194/acp-19-1013-2019, 2019.

Jenkins, B. M., Jones, A. D., Turn, S. Q., and Williams, R. B.: Emission Factors for Polycyclic Aromatic Hydrocarbons from Biomass Burning, Environmental Science & Technology, 30, 2462-2469, https://doi.org/10.1021/es950699m, 1996.

Jia, Y. L., Stone, D., Wang, W. T., Schrlau, J., Tao, S., and Simonich, S. L. M.: Estimated Reduction in Cancer Risk due to PAH Exposures If Source Control Measures during the 2008 Beijing Olympics Were Sustained, Environmental Health Perspectives, 119, 815-820, https://doi.org/10.1289/ehp.1003100, 2011.

Jobson, B. T., Parrish, D. D., Goldan, P., Kuster, W., Fehsenfeld, F. C., Blake, D. R., Blake, N. J., and Niki, H.: Spatial and temporal variability of nonmethane hydrocarbon mixing ratios and their relation to photochemical lifetime, Journal of Geophysical Research: Atmospheres, 103, 13557-13567, https://doi.org/10.1029/97jd01715, 1998.

Johansson, K. O., Dillstrom, T., Monti, M., El Gabaly, F., Campbell, M. F., Schrader, P. E., Popolan-Vaida, D. M., Richards-Henderson, N. K., Wilson, K. R., Violi, A., and Michelsen, H. A.: Formation and emission of large furans and oxygenated hydrocarbons from flames, Proceedings of the National Academy of Sciences, 113, 8374-8379, https://doi.org/10.1073/pnas.1604772113, 2016.

Kakareka, S. V., Kukharchyk, T. I., and Khomich, V. S.: Study of PAH emission from the solid fuels combustion in residential furnaces, Environmental Pollution, 133, 383-387, https://doi.org/10.1016/j.envpol.2004.01.009, 2005.

Karakoçak, B. B., Patel, S., Ravi, N., and Biswas, P.: Investigating the Effects of Stove Emissions on Ocular and Cancer Cells, Scientific Reports, 9, 1870, https://doi.org/10.1038/s41598-019-38803-4, 2019.

Karasek, F. W., and Tong, H. Y.: Semi-preparative high-performance liquid chromatographic analysis of complex organic mixtures, Journal of Chromatography A 332, 169-179, https://doi.org/10.1016/S0021-9673(01)83294-5, 1985.

Kaushal, L. A.: Examining the policy-practice gap- The issue of crop burning induced Particulate Matter pollution in Northwest India, Ecosystem Health and Sustainability, 6, 1846460, https://doi.org/10.1080/20964129.2020.1846460, 2020.

Kaza, S., Yao, L. C., Bhada-Tata, P., and Van Woerden, F.: What a waste 2.0: A global snapshot of solid waste managment to 2050 World Bank, Washington DC. USA, p71, 2018.

Kerminen, V.-M., Lihavainen, H., Komppula, M., Viisanen, Y., and Kulmala, M.: Direct observational evidence linking atmospheric aerosol formation and cloud droplet activation, Geophysical Research Letters, 32, L14803, https://doi.org/10.1029/2005gl023130, 2005.

Khillare, P. S., Hoque, R. R., Shridhar, V., Agarwal, T., and Balachandran, S.: Temporal variability of benzene concentration in the ambient air of Delhi: A comparative assessment of pre- and post-CNG periods, Journal of Hazardous Materials, 154, 1013-1018, https://doi.org/10.1016/j.jhazmat.2007.11.006, 2008.

Kiely, L., Spracklen, D. V., Wiedinmyer, C., Conibear, L., Reddington, C. L., Archer-Nicholls, S., Lowe, D., Arnold, S. R., Knote, C., Khan, M. F., Latif, M. T., Kuwata, M., Budisulistiorini, S. H., and Syaufina, L.: New estimate of particulate emissions from Indonesian peat fires in 2015, Atmos. Chem. Phys., 19, 11105-11121, https://doi.org/10.5194/acp-19-11105-2019, 2019.

Kim Oanh, N. T., Bætz Reutergårdh, L., and Dung, N. T.: Emission of Polycyclic Aromatic Hydrocarbons and Particulate Matter from Domestic Combustion of Selected Fuels, Environmental Science & Technology, 33, 2703-2709, https://doi.org/10.1021/es980853f, 1999.

Kim Oanh, N. T., Nghiem, L. H., and Phyu, Y. L.: Emission of Polycyclic Aromatic Hydrocarbons, Toxicity, and Mutagenicity from Domestic Cooking Using Sawdust Briquettes, Wood, and Kerosene, Environmental Science & Technology, 36, 833-839, https://doi.org/10.1021/es011060n, 2002.

Kim Oanh, N. T., Albina, D. O., Ping, L., and Wang, X.: Emission of particulate matter and polycyclic aromatic hydrocarbons from select cookstove–fuel systems in Asia, Biomass and Bioenergy, 28, 579-590, https://doi.org/10.1016/j.biombioe.2005.01.003, 2005.

Kim Oanh, N. T., Tipayarom, A., Bich, T. L., Tipayarom, D., Simpson, C. D., Hardie, D., and Sally Liu, L. J.: Characterization of gaseous and semi-volatile organic compounds emitted from field burning of rice straw, Atmospheric Environment, 119, 182-191, https://doi.org/10.1016/j.atmosenv.2015.08.005, 2015.

Kinghorn, R. M., and Marriott, P. J.: Enhancement of Signal-to-Noise Ratios in Capillary Gas Chromatography by Using a Longitudinally Modulated Cryogenic System, Journal of High Resolution Chromatography, 21, 32-38, 1998.

Kirkby, J., Curtius, J., Almeida, J., Dunne, E., Duplissy, J., Ehrhart, S., Franchin, A., Gagne, S., Ickes, L., Kurten, A., Kupc, A., Metzger, A., Riccobono, F., Rondo, L., Schobesberger, S., Tsagkogeorgas, G., Wimmer, D., Amorim, A., Bianchi, F., Breitenlechner, M., David, A., Dommen, J., Downard, A., Ehn, M., Flagan, R. C., Haider, S., Hansel, A., Hauser, D., Jud, W., Junninen, H., Kreissl, F., Kvashin, A., Laaksonen, A., Lehtipalo, K., Lima, J., Lovejoy, E. R., Makhmutov, V., Mathot, S., Mikkila, J., Minginette, P., Mogo, S., Nieminen, T., Onnela, A., Pereira, P., Petaja, T., Schnitzhofer, R., Seinfeld, J. H., Sipila, M., Stozhkov, Y., Stratmann, F., Tome, A., Vanhanen, J., Viisanen, Y., Vrtala, A., Wagner, P. E., Walther, H., Weingartner, E., Wex, H., Winkler, P. M., Carslaw, K. S., Worsnop, D. R., Baltensperger, U., and Kulmala, M.: Role of sulphuric acid, ammonia and galactic cosmic rays in atmospheric aerosol nucleation, Nature, 476, 429-U477, https://doi.org/10.1038/nature10343, 2011.

Ko, Y. C., Lee, C. H., Chen, M. J., Huang, C. C., Chang, W. Y., Lin, H. J., Wang, H. Z., and Chang, P. Y.: Risk factors for primary lung cancer among non-smoking women in Taiwan, International Journal of Epidemiology, 26, 24-31, https://doi.org/10.1093/ije/26.1.24, 1997.

Kocak, D., Ozel, M. Z., Gogus, F., Hamilton, J. F., and Lewis, A. C.: Determination of volatile nitrosamines in grilled lamb and vegetables using comprehensive gas chromatography – Nitrogen chemiluminescence detection, Food Chemistry, 135, 2215-2220, https://doi.org/10.1016/j.foodchem.2012.07.002, 2012.

Kochman, M., Gordin, A., Alon, T., and Amirav, A.: Flow modulation comprehensive two-dimensional gas chromatography–mass spectrometry with a supersonic molecular beam, Journal of Chromatography A, 1129, 95-104, https://doi.org/10.1016/j.chroma.2006.06.079, 2006.

Kodros, J. K., Carter, E., Brauer, M., Volckens, J., Bilsback, K. R., L'Orange, C., Johnson, M., and Pierce, J. R.: Quantifying the Contribution to Uncertainty in Mortality Attributed to Household, Ambient, and Joint Exposure to $PM_{2.5}$ From Residential Solid Fuel Use, Geohealth, 2, 25-39, https://doi.org/10.1002/2017gh000115, 2018.

Kortelainen, M., Jokiniemi, J., Tiitta, P., Tissari, J., Lamberg, H., Leskinen, J., Grigonyte-Lopez Rodriguez, J., Koponen, H., Antikainen, S., Nuutinen, I., Zimmermann, R., and Sippula, O.:

Time-resolved chemical composition of small-scale batch combustion emissions from various wood species, Fuel, 233, 224-236, https://doi.org/10.1016/j.fuel.2018.06.056, 2018.

Koss, A. R., Sekimoto, K., Gilman, J. B., Selimovic, V., Coggon, M. M., Zarzana, K. J., Yuan, B., Lerner, B. M., Brown, S. S., Jimenez, J. L., Krechmer, J., Roberts, J. M., Warneke, C., Yokelson, R. J., and de Gouw, J.: Non-methane organic gas emissions from biomass burning: identification, quantification, and emission factors from PTR-ToF during the FIREX 2016 laboratory experiment, Atmos. Chem. Phys., 18, 3299-3319, https://doi.org/10.5194/acp-18-3299-2018, 2018.

Kroll, J. H., and Seinfeld, J. H.: Chemistry of secondary organic aerosol: Formation and evolution of low-volatility organics in the atmosphere, Atmospheric Environment, 42, 3593-3624, https://doi.org/10.1016/j.atmosenv.2008.01.003, 2008.

Kroll, J. H., Donahue, N. M., Jimenez, J. L., Kessler, S. H., Canagaratna, M. R., Wilson, K. R., Altieri, K. E., Mazzoleni, L. R., Wozniak, A. S., Bluhm, H., Mysak, E. R., Smith, J. D., Kolb, C. E., and Worsnop, D. R.: Carbon oxidation state as a metric for describing the chemistry of atmospheric organic aerosol, Nature Chemistry, 3, 133-139, https://doi.org/10.1038/nchem.948, 2011.

Kulkarni, P., and Venkataraman, C.: Atmospheric polycyclic aromatic hydrocarbons in Mumbai, India, Atmospheric Environment, 34, 2785-2790, https://doi.org/10.1016/S1352-2310(99)00312-X, 2000.

Kumar, A.: Benzene and toluene profiles in ambient air of Delhi as determined by active sampling and GC analysis, 252-257 pp., 2006.

Kumar, P., Jain, S., Gurjar, B. R., Sharma, P., Khare, M., Morawska, L., and Britter, R.: New Directions: Can a “blue sky” return to Indian megacities?, Atmospheric Environment, 71, 198-201, https://doi.org/10.1016/j.atmosenv.2013.01.055, 2013.

Kumar, P., Khare, M., Harrison, R. M., Bloss, W. J., Lewis, A. C., Coe, H., and Morawska, L.: New directions: Air pollution challenges for developing megacities like Delhi, Atmospheric Environment, 122, 657-661, https://doi.org/10.1016/j.atmosenv.2015.10.032, 2015.

Kumar, V., Chandra, B. P., and Sinha, V.: Large unexplained suite of chemically reactive compounds present in ambient air due to biomass fires, Scientific Reports, 8, 626, https://doi.org/10.1038/s41598-017-19139-3, 2018.

Kumari, K., Kumar, S., Rajagopal, V., Khare, A., and Kumar, R.: Emission from open burning of municipal solid waste in India, Environmental Technology, 40, 2201-2214, https://doi.org/10.1080/09593330.2017.1351489, 2019.

Kurokawa, J., Ohara, T., Morikawa, T., Hanayama, S., Janssens-Maenhout, G., Fukui, T., Kawashima, K., and Akimoto, H.: Emissions of air pollutants and greenhouse gases over Asian regions during 2000–2008: Regional Emission inventory in ASia (REAS) version 2, Atmos. Chem. Phys., 13, 11019-11058, https://doi.org/10.5194/acp-13-11019-2013, 2013.

Kurokawa, J., and Ohara, T.: Long-term historical trends in air pollutant emissions in Asia: Regional Emission inventory in ASia (REAS) version 3, Atmos. Chem. Phys., 20, 12761–12793, https://doi.org/10.5194/acp-20-12761-2020, 2020.

Laaksonen, A., Hamed, A., Joutsensaari, J., Hiltunen, L., Cavalli, F., Junkermann, W., Asmi, A., Fuzzi, S., and Facchini, M. C.: Cloud condensation nucleus production from nucleation events at a highly polluted region, Geophysical Research Letters, 32, L06812, https://doi.org/10.1029/2004gl022092, 2005.

LaClair, R. W., Bueno, P. A., and Seeley, J. V.: A systematic analysis of a flow-switching modulator for comprehensive two-dimensional gas chromatography, Journal of Separation Science, 27, 389-396, https://doi.org/10.1002/jssc.200301668, 2004.

Lal, R. M., Nagpure, A. S., Luo, L. N., Tripathi, S. N., Ramaswami, A., Bergin, M. H., and Russell, A. G.: Municipal solid waste and dung cake burning: discoloring the Taj Mahal and human health impacts in Agra, Environmental Research Letters, 11, https://doi.org/10.1088/1748-9326/11/10/104009, 2016.

Lamarque, J. F., Bond, T. C., Eyring, V., Granier, C., Heil, A., Klimont, Z., Lee, D., Liousse, C., Mieville, A., Owen, B., Schultz, M. G., Shindell, D., Smith, S. J., Stehfest, E., Van Aardenne, J., Cooper, O. R., Kainuma, M., Mahowald, N., McConnell, J. R., Naik, V., Riahi, K., and van Vuuren, D. P.: Historical (1850-2000) gridded anthropogenic and biomass burning emissions of reactive gases and aerosols: methodology and application, Atmospheric Chemistry and Physics, 10, 7017-7039, https://doi.org/10.5194/acp-10-7017-2010, 2010.

Lanz, V. A., Alfarra, M. R., Baltensperger, U., Buchmann, B., Hueglin, C., and Prévôt, A. S. H.: Source apportionment of submicron organic aerosols at an urban site by factor analytical modelling of aerosol mass spectra, Atmos. Chem. Phys., 7, 1503-1522, https://doi.org/10.5194/acp-7-1503-2007, 2007.

Lanz, V. A., Alfarra, M. R., Baltensperger, U., Buchmann, B., Hueglin, C., Szidat, S., Wehrli, M. N., Wacker, L., Weimer, S., Caseiro, A., Puxbaum, H., and Prevot, A. S. H.: Source Attribution of Submicron Organic Aerosols during Wintertime Inversions by Advanced Factor Analysis of Aerosol Mass Spectra, Environmental Science & Technology, 42, 214-220, https://doi.org/10.1021/es0707207, 2008.

Larsen, J. C., and Larsen, P. B.: Air pollution and Health, Issues in environmental science and technology, edited by: Hester, R. E., and Harrison, R. M., Royal Society of Chemistry, London, UK, 1998.

Laskin, A., Laskin, J., and Nizkorodov, S. A.: Chemistry of Atmospheric Brown Carbon, Chemical Reviews, 115, 4335-4382, https://doi.org/10.1021/cr5006167, 2015.

Lauraguais, A., Coeur, C., Cassez, A., Deboudt, K., Fourmentin, M., and Choël, M.: Atmospheric reactivity of hydroxyl radicals with guaiacol (2-methoxyphenol), a biomass burning emitted compound: Secondary organic aerosol formation and gas-phase oxidation products, Atmospheric Environment, 86, 155–163, https://doi.org/10.1016/j.atmosenv.2013.11.074, 2014.

Lee, A., Goldstein, A. H., Kroll, J. H., Ng, N. L., Varutbangkul, V., Flagan, R. C., and Seinfeld, J. H.: Gas-phase products and secondary aerosol yields from the photooxidation of 16 different terpenes, Journal of Geophysical Research: Atmospheres, 111, https://doi.org/10.1029/2006jd007050, 2006.

Lee, B. H., Lopez-Hilfiker, F. D., Mohr, C., Kurtén, T., Worsnop, D. R., and Thornton, J. A.: An Iodide-Adduct High-Resolution Time-of-Flight Chemical-Ionization Mass Spectrometer: Application to Atmospheric Inorganic and Organic Compounds, Environmental Science & Technology, 48, 6309-6317, https://doi.org/10.1021/es500362a, 2014.

Lee, R. G. M., Coleman, P., Jones, J. L., Jones, K. C., and Lohmann, R.: Emission Factors and Importance of PCDD/Fs, PCBs, PCNs, PAHs and PM10 from the Domestic Burning of Coal and Wood in the U.K, Environmental Science & Technology, 39, 1436-1447, https://doi.org/10.1021/es048745i, 2005.

Leko: ChromaTOF 5.0. Accessed 10 08 2020. Available from: https://www.leco.com/product/chromatof-software, 2019.

Lelieveld, J., Evans, J. S., Fnais, M., Giannadaki, D., and Pozzer, A.: The contribution of outdoor air pollution sources to premature mortality on a global scale, Nature, 525, 367, https://doi.org/10.1038/nature15371, 2015.

Lemieux, P. M., Lutes, C. C., Abbott, J. A., and Aldous, K. M.: Emissions of Polychlorinated Dibenzo-p-dioxins and Polychlorinated Dibenzofurans from the Open Burning of Household Waste in Barrels, Environmental Science & Technology, 34, 377-384, https://doi.org/10.1021/es990465t, 2000.

Lemieux, P. M., Gullett, B. K., Lutes, C. C., Winterrowd, C. K., and Winters, D. L.: Variables Affecting Emissions of PCDD/Fs from Uncontrolled Combustion of Household Waste in Barrels, Journal of the Air & Waste Management Association, 53, 523-531, https://doi.org/10.1080/10473289.2003.10466192, 2003.

Leppalahti, J., and Koljonen, T.: Nitrogen evolution from coal, peat and wood during gasification - literature review, Fuel Processing Technology, 43, 1-45, https://doi.org/10.1016/0378-3820(94)00123-b, 1995.

Lerner, B. M., Gilman, J. B., Aikin, K. C., Atlas, E. L., Goldan, P. D., Graus, M., Hendershot, R., Isaacman-VanWertz, G. A., Koss, A., Kuster, W. C., Lueb, R. A., McLaughlin, R. J., Peischl, J., Sueper, D., Ryerson, T. B., Tokarek, T. W., Warneke, C., Yuan, B., and de Gouw, J. A.: An improved, automated whole air sampler and gas chromatography mass spectrometry analysis system for volatile organic compounds in the atmosphere, Atmos. Meas. Tech., 10, 291-313, https://doi.org/10.5194/amt-10-291-2017, 2017.

Lewis, A., Hopkins, J., Carslaw, D., Hamilton, J., Nelson, B., Stewart, G., Dernie, J., Passant, N., and Murrells, T.: An increasing role for solvent emissions and implications for future measurements of Volatile Organic Compounds, Philosophical Transactions of the Royal Society of London. Series A, Mathematical and Physical Sciences, 378, https://doi.org/10.1098/rsta.2019.0328, 2020.

Lewis, A. C., Carslaw, N., Marriott, P. J., Kinghorn, R. M., Morrison, P., Lee, A. L., Bartle, K. D., and Pilling, M. J.: A larger pool of ozone-forming carbon compounds in urban atmospheres, Nature, 405, 778-781, https://doi.org/10.1038/35015540, 2000.

Lewtas, J.: Air pollution combustion emissions: Characterization of causative agents and mechanisms associated with cancer, reproductive, and cardiovascular effects, Mutation Research/Reviews in Mutation Research, 636, 95-133, https://doi.org/10.1016/j.mrrev.2007.08.003, 2007.

Li, B. W., Ho, S. S. H., Gong, S. L., Ni, J. W., Li, H. R., Han, L. Y., Yang, Y., Qi, Y. J., and Zhao, D. X.: Characterization of VOCs and their related atmospheric processes in a central Chinese

city during severe ozone pollution periods, Atmospheric Chemistry and Physics, 19, 617-638, https://doi.org/10.5194/acp-19-617-2019, 2019.

Li, M., Zhang, S., Jiang, C., Zhu, G., Fowler, M., Achal, S., Milovic, M., Robinson, R., and Larter, S.: Two-dimensional gas chromatograms as fingerprints of sour gas-associated oils, Organic Geochemistry, 39, 1144-1149, https://doi.org/10.1016/j.orggeochem.2008.02.015, 2008.

Lidster, R. T., Hamilton, J. F., and Lewis, A. C.: The application of two total transfer valve modulators for comprehensive two-dimensional gas chromatography of volatile organic compounds, Journal of Separation Science, 34, 812-821, https://doi.org/10.1002/jssc.201000710, 2011.

Liljegren, J., and Stevens, P.: Kinetics of the Reaction of OH Radicals with 3-Methylfuran at Low Pressure, International Journal of Chemical Kinetics, 45, 787-794, 10.1002/kin.20814, 2013.

Lim, C. Y., Hagan, D. H., Coggon, M. M., Koss, A. R., Sekimoto, K., de Gouw, J., Warneke, C., Cappa, C. D., and Kroll, J. H.: Secondary organic aerosol formation from the laboratory oxidation of biomass burning emissions, Atmos. Chem. Phys., 19, 12797-12809, 10.5194/acp-19-12797-2019, 2019.

Lim, S. S., Vos, T., Flaxman, A. D., Danaei, G., Shibuya, K., Adair-Rohani, H., AlMazroa, M. A., Amann, M., Anderson, H. R., Andrews, K. G., Aryee, M., Atkinson, C., Bacchus, L. J., Bahalim, A. N., Balakrishnan, K., Balmes, J., Barker-Collo, S., Baxter, A., Bell, M. L., Blore, J. D., Blyth, F., Bonner, C., Borges, G., Bourne, R., Boussinesq, M., Brauer, M., Brooks, P., Bruce, N. G., Brunekreef, B., Bryan-Hancock, C., Bucello, C., Buchbinder, R., Bull, F., Burnett, R. T., Byers, T. E., Calabria, B., Carapetis, J., Carnahan, E., Chafe, Z., Charlson, F., Chen, H., Chen, J. S., Cheng, A. T.-A., Child, J. C., Cohen, A., Colson, K. E., Cowie, B. C., Darby, S., Darling, S., Davis, A., Degenhardt, L., Dentener, F., Des Jarlais, D. C., Devries, K., Dherani, M., Ding, E. L., Dorsey, E. R., Driscoll, T., Edmond, K., Ali, S. E., Engell, R. E., Erwin, P. J., Fahimi, S., Falder, G., Farzadfar, F., Ferrari, A., Finucane, M. M., Flaxman, S., Fowkes, F. G. R., Freedman, G., Freeman, M. K., Gakidou, E., Ghosh, S., Giovannucci, E., Gmel, G., Graham, K., Grainger, R., Grant, B., Gunnell, D., Gutierrez, H. R., Hall, W., Hoek, H. W., Hogan, A., Hosgood, H. D., Hoy, D., Hu, H., Hubbell, B. J., Hutchings, S. J., Ibeanusi, S. E., Jacklyn, G. L., Jasrasaria, R., Jonas, J. B., Kan, H., Kanis, J. A., Kassebaum, N., Kawakami, N., Khang, Y.-H., Khatibzadeh, S., Khoo, J.-P., Kok, C., Laden, F., Lalloo, R., Lan, Q., Lathlean, T., Leasher, J. L., Leigh, J., Li,

Y., Lin, J. K., Lipshultz, S. E., London, S., Lozano, R., Lu, Y., Mak, J., Malekzadeh, R., Mallinger, L., Marcenes, W., March, L., Marks, R., Martin, R., McGale, P., McGrath, J., Mehta, S., Memish, Z. A., Mensah, G. A., Merriman, T. R., Micha, R., Michaud, C., Mishra, V., Hanafiah, K. M., Mokdad, A. A., Morawska, L., Mozaffarian, D., Murphy, T., Naghavi, M., Neal, B., Nelson, P. K., Nolla, J. M., Norman, R., Olives, C., Omer, S. B., Orchard, J., Osborne, R., Ostro, B., Page, A., Pandey, K. D., Parry, C. D. H., Passmore, E., Patra, J., Pearce, N., Pelizzari, P. M., Petzold, M., Phillips, M. R., Pope, D., Pope, C. A., Powles, J., Rao, M., Razavi, H., Rehfuess, E. A., Rehm, J. T., Ritz, B., Rivara, F. P., Roberts, T., Robinson, C., Rodriguez-Portales, J. A., Romieu, I., Room, R., Rosenfeld, L. C., Roy, A., Rushton, L., Salomon, J. A., Sampson, U., Sanchez-Riera, L., Sanman, E., Sapkota, A., Seedat, S., Shi, P., Shield, K., Shivakoti, R., Singh, G. M., Sleet, D. A., Smith, E., Smith, K. R., Stapelberg, N. J. C., Steenland, K., Stöckl, H., Stovner, L. J., Straif, K., Straney, L., Thurston, G. D., Tran, J. H., Van Dingenen, R., van Donkelaar, A., Veerman, J. L., Vijayakumar, L., Weintraub, R., Weissman, M. M., White, R. A., Whiteford, H., Wiersma, S. T., Wilkinson, J. D., Williams, H. C., Williams, W., Wilson, N., Woolf, A. D., Yip, P., Zielinski, J. M., Lopez, A. D., Murray, C. J. L., and Ezzati, M.: A comparative risk assessment of burden of disease and injury attributable to 67 risk factors and risk factor clusters in 21 regions, 1990–2010: a systematic analysis for the Global Burden of Disease Study 2010, The Lancet, 380, 2224-2260, https://doi.org/10.1016/S0140-6736(12)61766-8, 2012.

Lipsky, E. M., and Robinson, A. L.: Effects of Dilution on Fine Particle Mass and Partitioning of Semivolatile Organics in Diesel Exhaust and Wood Smoke, Environmental Science & Technology, 40, 155-162, https://doi.org/10.1021/es050319p, 2006.

Liu, Q., Sasco, A. J., Riboli, E., and Hu, M. X.: Indoor Air Pollution and Lung Cancer in Guangzhou, People's Republic of China, American Journal of Epidemiology, 137, 145-154, https://doi.org/10.1093/oxfordjournals.aje.a116654, 1993.

Liu, S. M., Zhou, Y. M., Wang, X. P., Wang, D. L., Lu, J. C., Zheng, J. P., Zhong, N. S., and Ran, P. X.: Biomass fuels are the probable risk factor for chronic obstructive pulmonary disease in rural South China, Thorax, 62, 889-897, 10.1136/thx.2006.061457, 2007.

Liu, X., Huey, L. G., Yokelson, R. J., Selimovic, V., Simpson, I. J., Müller, M., Jimenez, J. L., Campuzano-Jost, P., Beyersdorf, A. J., Blake, D. R., Butterfield, Z., Choi, Y., Crounse, J. D., Day, D. A., Diskin, G. S., Dubey, M. K., Fortner, E., Hanisco, T. F., Hu, W., King, L. E., Kleinman, L., Meinardi, S., Mikoviny, T., Onasch, T. B., Palm, B. B., Peischl, J., Pollack, I. B., Ryerson, T.

B., Sachse, G. W., Sedlacek, A. J., Shilling, J. E., Springston, S., St. Clair, J. M., Tanner, D. J., Teng, A. P., Wennberg, P. O., Wisthaler, A., and Wolfe, G. M.: Airborne measurements of western U.S. wildfire emissions: Comparison with prescribed burning and air quality implications, Journal of Geophysical Research: Atmospheres, 122, 6108-6129, https://doi.org/10.1002/2016jd026315, 2017.

Liu, Y., Shao, M., Fu, L., Lu, S., Zeng, L., and Tang, D.: Source profiles of volatile organic compounds (VOCs) measured in China: Part I, Atmospheric Environment, 42, 6247-6260, https://doi.org/10.1016/j.atmosenv.2008.01.070, 2008.

Liu, Y., Siekmann, F., Renard, P., El Zein, A., Salque, G., Haddad, I., Temime-Roussel, B., Voisin, D., Thissen, R., and Monod, A.: Oligomer and SOA formation through aqueous phase photooxidation of methacrolein and methyl vinyl ketone, Atmospheric Environment, 49, https://doi.org/10.1016/j.atmosenv.2011.12.012, 2011.

Liu, Z. Y., and Phillips, J. B.: Comprehensive 2-dimensional gas-chromatography using an on-column thermal modulator device Journal of Chromatographic Science, 29, 227-231, 1991.

Loza, C. L., Craven, J. S., Yee, L. D., Coggon, M. M., Schwantes, R. H., Shiraiwa, M., Zhang, X., Schilling, K. A., Ng, N. L., Canagaratna, M. R., Ziemann, P. J., Flagan, R. C., and Seinfeld, J. H.: Secondary organic aerosol yields of 12-carbon alkanes, Atmos. Chem. Phys., 14, 1423-1439, https://doi.org/10.5194/acp-14-1423-2014, 2014.

Lu, H., Zhu, L., and Zhu, N.: Polycyclic aromatic hydrocarbon emission from straw burning and the influence of combustion parameters, Atmospheric Environment - ATMOS ENVIRON, 43, 978-983, https://doi.org/10.1016/j.atmosenv.2008.10.022, 2009.

Lu, Q., Zhao, Y., and Robinson, A. L.: Comprehensive organic emission profiles for gasoline, diesel, and gas-turbine engines including intermediate and semi-volatile organic compound emissions, Atmos. Chem. Phys., 18, 17637-17654, https://doi.org/10.5194/acp-18-17637-2018, 2018.

Lyu, R., Shi, Z., Alam, M. S., Wu, X., Liu, D., Vu, T. V., Stark, C., Xu, R., Fu, P., Feng, Y., and Harrison, R. M.: Alkanes and aliphatic carbonyl compounds in wintertime $PM_{2.5}$ in Beijing, China, Atmospheric Environment, 202, 244-255, https://doi.org/10.1016/j.atmosenv.2019.01.023, 2019.

Manzano, P., Arnáiz, E., Diego, J. C., Toribio, L., García-Viguera, C., Bernal, J. L., and Bernal, J.: Comprehensive two-dimensional gas chromatography with capillary flow modulation to

separate FAME isomers, Journal of Chromatography A, 1218, 4952-4959, https://doi.org/10.1016/j.chroma.2011.02.002, 2011.

Marriott, P. J., and Kinghorn, R. M.: Longitudinally modulated cryogenic system. A generally applicable approach to solute trapping and mobilization in gas chromatography, Analytical Chemistry, 69, 2582-2588, https://doi.org/10.1021/ac961310w, 1997.

May, A. A., Presto, A. A., Hennigan, C. J., Nguyen, N. T., Gordon, T. D., and Robinson, A. L.: Gas-particle partitioning of primary organic aerosol emissions: (1) Gasoline vehicle exhaust, Atmospheric Environment, 77, 128-139, https://doi.org/10.1016/j.atmosenv.2013.04.060, 2013.

May, A. A., Nguyen, N. T., Presto, A. A., Gordon, T. D., Lipsky, E. M., Karve, M., Gutierrez, A., Robertson, W. H., Zhang, M., Brandow, C., Chang, O., Chen, S. Y., Cicero-Fernandez, P., Dinkins, L., Fuentes, M., Huang, S. M., Ling, R., Long, J., Maddox, C., Massetti, J., McCauley, E., Miguel, A., Na, K., Ong, R., Pang, Y. B., Rieger, P., Sax, T., Truong, T., Vo, T., Chattopadhyay, S., Maldonado, H., Maricq, M. M., and Robinson, A. L.: Gas- and particle-phase primary emissions from in-use, on-road gasoline and diesel vehicles, Atmospheric Environment, 88, 247-260, https://doi.org/10.1016/j.atmosenv.2014.01.046, 2014.

McCulloch, A., Aucott, M. L., Benkovitz, C. M., Graedel, T. E., Kleiman, G., Midgley, P. M., and Li, Y.-F.: Global emissions of hydrogen chloride and chloromethane from coal combustion, incineration and industrial activities: Reactive Chlorine Emissions Inventory, Journal of Geophysical Research: Atmospheres, 104, 8391-8403, https://doi.org/10.1029/1999jd900025, 1999.

McDonald, J. D., Zielinska, B., Fujita, E. M., Sagebiel, J. C., Chow, J. C., and Watson, J. G.: Fine Particle and Gaseous Emission Rates from Residential Wood Combustion, Environmental Science & Technology, 34, 2080-2091, https://doi.org/10.1021/es9909632, 2000.

McMeeking, G. R., Kreidenweis, S. M., Baker, S., Carrico, C. M., Chow, J. C., Collett Jr., J. L., Hao, W. M., Holden, A. S., Kirchstetter, T. W., Malm, W. C., Moosmüller, H., Sullivan, A. P., and Wold, C. E.: Emissions of trace gases and aerosols during the open combustion of biomass in the laboratory, Journal of Geophysical Research: Atmospheres, 114, https://doi.org/10.1029/2009jd011836, 2009.

Micyus, N. J., McCurry, J. D., and Seeley, J. V.: Analysis of aromatic compounds in gasoline with flow-switching comprehensive two-dimensional gas chromatography, Journal of Chromatography A, 1086, 115-121, https://doi.org/10.1016/j.chroma.2005.06.015, 2005.

Miller, A., and Fisk, G. A.: Combustion Chemistry, Chem. & Eng. News, 31, 22-46, 1987.

Miller, S. L., Anderson, M. J., Daly, E. P., and Milford, J. B.: Source apportionment of exposures to volatile organic compounds. I. Evaluation of receptor models using simulated exposure data, Atmospheric Environment, 36, 3629-3641, https://doi.org/10.1016/S1352-2310(02)00279-0, 2002.

Ministry of Agriculture: Agricultural Statistics At a Glance 2012, 63-120, 2012.

Ministry of Agriculture: National Policy for Management of Crop Residues (NPMCR) Department of Agriculture & Cooperation (Natural Resource Management Division), Krishi Bhawan, New Delhi, 2014.

Mishra, V.: Indoor air pollution from biomass combustion and acute respiratory illness in preschool age children in Zimbabwe, International Journal of Epidemiology, 32, 847-853, https://doi.org/10.1093/ije/dyg240, 2003.

Monien, B. H., Herrmann, K., Florian, S., and Glatt, H.: Metabolic activation of furfuryl alcohol: formation of 2-methylfuranyl DNA adducts in Salmonella typhimurium strains expressing human sulfotransferase 1A1 and in FVB/N mice, Carcinogenesis, 32, 1533-1539, https://doi.org/10.1093/carcin/bgr126, 2011.

Monks, P. S.: Gas-phase radical chemistry in the troposphere, Chemical Society Reviews, 34, 376-395, https://doi.org/10.1039/b307982c, 2005.

Moran-Mendoza, O., Pérez-Padilla, J., Salazar-Flores, M., and Vazquez-Alfaro, F.: Wood smoke-associated lung disease: A clinical, functional, radiological and pathological description, The international journal of tuberculosis and lung disease : the official journal of the International Union against Tuberculosis and Lung Disease, 12, 1092-1098, 2008.

Mukhopadhyay, R., Sambandam, S., Pillarisetti, A., Jack, D., Mukhopadhyay, K., Balakrishnan, K., Vaswani, M., Bates, M. N., Kinney, P., Arora, N., and Smith, K.: Cooking practices, air quality, and the acceptability of advanced cookstoves in Haryana, India: an exploratory study to inform large-scale interventions, Global Health Action, 5, 19016, https://doi.org/10.3402/gha.v5i0.19016, 2012.

Murphy, B. N., Woody, M. C., Jimenez, J. L., Carlton, A. M. G., Hayes, P. L., Liu, S., Ng, N. L., Russell, L. M., Setyan, A., Xu, L., Young, J., Zaveri, R. A., Zhang, Q., and Pye, H. O. T.:

Semivolatile POA and parameterized total combustion SOA in CMAQv5.2: impacts on source strength and partitioning, Atmos. Chem. Phys., 17, 11107-11133, https://doi.org/10.5194/acp-17-11107-2017, 2017.

Murphy, D. M., Cziczo, D. J., Froyd, K. D., Hudson, P. K., Matthew, B. M., Middlebrook, A. M., Peltier, R. E., Sullivan, A., Thomson, D. S., and Weber, R. J.: Single-particle mass spectrometry of tropospheric aerosol particles, Journal of Geophysical Research: Atmospheres, 111, https://doi.org/10.1029/2006JD007340, 2006.

N'Dri, A. B., Kone, A. W., Loukou, S. K. K., Barot, S., and Gignoux, J.: Carbon and nutrient losses through biomass burning, and links with soild fertility and yam (dioscorea alata) production), Experimental Agriculture, 55, 738-751, https://doi.org/10.1017/s0014479718000327, 2019.

Naeher, L. P., Brauer, M., Lipsett, M., Zelikoff, J. T., Simpson, C. D., Koenig, J. Q., and Smith, K. R.: Woodsmoke Health Effects: A Review, Inhalation Toxicology, 19, 67-106, 10.1080/08958370600985875, 2007.

Nagpure, A. S., Ramaswami, A., and Russell, A.: Characterizing the Spatial and Temporal Patterns of Open Burning of Municipal Solid Waste (MSW) in Indian Cities, Environmental Science & Technology, 49, 12904-12912, 10.1021/acs.est.5b03243, 2015.

Nandy, B., Sharma, G., Garg, S., Kumari, S., George, T., Sunanda, Y., and Sinha, B.: Recovery of consumer waste in India – A mass flow analysis for paper, plastic and glass and the contribution of households and the informal sector, Resources, Conservation and Recycling, 101, 167-181, https://doi.org/10.1016/j.resconrec.2015.05.012, 2015.

NASA: MODIS/Terra+Aqua Land Cover Type Yearly L3 Global 500 m SIN Grid, https://doi.org/10.5067/MODIS/MCD12Q1.006, 2011.

NEERI: Air Quality Monitoring, Emission Inventory & Source Apportionment Studies for Delhi, 2008.

NEERI: Air Quality Assessment, Emissions Inventory and Source Apportionment Studies: Mumbai, Central Pollution Control Board, New Delhi, India, 2010.

Ng, N. L., Chhabra, P. S., Chan, A. W. H., Surratt, J. D., Kroll, J. H., Kwan, A. J., McCabe, D. C., Wennberg, P. O., Sorooshian, A., Murphy, S. M., Dalleska, N. F., Flagan, R. C., and Seinfeld, J. H.: Effect of NO_x level on secondary organic aerosol (SOA) formation from the photooxidation of terpenes, Atmos. Chem. Phys., 7, 5159-5174, 10.5194/acp-7-5159-2007, 2007a.

Ng, N. L., Kroll, J. H., Chan, A. W. H., Chhabra, P. S., Flagan, R. C., and Seinfeld, J. H.: Secondary organic aerosol formation from *m*-xylene, toluene, and benzene, Atmos. Chem. Phys., 7, 3909-3922, https://doi.org/10.5194/acp-7-3909-2007, 2007b.

Nisbet, I. C. T., and LaGoy, P. K.: Toxic equivalency factors (TEFs) for polycyclic aromatic hydrocarbons (PAHs), Regulatory Toxicology and Pharmacology, 16, 290-300, https://doi.org/10.1016/0273-2300(92)90009-X, 1992.

Integrated Surface Database (ISD): https://www.ncdc.noaa.gov/isd, 2019.

Novakov, T., and Penner, J. E.: Large contribution of organic aerosols to cloud-condensation-nuclei concentrations, Nature, 365, 823-826, 10.1038/365823a0, 1993.

NSSO: Energy used by Indian households 1993-1994: Fifth quinquennial survey on Consumer Expenditure New Delhi, India, 1997.

NSSO: Household Consumer Expenditure and Employment - Unemployment Situation in India 2002, New Delhi, India, 2003.

NSSO: Household Consumer Expenditure and Employment-Unemployment Situation in India 2003, New Delhi, India, 2005.

NSSO: Energy Sources of Indian Households for Cooking and Lighting , 2004-05, New Delhi, India, 2007a.

NSSO: Household Consumption of Various Goods and Services in India 2004-05, NSS 61st Round, New Delhi, India, 2007b.

NSSO: Household Consumer Expenditure in India, 2006-07, New Delhi, India, 2008.

NSSO: Energy Sources of Indian Households for Cooking and Lighting 2009-2010, New Delhi, India, 2012a.

NSSO: Household Consumption of Various Goods and Services in India 2009-2010, NSS 66st Round, New Delhi, India, 2012b.

NSSO: Household Consumption of Various Goods and Services in India 2011-2012, NSS 68th round, 2014.

NSSO: Energy Sources of Indian Households for Cooking and Lighting, 2011-12, New Delhi, India, 2015a.

NSSO: Energy Sources of Indian Households for Cooking and Lighting, 2011-12, NSS 68th Round, National Sample Survey Office, Ministry of Statistics and Programme Implementation, Government of India, 2015b.

OEHHA: Benzo[a]pyrene as a Toxic Air Contaminant, 1994.

Ohara, T., Akimoto, H., Kurokawa, J., Horii, N., Yamaji, K., Yan, X., and Hayasaka, T.: An Asian emission inventory of anthropogenic emission sources for the period 1980-2020, Atmos. Chem. Phys., 7, 4419-4444, https://doi.org/10.5194/acp-7-4419-2007, 2007.

Olivier, J. G. J., Van Aardenne, J. A., Dentener, F. J., Pagliari, V., Ganzeveld, L. N., and Peters, J. A. H. W.: Recent trends in global greenhouse gas emissions: regional trends 1970–2000 and spatial distribution of key sources in 2000, Environmental Sciences, 2, 81-99, https://doi.org/10.1080/15693430500400345, 2005.

Orozco-Levi, M., Garcia-Aymerich, J., Villar, J., Ramírez-Sarmiento, A., Antó, J. M., and Gea, J.: Wood smoke exposure and risk of chronic obstructive pulmonary disease, European Respiratory Journal, 27, 542, https://doi.org/10.1183/09031936.06.00052705, 2006.

Ots, R., Young, D. E., Vieno, M., Xu, L., Dunmore, R. E., Allan, J. D., Coe, H., Williams, L. R., Herndon, S. C., Ng, N. L., Hamilton, J. F., Bergström, R., Di Marco, C., Nemitz, E., Mackenzie, I. A., Kuenen, J. J. P., Green, D. C., Reis, S., and Heal, M. R.: Simulating secondary organic aerosol from missing diesel-related intermediate-volatility organic compound emissions during the Clean Air for London (ClearfLo) campaign, Atmos. Chem. Phys., 16, 6453-6473, https://doi.org/10.5194/acp-16-6453-2016, 2016.

Özel, M. Z., Hamilton, J. F., and Lewis, A. C.: New Sensitive and Quantitative Analysis Method for Organic Nitrogen Compounds in Urban Aerosol Samples, Environ. Sci. Technol, 45, 1497–1505, 2011.

Padhy, P. K., and Varshney, C. K.: Total non-methane volatile organic compounds (TNMVOC) in the atmosphere of Delhi, Atmospheric Environment, 34, 577-584, https://doi.org/10.1016/S1352-2310(99)00204-6, 2000.

Pagonis, D., Krechmer, J. E., de Gouw, J., Jimenez, J. L., and Ziemann, P. J.: Effects of gas–wall partitioning in Teflon tubing and instrumentation on time-resolved measurements of gas-phase organic compounds, Atmos. Meas. Tech., 10, 4687-4696, https://doi.org/10.5194/amt-10-4687-2017, 2017.

Pandey, A., Sadavarte, P., Rao, A., and Venkataraman, C.: Trends in multi-pollutant emissions from a technology-linked inventory for India: II. Residential, agricultural and informal industry sectors, Atmospheric Environment, 99, 341–352, https://doi.org/10.1016/j.atmosenv.2014.09.080, 2014.

Pandey, K., and Sahu, L. K.: Emissions of volatile organic compounds from biomass burning sources and their ozone formation potential over India, Current Science, 106, 1270-1279, 2014.

Pandharipande, S., Gujrati, M., Mulkutkar, N., and Pandey, S.: Comparative study of extraction & characterization of lignin from wet and dry coconut husk, International journal of Engineering Sciences & Research Technology 7, 659-666, https://doi.org/10.5281/zenodo.1228694, 2018.

Pant, P., and Harrison, R. M.: Critical review of receptor modelling for particulate matter: A case study of India, Atmospheric Environment, 49, 1-12, https://doi.org/10.1016/j.atmosenv.2011.11.060, 2012.

Parliament of India: Air (Prevention and Control of Pollution) Act, in, New Delhi, 1981.

Parmar, R., and Pamnani, A.: Revolution in Rural India through Solid Waste Management, International Journal of Engineering Research in Mechanical and Civil Engineering, 2018.

Passant, N.: Speciation of UK emissions of non-methane volatile organic compounds, Technical report., Abingdon, UK, 2002.

PerezPadilla, R., Regalado, J., Vedal, S., Pare, P., Chapela, R., Sansores, R., and Selman, M.: Exposure to biomass smoke and chronic airway disease in Mexican women - A case-control study, American Journal of Respiratory and Critical Care Medicine, 154, 701-706, https://doi.org/10.1164/ajrccm.154.3.8810608, 1996.

Peterson, L. A.: Electrophilic Intermediates Produced by Bioactivation of Furan, Drug Metabolism Reviews, 38, 615-626, https://doi.org/10.1080/03602530600959417, 2006.

Pettersson, E., Boman, C., Westerholm, R., Boström, D., and Nordin, A.: Stove Performance and Emission Characteristics in Residential Wood Log and Pellet Combustion, Part 2: Wood Stove, Energy & Fuels, 25, 315-323, https://doi.org/10.1021/ef1007787, 2011.

Pfister, G. G., Wiedinmyer, C., and Emmons, L. K.: Impacts of the fall 2007 California wildfires on surface ozone: Integrating local observations with global model simulations, Geophysical Research Letters, 35, L19814, https://doi.org/10.1029/2008GL034747, 2008.

Phillips, J. B., and Xu, J.: Comprehensive multi-dimensional gas chromatography, Journal of Chromatography A, 703, 327-334, https://doi.org/10.1016/0021-9673(95)00297-Z, 1995.

Phillips, J. B., Gaines, R. B., Blomberg, J., van der Wielen, F. W. M., Dimandja, J.-M., Green, V., Granger, J., Patterson, D., Racovalis, L., de Geus, H.-J., de Boer, J., Haglund, P., Lipsky, J., Sinha, V., and Ledford Jr., E. B.: A Robust Thermal Modulator for Comprehensive Two-

Dimensional Gas Chromatography, Journal of High Resolution Chromatography, 22, 3-10, https://doi.org/10.1002/(SICI)1521-4168(19990101)22:1<3::AID-JHRC3>3.0.CO;2-U, 1999.

Planning Commission: Report of the Task Force on Waste to Energy (Volume I) (in the context of Integrated MSW management), Planning commission, New Delhi, India, 2014.

Pokhrel, A. K., Smith, K. R., Khalakdina, A., Deuja, A., and Bates, M. N.: Case–control study of indoor cooking smoke exposure and cataract in Nepal and India, International Journal of Epidemiology, 34, 702-708, 10.1093/ije/dyi015, 2005.

Poliak, M., Kochman, M., and Amirav, A.: Pulsed flow modulation comprehensive two-dimensional gas chromatography, Journal of Chromatography A, 1186, 189-195, https://doi.org/10.1016/j.chroma.2007.09.030, 2008.

Ponette-Gonzalez, A. G., Curran, L. M., Pittman, A. M., Carlson, K. M., Steele, B. G., Ratnasari, D., Mujiman, and Weathers, K. C.: Biomass burning drives atmospheric nutrient redistribution within forested peatlands in Borneo, Environmental Research Letters, 11, 085003, https://doi.org/10.1088/1748-9326/11/8/085003, 2016.

Pope, D., Bruce, N., Dherani, M., Jagoe, K., and Rehfuess, E.: Real-life effectiveness of 'improved' stoves and clean fuels in reducing $PM_{2.5}$ and CO: Systematic review and meta-analysis, Environment International, 101, 7-18, https://doi.org/10.1016/j.envint.2017.01.012, 2017.

Pravallika, S.: Gas Chromatography a Mini Review, Research and Reviews Journal of Pharmaceutical Analysis, 5 55-62, 2016.

Presto, A. A., Nguyen, N. T., Ranjan, M., Reeder, A. J., Lipsky, E. M., Hennigan, C. J., Miracolo, M. A., Riemer, D. D., and Robinson, A. L.: Fine particle and organic vapor emissions from staged tests of an in-use aircraft engine, Atmospheric Environment, 45, 3603-3612, https://doi.org/10.1016/j.atmosenv.2011.03.061, 2011.

Priestley, M., Le Breton, M., Bannan, T. J., Leather, K. E., Bacak, A., Reyes-Villegas, E., De Vocht, F., Shallcross, B. M. A., Brazier, T., Anwar Khan, M., Allan, J., Shallcross, D. E., Coe, H., and Percival, C. J.: Observations of Isocyanate, Amide, Nitrate, and Nitro Compounds From an Anthropogenic Biomass Burning Event Using a ToF-CIMS, Journal of Geophysical Research: Atmospheres, 123, 7687-7704, https://doi.org/10.1002/2017JD027316, 2018.

Putaud, J.-P., Raes, F., Van Dingenen, R., Brüggemann, E., Facchini, M. C., Decesari, S., Fuzzi, S., Gehrig, R., Hüglin, C., Laj, P., Lorbeer, G., Maenhaut, W., Mihalopoulos, N., Müller, K., Querol, X., Rodriguez, S., Schneider, J., Spindler, G., Brink, H. t., Tørseth, K., and

Wiedensohler, A.: A European aerosol phenomenology—2: chemical characteristics of particulate matter at kerbside, urban, rural and background sites in Europe, Atmospheric Environment, 38, 2579-2595, https://doi.org/10.1016/j.atmosenv.2004.01.041, 2004.

Radke, L., Hegg, D., Hobbs, P., Nance, D., Lyons, J., Laursen, K., Weiss, R., Riggan, P., and Ward, D. E.: Particulate and trace gas emissions from large biomass fires in North America, in: Levine, J.S. (ed.) Global Biomass Burning: Atmospheric, Climatic, and Biospheric Implications, The MIT Press, Cambridge, Massachusetts, 209-216, 1991.

Rajamanikam, R., Poyyamoli, G., Kumar, S., and R, L.: The role of non-governmental organizations in residential solid waste management: A case study of Puducherry, a coastal city of India, Waste Management & Research, 32, 867-881, https://doi.org/10.1177/0734242x14544353, 2014.

Ramankutty, N., Evan, A. T., Monfreda, C., and Foley, J. A.: Farming the planet: 1. Geographic distribution of global agricultural lands in the year 2000, Global Biogeochemical Cycles, 22, https://doi.org/10.1029/2007gb002952, 2008.

Ramirez-Venegas, A., Sansores, R. H., Perez-Padilla, R., Regalado, J., Velazquez, A., Sanchez, C., and Mayar, M. E.: Survival of patients with chronic obstructive pulmonary disease due to biomass smoke and tobacco, American Journal of Respiratory and Critical Care Medicine, 173, 393-397, https://doi.org/10.1164/rccm.200504-568OC, 2006.

Ramírez, N., Cuadras, A., Rovira, E., Marcé Rosa, M., and Borrull, F.: Risk Assessment Related to Atmospheric Polycyclic Aromatic Hydrocarbons in Gas and Particle Phases near Industrial Sites, Environmental Health Perspectives, 119, 1110-1116, https://doi.org/10.1289/ehp.1002855, 2011.

Ramírez, N., Özel, M. Z., Lewis, A. C., Marcé, R. M., Borrull, F., and Hamilton, J. F.: Determination of nicotine and N-nitrosamines in house dust by pressurized liquid extraction and comprehensive gas chromatography—Nitrogen chemiluminiscence detection, Journal of Chromatography A, 1219, 180-187, https://doi.org/10.1016/j.chroma.2011.11.017, 2012.

Ramírez, N., Özel, M. Z., Lewis, A. C., Marcé, R. M., Borrull, F., and Hamilton, J. F.: Exposure to nitrosamines in thirdhand tobacco smoke increases cancer risk in non-smokers, Environment International, 71, 139-147, https://doi.org/10.1016/j.envint.2014.06.012, 2014.

Ramírez, N., Vallecillos, L., Lewis, A. C., Borrull, F., Marcé, R. M., and Hamilton, J. F.: Comparative study of comprehensive gas chromatography-nitrogen chemiluminescence detection and gas chromatography-ion trap-tandem mass spectrometry for determining nicotine and carcinogen organic nitrogen compounds in thirdhand tobacco smoke, Journal of Chromatography A, 1426, 191-200, https://doi.org/10.1016/j.chroma.2015.11.035, 2015.

Ravindranath, V., Boyd, M. R., and Burka, L. T.: Reactive metabolites from the bioactivation of toxic methylfurans, Science, 224, 884-886, https://doi.org/10.1126/science.6719117, 1984.

Reddy, M. S., and Venkataraman, C.: Inventory of aerosol and sulphur dioxide emissions from India. Part II—biomass combustion, Atmospheric Environment, 36, 699-712, https://doi.org/10.1016/S1352-2310(01)00464-2, 2002.

Ren, Q. Q., and Zhao, C. S.: Evolution of fuel-N in gas phase during biomass pyrolysis, Renewable & Sustainable Energy Reviews, 50, 408-418, https://doi.org/10.1016/j.rser.2015.05.043, 2015.

Reyes-Villegas, E., Panda, U., Darbyshire, E., Cash, J., Joshi, R., Langford, B., Di Marco, C. F., Mullinger, N., Acton, J., Drysdale, W., Nemitz, E., Flynn, M., Voliotis, A., McFiggans, G., Coe, H., Lee, J., Hewitt, C. N., Heal, M. R., Gunthe, S. S., Shivani, S., Gadi, R., Singh, S., Soni, V., and Allan, J.: PM1 chemical composition and source apportionment at two sites in Delhi, India across multiple seasons. , Atmos. Chem. Phys. Discuss. , https://doi.org/10.5194/acp-2020-894, 2020.

Rinne, S. T., Rodas, E. J., Bender, B. S., Rinne, M. L., Simpson, J. M., Galer-Unti, R., and Glickman, L. T.: Relationship of pulmonary function among women and children to indoor air pollution from biomass use in rural Ecuador, Respiratory Medicine, 100, 1208-1215, https://doi.org/10.1016/j.rmed.2005.10.020, 2006.

Robinson, A. L., Donahue, N. M., Shrivastava, M. K., Weitkamp, E. A., Sage, A. M., Grieshop, A. P., Lane, T. E., Pierce, J. R., and Pandis, S. N.: Rethinking organic aerosols: Semivolatile emissions and photochemical aging, Science, 315, 1259-1262, https://doi.org/10.1126/science.1133061, 2007.

Rubin, J. I., Kean, A. J., Harley, R. A., Millet, D. B., and Goldstein, A. H.: Temperature dependence of volatile organic compound evaporative emissions from motor vehicles,

Journal of Geophysical Research: Atmospheres, 111, D03305, https://doi.org/10.1029/2005jd006458, 2006.

Sadavarte, P., and Venkataraman, C.: Trends in multi-pollutant emissions from a technology-linked inventory for India: I. Industry and transport sectors, Atmospheric Environment, 99, 353-364, https://doi.org/10.1016/j.atmosenv.2014.09.081, 2014.

Sahu, L. K., and Saxena, P.: High time and mass resolved PTR-TOF-MS measurements of VOCs at an urban site of India during winter: Role of anthropogenic, biomass burning, biogenic and photochemical sources, Atmospheric Research, 164-165, 84-94, https://doi.org/10.1016/j.atmosres.2015.04.021, 2015.

Sahu, L. K., Yadav, R., and Pal, D.: Source identification of VOCs at an urban site of western India: Effect of marathon events and anthropogenic emissions, Journal of Geophysical Research: Atmospheres, 121, 2416-2433, https://doi.org/10.1002/2015jd024454, 2016.

Sambandam, S., Balakrishnan, K., Ghosh, S., Sadasivam, A., Madhav, S., Ramasamy, R., Samanta, M., Mukhopadhyay, K., Rehman, H., and Ramanathan, V.: Can Currently Available Advanced Combustion Biomass Cook-Stoves Provide Health Relevant Exposure Reductions? Results from Initial Assessment of Select Commercial Models in India, EcoHealth, 12, 25-41, https://doi.org/10.1007/s10393-014-0976-1, 2015.

Sander, S. P., Friedl, R. R., Abbatt, J. P. D., Barker, J. P., Burkholder, J. B., Golden, D. M., Kolb, C. E., Kurylo, M. J., Moortgat, G. K., Winer, A. M., Huie, R. E., and Orkin, V. L.: Photochemical data in: Chemical Kinetics and Photochemical Data for Use in Atmospheric Studies: Evaluation Number 17 NASA, California, USA, 2011.

Saud, T., Mandal, T. K., Gadi, R., Singh, D. P., Sharma, S. K., Saxena, M., and Mukherjee, A.: Emission estimates of particulate matter (PM) and trace gases (SO_2, NO and NO_2) from biomass fuels used in rural sector of Indo-Gangetic Plain, India, Atmospheric Environment, 45, 5913-5923, https://doi.org/10.1016/j.atmosenv.2011.06.031, 2011.

Saud, T., Gautam, R., Mandal, T. K., Gadi, R., Singh, D. P., Sharma, S. K., Dahiya, M., and Saxena, M.: Emission estimates of organic and elemental carbon from household biomass fuel used over the Indo-Gangetic Plain (IGP), India, Atmospheric Environment, 61, 212-220, https://doi.org/10.1016/j.atmosenv.2012.07.030, 2012.

Schauer, J. J., Kleeman, M. J., Cass, G. R., and Simoneit, B. R. T.: Measurement of Emissions from Air Pollution Sources. 3. C_1−C_{29} Organic Compounds from Fireplace Combustion of

Wood, Environmental Science & Technology, 35, 1716-1728, https://doi.org/10.1021/es001331e, 2001.

Seeley, J. V., Kramp, F., and Hicks, C. J.: Comprehensive Two-Dimensional Gas Chromatography via Differential Flow Modulation, Analytical Chemistry, 72, 4346-4352, https://doi.org/10.1021/ac000249z, 2000.

Seeley, J. V., Micyus, N. J., McCurry, J. D., and Seeley, S. K.: Comprehensive two-dimensional gas chromatography with a simple fluidic modulator, American Laboratory, 38, 24-26, 2006.

Seeley, J. V., Micyus, N. J., Bandurski, S. V., Seeley, S. K., and McCurry, J. D.: Microfluidic Deans Switch for Comprehensive Two-Dimensional Gas Chromatography, Analytical Chemistry, 79, 1840-1847, https://doi.org/10.1021/ac061881g, 2007a.

Seeley, J. V., Seeley, S. K., Libby, E. K., Breitbach, Z. S., and Armstrong, D. W.: Comprehensive two-dimensional gas chromatography using a high-temperature phosphonium ionic liquid column, Analytical and Bioanalytical Chemistry, 390, 323-332, https://doi.org/10.1007/s00216-007-1676-2, 2008a.

Seeley, J. V., Libby, E. M., Seeley, S. K., and McCurry, J. D.: Comprehensive two-dimensional gas chromatography analysis of high-ethanol containing motor fuels, Journal of Separation Science, 31, 3337-3346, doi:10.1002/jssc.200800258, 2008b.

Seeley, S., V Bandurski, S., G Brown, R., D McCurry, J., and V Seeley, J.: A Comprehensive Two-Dimensional Gas Chromatography Method for Analyzing Extractable Petroleum Hydrocarbons in Water and Soil, 657-663 pp., 2007b.

Sehgal, M., Suresh, R., Sharma, V. P., and Gautam, S. K.: Variations in air quality at filling stations, Delhi, India, International Journal of Environmental Studies, 68, 845-849, 2011.

Seinfeld, J. H., and Spyros, N. P.: Atmospheric Chemistry and Physics: From Air Pollution to Climate Change, in, Wiley, California, USA, 2006.

Seinfeld, J. H., and Pandis, S. N.: Atmospheric Chemistry and Physics: From Air Pollution to Climate Change, Wiley, 2012.

Sekimoto, K., Koss, A. R., Gilman, J. B., Selimovic, V., Coggon, M. M., Zarzana, K. J., Yuan, B., Lerner, B. M., Brown, S. S., Warneke, C., Yokelson, R. J., Roberts, J. M., and de Gouw, J.: High- and low-temperature pyrolysis profiles describe volatile organic compound emissions from western US wildfire fuels, Atmos. Chem. Phys., 18, 9263-9281, https://doi.org/10.5194/acp-18-9263-2018, 2018.

Semard, G., Gouin, C., Bourdet, J., Bord, N., and Livadaris, V.: Comparative study of differential flow and cryogenic modulators comprehensive two-dimensional gas chromatography systems for the detailed analysis of light cycle oil, Journal of Chromatography A, 1218, 3146-3152, https://doi.org/10.1016/j.chroma.2010.08.082, 2011.

Sengupta, D., Samburova, V., Bhattarai, C., Watts, A. C., Moosmüller, H., and Khlystov, A. Y.: Polar semi-volatile organic compounds in biomass burning emissions and their chemical transformations during aging in an oxidation flow reactor, Atmos. Chem. Phys. Discuss., 2020, 1-50, https://doi.org/10.5194/acp-2019-1179, 2020.

Serrano, G., Paul, D., Kim, S.-J., Kurabayashi, K., and Zellers, E. T.: Comprehensive Two-Dimensional Gas Chromatographic Separations with a Microfabricated Thermal Modulator, Analytical Chemistry, 84, 6973-6980, https://doi.org/10.1021/ac300924b, 2012.

Shafizadeh, F.: Introduction to pyrolysis of biomass, Journal of Analytical and Applied Pyrolysis, 3, 283-305, https://doi.org/10.1016/0165-2370(82)80017-X, 1982.

Sharma, G., Sinha, B., Pallavi, Hakkim, H., Chandra, B. P., Kumar, A., and Sinha, V.: Gridded Emissions of CO, NO_x, SO_2, CO_2, NH_3, HCl, CH_4, $PM_{2.5}$, PM_{10}, BC, and NMVOC from Open Municipal Waste Burning in India, Environmental Science & Technology, 53, 4765-4774, https://doi.org/10.1021/acs.est.8b07076, 2019.

Sharma, S., Goel, A., Gupta, D., Kumar, A., Mishra, A., Kundu, S., Chatani, S., and Klimont, Z.: Emission inventory of non-methane volatile organic compounds from anthropogenic sources in India, Atmospheric Environment, 102, 209-219, https://doi.org/10.1016/j.atmosenv.2014.11.070, 2015.

Sheesley, R. J., Schauer, J. J., Chowdhury, Z., Cass, G. R., and Simoneit, B. R. T.: Characterization of organic aerosols emitted from the combustion of biomass indigenous to South Asia, Journal of Geophysical Research: Atmospheres, 108, 4285, https://doi.org/10.1029/2002jd002981, 2003.

Sheffield, P. E., Zhou, J., Shmool, J. L. C., and Clougherty, J. E.: Ambient ozone exposure and children's acute asthma in New York City: a case-crossover analysis, Environmental Health, 14, 25, https://doi.org/10.1186/s12940-015-0010-2, 2015.

Shen, H. Z., Huang, Y., Wang, R., Zhu, D., Li, W., Shen, G. F., Wang, B., Zhang, Y. Y., Chen, Y. C., Lu, Y., Chen, H., Li, T. C., Sun, K., Li, B. G., Liu, W. X., Liu, J. F., and Tao, S.: Global Atmospheric Emissions of Polycyclic Aromatic Hydrocarbons from 1960 to 2008 and Future

Predictions, Environmental Science & Technology, 47, 6415-6424, https://doi.org/10.1021/es400857z, 2013.

Shrivastava, M., Cappa, C. D., Fan, J., Goldstein, A. H., Guenther, A. B., Jimenez, J. L., Kuang, C., Laskin, A., Martin, S. T., Ng, N. L., Petaja, T., Pierce, J. R., Rasch, P. J., Roldin, P., Seinfeld, J. H., Shilling, J., Smith, J. N., Thornton, J. A., Volkamer, R., Wang, J., Worsnop, D. R., Zaveri, R. A., Zelenyuk, A., and Zhang, Q.: Recent advances in understanding secondary organic aerosol: Implications for global climate forcing, Reviews of Geophysics, 55, 509-559, https://doi.org/10.1002/2016rg000540, 2017.

Simon, G. L., Bailis, R., Baumgartner, J., Hyman, J., and Laurent, A.: Current debates and future research needs in the clean cookstove sector, Energy for Sustainable Development, 20, 49-57, https://doi.org/10.1016/j.esd.2014.02.006, 2014.

Simoneit, B. R. T., Rogge, W. F., Mazurek, M. A., Standley, L. J., Hildemann, L. M., and Cass, G. R.: Lignin pyrolysis products, lignans, and resin acids as specific tracers of plant classes in emissions from biomass combustion, Environmental Science & Technology, 27, 2533-2541, https://doi.org/10.1021/es00048a034, 1993.

Simoneit, B. R. T.: Biomass burning — a review of organic tracers for smoke from incomplete combustion, Applied Geochemistry, 17, 129-162, https://doi.org/10.1016/S0883-2927(01)00061-0, 2002.

Sindelarova, K., Granier, C., Bouarar, I., Guenther, A., Tilmes, S., Stavrakou, T., Müller, J. F., Kuhn, U., Stefani, P., and Knorr, W.: Global data set of biogenic VOC emissions calculated by the MEGAN model over the last 30 years, Atmos. Chem. Phys., 14, 9317-9341, https://doi.org/10.5194/acp-14-9317-2014, 2014.

Singh, A. K., Tomer, N., and Jain, C. L.: Monitoring, Assessment and Status of Benzene, Toluene and Xylene Pollution in the Urban Atmosphere of Delhi, India Research Journal of Chemical Sciences, 2, 45-49, 2012.

Singh, D. P., Gadi, R., Mandal, T. K., Saud, T., Saxena, M., and Sharma, S. K.: Emissions estimates of PAH from biomass fuels used in rural sector of Indo-Gangetic Plains of India, Atmospheric Environment, 68, 120-126, https://doi.org/10.1016/j.atmosenv.2012.11.042, 2013.

Singh, R., Shukla, A., Gangopadhyay, S., and Adhikary, S.: A pilot study of benzene in different corridors of Delhi, Indian Journal of Air Pollution Control, 10, 21-24, 2010.

Singh, R., Gaur, M., and Shukla, A.: Seasonal and Spatial Variation of BTEX in Ambient Air of Delhi, Scientific Research Publishing, 7, 670-688, 2016.

Sirithian, D., Thepanondh, S., Sattler, M. L., and Laowagul, W.: Emissions of volatile organic compounds from maize residue open burning in the northern region of Thailand, Atmospheric Environment, 176, 179-187, https://doi.org/10.1016/j.atmosenv.2017.12.032, 2018.

Isotope Distribution Calculator and Mass Spec Plotter: https://www.sisweb.com/mstools/isotope.htm, access: 14 July 2020, 2016.

Sjöström, E.: Wood Chemistry: Fundamentals and Applications, 2nd ed., Academic Press, San Diego, USA, 1993.

Smith, J. N., Dunn, M. J., VanReken, T. M., Iida, K., Stolzenburg, M. R., McMurry, P. H., and Huey, L. G.: Chemical composition of atmospheric nanoparticles formed from nucleation in Tecamac, Mexico: Evidence for an important role for organic species in nanoparticle growth, Geophysical Research Letters, 35, L04808, https://doi.org/10.1029/2007gl032523, 2008.

Smith, K., Kishore, U. R., Lata, V. V. N., Joshi, K., Zhang, V., Rasmussen, J., Khalil, R. A., and Khalil, M. A. K.: Greenhouse gases from small-scale combustion devices in developing countries: Household stoves in India, EPA, Research Triangle Park, N. C, 2000.

Smith, K. R., McCracken, J. P., Weber, M. W., Hubbard, A., Jenny, A., Thompson, L. M., Balmes, J., Diaz, A., Arana, B., and Bruce, N.: Effect of reduction in household air pollution on childhood pneumonia in Guatemala (RESPIRE): a randomised controlled trial, The Lancet, 378, 1717-1726, https://doi.org/10.1016/S0140-6736(11)60921-5, 2011.

Smith, K. R., Bruce, N., Balakrishnan, K., Adair-Rohani, H., Balmes, J., Chafe, Z., Dherani, M., Hosgood, H. D., Mehta, S., Pope, D., and Rehfuess, E.: Millions Dead: How Do We Know and What Does It Mean? Methods Used in the Comparative Risk Assessment of Household Air Pollution, Annual Review of Public Health, 35, 185-206, https://doi.org/10.1146/annurev-publhealth-032013-182356, 2014.

Sotiropoulou, R. E. P., Tagaris, E., Pilinis, C., Anttila, T., and Kulmala, M.: Modeling New Particle Formation During Air Pollution Episodes: Impacts on Aerosol and Cloud Condensation Nuclei, Aerosol Science and Technology, 40, 557-572, https://doi.org/10.1080/02786820600714346, 2006.

Spracklen, D. V., Jimenez, J. L., Carslaw, K. S., Worsnop, D. R., Evans, M. J., Mann, G. W., Zhang, Q., Canagaratna, M. R., Allan, J., Coe, H., McFiggans, G., Rap, A., and Forster, P.: Aerosol mass spectrometer constraint on the global secondary organic aerosol budget, Atmos. Chem. Phys., 11, 12109-12136, https://doi.org/10.5194/acp-11-12109-2011, 2011.

Squires, F. A., Nemitz, E., Langford, B., Wild, O., Drysdale, W. S., Acton, W. J. F., Fu, P., Grimmond, C. S. B., Hamilton, J. F., Hewitt, C. N., Hollaway, M., Kotthaus, S., Lee, J., Metzger, S., Pingintha-Durden, N., Shaw, M., Vaughan, A. R., Wang, X., Wu, R., Zhang, Q., and Zhang, Y.: Measurements of traffic dominated pollutant emissions in a Chinese megacity, Atmos. Chem. Phys. Discuss., 2020, 1-33, https://doi.org/10.5194/acp-2019-1105, 2020.

Srivastava, A., Joseph, A. E., Patil, S., More, A., Dixit, R. C., and Prakash, M.: Air toxics in ambient air of Delhi, Atmospheric Environment, 39, 59-71, https://doi.org/10.1016/j.atmosenv.2004.09.053, 2005a.

Srivastava, A., Joseph, A. E., More, A., and Patil, S.: Emissions of VOCs at Urban Petrol Retail Distribution Centres in India (Delhi and Mumbai), Environmental Monitoring and Assessment, 109, 227-242, https://doi.org/10.1007/s10661-005-6292-z, 2005b.

Srivastava, A., Sengupta, B., and Dutta, S. A.: Source apportionment of ambient VOCs in Delhi City, Science of The Total Environment, 343, 207-220, https://doi.org/10.1016/j.scitotenv.2004.10.008, 2005c.

Srivastava, A., and Majumdar, D.: Emission inventory of evaporative emissions of VOCs in four metro cities in India, 315-322 pp., 2009.

Stein, S. E.: National Institute and Standards and Technology (NIST) Mass Spectral Search Program. Version 2.0g. Last Access 16 Febuary 2021. Available from: https://www.nist.gov/system/files/documents/srd/Ver20Man.pdf, 2011.

Stewart, G. J., Nelson, B. S., Drysdale, W. S., Acton, W. J. F., Vaughan, A. R., Hopkins, J. R., Dunmore, R. E., Hewitt, C. N., Nemitz, E. G., Mullinger, N., Langford, B., Shivani, Villegas, E. R., Gadi, R., Rickard, A. R., Lee, J. D., and Hamilton, J. F.: Sources of non-methane hydrocarbons in surface air in Delhi, India, Faraday Discussions 226, 409-431, https://doi.org/10.1039/D0FD00087F, 2021.

Stockwell, C. E., Yokelson, R. J., Kreidenweis, S. M., Robinson, A. L., DeMott, P. J., Sullivan, R. C., Reardon, J., Ryan, K. C., Griffith, D. W. T., and Stevens, L.: Trace gas emissions from combustion of peat, crop residue, domestic biofuels, grasses, and other fuels: configuration

and Fourier transform infrared (FTIR) component of the fourth Fire Lab at Missoula Experiment (FLAME-4), Atmos. Chem. Phys., 14, 9727-9754, 10.5194/acp-14-9727-2014, 2014.

Stockwell, C. E., Veres, P. R., Williams, J., and Yokelson, R. J.: Characterization of biomass burning emissions from cooking fires, peat, crop residue, and other fuels with high-resolution proton-transfer-reaction time-of-flight mass spectrometry, Atmos. Chem. Phys., 15, 845-865, https://doi.org/10.5194/acp-15-845-2015, 2015.

Stockwell, C. E., Christian, T. J., Goetz, J. D., Jayarathne, T., Bhave, P. V., Praveen, P. S., Adhikari, S., Maharjan, R., DeCarlo, P. F., Stone, E. A., Saikawa, E., Blake, D. R., Simpson, I. J., Yokelson, R. J., and Panday, A. K.: Nepal Ambient Monitoring and Source Testing Experiment (NAMaSTE): emissions of trace gases and light-absorbing carbon from wood and dung cooking fires, garbage and crop residue burning, brick kilns, and other sources, Atmos. Chem. Phys., 16, 11043-11081, https://doi.org/10.5194/acp-16-11043-2016, 2016.

Streets, D. G., and Waldhoff, S. T.: Biofuel use in Asia and acidifying emissions, Energy, 23, 1029-1042, https://doi.org/10.1016/S0360-5442(98)00033-4, 1998.

Streets, D. G., Bond, T. C., Carmichael, G. R., Fernandes, S. D., Fu, Q., He, D., Klimont, Z., Nelson, S. M., Tsai, N. Y., Wang, M. Q., Woo, J. H., and Yarber, K. F.: An inventory of gaseous and primary aerosol emissions in Asia in the year 2000, Journal of Geophysical Research: Atmospheres, 108, 8809, https://doi.org/10.1029/2002JD003093, 2003.

Strollo, C. M., and Ziemann, P. J.: Products and mechanism of secondary organic aerosol formation from the reaction of 3-methylfuran with OH radicals in the presence of NO_x, Atmospheric Environment, 77, 534-543, https://doi.org/10.1016/j.atmosenv.2013.05.033, 2013.

Taipale, R., Ruuskanen, T. M., Rinne, J., Kajos, M. K., Hakola, H., Pohja, T., and Kulmala, M.: Technical Note: Quantitative long-term measurements of VOC concentrations by PTR-MS - measurement, calibration, and volume mixing ratio calculation methods, Atmos. Chem. Phys., 8, 6681-6698, https://doi.org/10.5194/acp-8-6681-2008, 2008.

Talapatra, A., and Srivastava, A.: Ambient Air Non-Methane Volatile Organic Compound (NMVOC) Study Initiatives in India - a Review, Journal of Environmental Protection,, 2, 21-36, 2011.

Talyan, V., Dahiya, R. P., and Sreekrishnan, T. R.: State of municipal solid waste management in Delhi, the capital of India, Waste Management, 28, 1276-1287, https://doi.org/10.1016/j.wasman.2007.05.017, 2008.

Tapia, A., Villanueva, F., Salgado, M. S., Cabañas, B., Martínez, E., and Martín, P.: Atmospheric degradation of 3-methylfuran: kinetic and products study, Atmos. Chem. Phys., 11, 3227-3241, https://doi.org/10.5194/acp-11-3227-2011, 2011.

Thurston, G. D., and Spengler, J. D.: A quantitative assessment of source contributions to inhalable particulate matter pollution in metropolitan Boston, Atmospheric Environment 19, 9-25, https://doi.org/10.1016/0004-6981(85)90132-5, 1985.

Tomaz, S., Shahpoury, P., Jaffrezo, J.-L., Lammel, G., Perraudin, E., Villenave, E., and Albinet, A.: One-year study of polycyclic aromatic compounds at an urban site in Grenoble (France): Seasonal variations, gas/particle partitioning and cancer risk estimation, Science of The Total Environment, 565, 1071-1083, https://doi.org/10.1016/j.scitotenv.2016.05.137, 2016.

Tong, H. Y., Shore, D. L., Karasek, F. W., Helland, P., and Jellum, E.: Identification of organic compounds obtained from incineration of municipal waste by high-performance liquid chromatographic fractionation and gas chromatography-mass spectrometry, Journal of Chromatography A, 285, 423-441, https://doi.org/10.1016/S0021-9673(01)87784-0, 1984.

United Nations: World urbanization trends 2014: key facts, in: World Urbanisation Prospects, UN, New York, USA, 1, 2014.

United Nations: World Urbanization Prospects: The 2018 Revision (ST/ESA/SER.A/420), United Nations: Department of Economic and Social Affairs, Population Division New York, 2019.

Varshney, C. K., and Padhy, P. K.: Emissions of Total Volatile Organic Compounds from Anthropogenic Sources in India, Journal of Industrial Ecology, 2, 93-105, https://doi.org/10.1162/jiec.1998.2.4.93, 1998.

Vendeuvre, C., Ruiz-Guerrero, R., Bertoncini, F., Duval, L., and Thiébaut, D.: Comprehensive Two-Dimensional Gas Chromatography for Detailed Characterisation of Petroleum Products, Oil & Gas Science and Technology, 62, 43-55, 2007.

Venkataraman, C., and Rao, G. U. M.: Emission Factors of Carbon Monoxide and Size-Resolved Aerosols from Biofuel Combustion, Environmental Science & Technology, 35, 2100-2107, https://doi.org/10.1021/es001603d, 2001.

Venkataraman, C., Negi, G., Brata Sardar, S., and Rastogi, R.: Size distributions of polycyclic aromatic hydrocarbons in aerosol emissions from biofuel combustion, Journal of Aerosol Science, 33, 503-518, https://doi.org/10.1016/S0021-8502(01)00185-9, 2002.

Venkataraman, C., Habib, G., Eiguren-Fernandez, A., Miguel, A. H., and Friedlander, S. K.: Residential biofuels in south Asia: Carbonaceous aerosol emissions and climate impacts, Science, 307, 1454-1456, https://doi.org/10.1126/science.1104359, 2005.

Venkataraman, C., Sagar, A. D., Habib, G., Lam, N., and Smith, K. R.: The Indian National Initiative for Advanced Biomass Cookstoves: The benefits of clean combustion, Energy for Sustainable Development, 14, 63-72, https://doi.org/10.1016/j.esd.2010.04.005, 2010.

Vilaseca, A., Guy, I., Charles, B., Guinaudeau, H., de Arias, A. R., and Fournet, A.: Chemical Composition and Insecticidal Activity of Hedeoma mandoniana Essential Oils, Journal of Essential Oil Research, 16, 380-383, https://doi.org/10.1080/10412905.2004.9698749, 2004.

Villanueva, F., Barnes, I., Monedero, E., Salgado, S., Gómez, M. V., and Martin, P.: Primary product distribution from the Cl-atom initiated atmospheric degradation of furan: Environmental implications, Atmospheric Environment, 41, 8796-8810, https://doi.org/10.1016/j.atmosenv.2007.07.053, 2007.

Vineis, P., and Husgafvel-Pursiainen, K.: Air pollution and cancer: biomarker studies in human populations Carcinogenesis, 26, 1846-1855, https://doi.org/10.1093/carcin/bgi216, 2005.

Wagner, P., and Kuttler, W.: Biogenic and anthropogenic isoprene in the near-surface urban atmosphere — A case study in Essen, Germany, Science of The Total Environment, 475, 104-115, https://doi.org/10.1016/j.scitotenv.2013.12.026, 2014.

Wang, F. C.-Y., and Walters, C. C.: Pyrolysis Comprehensive Two-Dimensional Gas Chromatography Study of Petroleum Source Rock, Analytical Chemistry, 79, 5642-5650, https://doi.org/10.1021/ac070166j, 2007.

Wang, H. K., Huang, C. H., Chen, K. S., Peng, Y. P., and Lai, C. H.: Measurement and source characteristics of carbonyl compounds in the atmosphere in Kaohsiung city, Taiwan, Journal of Hazardous Materials, 179, 1115-1121, https://doi.org/10.1016/j.jhazmat.2010.03.122, 2010.

Wang, H. L., Lou, S. R., Huang, C., Qiao, L. P., Tang, X. B., Chen, C. H., Zeng, L. M., Wang, Q., Zhou, M., Lu, S. H., and Yu, X. N.: Source Profiles of Volatile Organic Compounds from

Biomass Burning in Yangtze River Delta, China, Aerosol Air Qual. Res., 14, 818-828, https://doi.org/10.4209/aaqr.2013.05.0174, 2014.

Wang, L., Slowik, J. G., Tripathi, N., Bhattu, D., Rai, P., Kumar, V., Vats, P., Satish, R., Baltensperger, U., Ganguly, D., Rastogi, N., Sahu, L. K., Tripathi, S. N., and Prévôt, A. S. H.: Source characterization of volatile organic compounds measured by PTR-ToF-MS in Delhi, India, Atmos. Chem. Phys. Discuss., 2020, 1-27, https://doi.org/10.5194/acp-2020-11, 2020.

Warneke, C., Roberts, J. M., Veres, P., Gilman, J., Kuster, W. C., Burling, I., Yokelson, R., and de Gouw, J. A.: VOC identification and inter-comparison from laboratory biomass burning using PTR-MS and PIT-MS, International Journal of Mass Spectrometry, 303, 6-14, https://doi.org/10.1016/j.ijms.2010.12.002, 2011.

Wei, S. Y., Shen, G. F., Zhang, Y. Y., Xue, M., Xie, H., Lin, P. C., Chen, Y. C., Wang, X. L., and Tao, S.: Field measurement on the emissions of PM, OC, EC and PAHs from indoor crop straw burning in rural China, Environmental Pollution, 184, 18-24, https://doi.org/10.1016/j.envpol.2013.07.036, 2014.

Wells, K. C., Millet, D. B., Payne, V. H., Deventer, M. J., Bates, K. H., de Gouw, J. A., Graus, M., Warneke, C., Wisthaler, A., and Fuentes, J. D.: Satellite isoprene retrievals constrain emissions and atmospheric oxidation, Nature, 585, 225-233, https://doi.org/10.1038/s41586-020-2664-3, 2020.

Wendt, J. O. L., Pershing, D. W., Lee, J. W. L., and Glass, J. W.: Pulverized coal combustion: NO_x formation mechanisms under fuel rich and staged combustion conditions, Symposium (International) on Combustion, 17, 77-87, 1979.

Went, F. W.: Blue Hazes in the Atmosphere, Nature, 187, 641, https://doi.org/10.1038/187641a0, 1960.

West, S. K., Bates, M. N., Lee, J. S., Schaumberg, D. A., Lee, D. J., Adair-Rohani, H., Chen, D. F., and Araj, H.: Is Household Air Pollution a Risk Factor for Eye Disease?, International Journal of Environmental Research and Public Health, 10, 5378-5398, https://doi.org/10.3390/ijerph10115378, 2013.

WHO: Ambient (outdoor) air pollution in cities database 2014, World Health Organization, Geneva, Switzerland, 2014.

WHO: IARC monographs on the evaluation of carcinogenic risks to humans, Internal report 14/002 World Health Organisation, Lyon, France, 2016.

Wiedinmyer, C., Akagi, S. K., Yokelson, R. J., Emmons, L. K., Al-Saadi, J. A., Orlando, J. J., and Soja, A. J.: The Fire INventory from NCAR (FINN): a high resolution global model to estimate the emissions from open burning, Geosci. Model Dev., 4, 625-641, https://doi.org/10.5194/gmd-4-625-2011, 2011.

Wiedinmyer, C., Yokelson, R. J., and Gullett, B. K.: Global Emissions of Trace Gases, Particulate Matter, and Hazardous Air Pollutants from Open Burning of Domestic Waste, Environmental Science & Technology, 48, 9523-9530, https://doi.org/10.1021/es502250z, 2014.

Wiriya, W., Chantara, S., Sillapapiromsuk, S., and Lin, N. H.: Emission Profiles of PM10-Bound Polycyclic Aromatic Hydrocarbons from Biomass Burning Determined in Chamber for Assessment of Air Pollutants from Open Burning, Aerosol Air Qual. Res., 16, 2716-2727, https://doi.org/10.4209/aaqr.2015.04.0278, 2016.

Woody, M. C., Baker, K. R., Hayes, P. L., Jimenez, J. L., Koo, B., and Pye, H. O. T.: Understanding sources of organic aerosol during CalNex-2010 using the CMAQ-VBS, Atmos. Chem. Phys., 16, 4081-4100, https://doi.org/10.5194/acp-16-4081-2016, 2016.

World Bank: Urban development series, What a Waste, A global review of Solid Waste Managment, Washington, USA, 13-16, 2012.

World Bank: Tracking SDG 7: The Energy Progress Report 2020. Chapter 2: Access To Clean Fuels And Technologies For Cooking, International Bank for Reconstruction and Development, Washington, DC, 2020.

World Health Organization: Burden of disease attributable to ambient air pollution, in: Ambient Air Pollution: a global assessment of exposure and burden of disease, World Health Organisation, Geneva, Switzerland, 39-48, 2016.

World Health Organization: Burden of disease from ambient air pollution for 2016, WHO, Geneva: Switzerland, 2018a.

World Health Organization: Household air pollution and health. Accessed 05 Aug 2020. Available from https://www.who.int/news-room/fact-sheets/detail/household-air-pollution-and-health, 2018b.

WorldPop: India 100m population. DOI 10.5258/SOTON/WP00532, 2017.

Worton, D. R., Decker, M., Isaacman-VanWertz, G., Chan, A. W. H., Wilson, K. R., and Goldstein, A. H.: Improved molecular level identification of organic compounds using comprehensive two-dimensional chromatography, dual ionization energies and high

resolution mass spectrometry, Analyst, 142, 2395-2403, https://doi.org/10.1039/c7an00625j, 2017.

Wróblewski, T., Ziemczonek, L., Szerement, K., and Karwasz, G. P.: Proton affinities of simple organic compounds, Czechoslovak Journal of Physics, 56, B1110-B1115, https://doi.org/10.1007/s10582-006-0335-8, 2006.

Xue, W. L., and Warshawsky, D.: Metabolic activation of polycyclic and heterocyclic aromatic hydrocarbons and DNA damage: A review, Toxicology and Applied Pharmacology, 206, 73-93, https://doi.org/10.1016/j.taap.2004.11.006, 2005.

Yamada, H., Inomata, S., and Tanimoto, H.: Evaporative emissions in three-day diurnal breathing loss tests on passenger cars for the Japanese market, Atmospheric Environment, 107, 166-173, https://doi.org/10.1016/j.atmosenv.2015.02.032, 2015.

Yao, Z., Shen, X., Ye, Y., Cao, X., Jiang, X., Zhang, Y., and He, K.: On-road emission characteristics of VOCs from diesel trucks in Beijing, China, Atmospheric Environment, 103, 87-93, https://doi.org/10.1016/j.atmosenv.2014.12.028, 2015.

Yee, L. D., Kautzman, K. E., Loza, C. L., Schilling, K. A., Coggon, M. M., Chhabra, P. S., Chan, M. N., Chan, A. W. H., Hersey, S. P., Crounse, J. D., Wennberg, P. O., Flagan, R. C., and Seinfeld, J. H.: Secondary organic aerosol formation from biomass burning intermediates: phenol and methoxyphenols, Atmos. Chem. Phys., 13, 8019-8043, https://doi.org/10.5194/acp-13-8019-2013, 2013.

Yevich, R., and Logan, J. A.: An assessment of biofuel use and burning of agricultural waste in the developing world, Global Biogeochemical Cycles, 17, 1095, https://doi.org/10.1029/2002GB001952, 2003.

Yokelson, R. J., Griffith, D. W. T., and Ward, D. E.: Open-path Fourier transform infrared studies of large-scale laboratory biomass fires, Journal of Geophysical Research: Atmospheres, 101, 21067-21080, https://doi.org/10.1029/96JD01800, 1996.

Yokelson, R. J., Bertschi, I. T., Christian, T. J., Hobbs, P. V., Ward, D. E., and Hao, W. M.: Trace gas measurements in nascent, aged, and cloud-processed smoke from African savanna fires by airborne Fourier transform infrared spectroscopy (AFTIR), Journal of Geophysical Research: Atmospheres, 108, https://doi.org/10.1029/2002jd002322, 2003.

Yokelson, R. J., Christian, T. J., Karl, T. G., and Guenther, A.: The tropical forest and fire emissions experiment: laboratory fire measurements and synthesis of campaign data, Atmos. Chem. Phys., 8, 3509-3527, https://doi.org/10.5194/acp-8-3509-2008, 2008.

Yokelson, R. J., Burling, I. R., Urbanski, S. P., Atlas, E. L., Adachi, K., Buseck, P. R., Wiedinmyer, C., Akagi, S. K., Toohey, D. W., and Wold, C. E.: Trace gas and particle emissions from open biomass burning in Mexico, Atmos. Chem. Phys., 11, 6787-6808, https://doi.org/10.5194/acp-11-6787-2011, 2011.

Yokelson, R. J., Burling, I. R., Gilman, J. B., Warneke, C., Stockwell, C. E., de Gouw, J., Akagi, S. K., Urbanski, S. P., Veres, P., Roberts, J. M., Kuster, W. C., Reardon, J., Griffith, D. W. T., Johnson, T. J., Hosseini, S., Miller, J. W., Cocker Iii, D. R., Jung, H., and Weise, D. R.: Coupling field and laboratory measurements to estimate the emission factors of identified and unidentified trace gases for prescribed fires, Atmos. Chem. Phys., 13, 89-116, https://doi.org/10.5194/acp-13-89-2013, 2013.

Young Koo, Y. K., Kim, W., and Jo, Y. M.: Release of Harmful Air Pollutants from Open Burning of Domestic Municipal Solid Wastes in a Metropolitan Area of Korea, Aerosol Air Qual. Res., 13, 1365-1372, https://doi.org/10.4209/aaqr.2012.10.0272, 2013.

Yu, F., and Luo, G.: Modeling of gaseous methylamines in the global atmosphere: impacts of oxidation and aerosol uptake, Atmos. Chem. Phys., 14, 12455-12464, 10.5194/acp-14-12455-2014, 2014.

Yu, S., Bhave, P. V., Dennis, R. L., and Mathur, R.: Seasonal and Regional Variations of Primary and Secondary Organic Aerosols over the Continental United States: Semi-Empirical Estimates and Model Evaluation, Environmental Science & Technology, 41, 4690-4697, https://doi.org/10.1021/es061535g, 2007.

Yuan, B., Hu, W. W., Shao, M., Wang, M., Chen, W. T., Lu, S. H., Zeng, L. M., and Hu, M.: VOC emissions, evolutions and contributions to SOA formation at a receptor site in eastern China, Atmos. Chem. Phys., 13, 8815-8832, https://doi.org/10.5194/acp-13-8815-2013, 2013.

Yuan, B., Koss, A., Warneke, C., Gilman, J. B., Lerner, B. M., Stark, H., and de Gouw, J. A.: A high-resolution time-of-flight chemical ionization mass spectrometer utilizing hydronium ions (H_3O^+ ToF-CIMS) for measurements of volatile organic compounds in the atmosphere, Atmos. Meas. Tech., 9, 2735-2752, 10.5194/amt-9-2735-2016, 2016.

Yuan, B., Koss, A. R., Warneke, C., Coggon, M., Sekimoto, K., and de Gouw, J. A.: Proton-Transfer-Reaction Mass Spectrometry: Applications in Atmospheric Sciences, Chemical Reviews, 117, 13187-13229, https://doi.org/10.1021/acs.chemrev.7b00325, 2017.

Yucra, S., Tapia, V., Steenland, K., Naeher, L. P., and Gonzales, G. F.: Association Between Biofuel Exposure and Adverse Birth Outcomes at High Altitudes in Peru: A Matched Case-control Study, International Journal of Occupational and Environmental Health, 17, 307-313, 2011.

Zhang, H., Zhang, Y., Huang, Z., Acton, W. J. F., Wang, Z., Nemitz, E., Langford, B., Mullinger, N., Davison, B., Shi, Z., Liu, D., Song, W., Yang, W., Zeng, J., Wu, Z., Fu, P., Zhang, Q., and Wang, X.: Vertical profiles of biogenic volatile organic compounds as observed online at a tower in Beijing, Journal of Environmental Sciences, 95, 33-42, https://doi.org/10.1016/j.jes.2020.03.032, 2020.

Zhang, Q., Jimenez, J. L., Canagaratna, M. R., Allan, J. D., Coe, H., Ulbrich, I., Alfarra, M. R., Takami, A., Middlebrook, A. M., Sun, Y. L., Dzepina, K., Dunlea, E., Docherty, K., DeCarlo, P. F., Salcedo, D., Onasch, T., Jayne, J. T., Miyoshi, T., Shimono, A., Hatakeyama, S., Takegawa, N., Kondo, Y., Schneider, J., Drewnick, F., Borrmann, S., Weimer, S., Demerjian, K., Williams, P., Bower, K., Bahreini, R., Cottrell, L., Griffin, R. J., Rautiainen, J., Sun, J. Y., Zhang, Y. M., and Worsnop, D. R.: Ubiquity and dominance of oxygenated species in organic aerosols in anthropogenically-influenced Northern Hemisphere midlatitudes, Geophysical Research Letters, 34, https://doi.org/10.1029/2007GL029979, 2007.

Zhang, Q., Streets, D. G., Carmichael, G. R., He, K. B., Huo, H., Kannari, A., Klimont, Z., Park, I. S., Reddy, S., Fu, J. S., Chen, D., Duan, L., Lei, Y., Wang, L. T., and Yao, Z. L.: Asian emissions in 2006 for the NASA INTEX-B mission, Atmos. Chem. Phys., 9, 5131-5153, https://doi.org/10.5194/acp-9-5131-2009, 2009.

Zhang, Y., and Tao, S.: Global atmospheric emission inventory of polycyclic aromatic hydrocarbons (PAHs) for 2004, Atmospheric Environment, 43, 812-819, https://doi.org/10.1016/j.atmosenv.2008.10.050, 2009.

Zhao, X. C., and Wang, L. M.: Atmospheric Oxidation Mechanism of Furfural Initiated by Hydroxyl Radicals, Journal of Physical Chemistry A, 121, 3247-3253, https://doi.org/10.1021/acs.jpca.7b00506, 2017.

Zhao, Y., Nguyen, N. T., Presto, A. A., Hennigan, C. J., May, A. A., and Robinson, A. L.: Intermediate Volatility Organic Compound Emissions from On-Road Gasoline Vehicles and Small Off-Road Gasoline Engines, Environmental Science & Technology, 50, 4554-4563, https://doi.org/10.1021/acs.est.5b06247, 2016.

Zhao, Y. L., Nguyen, N. T., Presto, A. A., Hennigan, C. J., May, A. A., and Robinson, A. L.: Intermediate Volatility Organic Compound Emissions from On-Road Diesel Vehicles: Chemical Composition, Emission Factors, and Estimated Secondary Organic Aerosol Production, Environmental Science & Technology, 49, 11516-11526, https://doi.org/10.1021/acs.est.5b02841, 2015.